CR-134655

1 August 1974

FINAL REPORT

EXTENDED TEMPERATURE RANGE ACPS THRUSTER INVESTIGATION

by

A. L. Blubaugh
L. Schoenman

Aerojet Liquid Rocket Company
Sacramento, California 95812

Prepared for

NASA Lewis Research Center
Contract NAS 3-16775

1. Report No.	2. Government Accession No.	3. Recipient's Catalog No.
CR-134655		

4. Title and Subtitle	5. Report Date
Extended Temperature Range ACPS Thruster Investigation	1 August 1974
	6. Performing Organization Code
7. Author(s)	8. Performing Organization Report No.
A. L. Blubaugh L. Schoenman	
9. Performing Organization Name and Address	10. Work Unit No.
	R5231
Aerojet Liquid Rocket Company Sacramento, California 95812	11. Contract or Grant No.
	NAS 3-16775
12. Sponsoring Agency Name and Address	13. Type of Report and Period Covered
NASA Lewis Research Center 21000 Brookpark Road Cleveland, Ohio 44135	Final
	14. Sponsoring Agency Code

15. Supplementary Notes

16. Abstract

A successful hot fire demonstration of Pulsing Liquid Hydrogen/Liquid Oxygen and Gaseous Hydrogen/Liquid Oxygen ACPS Thrusters has resulted from the most recent efforts* in the continuing search for a simple, lightweight and high performance reaction control system (RCS) by the NASA. The use of liquid cryogenic propellants has heretofore required extensive periods of engine thermal conditioning or the use of complex equipment to convert both liquid propellants to gas prior to delivery to the engine.

Significant departures from conventional injector design practice were employed to achieve an operable design. The work presented includes thermal and injector manifold priming analyses, the results of subscale injector chilldown tests and the results of 168 full scale, 550 N (1250 lbF) rocket engine tests. Ignition experiments at propellant temperatures ranging from cryogenic (25°K (45°R)) to ambient led to the generation of a universal spark ignition system which can reliably ignite an engine when supplied with liquid, two phase, or gaseous propellants. Electrical power requirements for the spark igniter are very low (10 mJ).

*Extended temperature range ACPS thruster investigation, NAS 3-16775.

17. Key Words (Suggested by Author(s))	18. Distribution Statement
Cryogenic APS Thrusters, Pulsing, LO_2, LH_2	Publicly Available

19. Security Classif. (of this report)	20. Security Classif. (of this page)	21. No. of Pages	22. Price*
Unclassified	Unclassified	201	

* For sale by the National Technical Information Service, Springfield, Virginia 22151

TABLE OF CONTENTS

TABLE OF CONTENTS (cont.)

TABLE LIST

FIGURE LIST

FIGURE LIST (cont.)

FIGURE LIST (cont.)

FIGURE LIST (cont.)

ABSTRACT

A successful hot fire demonstration of Pulsing Liquid Hydrogen/Liquid Oxygen and Gaseous Hydrogen/Liquid Oxygen ACPS Thrusters has resulted from the most recent efforts* in the continuing search for a simple, lightweight and high performance reaction control system (RCS) by the NASA. The use of liquid cryogenic propellants has heretofore required extensive periods of engine thermal conditioning or the use of complex equipment to convert both liquid propellants to gas prior to delivery to the engine.

Significant departures from conventional injector design practice were employed to achieve an operable design. The work presented includes thermal and injector manifold priming analyses, the results of subscale injector chilldown tests and the results of 168 full scale, 550 N (1250 lbF) rocket engine tests. Ignition experiments at propellant temperatures ranging from cryogenic (25°K (45°R)) to ambient led to the generation of a universal spark ignition system which can reliably ignite an engine when supplied with liquid, two phase, or gaseous propellants. Electrical power requirements for the spark igniter are very low (10 mJ).

*Extended temperature range ACPS thruster investigation, NAS 3-16775.

I. INTRODUCTION

During the early phase of the Space Shuttle vehicle definition and propulsion system studies (1971), several candidate auxiliary propulsion system concepts were proposed and evaluated by both the NASA Centers and vehicle contractor specialists[1,2,3]. From these extensive study and vehicle optimization efforts, it was concluded that the simplest, lightest-weight, highest performing nonintegrated Auxiliary Propulsion System for the Space Shuttle application (1.5→2.3 million lb-sec I_t) would be a liquid hydrogen/liquid oxygen (L/L) ACPS of the type shown in Figure 1. It was suggested that this would be a near ideal system if it could be made to work in a satisfactory manner. However, major technical questions concerning the feasibility and operability of such a system had not been properly addressed and, therefore, many questions such as ignition and transient flow characteristics of liquid cryogenic propellants, remained unanswered.

An extensive technology program was initiated by NASA-Lewis in June of 1972, as a continuing technology effort aimed at finalizing the cryogenic S.S. ACPS technology package, and at the same time resolving several of the very basic and difficult technical issues associated with a L/L ACPS thruster concept. Some of the anticipated critical technology issues directly related to the L/L pulsing auxiliary thruster concept were: low temperature ignition, pulse mode operation, delivered performance and combustion stability[4] and thruster heat rejection rates to the propellant feed lines.

From the onset of the subject technical effort, it was obvious that extreme care in maintaining thermal control over the cryogenic propellants, the propellant feed system, the thruster interface[1,2] and the combustion zone of the thruster assembly would be vitally important to successful thruster operation. Furthermore, a "clean sheet" design approach to this difficult technical undertaking was adopted and no design restraints or ties to conventionality were imposed.

In order to address all of the key technical problems early in the effort, comprehensive analyses were conducted in each of the following areas:

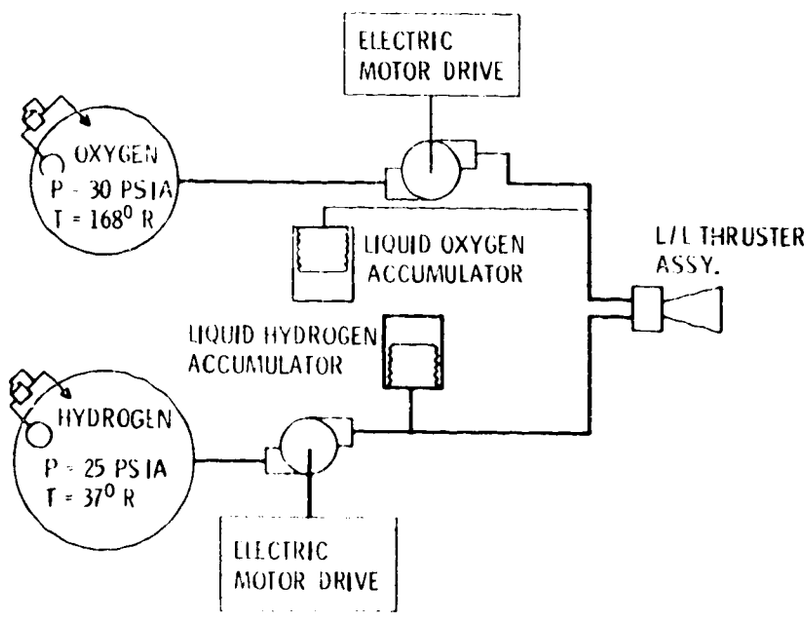

Figure 1. Liquid Hydrogen/Liquid Oxygen APS Schematic

I, Introduction (cont.)

Propellant physical properties
Material selection
Low temperature ignition
Valve sequencing and feed system interactions
Manifold fill and venting characteristics
Combustion stability (high and low frequency)
Component cooling and heat soak

These were combined into four broad areas for further parametric analyses that covered all technical areas of concern. These areas are (1) thruster thermal management, (2) ignition requirements and limitations, (3) performance and operational characteristics, and (4) thruster component and feed system interactions. The results of these parametric analyses provided design guidance in what were concluded to be the three key technology areas requiring demonstration.

(1) A reliable ignition system which could provide rapid ignition at low power levels with a wide range of propellant supply temperatures.

(2) Low residual volume thruster designs which would not vapor lock on start.

(3) A means of minimizing heat leak from the thruster to the propellant supply system.

Two critical experimental activities were conducted in support of the parametric analyses prior to design selections. One was a series of critical ignition limits experiments undertaken to verify the analytically predicted limits of ignitability of cryogenic hydrogen/oxygen mixtures. The other involved the chilldown and priming characteristics of various low thermal capacitance and primed manifold concepts.

I, Introduction (cont.)

Detailed design analyses were conducted on two different thruster systems corresponding to two different engine design points. The first system, (Design Point 1) referred to as the Liquid-Liquid (L/L) system was optimized for LH_2 at 25°K (45°R) and LO_2 at 83°K (150°R) at the valves. The second system (Design Point 2) uses slightly warmer supercritical H_2 and is referred to herein as the Gas-Liquid (G/L) system. The G/L system was optimized for both propellants at 83°K (150°R) at the thruster valves. The design point conditions for each system and operating ranges are defined in Table I.

TABLE I

THRUSTER DESIGN POINT AND OPERATING CONDITIONS

Nominal Conditions	Experimental Operating Range
Thrust: 5560 N (1250 lb_f)	2780-8340 N (625-1875 lb_f)
Chamber Pressure: 345 N/cm^2 (500 psia)	172-517 N/cm^2 (250-750 psia)
Overall Mixture Ratio (O/F): 4.5	3.5 - 5.0
Nozzle Expansion Ratio: 40:1	

	H_2 Temp °K/(°R)			O_2 Temp		
	Nom.	Min.	Max.	Nom.	Min.	Max.
Design Point 1 (L/L System)	25 (45)	21 (37)	42 (75)	83 (150)	56 (100)	111 (200)
Design Point 2 (G/L System)	83 (150)	56 (100)	111 (200)	83 (150)	56 (100)	111 (200)

Four full thruster designs were prepared which integrated the results of the above analyses and experiments. Two of the designs were for the L/L system and two were for the G/L system. Each design was analyzed in detail using an engine simulation model to predict fill, ignition and shutdown

transients. The nominal design point, operating range, and performance and response goals established by the NASA for these thrusters are provided in Table I. Following NASA review of the 4 designs one of the L/L designs and one of the G/L designs were selected for further evaluation. Two thruster assemblies were fabricated and tested, first at sea level using heat sink nozzles and then at simulated altitude using cooled thrust chambers.

II. SUMMARY

A. ANALYTICAL FEASIBILITY STUDIES AND SUPPORTING EXPERIMENTS

1. Complete Thruster

Two thermal management approaches were evaluated for each design point. The first approach maintains the valve, injector manifolding, igniter and propellants at the valve at cryogenic temperatures via a low velocity propellant recirculation loop which is integrated into the thruster design. Such a design provided a high confidence level by insuring that the thruster is cold and ready to run at all times. This design does not require any major technology advances. The heat load resulting from the need for continuous cooling, however, was computed to range from 25 to 50 BTU/hr (7 to 14 W) which was at least an order of magnitude greater than the systems study Reference 1 considered acceptable.

The second approach evaluated employed a thermal stand-off between the valve and thruster to reduce heat leaks to the system to 1 to 2 BTU/hr (0.3 to 0.6 W). In this approach, the complete thruster (including the propellant manifolding) would be at the vehicle ambient temperature or higher, depending upon the heat soak out levels from long burns. Various methods of accelerating the internal manifold wall chilldown and propellant bleed-in rates were considered. These included the use of (1) low thermal conductivity nonmetallic coating for the manifolds and (2) low thermal capacitance metallic liners in a dual wall manifolding configuration. The latter was selected for further subscale experimental verification since analyses showed that chill-in times in the order of 0.020 sec were possible and that liner thermal cycle capabilities in the order of $10^5 \rightarrow 10^6$ cycles could be expected with conventional stainless steel materials. The nonmetallic coating was rejected due to concern about spalling and subsequent orifice plugging during repeated thermal cycling. Subsequent testing of the dual

wall manifolding using a 0.013 cm (0.005 in.) CRES 347 liner showed predicted chilldown rates could be achieved, and that pressures in excess of 1000 psi (690 N/cm^2) could be accommodated without distortion.

The thermal management approach selected for the Liquid-Liquid System is illustrated in Figure 2. Propellants from the valves pass through thermal standoffs into low volume dual wall manifolding located within the injector. The injector face is actively cooled during firing by diverting a portion of the LH_2 through dump circuits located in the injector face. Chamber cooling is accomplished by generating a low temperature fuel rich gas barrier at the chamber wall. The low manifold volumes are required for good pulsing performance and response.

The selected Gas/Liquid System shown in Figure 3 uses a similar oxidizer feed system but takes advantage of the lower density of the gaseous fuel. Regenerative cooling a portion of the combustion chamber is possible with the 83°K (150°R) fuel because (1) the vapor lock effect was markedly reduced to the point where a dual wall manifolding is no longer required, and (2) residual mass of the gaseous fuel in the channels no longer imposes a significant performance loss.

2. Ignition Limits

The thruster thermal analysis showed that it would be difficult to control the density of the small quantities of propellant reaching the igniter and it was thus necessary to develop an igniter which could perform its function independent of the state of the propellant being supplied. A series of ignition limits analyses supported by ignition experiments employing liquid, two phase, and gaseous propellants resulted in the conclusion that a modified form of the 4-stage spark/ox torch igniter developed

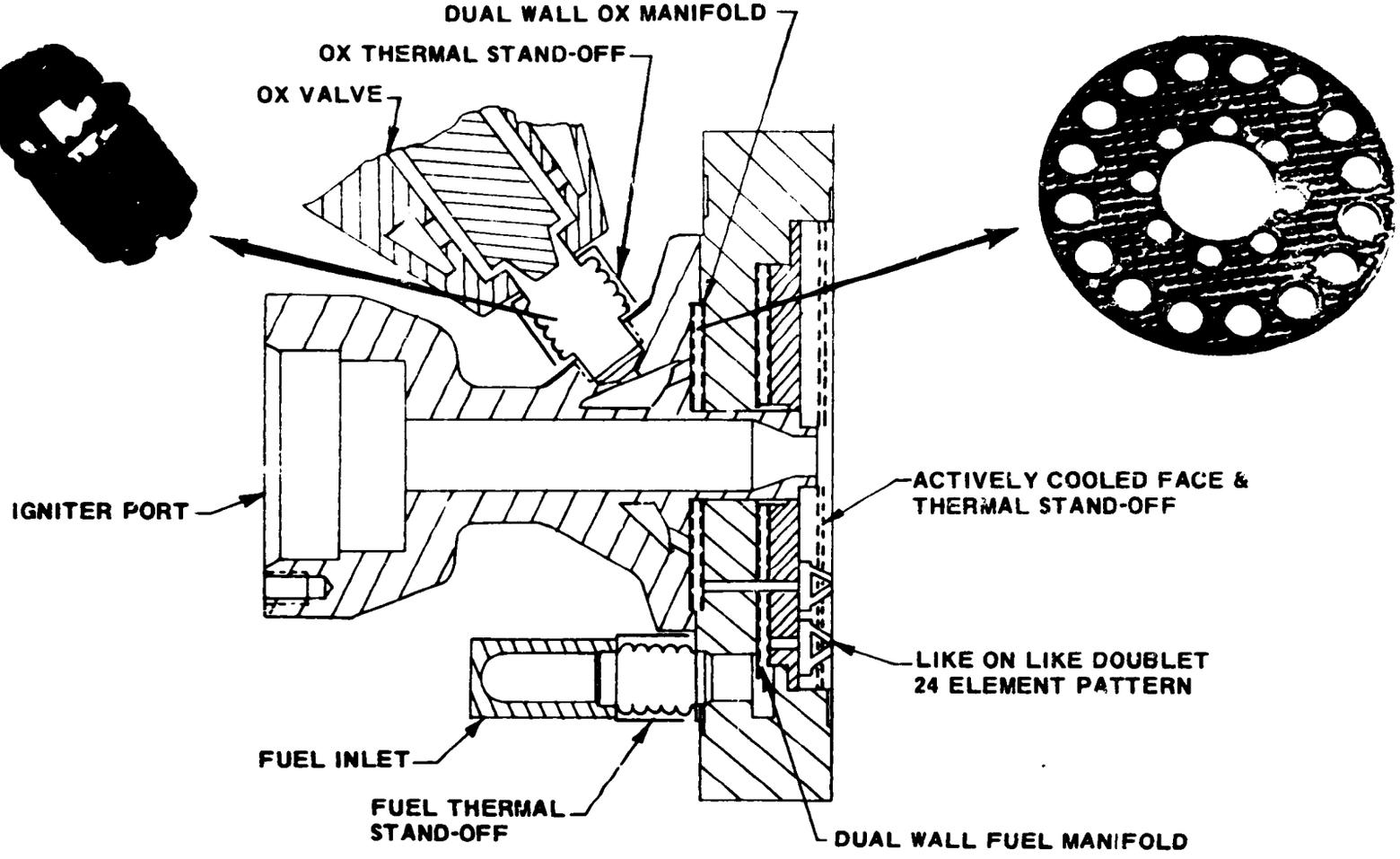

Figure 2. Thermally Isolated L/L Injector with Dual Wall Manifolding

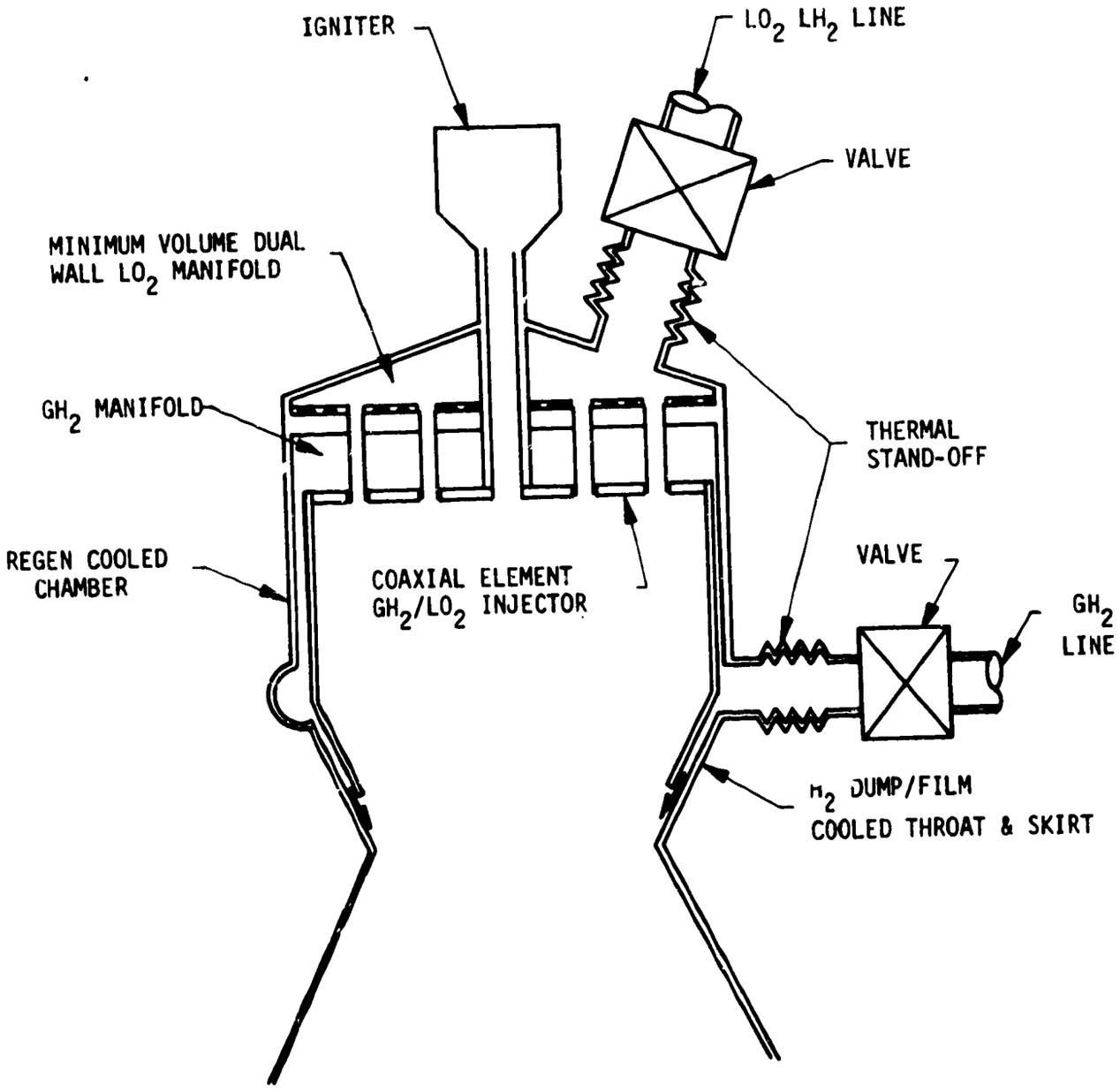

Figure 3. Gas/Liquid Thruster Thermal Management Schematic

by ALRC under Contract NAS 3-14348 could, in a sense, act as a universal igniter and that rapid ignition (less than 0.02 sec) could be achieved at very low spark energy levels (10 mJ).

II, Summary (cont.)

B. FABRICATION OF SELECTED DESIGNS

The following experimental hardware was fabricated following completion of the detail designs and NASA design approvals.

Igniters - 2 ox torch universal igniter assemblies of the same design.

Injectors - 1, LH_2/LO_2 injector incorporating a 24 element like-on-like doublet pattern, the dual wall low volume manifold concept, and close coupled thermally isolated valves in both propellant circuits. One GH_2/LO_2 injector incorporating a 36 element coaxial tube pattern and the dual wall low volume manifolding, and close coupled thermally isolated valve in the ox circuit only. The fuel circuit of the injector was of conventional design fed from the discharge of a regeneratively cooled chamber. Both injectors contain injector face, body and valve thermal instrumentation and pressure ports.

Chambers - One 8.9 cm (3-1/2") long regeneratively cooled combustion chamber with integral acoustic resonator cavity and close coupled, thermally isolated valve. This chamber mates with the Gas/Liquid injector, heat sink throat sections and cooled chamber.

Two heat sink copper throats and 2 cylindrical L* extensions 3.8 cm (1.5") and 5.1 cm (2.0") in length. Useable directly with the L/L injector and as additions to the above regeneratively cooled chamber.

All chamber sections including the regeneratively cooled contains chamber pressure ports and gas side thermal instrumentation which allow computation of the axial and circumferential heat flux profiles. Ports for high frequency

transducers (Photocon and Kistler) and a pulse gun are provided in the heat sink chambers.

Two cooled chambers: one columbium (barrier cooled) chamber that mates to the Liquid/Liquid injector; one Haynes nozzle for use with the Gas/Liquid injector. One uncooled spacer (L/L) and one dump cooled section (G/L). The uncooled spacer was designed to provide a heat soak barrier between the columbium chamber and the L/L injector. The dump cooled section delivers film coolant to the Haynes nozzle, and forms the convergent section of the G/L cooled chamber mating the regen section to the Haynes throat-nozzle-skirt section.

Valves - Main valves employed in testing are modifications of standard Control Components, Inc., gas actuated, fast response, soft seal, cryogenic poppet valves. Four sets of valve seats (which become an integral part of the chamber) were purchased. Each seat assembly contains a bleed port which allows propellant to be circulated through the valve while the valve is in the closed position. Thus, propellants pass through the thruster only when firing. Two poppet assemblies, which are interchangeable between the Liquid-Liquid and Gas-Liquid thrusters, were also purchased. Two smaller fast response Valcor solenoid valves were employed for the igniter.

C. TEST RESULTS

1. Ignition in the Igniter Only Mode

A series of 251 tests were conducted with the prototype igniter prior to its installation into the full thruster. Rapid and repeatable ignitions

were demonstrated over the following test conditions:

Temperature at oxidizer valve	74 to 289°K (134 to 520°R)
Temperature at fuel valve	24 to 288°K (44 to 518°R)
Pressure at oxidizer valve	227 - 627 N/cm^2 (330 to 910 psia)
Pressure at fuel valve	213 - 627 N/cm^2 (309 to 910 psia)
Ambient pressure	Less than .34 N/cm^2 (0.5 psia)
Hardware temperature	83 to 294°K (150 to 530°R)

Proper ignition was demonstrated with LH_2/LO_2, GH_2/LO_2, GH_2/LO_2 + GO_2, GH_2/GO_2 at power levels at 10 mJ. Ignition was detected in the ignition chamber under all propellant supply conditions within .02 sec from the time fuel and oxidizer are sensed in the igniter manifolds. Igniter durability and cooling was demonstrated by continuous firings of up to 10 sec and pulses consisting of 20 firings in rapid succession. No cooling problems were noted.

2. Full Thruster Sea Level Tests

a. Response

A series of 66 hot fire tests with LH_2/LO_2 and 48 tests with GH_2/LO_2 were conducted. The response goal of 0.075 sec from electrical signal to 90% thrust, using nonprimed and nonconditioned hardware, was demonstrated at the design condition (P_c 500) with both the LH_2/LO_2 and the GH_2/LO_2 injectors.

Of the 0.075-sec response demonstrated, 0.050 sec was associated with electrical energization of the main valve solenoid and 0.025 sec with valve travel, ignition and thrust rise. Thrust rise, 0 to 90%, was accomplished in less than 0.01 sec when a slight oxidizer lead (.005 sec) was employed. Thrust rise rates experienced with simultaneous flow or fuel leads, as measured by the close coupled Ramapo flow meter, were in the order of .02 to .03 sec from 0 to 90% thrust.

II, C, Test Results (cont.)

A number of tests were conducted in a 50% throttled conditioned obtained by reducing the supply tank pressures. The response of the LH_2/LO_2 thruster in this mode was .090 sec from signal to 90% thrust. The response of the GH_2/LO_2 thruster was the same as the design point.

Bit impulse was found to be repeatable (±3%) at 222 N-sec. (50 lb sec) in pulse trains up to 6 pulses. First starts and subsequent restarts provided the same total impulse.

b. Stability

Both designs were found to be stable with quarter wave tube corner resonators tuned to 18,000 Hz. Throttling to 50% of the design flow was demonstrated without encountering chugging.

The LH_2/LO_2 thruster, when bombed with a 2 gr RDX charge, was found to recover from 100% over pressure in 1 millisecond.

c. Performance

Tests of each injector design were conducted on 35 and 43 cm (14 and 17 in.) L* chambers. The steady state energy release efficiency at the design mixture ratio of 4.5 is as follows:

	14 L*	17 L*
LH_2/LO_2	91%	96%
GH_2/LO_2	99%	100%

The predicted deliverable vacuum specific impulse of a 43 cm (17 in.) L* 40:1 area ratio cooled chamber is 4187 N-sec/Kg (427 lb-sec/lb) for the Liquid-Liquid System and 4246 N-sec/Kg (433 lb-sec/lb) for the Gas-Liquid System. These indicated steady state performance levels were achieved within .10 sec of main stage ignition. Performance losses prior to .10 sec include those

associated with initial feed system pressure oscillations, valve opening rates and manifold fill and chill-in rates. Pulse mode performance efficiency remained above 90% of steady state values for impulse bits down to 889 N-sec (200 lb-sec). Performance at 222 N-sec (50 lb-sec) total impulse was measured to be 75% of steady state.

d. Component Cooling

Test durations ranged from .05 sec of fire to 7.7 sec. All essential components were instrumented to determine the maximum temperatures and time required to achieve steady state thermal conditions. These measurements indicated that the Gas-Liquid and Liquid-Liquid injector faces were operating below 394°K (250°F); that the gas-side walls of the regeneratively cooled chamber were less than 589°K (600°F) and that throat nozzle cooling should not be a problem. No component overheating or damage was noted in the 114 hot fire tests conducted.

3. Cooled Chamber Tests

Ten cooled chamber tests were made with the L/L hardware and 44 tests with the G/L hardware.

a. Liquid/Liquid

(1) Heat Transfer

The coating on the columbium chamber was eroded on the ninth test and a burn through of the chamber occurred on the tenth test. The erosion was the result of high temperature injector induced heat streaks.

II, C, Test Results (cont.)

The heat streaks were not discovered during sea level testing because they were mitigated by the high thermal conductivity of the copper workhorse chambers used for sea level testing. Although thermocouples were not located in the worst streaks recovery temperatures of ∿1420°K (2100°F) were measured with the columbium chamber as opposed to a recovery temperature of 1090°K (1500°F) inferred from the sea level testing.

(2) Performance

The delivered vacuum specific impulse was 4178 - 4187 N-sec/Kg (426 - 427 lb_f-sec/lb_m) with the cooled chamber in good agreement with the performance prediction extrapolated from the sea level test results.

b. Gas/Liquid

(1) Heat Transfer

The fuel film coolant (ffc) flow rate to the nozzle was reduced in four steps from approximately 37% to 18% of the fuel flow. With ∿18% ffc and steady state operation, the throat temperature was 887°K (1100°F) and the maximum extrapolated steady state skirt temperature was 1200°K (1700°F). Further reduction in the coolant flow rate is possible based on a 1144°K (1600°F) operating limit for the throat and a 1422°K (2100°F) operating limit for the skirt.

Fuel inlet temperatures were varied from 35.6°K (64°R) to approximately 111°K (200°R). This overlap into the Liquid/Liquid operating range did not adversely affect operation of the regen cooled section or dump cooled section.

II, C, Test Results (cont.)

The pulse mode of operation was demonstrated over a wide range of pressure, mixture ratio, and fuel inlet temperature conditions. Duty cycle effects were investigated. A total of 417 firings were made. A worst case duty cycle (30 to 40% on time) was found that resulted in higher throat temperatures than achieved with steady state operation.

(2) Performance

Steady state delivered vacuum specific impulse of 4266 N-sec/Kg (435 lb_f-sec/lb_m) was demonstrated with 18% fuel film cooling. A minimum repeatable bit impulse of 196 N-sec (44 lb_f-sec) was demonstrated and a 245 N-sec (55 lb_f-sec) bit impulse with a 3986 N-sec/Kg (406.5 lb_f-sec/lb_m) performance.

III. CONCLUSIONS AND RECOMMENDATIONS

The experimental data acquired to date has demonstrated that pulsing HO cryogenic thrusters in 2669-5560 N (600-1250 lb_f) thrust class at 172-344 N/cm^2 (250-500 psia) are viable candidates for space shuttle and tug engine systems. The designs which have been successfully tested demonstrate a 0.075 sec response from signal to 90% thrust, do not require prechilling prior to firing, are thermally isolated from the valve and thus do not represent a significant heat leak into the propellant feed system. The data show that ignition is rapid and repeatable, bit impulse is repeatable within $\pm$3% down to 222 N-sec (50 lb-sec). Lower impulses have not been explored but are possible with the full thruster. Operation in the igniter only mode, which is effectively a 222 N (50 lb_f) thruster, could, with further development, lead to repeatable, high performance impulses down to 5 lb_f sec.

The injector patterns and element quantity were selected on the basis of analyses and data reported in literature, without the benefit of single element

cold flow or subscale experimentation specific to operating conditions and propellants. Nonetheless, the performance realized is quite respectable. Further activities in the optimization of the Liquid-Liquid injector pattern could result in a 1 to 2% improvement in delivered performance.

Accurate measurement of performance in short pulses is limited by (1) accuracy of available fast responding cryogenic propellant flow measuring devices, (2) the ability to close couple flow meters and thrusters without influencing thrust measurement, and (3) heat leaks from the test stand to the feed system. Additional work and testing is required in order to assess the true bit specific impulse capabilities of the design being tested.

The erosion of the columbium chamber was caused by injector heat streaks. The streaking could be mitigated by modification of the liquid/liquid injector pattern. This would involve rearranging the elements to eliminate areas of low mass injection and/or increasing the size of the outboard fuel elements. It is seldom with doublet elements that compatibility is achieved with the first injector, as mentioned above, without the benefit of single element cold flow, subscale experimentation or full scale cold flow experiments to measure mass and mixture ratio distribution.

The operation of the Gas/Liquid cooled chamber with hydrogen inlet temperatures as low as 35.5°K (64°R) is a considerable accomplishment and suggests that this concept has application over a wide range of propellant temperatures, and therefore, separate designs for liquid/liquid and gas/liquid operation may not be required. This concept has been tested with hydrogen inlet temperatures ranging from 35.5°K (64°R) (this program) to 333°K (600°R) (Ref. 5).

III, Conclusions and Recommendations (cont.)

Useful follow-on activities would include:

(1) Further optimization of the dual wall manifolding concept including manifold limit and life cycle durability testing.

(2) Design development of an integrated flightweight thruster assembly including flightweight valves.

(3) Life and durability testing of the flightweight design.

(4) Demonstration of a complete propulsion system including pump, high pressure run tanks, lines and thrusters at simulated vacuum conditions.

(5) Development and life test demonstration of a small (10-100 lb_f) universal HO thruster which can serve as a standard shuttle ignition system and/or Vernier engine.

(6) Optimize the liquid/liquid injector pattern to mitigate the heat streaking to the point where it is compatible with a columbium chamber.

(7) Investigate the applicability of the gas/liquid design to liquid/liquid operation.

IV. FEASIBILITY ANALYSES AND CONCEPTUAL DESIGN

A. OVERALL THRUSTER THERMAL MANAGEMENT AND CONFIGURATION

The overall thermal management problem associated with an all cryogenic hydrogen/oxygen pulsing thruster is one of great complexity and "thermal conflict", namely, the fuel is cold enough to freeze ($\simeq$ 100°R) the oxidizer, the oxidizer is warm enough to "boil" ($\simeq$ 55°R) the fuel, and the thruster itself is normally warm enough (540°R) to "boil" both propellants. The result of large and unexpected thermally-induced propellant density changes for any sustained period of time can be a loss of flow control in terms of both flow rate and mixture ratio distribution. Poor propellant flow control can be detrimental to the thruster operation in several ways:

IV, A, Overall Thruster Thermal Management and Configuration (cont.)

a. Poor pulse repeatability due to nonreproducible startup and shutdown transients.

b. Erratic ignition resulting from uncontrolled local and overall mixture ratios at startup.

c. Low pulse specific impulse from nonuniform manifold filling and venting processes.

d. Local overheating and possible failure from excessive local mixture ratios due to oxygen boiling or freezing in one part of the injector which forces an excess of oxygen out of another part.

Satisfactory theoretical solutions to these problems were found by (1) controlling the thermal energy within the thruster in both steady state and transient operation, and (2) controlling the rate at which the energy in the hardware is transferred to the propellants during thruster startup and steady state operation. The generation of fabricable and durable designs which could fulfill the requirements of the analytical solutions was a second activity which paralleled and directed, but was not permitted to restrict the analytical design processes.

Many candidate injector/thruster concepts were evaluated. Several typical concepts are shown in Figure 4. In Figure 4a, propellant is injected as received from the feed lines. In Figures 4b-c, propellants are changed from a liquid to gas by using the heat rejected through a full or partial regeneratively cooled thrust chamber during steady state operation. An energy balance showed there was sufficient heat to provide full gasification of both propellants. Residual (sink) energy in such a thruster could be utilized during start transients.

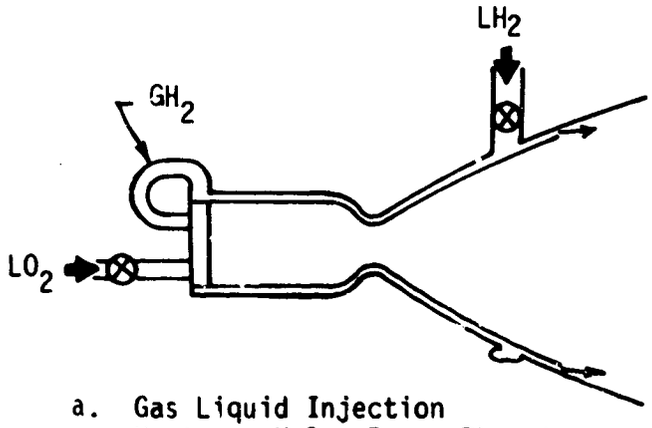

a. Gas Liquid Injection
Upstream Valve Regen Throat

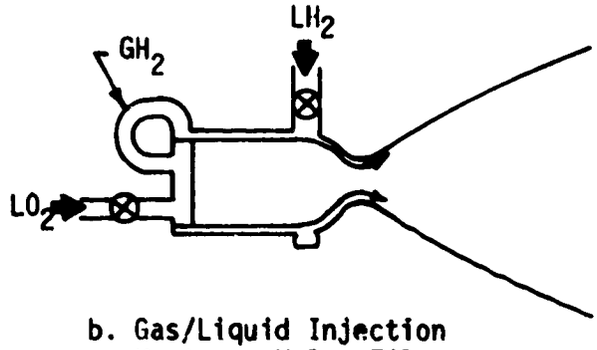

b. Gas/Liquid Injection
Upstream Valve Film
Cooled Throat

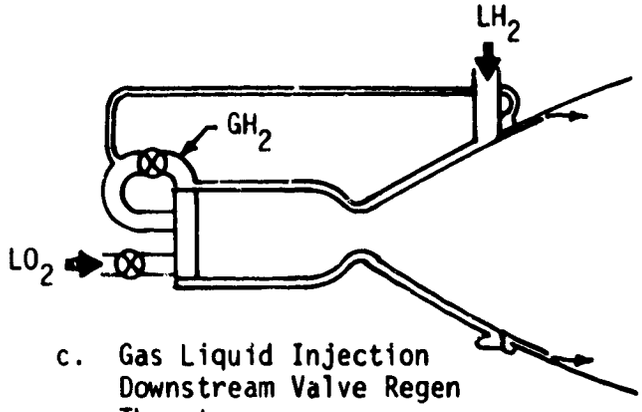

c. Gas Liquid Injection
Downstream Valve Regen
Throat

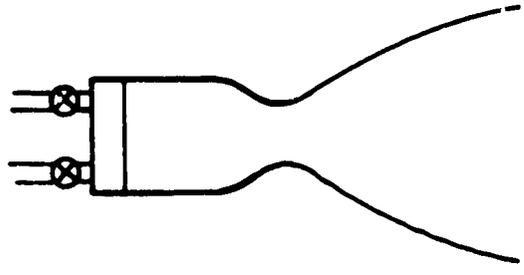

d. Liquid/Liquid
Injection Film Cooled
Chamber

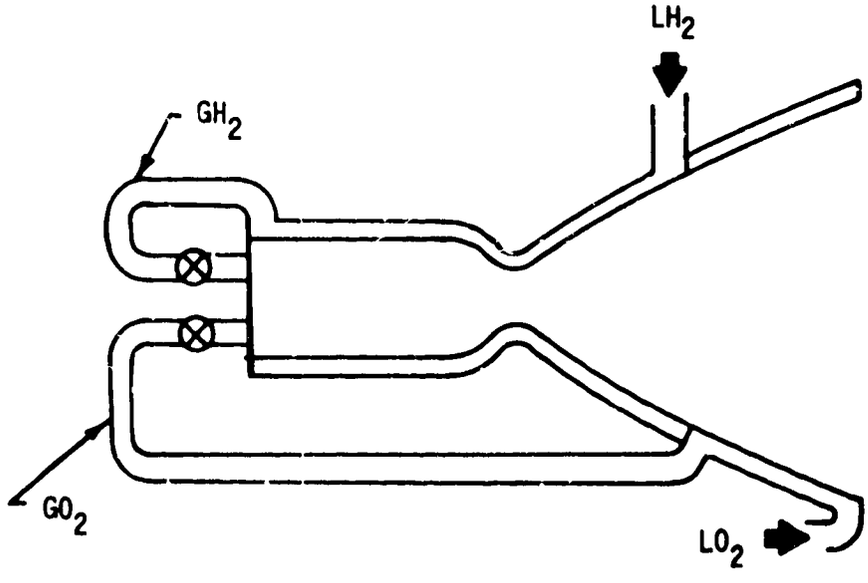

e. Gas/Gas Injection
Oxygen Regeneratively Cooled Skirt

Figure 4. Candidate Propellant Thermal Management Concepts

IV, A, Overall Thruster Thermal Management and Configuration (cont.)

Other evaluations included propellant valves located upstream and downstream of the cooling jackets and the use of interpropellant heat exchangers integral to or separate from the injector.

The results of all these analyses clearly indicated that liquid phase oxidizer injection was most desirable. The task of maintaining the oxygen in a high density liquid phase was less difficult than that of the 25°K fuel (45°R). It was also determined that the volume and heat transfer surface of the oxidizer manifold had to be minimized in order to produce acceptable pulsing characteristics over a wide range of inlet temperatures. Analyses showed oxidizer dribble volumes to be more critical than fuel and limited to 5 to 7 cc (0.3 to 0.4 cu in.) if the pulsing performance goals of Table I were to be achieved. Since the fuel dribble volume requirements were less critical ($\approx$ 3 cc (1 cu/in.) for LH_2 and 6-12 cc (5-10 $in.^3$) for GH_2) due to the low fuel density and high performance of a fuel rich blowdown, there was little need to locate a fuel valve downstream from a cooling jacket.*

The use of a regeneratively cooled chamber between the valve and injector made predicting the density of the fuel at the injector (with liquid at the valve) very difficult during transients and in pulsing. The simplest, lightest weight thruster concept was determined to be the LH_2/LO_2 injection scheme in which both propellants are supplied directly to the injector from the feed system. Direct injection in conjunction with a simple film cooled chamber, Figure 4a, provides the required volume-surface relations and reasonable performance and design margins. If 83°K (150°R) GH_2 is delivered to the valve, the density change is reduced sufficiently to allow consideration of full or partial

*A valve located downstream of a chamber cooling jacket is not desirable because the jacket is always under pressure and even a small chamber crack could result in loss of large quantity of propellants if undetected.

regenerative cooling. Fill time and residual volume effects with GH_2 were found to be small. Chamber cooling is dictated by the life cycle requirements and limitations imposed by re-entry heating. This precludes the use of copper for regenerative cooling (Reference 5) at and downstream of the throat and leads to the selection of the chamber cooling system shown in Figure 4b for design point 2.

Further analyses showed that the state of the propellant to the igniter could not be guaranteed because of the low flow rates and wide range of duty cycles. Thus, an igniter design which could operate in the L/L, G/L, or G/G mode was required.

Thermal analyses of the thruster-vehicle-feed line interface showed that refrigeration of the entire thruster for good pulsing response would result in heat inputs to the propellant feed system which were completed unacceptable[2,3] even with the best available insulation surrounding the thruster. Thus, it was necessary to limit or even eliminate, if possible, the need for prefire hardware thermal conditioning.

The two concepts investigated in detail during the feasibility studies are shown schematically in Figure 5a and b. The first approach (left) maintains only the valves, injector manifolding and igniter at cryogenic temperature such that only the most essential components are primed to fire at all times. The temperature conditioning is obtained by low velocity recirculation of propellants through the feed system. Each valve and manifold are integral to maintain low volume and are thermally isolated from both the surrounding structure and the injector face and combustion chamber to as large an extent as possible. Propellant is ducted from the manifold to the face and injector orifices through a series of long thin wall tubes which, in addition to allowing rapid starts, also limit heat flow when the engine is not in use. An actual

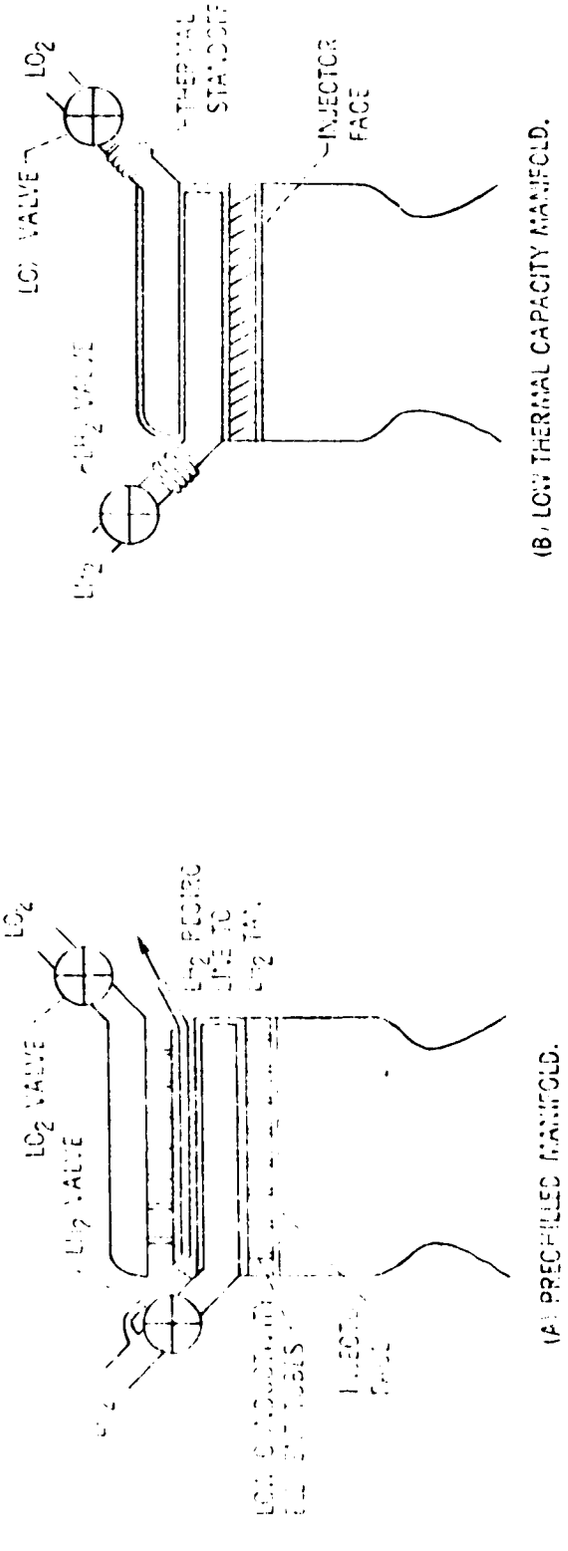

Figure 5. Thermal Management Concepts Investigated

design of this type is shown in Figure 6. The requirements for low volume (few short tubes), thermal insulation (few long tubes) and high performance and good compatibility (many short tubes) were in direct opposition as illustrated in Figure 7 and compromises had to be made. Heat leaks of 7 to 14 W (25 to 50 Btu/hr) are at least an order of magnitude greater than those found acceptable in the systems study of References 1 and 2.

The second approach which was analytically evaluated (Figure 5 (right)) employs a more efficient thermal standoff between the valve and thruster such that propellant can be bled up to the valve without cooling the injector or the thruster. This design concept was predicted to result in poorer start and pulse characteristics than the primed design because of the period required to cool the manifolding. It does, however, reduce the heat leak to the propellant feed system for the same manifold volume to approximately 0.6 W (2 Btu/hr) which is compatible with the feed system requirements of References 1 and 2. In order to obtain a fast and repeatable starting characteristic from a non-primed design with liquid propellants, it was deemed necessary to accelerate the chill-in and at the same time, limit the heat input to the propellant. This can be accomplished by constructing the propellant flow passages of a thermally insulating material, Curve a, Figure 8, or a structure having a very low heat capacity as shown in Curves b & e, Figure 8. Both approaches accelerate the manifold surface chilldown period and allow the propellant-hardware thermal transients to be completed rapidly as compared to conventionally constructed manifolds, Curves c and d. The low heat capacity approach was considered superior to the insulating approach because it allowed reliable all metal construction. The mechanical and adhesive properties of non-metallic insulators are generally poor and not as reliable at cryogenic temperatures.

A series of engine simulation analyses such as shown in Figure 9, were conducted for conventional, primed, and low thermal capacity manifolds corresponding to Design Points 1 and 2 of Table I. Analytical variables

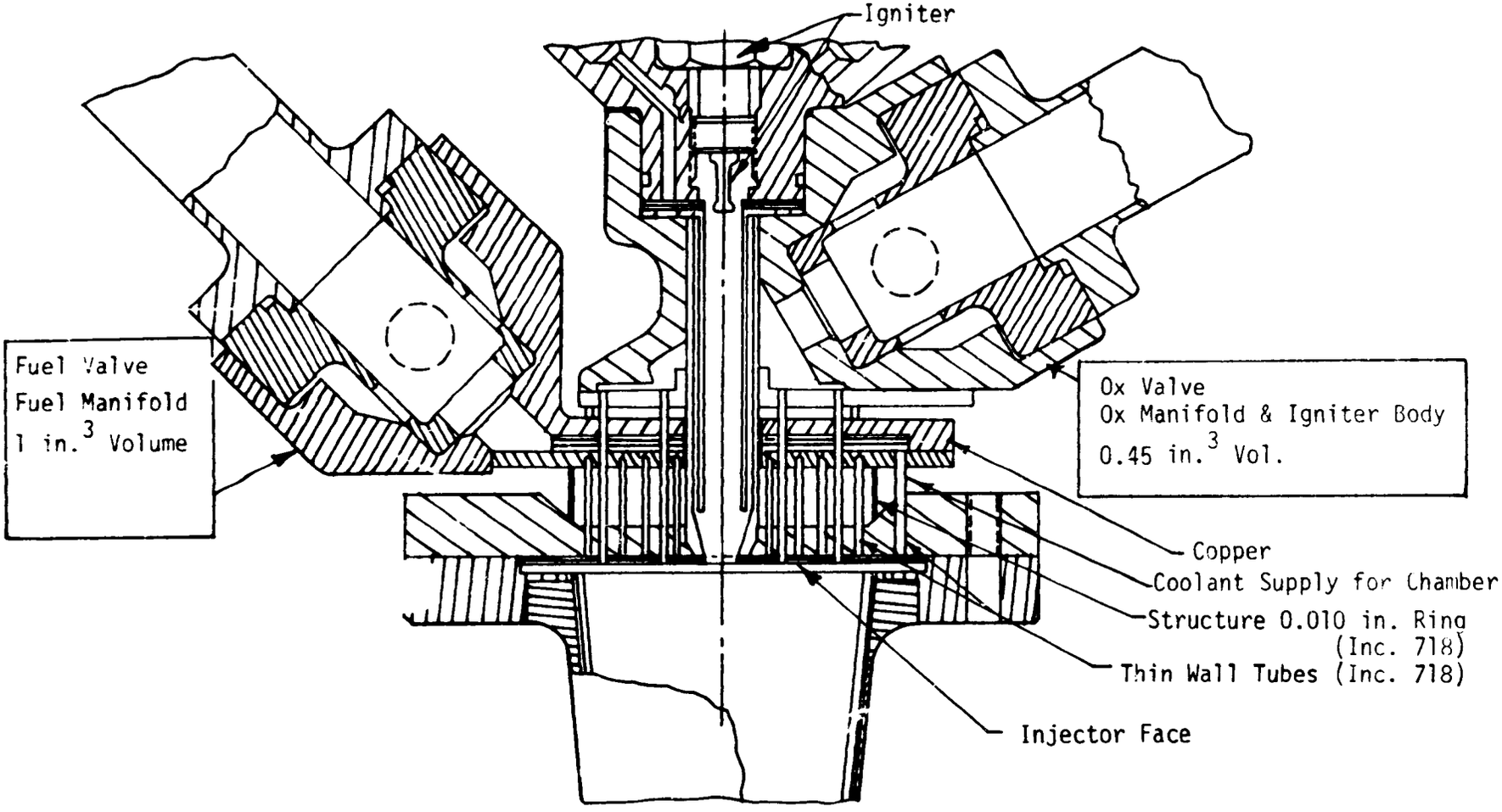

Figure 6. Thermally Isolated Manifold Prechilled Injector

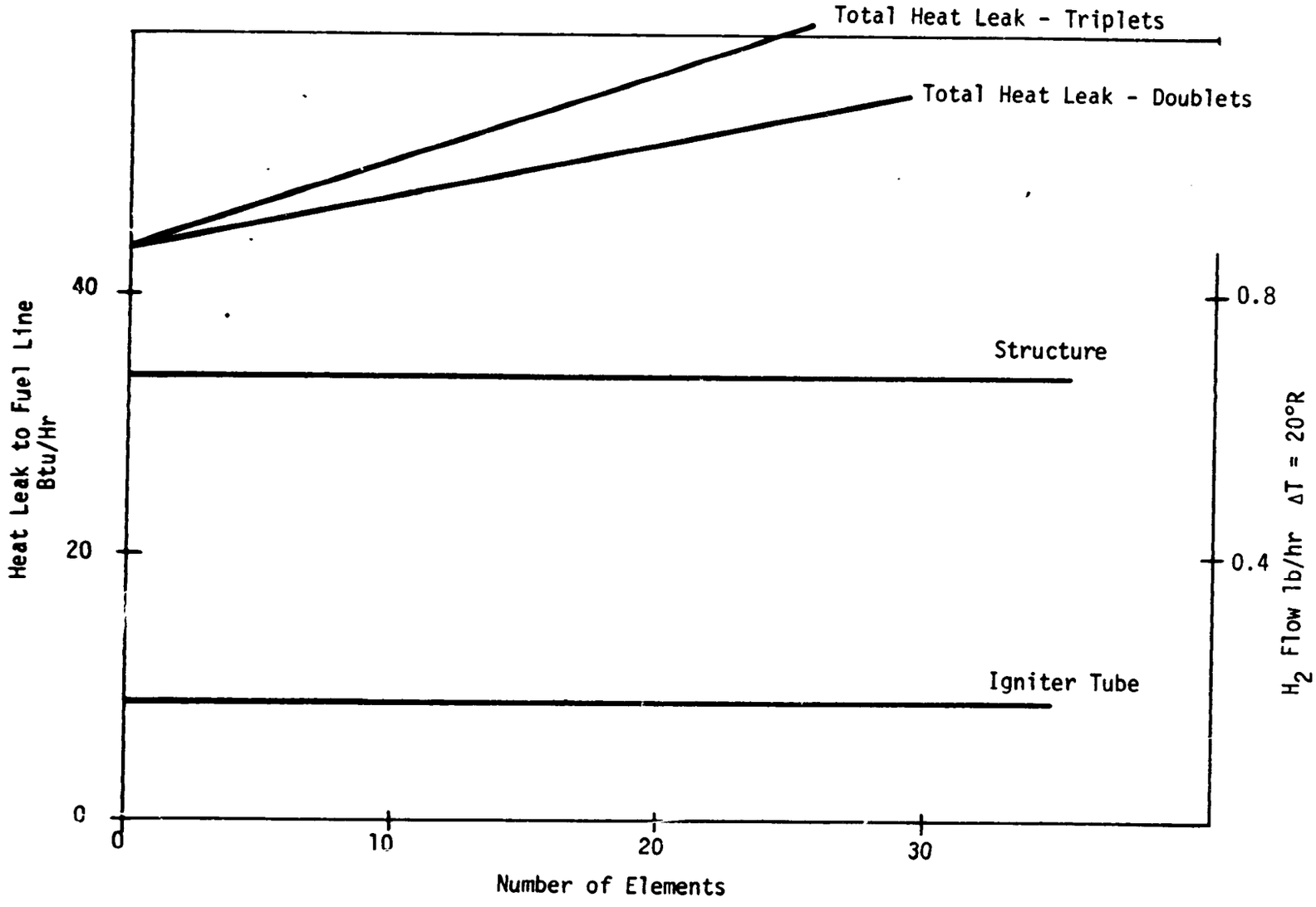

Figure 7. Feed System Heat Leak for Prechilled Injector

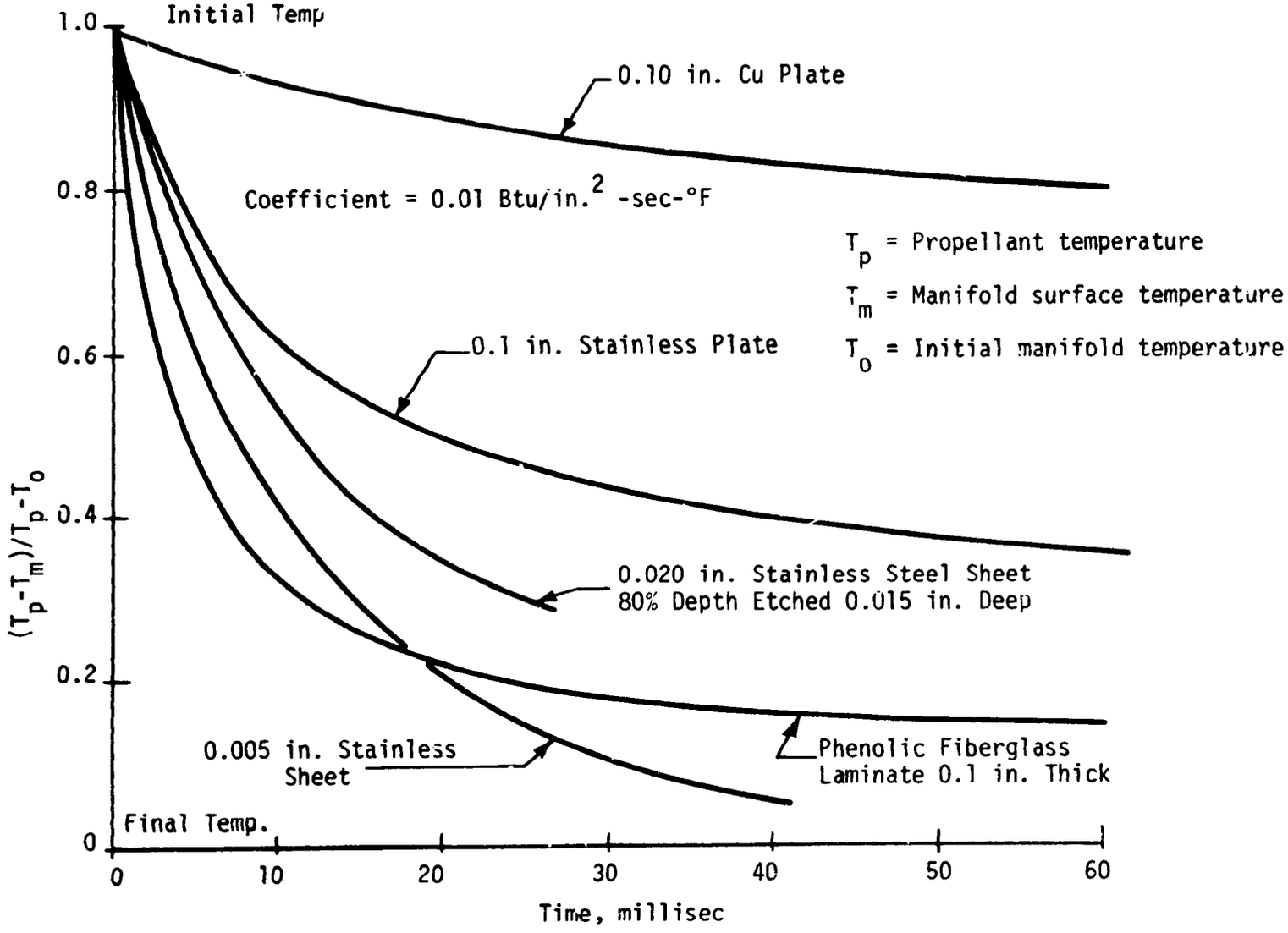

Figure 8. Manifold Cool Down Times

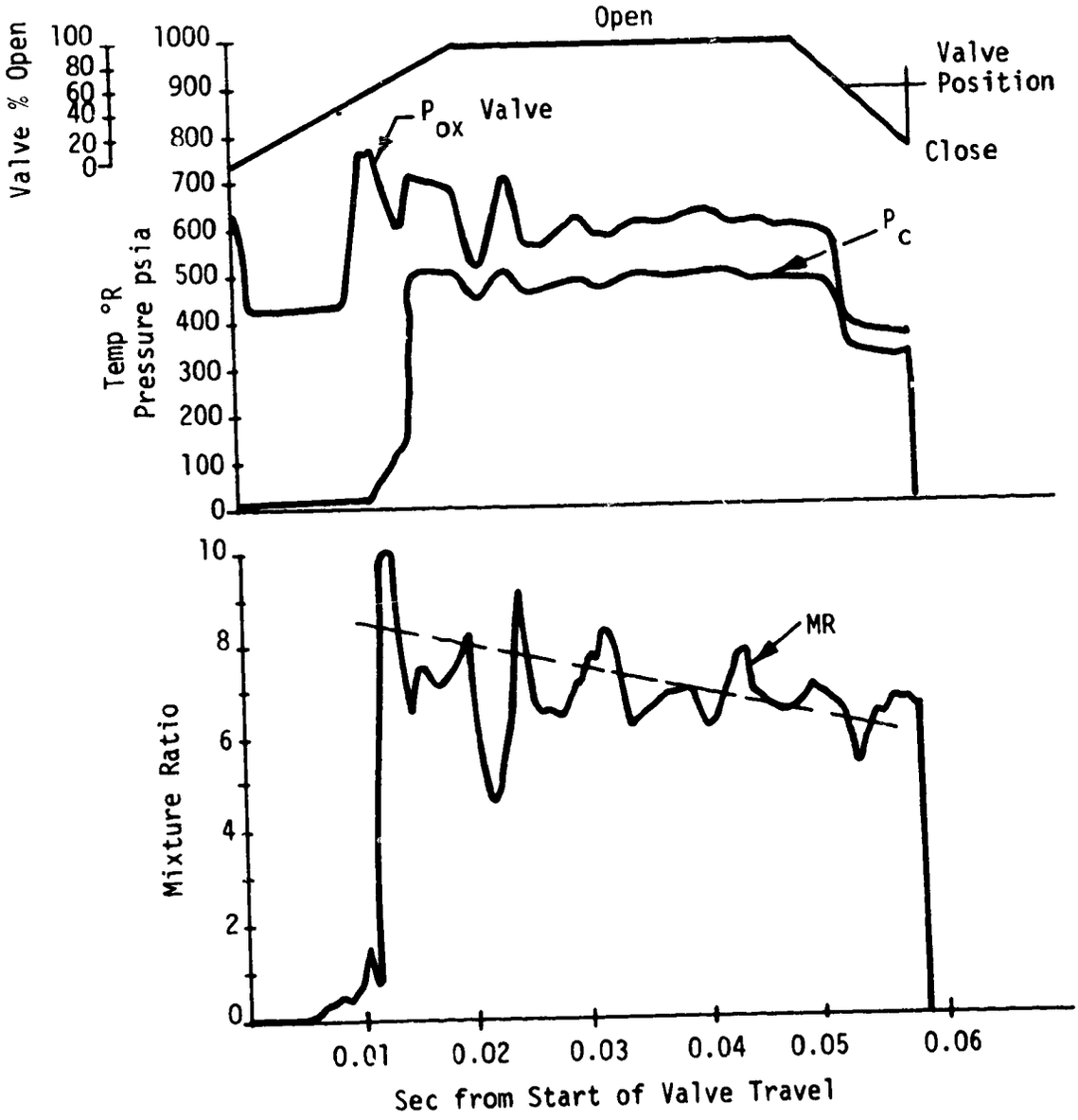

Figure 9. Typical Engine Simulation Analysis Predicted 50 lbF Sec (222 N-S) L/L Pulse

included manifold volume and surface, number of injection elements, valve sequencing and timing and propellant supply temperatures and pressures. The 222 N-sec (50 lb_f sec) pulse shown in Figure 9 corresponds to a nominal 345 N/cm^2 (500 psia) firing with LH_2/LO_2 propellants in a low thermal capacity injector design. Manifold fill, ignition and P_c rise are predicted to be rapid 0.016 sec from start of lagging valve travel. The MR is noted to have two transients which influence pulsing performance. One is oscillatory and follows the perturbation of the feed system caused by the rapid valve openings. The other is an overall decreasing value (shown dashed) and is caused by heat addition to the propellants in the manifolding. The heat addition has more of an influence on the LH_2, thus, resulting in a higher than nominal MR during the early portion of the pulse. The MR is predicted to approach the nominal core value about .06 sec following the start of valve travel.

Comparisons of the resulting "DC" portion of the MR shift at .03 sec following 90% P_c for the candidate manifolding concepts is shown in Figure 10. The larger quantity of elements and/or number of orifices results in additional surfaces to be cooled and, thus, a greater shift in early time MR. The influence of element type is also indicated. The performance penalty for the low capacity design was predicted to be small compared to the losses resulting if the propellant needed for continuous cooling were charged against a single pulse.

B. INJECTOR/MANIFOLDING DESIGN CONCEPTS AND SUPPORTING EXPERIMENTS

Several baseline injector concepts, Figures 2 and 6, were configured to match the analytically required thermal and hydraulic characteristics. Each design was evaluated for fabricability and using engine simulation model which computed the startup, ignition as well as shutdown transients as shown in Figure 9. The results of the feasibility analyses indicated the desired thermal objectives could be achieved by either of three basic design approaches: (a)

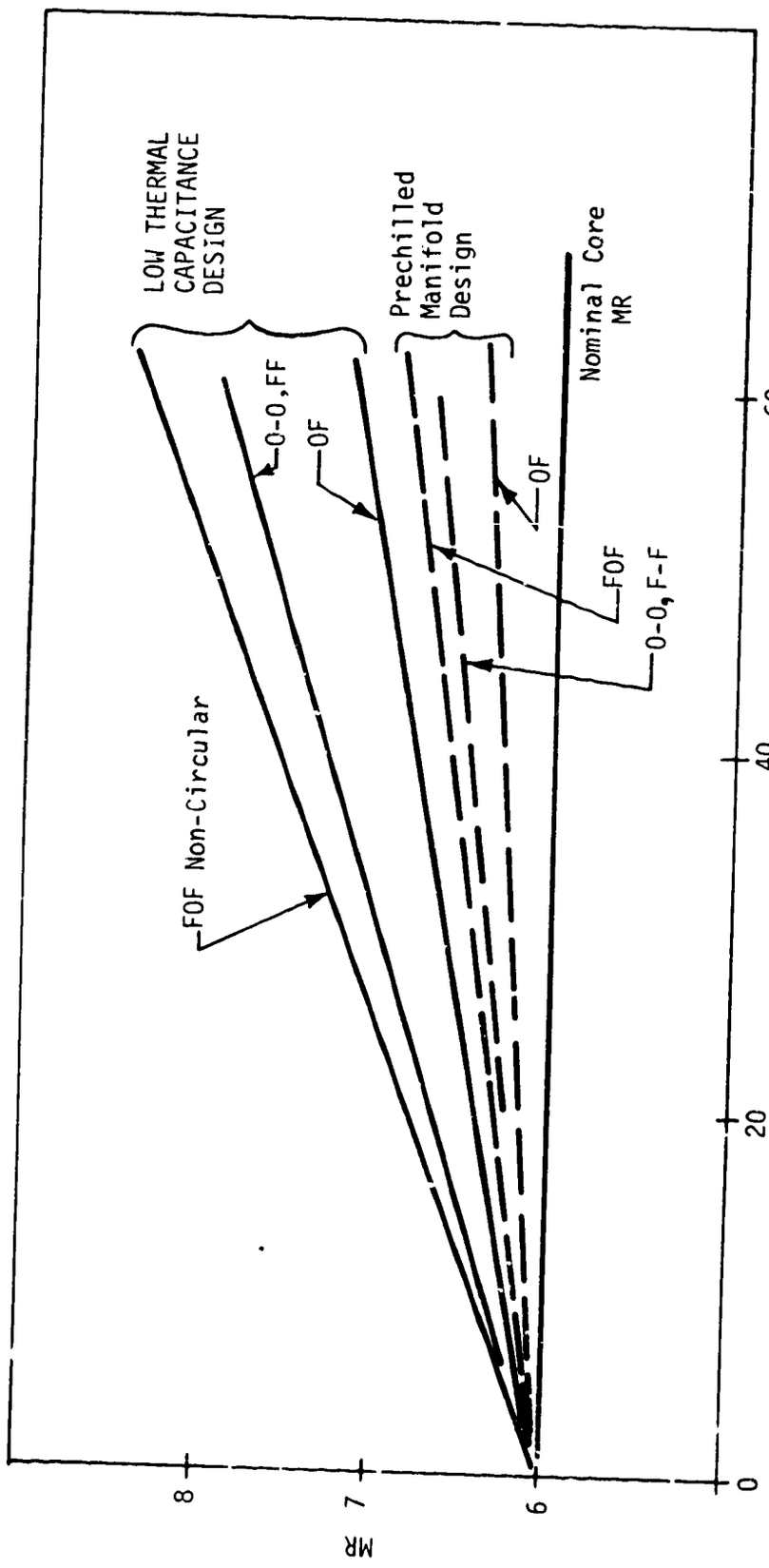

Figure 10. LH_2/LO_2 Pulsing MR Shift, Core MR 0.03 sec from 90% P_c

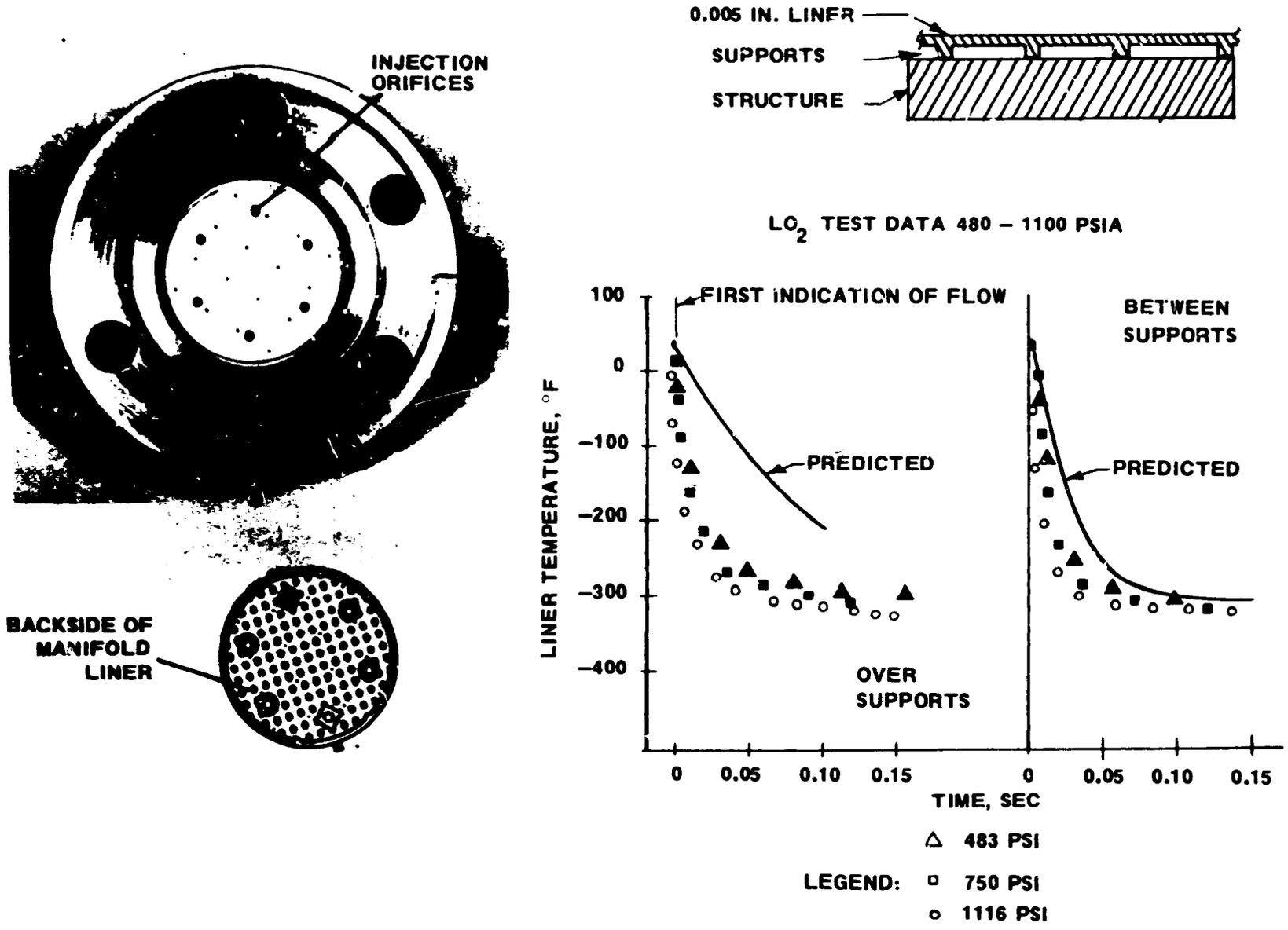

Figure 11. Dual Wall Manifolding Schematic

conventionally constructed and manifolded designs preprimed to allow rapid response, (b) a low thermal capacitance design which does not require temperature conditioning and which is fabricated from thin walled tubular, platelet or honeycombed materials, or (3) an insulated manifold design using materials having very low thermal conductivities. The last was rejected for fabrication and reliability reasons.

Small-scale injector body chilldown experiments were conducted in support of the above thermally isolated manifold and low thermal capacity manifold design analyses. The former employed long L/D, 0.015 cm (0.006-in.) wall stainless steel tubing for a major portion of the injector element, simulating the design shown in Figure 6. The relative tube length and volume was typical of the cooled manifold/warm face design. The latter employed a locally supported 0.013 cm (0.005-in.) thick chemically etched stainless steel manifold liner corresponding to Curve "e" in Figure 8 and shown in Figure 11. The support spacing and diameter was determined from a structural analysis for a design pressure of 690 N/cm^2 (1000 psi). The required forming and brazing processes were demonstrated to be practical in both cases. The tube, however, required careful handling in order to avoid bending and subsequent buckling.

Laboratory experiments conducted with tubing demonstrated that the complete thermal chilldown transient could be accomplished in less than 0.030 sec when the tube, initially at ambient temperature, was subjected to a sudden flow of LO_2 at a supply pressure greater than 138 N/cm^2 (200 psia). Figure 11 illustrates the dual wall manifolding chilldown test results where the initially ambient temperature dual wall manifold is exposed to sudden flows of LO_2 at pressures of 333, 516, and 769 N/cm^2 (483, 750 and 1116 psi). These tests demonstrated the structural durability of the approach and showed that the actual chilldown rates met and exceeded the predicted values. Manifold surface temperatures reached the LO_2 liquidus temperature within 0.020 sec from

first indication of propellant flow. The photoetched liners, which were bonded to the support structures, also proved to be much more durable than the tubing of approximately the same thickness.

The more favorable feed system heat leak and structural characteristics of the dual wall manifold resulted in a decision to employ this concept in the full-scale injector designs.

C. OTHER INJECTOR DESIGN CONSIDERATIONS

1. Injection Element Type and Quantity

Injector element types analyzed included H-O-H noncircular orifice triplets, a coaxial and like-doublet elements. Each of these elements were deemed to be good compromises between performance, chamber wall compatibility and injector face heat flux levels. The four main requirements dominating selection were:

1. Stable combustion.
2. Low face heat flux.
3. Chamber wall compatibility.
4. Reasonable steady state performance.

a. LH_2 Injection

For LH_2 injection, elements having low thermal contact area with the propellants were more desirable. The tendency to shift the pulsing MR to a more oxidizer rich condition or leak energy back into the feed system, depending upon the design, increased with the number of elements as shown in Figures 7 and 10. For LH_2, the non-circular triplet and coaxial tube element were less favorable than the circular doublet because they maximized the warm surface to flow area of the fuel circuit, giving a greater tendency to thermally choke. The quantity of coaxial tube elements which could be utilized with LH_2 was limited, for fabrication reasons, to 15. This

is due to the small annular gap size which resulted from the required high fuel/oxidizer injection velocity ratios for this shear mixing element. The annulus size for as few as 15 elements was about 0.018 cm (0.007 in.) and considered very difficult to control in fabrication. The selected 24 element like-on-like doublet pattern is shown in Figure 12. The outer row consists of 16 fuel pairs oriented 15 degrees to the chamber wall. Successive inner rows consisted of 16 ox pairs, 8 fuel pairs, and 8 ox pairs. The 15 degree element orientation and placement of fuel in the outer row was for maximum chamber wall compatibility based on the data of Reference 6. The inner row of oxidizer elements was highly desirable for augmenting the central igniter which normally would run fuel rich.

b. GH_2 Injection

The lower GH_2 fuel density allowed much larger fuel injection orifice areas to be employed and eliminated the thermal choking problem. The coaxial tube design was selected for GH_2/LO_2 application because of the outstandingly successful history of this element in each of the four areas governing the evaluation. The quantity of elements selected was based on face cooling requirements and the use of standard sizes of small diameter thin wall Ni tubing. The selected design shown in Figure 13 contains 36 elements uniformly distributed over the face in 3 equally spaced rows. The resulting fuel annulus which provided an H/O injection velocity ratio of 12 was 0.043 cm (0.017 in.). An oxidizer tube tip recess of 1 tube diameter, 0.163 cm (0.064 in.) was based on the data of Reference 7.

2. Injector Face Cooling

The major factor in face cooling is the selection of an injection pattern which recirculates unburned, relatively cool propellants. Each of the elements discussed earlier was configured to insure a fuel rich environment near the injector face. In the selected LH_2/LO_2 (O-O, F-f) doublet element, for example, long oxidizer and short fuel impingement lengths were employed. In

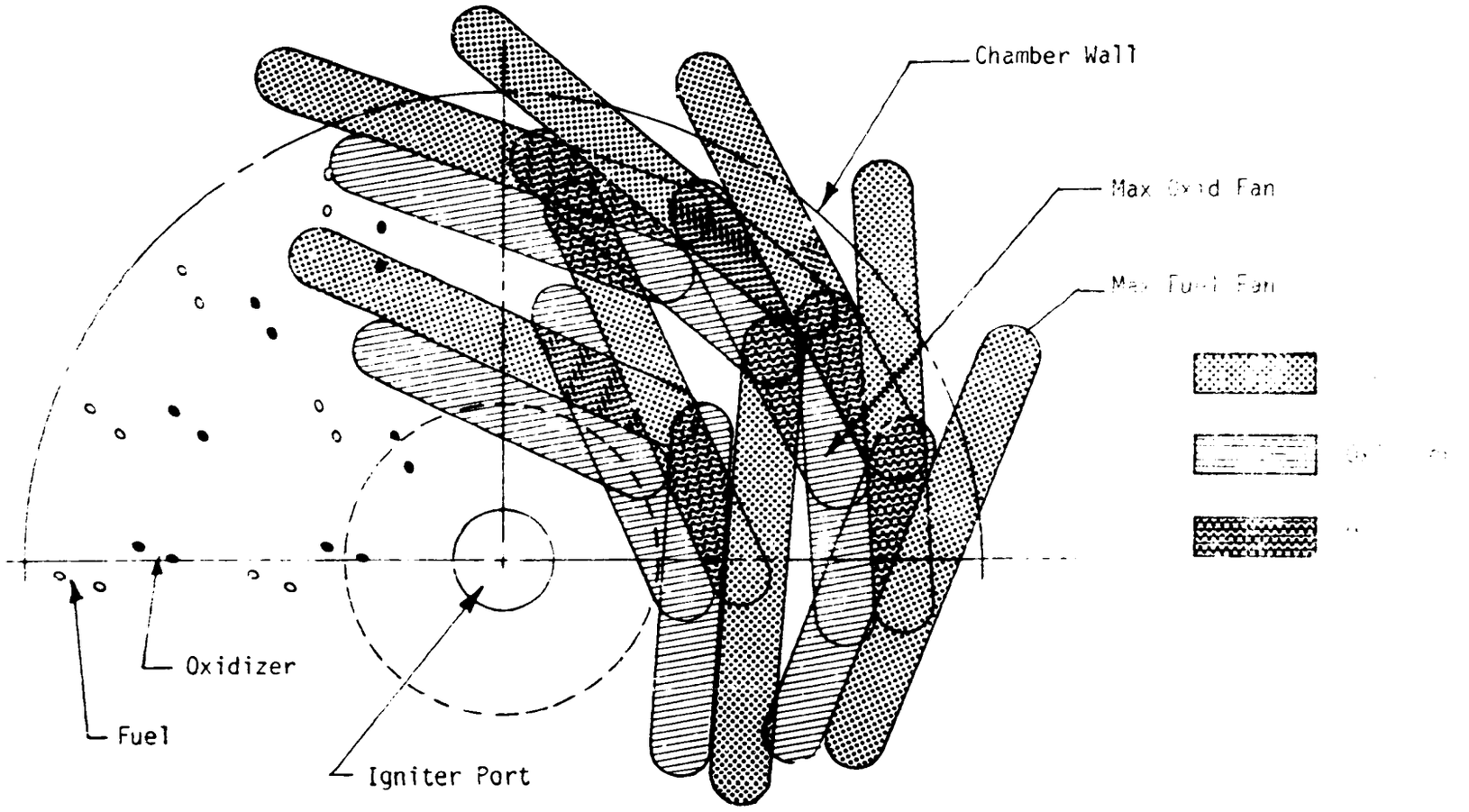

Figure 12. Doublet Element Injection Pattern and Predicted Fan Spray Characteristics

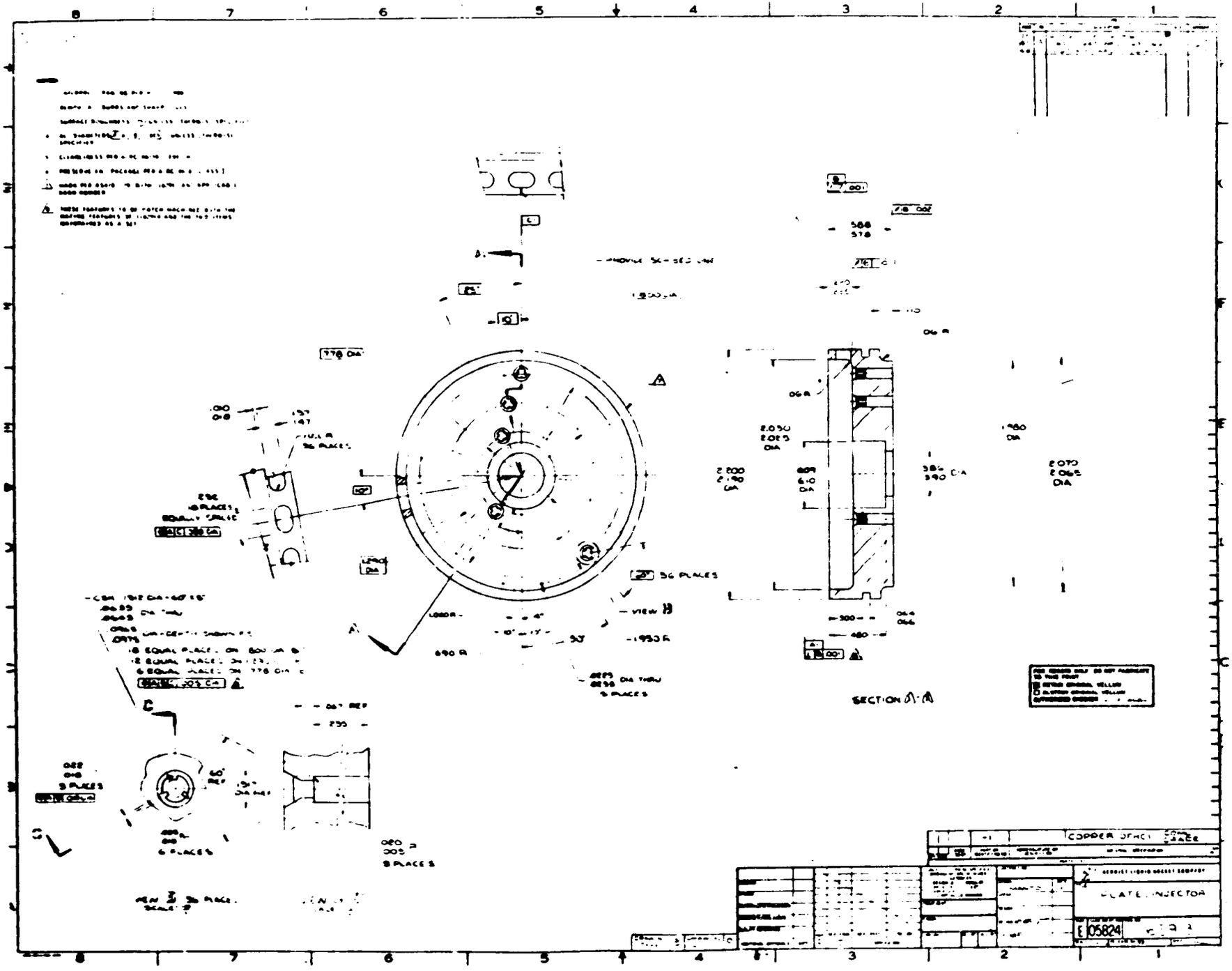

Figure 13. G/L Coaxial Injector Face Plate

addition, an actively (dump) cooled circuit which utilized 7% of the fuel was incorporated within the injector design to preclude heat penetration to the manifolds during periods of sustained firing. This circuit positioned between the combustion gases and the propellant injection orifices is described in detail in a later section.

In the GH_2/LO_2 co-axial element, the oxidizer leaving the injector was completely surrounded by fuel. The fuel discharging through a copper face at high velocity also provided regenerative cooling capacity as shown in Figure 14. The level of face cooling necessary was obtained by proper selection of face thickness and element quantity using the equations provided in Reference 5.

3. Stability (High Frequency)

A full combustion stability analysis was undertaken and the most likely modes of instability identified as follows:

Mode	(KHZ)	Comments
1-L	6	Nozzle damping
2-L	12	
1-T	16	Resonator
1-T + 1-L	17	
2T	27	Frequency too high
1R	33	Frequency too high

The 1-L mode was not considered significant because it could easily be eliminated by proper selection of chamber length. The 1-T and 1-T + 1R modes were thought to be both most likely to occur and potentially most destructive. The energy level of higher modes was considered to be small. Helmholtz and 1/4 wave tube resonators tuned to attenuate the 1-T and 1-T + 1R modes were evaluated. A 1/4 wave tube corner cavity providing an effective area equal to 20% of the injector face area, as shown in Figure 15, was incorporated into the necessary provisions for cooling the cavity.

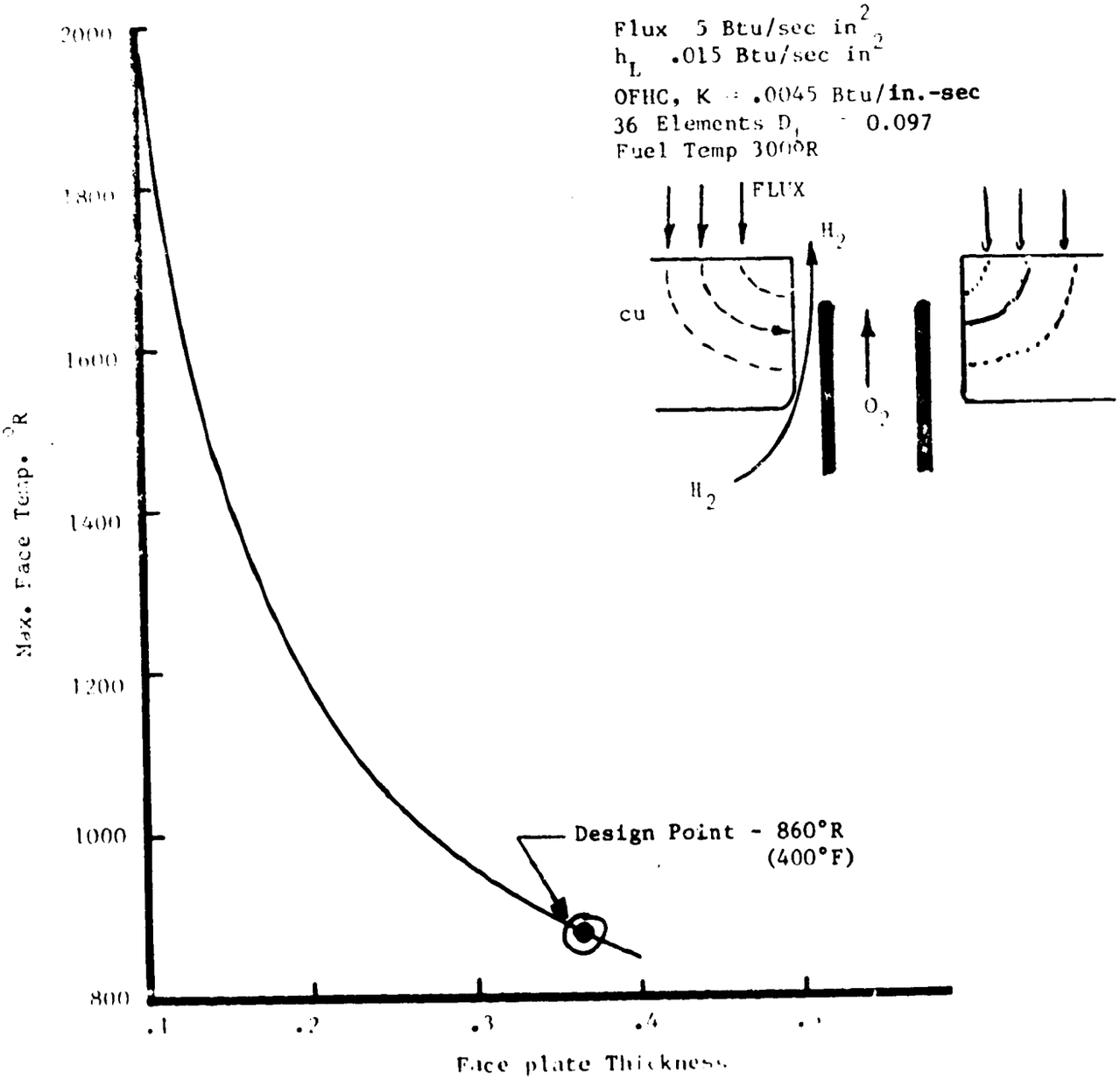

Figure 14. Element Coaxial Injector Face Temperature

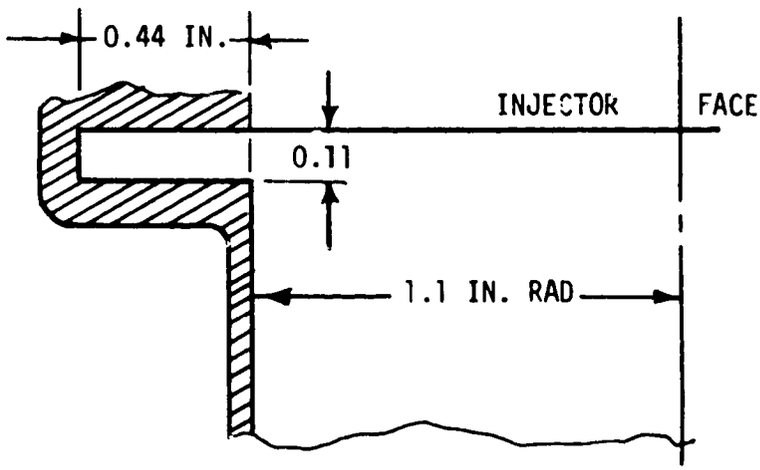

QUARTER WAVE TUBE

20% OPENING f_{1T} 16,000 Hz

$\overset{*}{V}$ = 2500 fPS

Figure 15. Resonator Cavity Design for LH_2/LO_2 and GH_2/LO_2 Injector

IV, C, Other Injector Design Considerations (cont.)

4. Stability (Chugging)

The low frequency chugging modes were evaluated via a conventional double dead time analysis by assuming an appropriate range of values for vaporization and mixing times. The pressure drops for each of the injection elements were selected on the basis of these results which are shown in Figure 16. The selected oxidizer $\Delta P/P_c$ was 0.27 based on a chamber pressure of 34.5 N/cm^2 (50 psia). The fuel $\Delta P/P_c$ was 0.20 for LH_2 and 0.09 for the GH_2 injector design.

D. IGNITION SYSTEM ANALYSIS AND DESIGN CONSIDERATIONS

Igniter design considerations included energy level requirements, propellant flow requirements and mixture ratios, ignition source (spark plug or other energy sources), propellant inlet sequencing, overall total ignition energy requirements (torch vs other igniter approaches) and inlet temperature and chamber pressure limitations.

Preliminary ignition system analyses indicated that it would be extremely difficult to control the density of the small quantities of propellant reaching any igniter design concept and it would be necessary to develop an igniter which could perform its function almost independent of the physical state or quantity of the propellants being supplied to the unit. Two criteria were set for igniter design. The first is that the mixture ratio in the spark zone should be centered in the broadest band of the H-O ignitability range. As shown in Figure 17, this corresponds to a MR range about 8-50. Igniter cooling considerations make operating near stoichiometric conditions undesirable, giving a desired MR range of about 40-50. The second criterion is that the total energy level of the igniter torch should be sufficiently high even in a low flow vapor locked condition to insure reliable ignition of liquid phase main stage propellants. Additional gas residence time-quenching analyses indicated the use of 3.5% of the total flow for the igniter would provide an order of magnitude safety factor.

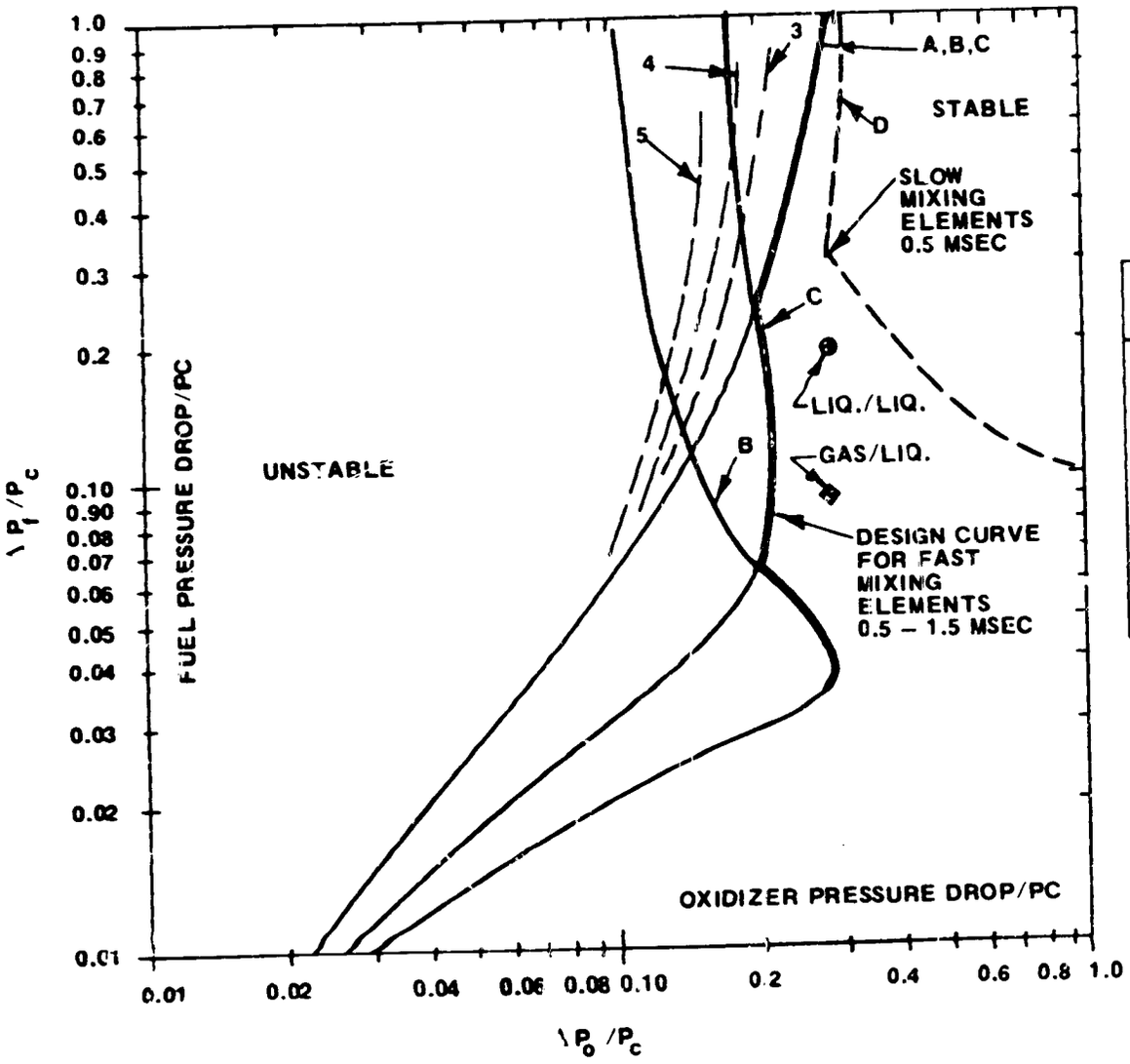

LEGEND	MIX TIME	OXID. VAP.	FUEL VAP.
A	0.05	1.0	0.000
B	0.05	1.0	0.050
C	0.15	1.0	0.000
D	0.5	1.0	0.000
3	0.05	0.5	0.0
4	0.05	0.5	0.0
5	0.05	0.5	0.0

Figure 16. Double Dead Band Chugging Analysis

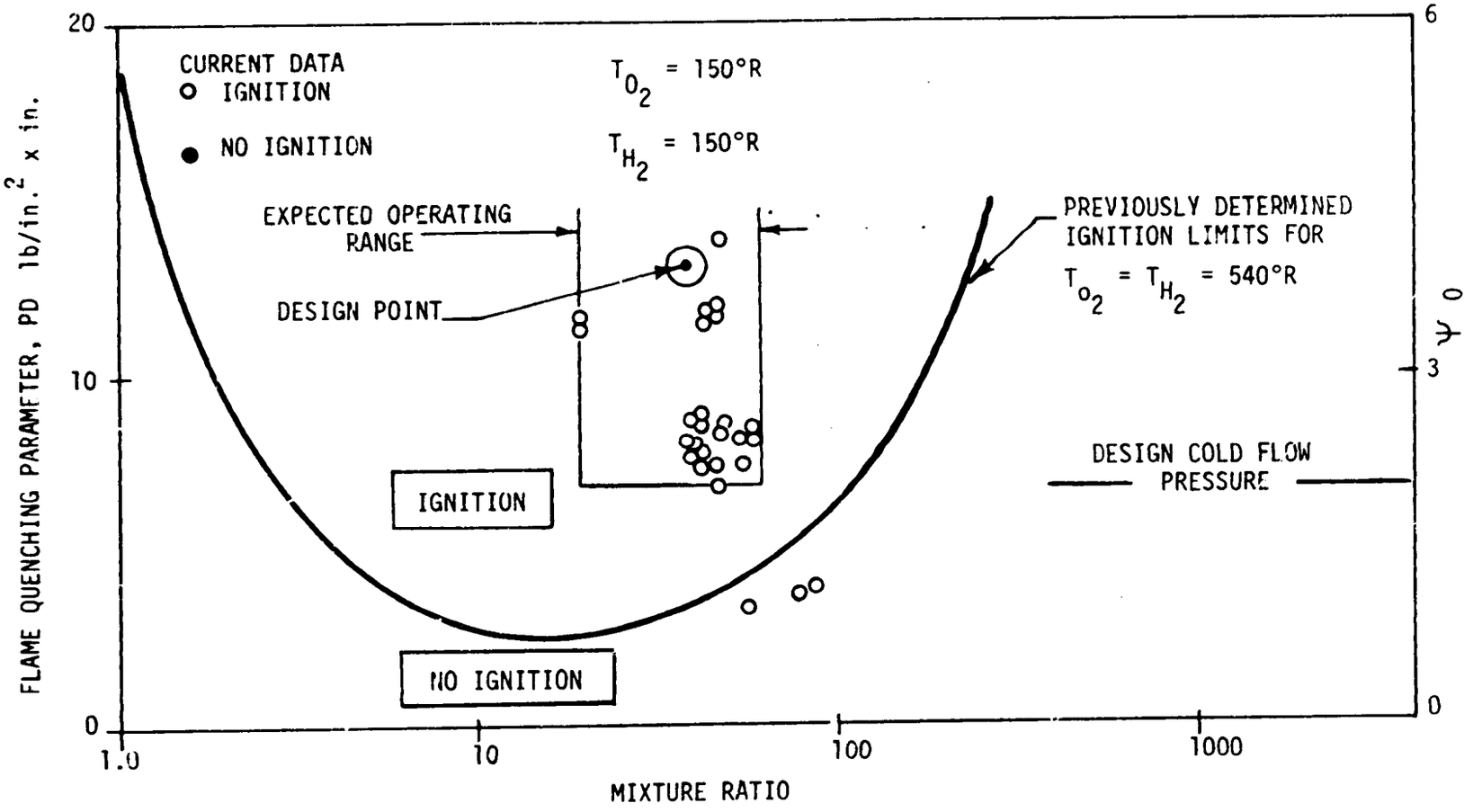

Figure 17. O_2/H_2 Ignitability and Results of Ignition Limits Test

IV, D, Ignition System Analysis and Design Considerations (cont.)

An igniter designed to provide reliable and rapid thruster ignition while accepting H_2 and O_2 in a gas, liquid, or two-phase state was configured based on MR and flow data requirements and the successful results of the 4 stage ignition system developed in Reference 8. The only operational constraint assumed was that both fuel and oxidzer could be supplied to the igniter assembly at the same temperature. This could easily be accomplished by the use of tangent or coaxial feed lines or other forms of interpropellant heat exchanger. Since the quantity of propellants employed in the igniter are very small such a device would also be very small.

The igniter design point conditions are shown in Table II.

TABLE II

ETR IGNITER SPECIFICATIONS

Design Point	Range
T_{O_2} = 83.5°K (150°R)	55.5 - 289°K (100 - 520)
T_{H_2} = 83.5°K (150°R)	19.5 - 289°K (35 - 520)
P_{ov} = 448 N/cm^2 (650 psia)	207 - 620 N/cm^2 (300 - 900)
P_{fv} = 448 N/cm^2 (650 psia)	207 - 620 N/cm^2 (300 - 900)
$\dot{w}_{O_2}$ = .0453 Kg/sec (0.100 lb/sec)	
$\dot{w}_{H_2}$ Total = .00905 Kg/sec (0.020 lb/sec)	
$MR_{overall}$ = 5	
MR_{core} = 50	
$\dot{w}_{H_2}$ core = .000905 Kg/sec (0.002 lb/sec)	
$\dot{w}_{H_2}$ coolant = .00815 Kg/sec (0.018 lb/sec)	
Spark Energy = 10 mJ/spark	
Spark Rate = 500 sparks/sec	

IV, D, Ignition System Analysis and Design Considerations (cont.)

Spark energy effects were investigated experimentally and it was concluded that 10 mJ was sufficient to provide reliable ignition under all circumstances where an ignitable mixture was present in the spark gap area.

The above analyses, coupled with the results of a series of 43 laboratory ignition limit tests (Data Figure 17), resulted in the conclusion that an oxidizer torch igniter design was capable of providing ignition over the required range of temperatures, flow rates and mixture ratios. Ignition delays of less than 0.020 sec were consistently demonstrated with gaseous, two phase and liquid propellants at inlet temperatures ranging from 84 to 295°R (150 to 530°R) mixture ratios from half to two times the nominal values, and flow rates down to 25% of design values. Subsequent testing provided comparable data for fuel temperatures of 30°K (49°R). Power levels of 0.010 mJ required for ignition have been demonstrated to be compatible with very long electrode life (Reference 8). Thus, the design of a universal igniter, which is insertable to the central igniter port of the injector appeared feasible. The 4-stage spark/ox torch igniter concept developed under Contract NAS 3-14348, was redesigned to: accept liquid and gas phase propellants, provide the proper cold flow pressure over the propellant temperature range of interest, integrate the valves to reduce volume, and interface with the design point 1 and 2 injectors.

1. Igniter Operation

The 4-stage ignition process functions as follows: Stage (1) spark discharge, Stage (2) ignition and combustion of a highly ignitable oxidizer rich torch (MR 20 to 60), Stage (3) fuel augmentation (MR 2-5 to provide the necessary cold flow pressure, higher exhaust temperatures, required igniter chamber cooling and more efficient igniter operation, and Stage (4) thruster ignition. A schematic of the igniter design is shown in Figure 18 and a photograph of the igniter assembly in the igniter only test mode is shown in Figure 19. In this design, all of the igniter oxygen flows through the gap between electrodes. A small quantity of the igniter hydrogen (10%) is injected at the downstream face of the electrodes. Ignition takes place in this highly oxygen enriched environment. Cooling of the electrodes is achieved via proper injection of the fuel and oxidizer.

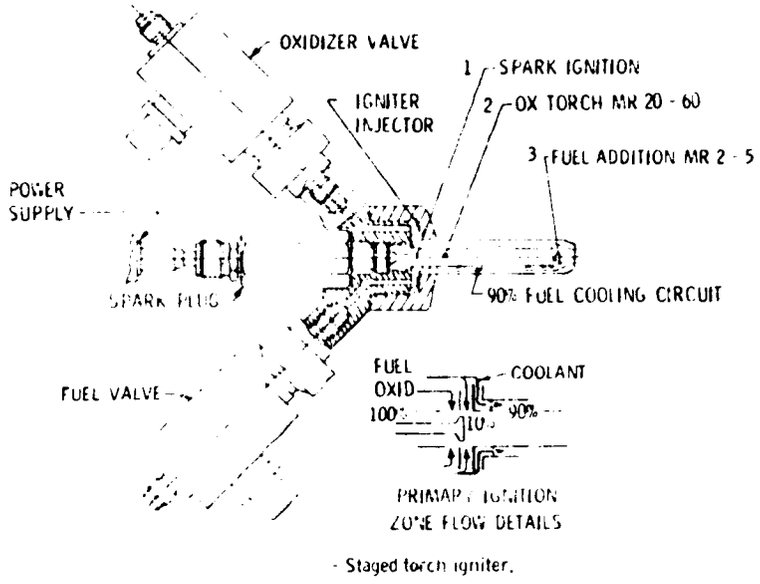

- Staged torch igniter.

Figure 18. Flow Schematic Staged Torch Igniter

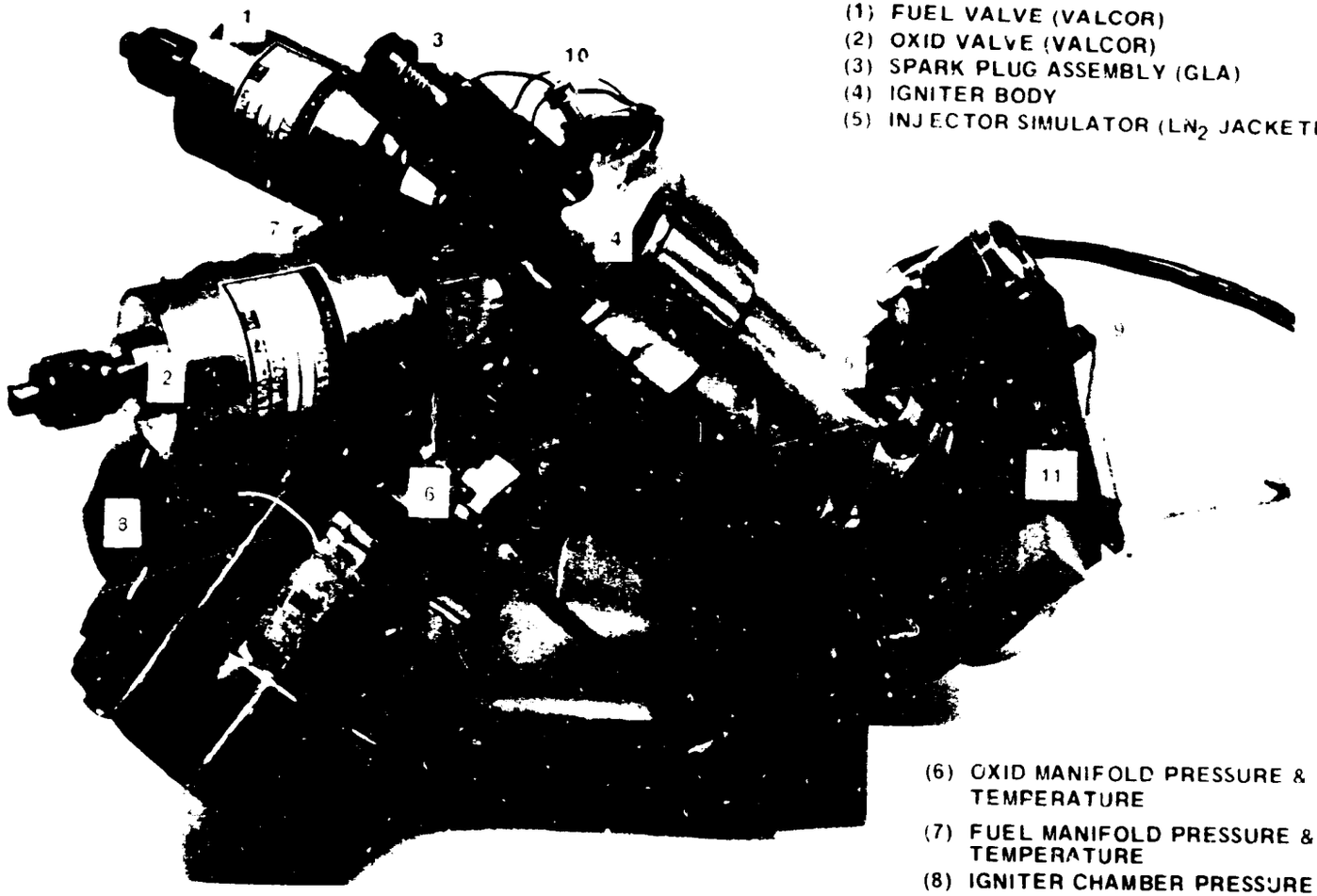

Figure 19. Assembly for ETR Igniter-Only Checkout Testing

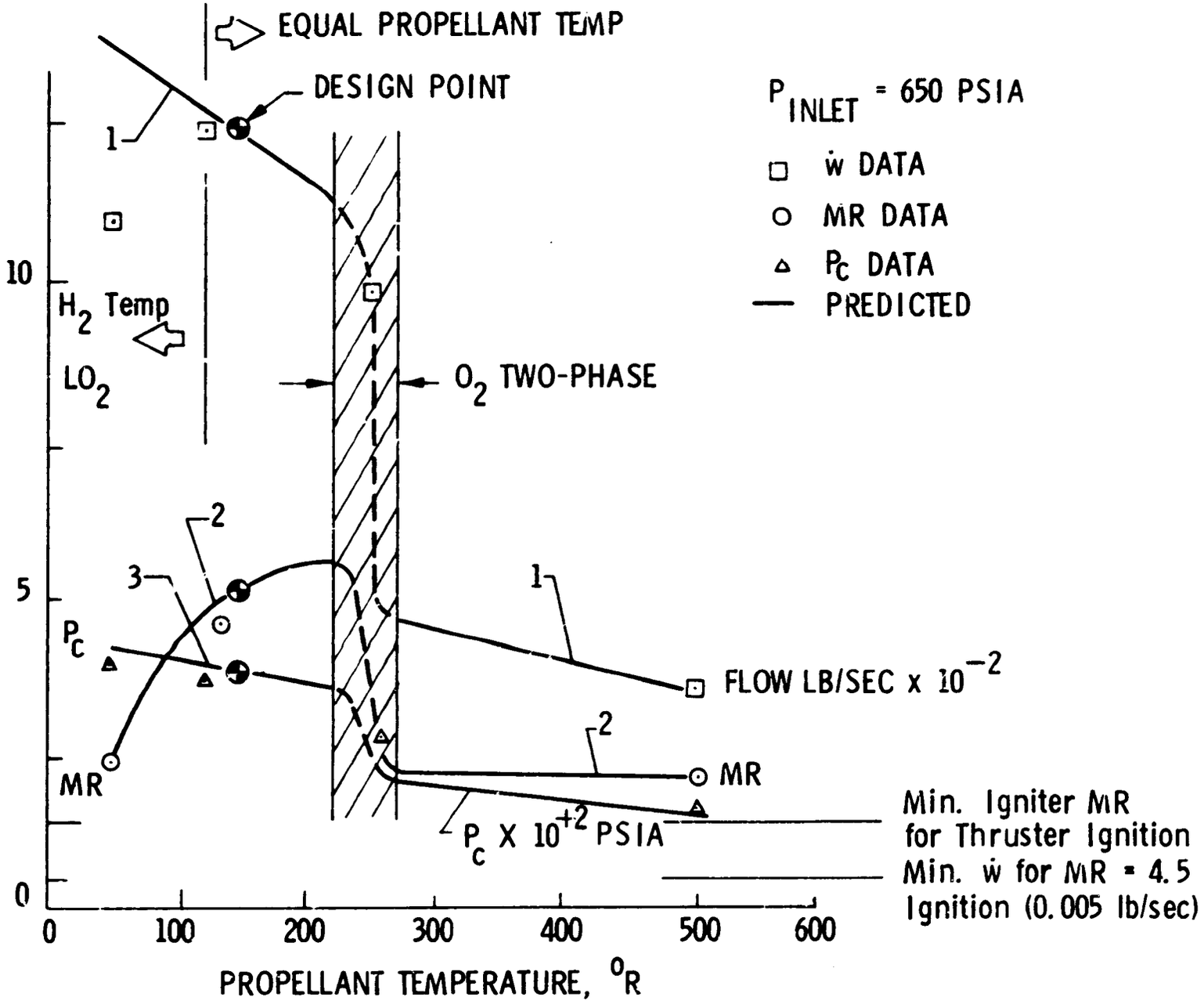

Figure 20. Igniter Flow Characteristics Vs Propellant Temperature

IV, D, Ignition System Analysis and Design Considerations (cont.)

always is present in the spark region (20-60), and the total flow which ignites the main stage is always at a high energy level MR = 2 at 2000°K (3600°R) MR = 6 at 3500°K (6300°R). Figure 20 also shows the igniter chamber pressure which is within the limits required to avoid flame quenching and spark stand off.

Cooling analyses indicated that the relative shift in core and total mixture ratios and igniter total flow rates produced compensating variables which make the maximum igniter wall temperatures relatively insensitive to the propellant supply temperature, as indicated in Table III.

TABLE III

IGNITER FLOW & THERMAL CHARACTERISTICS

Prop. Temp. °R	$\dot{w}$ lb/sec	P_c psia	Core MR	Torch M	Temp °R Core	Temp °R Exh.	Cool % Total	Max Wall Temp °F
Liquid	.14	410	25	2.5	4800	4000	26	1050
150	.12	380	50	5.0	3100	6000	15	875
530	.035	140	20	2.0	5400	3500	30	850

V. DESCRIPTION OF SELECTED DESIGNS

A. LIQUID-LIQUID SYSTEM

1. Injector

The injector designed to operate with LH_2/LO_2 is a 24-element, like-on-like doublet having the following components as shown in Figure 21.

- An actively fuel-cooled face to preclude thermal penetration to the injection orifices.
- Dual wall, low thermal capacity, low volume manifolding in both propellant circuits to allow rapid propellant bleed-in and fill and thus good pulsing performance.

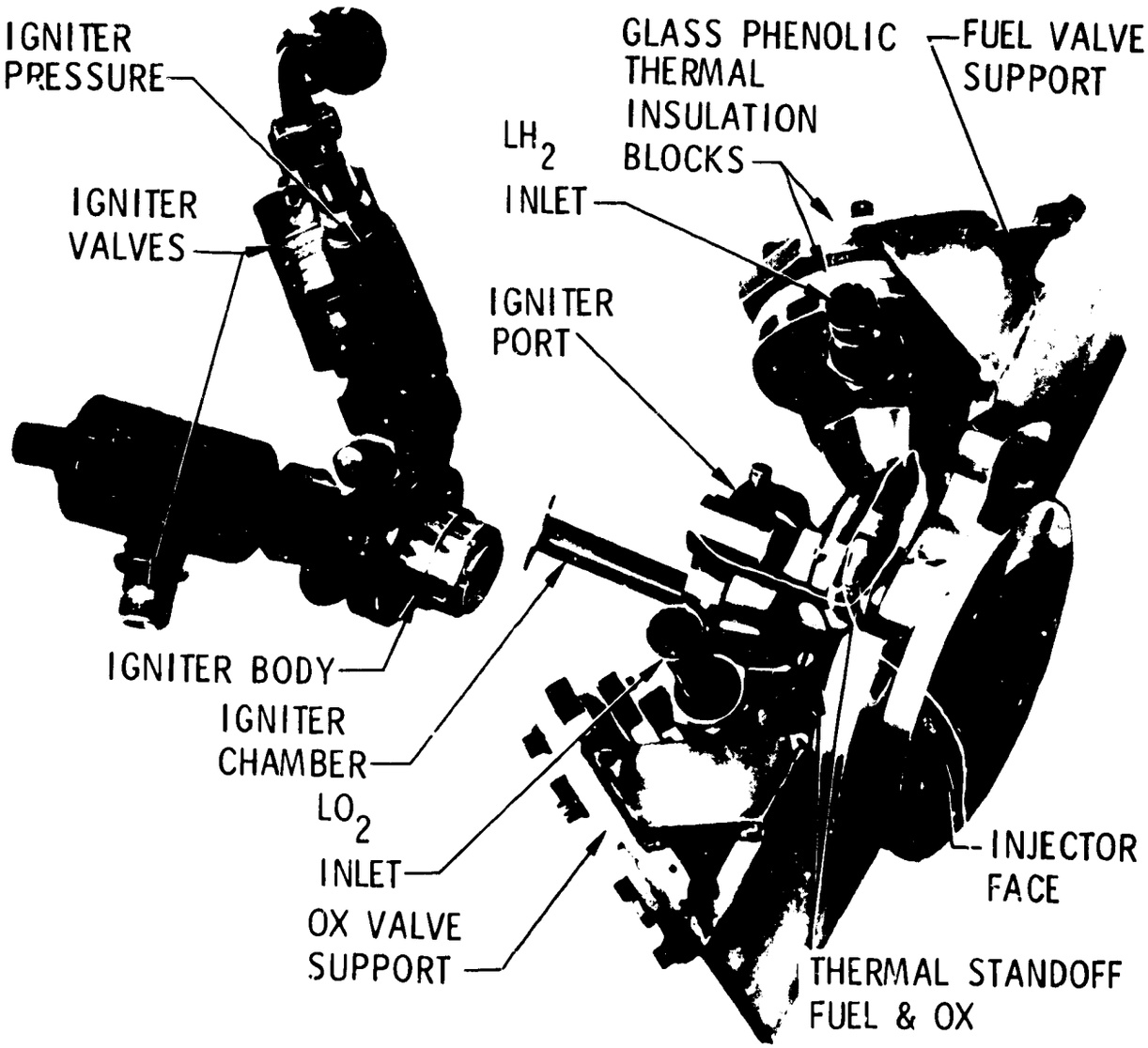

Figure 21. LH_2/LO_2 Injector Assembly

- Low volume, integral valve seat assemblies which are thermally uncoupled from the injector body.
- An injector-chamber interface which forms a cooled corner resonator cavity tuned as a quarter-wave tube to suppress the 1-T and 1-L instability mode of 17 and 16 KHz.
- A central port which accommodates the four-stage ox-torch igniter.

a. Injector Pattern

The propellant injection pattern consists of 48 contour-inlet self-impinging fuel orifices and 48 contoured inlet self-impinging oxidizer orifices (four orifices per element) positioned in alternate fuel and oxidizer rows which are equally spaced. The pattern is oriented with fuel in the outside row to provide a fuel rich barrier for chamber cooling. The selected orifice and spray overlap pattern are shown in Figure 12. The fuel orifices provide impingement close to the face (0.068 in. (0.173 cm) angle = 35 deg) and are sized at 0.028 in. (0.071 cm). The oxidizer orifice diameters are 0.034 in. (0.086 cm) and have a longer impingement distance (0.092 in. (0.234 cm) angle = 25 deg).

b. Face Cooling

Figure 22 provides a photograph of the platelet stack which form the propellant injection orifices and the active face cooling bleed circuit. The face cooling circuit, a two-pass design using 7% of the fuel as face coolant, is positioned between the injection orifices and the combustion gases and forms the diamond shaped cup around each orifice. The coolant, after passing through a metering platelet, makes the first pass in a radial outflow direction within a low conductivity stainless steel laminate; then counter-flows through a cross-over network to a radial inflow cooling circuit formed from a high thermal conductivity material (copper). Fuel for the face bleed is metered from this inflow pass through high velocity cooling channels before being discharged into the combustion chamber via the face bleed ports. The final flame surface of the injector face is formed of a thin laminate of Ni 200 to provide additional oxidization protection to the copper cooling surfaces. The injector face was instrumented with 6 thermocouples during fabrication.

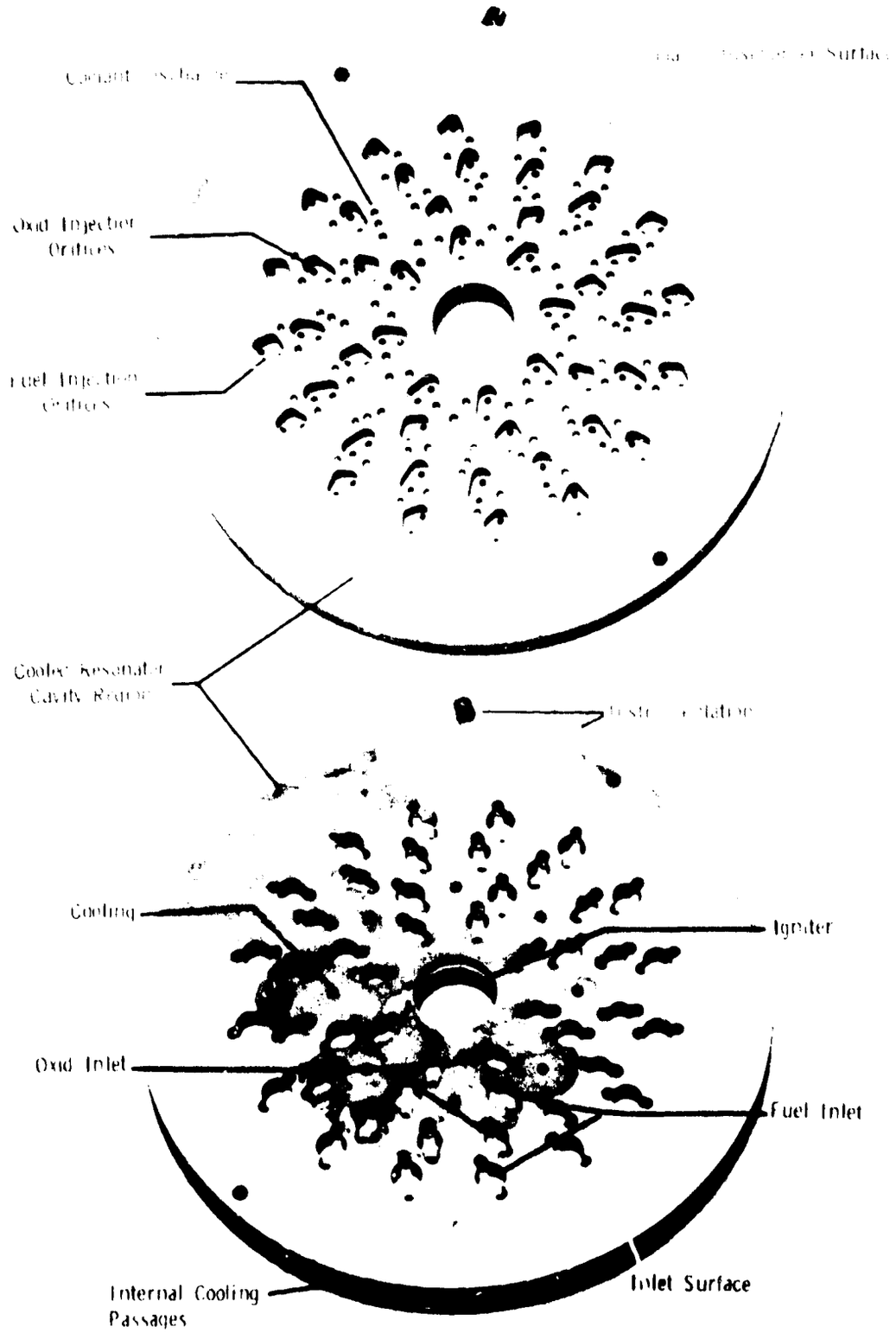

Figure 22. Like-on-Like Doublet Face Plate Assembly (A Composite Copper, Nickel and Stainless Steel Structure with Integral Cooling and Insulation Surfaces)

V, A, Liquid-Liquid System (cont.)

2. Thermal Stand Off

Each valve thermal stand off is formed from a 8.9 cm (3.5") length of .0203 cm (.008") wall, .354 dia CRES 321 tube, compressed as a bellows to an effective length of 1.26 cm (.5 in.) Axial compression of the thin wall tube allows the desired thermal isolation to be achieved while minimizing the propellant volume. The lower end of the fuel and oxidizer bellows assemblies are brazed to the injector body while the upper end is electron beam welded to the valve; thus avoiding the use of seals and flanges. The measured propellant volumes between the valve seat and the discharge end of the propellant injection orifices are 7.4 cm^3 (.45 $in.^3$) for the oxidizer and 10.5 cm^3 (.64 $in.^3$) for the fuel circuit.

3. Valves

The valves employed for the demonstration are modifications of standard N_2 actuated, teflon seat poppet valve manufactured by Control Components Inc. The valves are structurally tied to the injector through laminated, low thermal conductivity glass phenolic rings which can be seen in the photograph in Figure 21. Each propellant valve contains a high point bleed port at the upstream edge of the seat allowing the valve to be conditioned to cryogenic temperatures.

Upon actuation, the contoured nose of the poppet valve is withdrawn a total of 1.77 cm (.5 in.) in a .025 sec interval providing a prescribed time dependent valve flow coefficient which was optimized to provide a smooth start transient. Fuel and oxidizer valves are of the same design.

4. Manifolds and Flow Paths

With the liquid-liquid injector the LO_2 coming from the valve passes through the thermal standoff into a low tapered toroidal flow

V, A, Liquid-Liquid System (cont.)

distribution manifold. The oxidizer then passes through 12 equally spaced flow distribution orifices discharging into a disk shaped dual wall plenum which in turn, supplies propellant to the 48 orifices. Flow from the fuel valve located opposite the oxidizer valve, bifurcates and flows through 2 short, thin wall lines prior to passing through two symmetrically located thermal standoffs. The fuel discharges directly into the dual wall fuel manifold from which the 48 doublet fuel orifices and face cooling circuit are supplied.

5. Chambers

The injector checkout testing was accomplished with pressure and temperature instrumented copper heat sink chambers of 35.5 and 45.2 cm L* (14 and 17.8 in.).

B. GAS LIQUID SYSTEM

1. Injector

The GH_2/LO_2 injector is a 36-element coaxial tube type with elements positioned in three radial rows. The basic design is shown conceptually in Figure 3. This design contains the following features.

- A fuel internal regeneratively cooled copper face.
- A dual wall low thermal capacitance low volume oxidizer manifold.
- A low volume integral oxidizer valve welded to but thermally uncoupled from the injector body.
- An all metallic injector chamber interface seal which provides a cooled corner cavity resonator and allows the injector to receive fuel from the discharge of a regeneratively cooled combustion chamber.
- A central port which accommodates the universal four stage oxidizer torch igniter.

V, B, Gas Liquid System (cont.)

a. Valve and Manifolding

The oxidizer valve and manifolding are identical with the liquid/liquid design. Oxidizer flows from the valve via the thermal standoff into a tapered annular cavity which functions as a flow distributor to eliminate the dynamic forces resulting from the high velocity inlet lines. LOX discharges from the distribution manifold via 12 equally spaced orifices and flows radially inward and outward within the disk-shaped cavity to each of the elements. Low thermal capacitance plates applied at both faces of the disk cavity minimize heat addition following final mixing and distribution. The controlling resistance is provided by the chamfered entrance, .0876 cm (0.0345-in.-dia) flow restrictor at the inlet to each tube. The 36 oxidizer injection elements are formed from Nickel 200 tubing of .195 cm, .023 cm (0.0625 in. dia, 0.008 in.) wall.

The fuel circuit of the injector is designed to accept flow from the regeneratively cooled chamber. Fuel enters the disk-shaped manifold via six equally spaced tubes in the chamber forward flange. Initial flow is both circumferential and radially inward. Eighteen slots in the copper face plate aid in providing a uniform radial inward flow pattern. Fuel flows radially inward and then is discharged at 960 fps through the 0.043 cm (0.017 in.) annular slots formed by the copper face and nickel tubes. Each tube is centered by 3 axial ribs which are an integral part of the copper face. Face cooling is provided by the high velocity fuel flow through the annular gap.

The injector fuel volumes is 14.9 cm^3 (0.91 $in.^3$) and the oxidizer volume is 7.37 cm^3 (0.45 in.)

2. Chamber

The combustion chamber illustrated schematically in Figure 3 and shown in Figure 23 comprised of a 8.9 cm (3-1/2 in.) long regenerative section attached to a dump and film cooled nozzle. The fuel enters the chamber via an integral side-mounted valve which is connected to the chamber by a thermal

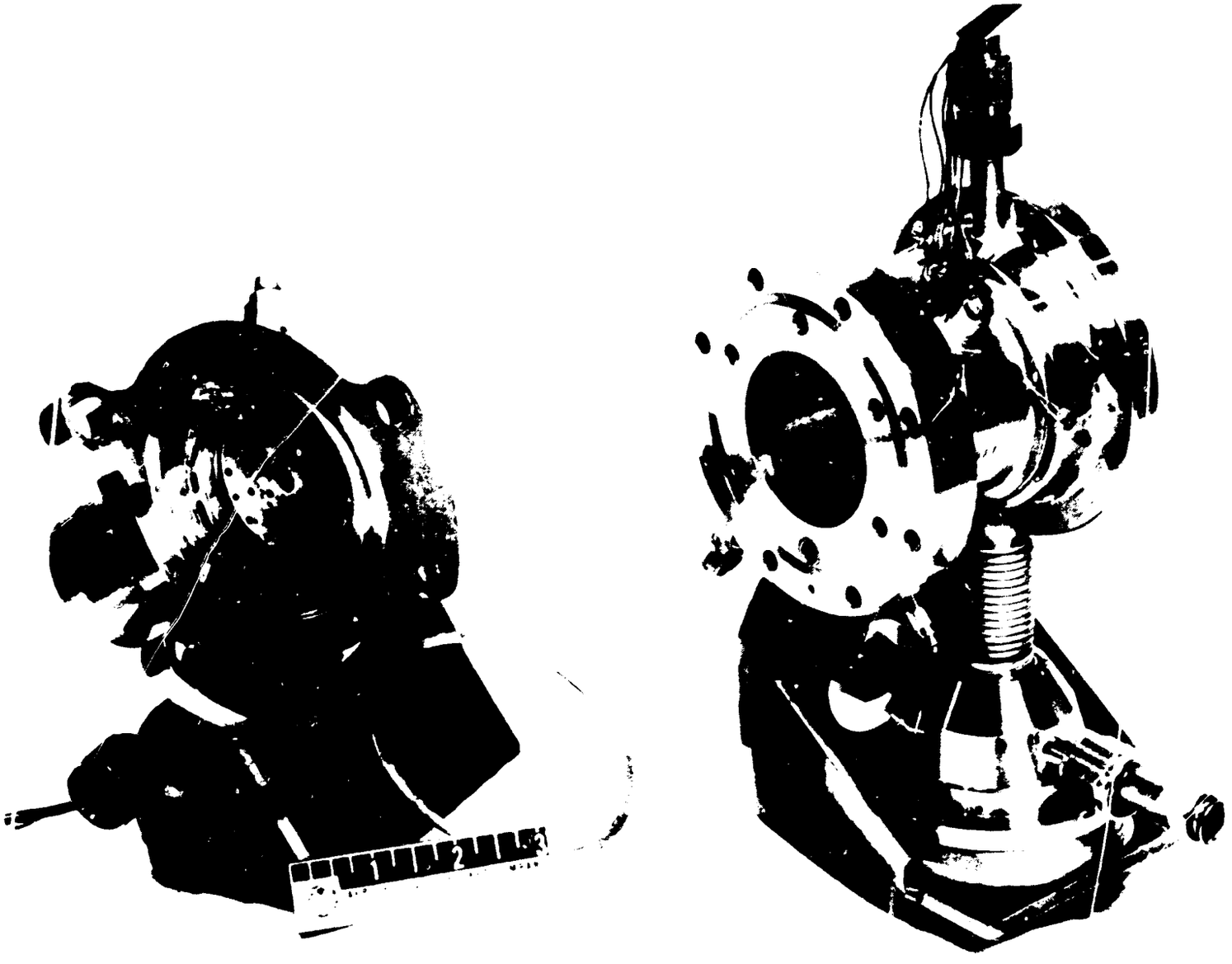

Figure 23. GH_2/LO_2 Injector-Chamber Assembly

standoff appropriately sized to pass the lower density gaseous fuel. Flow from the thermal standoff discharges into a constant velocity manifold. Then 75% of the fuel flows forward through 60 slots 0.386 cm (0.150 in.) deep and 0.081 cm (0.032 in.) wide which are machined in a copper liner. This liner is bonded to a 0.152 cm thick (0.060-in.) steel case which provides the necessary structural support. Flow discharging from the coolant channels is collected in a manifold and supplied to the injector via six equally spaced 0.635 cm (0.25-in.) tubes. Flow in the discharge manifold provides the cooling for the corner resonator cavity.

Nominally, 25% of the fuel flow is required for film cooling the nozzle and skirt. This coolant is supplied via a tap off from the main manifold and separately orificed (for experimental purposes) to a film coolant distribution manifold. The coolant injection ring is 5.1 cm (2.0 in.) long and contains 90 .081 cm wide (0.032-in.) channels which are .068 cm (0.027 in.) deep.

The following table defines essential 40:1 nozzle dimensions for use with both design point injectors:

TABLE IV

NOZZLE FOR ALTITUDE TESTS

Chamber length	18 cm	(7 in.)
L*	43 cm	(17 in.)
Chamber diameter	5.59 cm	(2.2 in.)
Throat diameter	3.35 cm	(1.32 in.)
ε_c	2.77	
ε_e	40:1	
Nozzle length	120% Rao, 28.3 cm (11.162 in.)	
Nozzle efficiency	99.5%	

V, Description of Selected Designs (cont.)

C. FOUR STAGE IGNITION SYSTEM

The igniter is a small thruster which can accept either liquidous, two phase, or gaseous propellants, ignite these using a very low energy spark, and produce a hot gas torch of sufficient energy to provide reliable rapid main stage ignition.

A schematic drawing of the igniter assembly is shown in Figure 18. The ignition system consists of 5 major components: (1) a GLA spark plug, (2) Model 427200-4871 Valcor coaxial type poppet valves; (3) a stainless steel/nickel body which forms or contains all manifolding and seals, propellant metering and injection orifices, a platform for mounting the spark plug and valves plus all necessary instrumentation ports and a flange for attachment to the injector, (4) a hydrogen cooled nickel chamber, and (5) a high voltage GLA capacitance discharge power supply (not shown).

The ten percent of the fuel for the core flow is injected via 24 radial inflow rectangular orifices which are formed by a bonded photoetched Ni plate. The 90% of the fuel bypassing the core flows through a stainless steel metering platelet and then into 12 slotted coolant passages .122 cm wide, .076 cm deep (.048 in. x .030 in.) formed by the nickel chamber and the internal cavity of the injector into which the igniter is inserted. The passage dimensions and flow are selected to provide the necessary cooling of the nickel chamber which contains the high mixture ratio hot gas.

The oxygen flows from the valve through a balancing orifice into a low volume manifold and is injected via 6 like-on-like doublet elements which produces 6 axial fans which flow radially inward to the center electrode. The 12-oxidizer orifices are formed by a single photoetched Nickel platelet bonded to the lower face of the igniter body. All of the oxygen flows through the annular spark gap formed between the central electrode and the igniter chamber wall and provides the required electrode cooling.

V, C, Four Stage Ignition System (cont.)

The power supply employed was a GLA Model 48136 variable energy system. The unit was calibrated at a 0.127 cm (0.050 in.) spark gap to give the following energy levels and spark rates.

10 mJ	500 sparks/sec
25 mJ	500 sparks/sec
50 mJ	300 sparks/sec
100 mJ	150 sparks/sec

VI. EXPERIMENTAL RESULTS

A. IGNITION TESTS

Full-scale igniter assembly tests were conducted with the hardware shown in Figure 19, prior to initiation of complete injector/thruster testing. Approximately 250 hot tests were conducted with this prototype igniter. Rapid and repeatable ignitions were demonstrated over the following range of test conditions:

Temperature at oxidizer valve	74 to 289°K (134-520°R)
Temperature at fuel valve	24 to 288°K (44 to 518°R)
Pressure at oxidizer valve	228 to 627 N/cm^2 (330-910 psia)
Pressure at fuel valve	213 to 637 N/cm^2 (309-924 psia)
Ambient pressure	Less than 0.34 N/cm^2 (0.5 psia)
Hardware temperature	83 to 294°K (150-530°R)

Satisfactory ignitions were demonstrated with LH_2/LO_2, GH_2/LO_2, $GH_2/LO_2 + GO_2$, GH_2/GO_2 at energy levels of 10 mJ. Ignition was detected by the igniter chamber pressure which rose within 0.02 sec from the time fuel and oxidizer were sensed in the igniter manifolds under all propellant supply conditions. Thermocouples located in the igniter throat and exhaust stream verified the ignition. Igniter durability and cooling was also demonstrated

VI, A, Ignition Tests (cont.)

by continuous firings of up to 10 sec and pulses consisting of 20 firings in rapid succession. No cooling problems were encountered. Typical igniter oscillograph traces and ignition delay times are shown in Figure 24 for (a) LO_2/GH_2 warm hardware, (b) LO_2/GH_2 cold hardware, (c) GO_2/GH_2 warm hardware, and (d) LO_2/LH_2 cold hardware.

B. INJECTOR TESTS

1. LH_2/LO_2 Testing

A series of 66 sea level hot firings, Table V, were made with a full engine assembly using heat sink chamber as shown in Figure 23. Table V provides a summary of the propellant supply and operating conditions demonstrated. Specific test conditions are itemized in Table VI.

TABLE V

SUMMARY OF LH_2/LO_2 TEST CONDITIONS (66 FULL THRUSTER FIRINGS)

P_c	163 - 338 N/cm^2 (237 - 490 psia)
MR	3 - 10
Fuel Temperature	27 - 39°K (49 - 70°R)
Oxidizer Temperature	93 - 102°K (166 - 184°R)
Injector Body Temperature*	89 - 294°K (160 - 530°R)
Injector Face*	278 - 333°K (500 - 600°R)
Duration min/max	0.076/7.7 sec

*At fire signal.

In order to investigate the first start, hot restart, and steady state performance characteristics, fire sequences consisting typically of a short pulse (0.1 sec), a long burn 2.0 sec and a repeat short pulse were executed. The first pulse provided data for a warm manifold dry start; the long burn gave steady state performance and thermal data; and the following pulse provided data for the performance and start characteristics with cold manifolds containing some residual propellants and a hot injector face. The longest

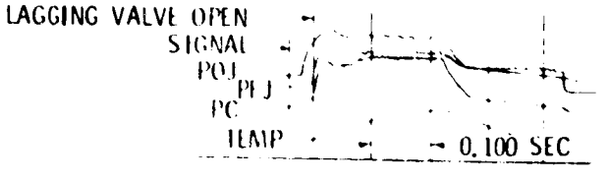

(A) TEST 197 PULSE 5 150° R, LO_2-GH_2 WARM HARDWARE, IGNITION DELAY 0.006 SEC.

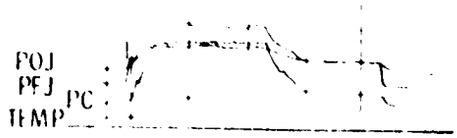

(B) TEST 203 PULSE 4 150° R, LO_2-GH_2 COLD HARDWARE, IGNITION DELAY 0.010 SEC.

(C) TEST 178 PULSE 2 530° R, GO_2-GH_2 WARM HARDWARE, IGNITION DELAY 0.005 SEC.

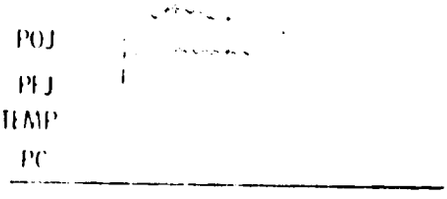

(D) TEST 108 PULSE 4 150° R, LO_2-LH_2 COOL HARDWARE, IGNITION DELAY 0.010 SEC.

Figure 24. Typical Igniter Start and Firing Transients

TABLE VI

PRIMARY [illegible] TESTING [illegible]

Test No.	Pulse Duration	MR	P_c	P_{fm}	T_F	T_o	Valve Sequence & Flow Time, sec IFV	IFV	MOV	MFV	FMO/FMF	T_{ign}/T_{ign}	90% Thrust	Comments
[illegible]														
		A		533		169								
		A		504										
		A			50	166								
		A		510	58	17								
		A		480	+7	17								Ignition system failure
		A		441	7	167								
		A			56	181								RFF on failed to start time
		A		521										LH_2 leak at flow meter
		A		443	+9	176								He in lines
														LH_2 leak at flow meter
														Solenoid leak due to He in lines
														Solenoid leak due to He in lines
														Flowed 15%
														Flowed 15%
														Flowed 15%
		A		503										
		A		430	6	176								
				443										
		A				176								Oxidizer injector valve [illegible] gas flow
														Oxidizer injector valve [illegible] gas flow
														Oxidizer injector valve [illegible] gas flow
														15%
														15%
		A		473										Fuel injector valve signal at 15%
		A		478	5	179								Oxidizer injector [illegible] gas injector valve
		A		394										
		A		472	4	16								Oxidizer injector valve [illegible] gas flow
				440										
		A		510										
		A		502		169								Oxidizer injector [illegible] gas flow
				460										
				440		176								
				433										
				448		176								
				444										
				464										
				433										
					43	71								
				433										
						176								
														15%
														15%
					5	74								Oxidizer injector valve [illegible] gas flow
				434										
		A												Fuel Test 2 or 3?
		A				174								Fuel Test 2 or 3?
				433										
				434										
				434										
				439										
				435										
		A				142								
														Oxidizer injector valve [illegible] gas flow
														Oxidizer injector valve [illegible] gas flow
					50	144								
				434										
				432										
				434										
				439										
				433										
														Cold prop to injector 15%
														Cold prop to injector 15%
		A												Cold prop to injector 15%
		A												Cold prop to injector 15%

Symbol

MR	Mixture Ratio	IFV	Igniter Fuel Valve
P_c	Chamber Pressure	MOV	Main Oxidizer Valve
L*	Chamber Characteristic Length	MFV	Main Fuel Valve
P_{fm}	Prefire Oxidizer Manifold Temperature	FMO/FMF	Time to Main Oxidizer Flow/Time to Main Fuel Flow
T_o	Fuel Temperature	T_{ign}/T_{ign}	Time to Igniter Ignition/Time to Injector Ignition
T_F	Oxidizer Temperature	90 F	Time to 90% Thrust
T_o	Igniter Oxidizer Valve		

single burn of the test series was 7.7 sec and was limited by the thermal capacity of the heat sink copper chambers. Several additional series of 6 successive pulses of equal on-times variable coast periods were conducted to establish pulse repeatability.

a. Pulse Characteristics

Figure 25 is a record of the first checkout firing of the engine. The mainstage valve sequencing employed a .005 sec ox lead with a .02 sec full travel time for both valves. The only variation in this first pulse from the planned optimum was that the igniter was permitted to operate for .050 sec prior to main stage ignition in order to more easily observe, first the igniter, and then the main stage ignition. In subsequent tests, the igniter lead was reduced and valve timing varied until the .075 sec signal to 90% thrust goal was demonstrated. Comparison of this and subsequent pulses with the engine firing simulations showed all aspects of the analyses to be quite accurate. The lower portion of Figure 26 shows the sequence of events and timing employed in demonstrating the minimum impulse. The parameters shown include; igniter pressure, valve position, chamber pressure and thrust. The upper portion of the figure shows the thrust time trace for 5 successive minimum impulses. Coast time between pulses range from 1.6 to 5.0 sec. The measured impulse is indicated above each trace. The average impulse was 51.7 lbF sec and was repeatable within $\pm$ 3%. No significant thrust differences were noted on the first pulse (with warm dry manifolds) and subsequent pulses (which were at various levels of chill-in and contained some residual propellants in the manifolding). Of the 0.075 sec response demonstrated, 0.050 sec was associated with electrical energization of the main valve solenoid and 0.025 sec with valve travel, ignition and thrust rise. Thrust rise, 0 to 90%, was accomplished in less than 0.01 sec when a slight oxidizer lead (.005 sec) was employed.

In the course of verifying the optimum valve sequencing, both fuel leads and lags were investigated. The thrust rise rates experienced with simultaneous flow or fuel leads, as measured by the close coupled Ramapo

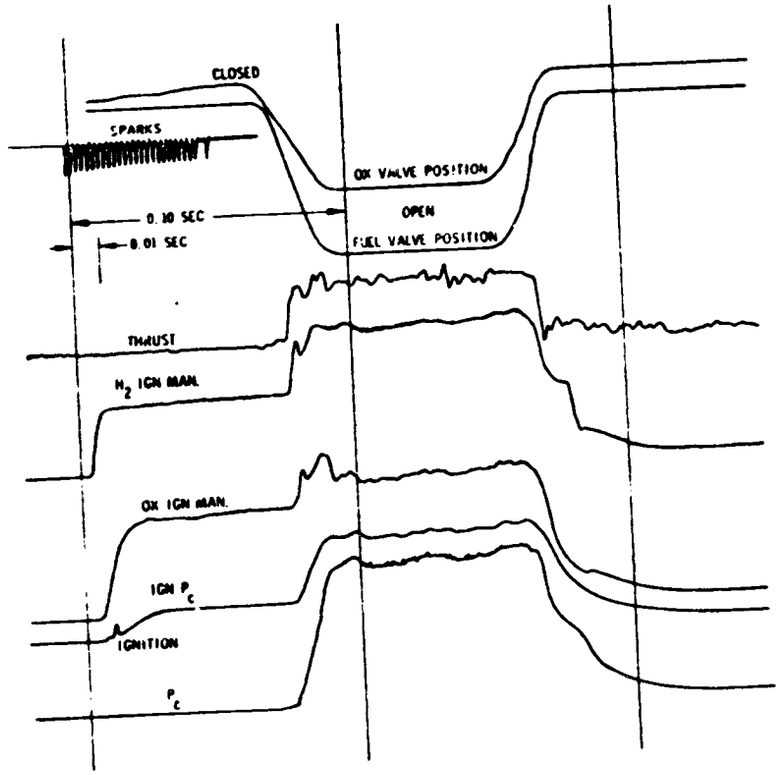

Figure 25. First LH_2/LO_2 Full Thruster Checkout Firing

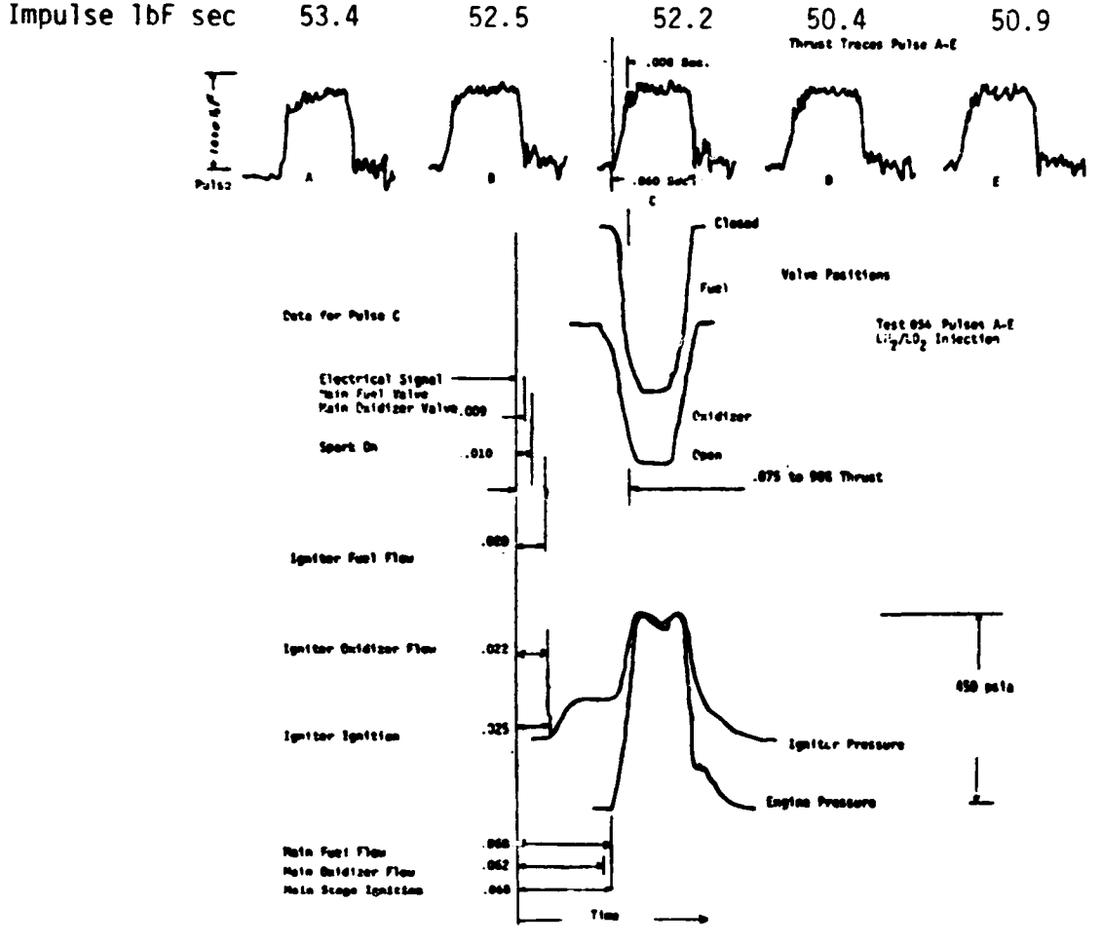

Figure 26. Sequence and Response Data, Minimum Impulse Series (Electrical Pulse = .076 sec, Test 054)

flowmeter, were in the order of 0.02 to 0.03 sec from 0 to 90% thrust. This compares to the 0.01 sec obtained with a slight oxidizer lead and verifies the prediction of minimum ignition delay with an ox lead. A number of tests were conducted in a 50% throttled condition obtained by reducing the supply tank pressures (172 N/cm^2 (250 psia)). The response of the LH_2/LO_2 thruster in this mode was 0.090 sec from signal to 90% thrust.

A series of pulses at other pulse widths and varying coast times were also conducted. A typical test series is shown in Figure 27. Excellent impulse repeatability was obtained at all test conditions. Figure 28 shows the linearity and repeatability of electrical pulse widths from 0.076 to 0.234 sec using a data sample from 20 firings. All samples fell within $\pm$3% of the nominal total impulse. These data include initial pulses after long coasts and subsequent restarts.

b. Pulsing Performance

The effect of successive reductions in firing durations on the thruster performance is shown in Figure 29. The data for 31 firings at 172 and 345 N/cm^2 (250 and 500 psia) are based on the integrals of measured thrust and total propellant flows including those of the priming startup and shutdown transients. Each data point compares the full pulse specific impulse to that which would be attained at the same propellant supply pressures after all transient effects were damped: i.e., % of steady state I_s. These data thus represent the loss in performance due to valve sequencing, mixture ratio shifts resulting from feed system flow oscillations from the valve openings, manifold priming and blowdown. The curve drawn through the upper limits of the data corresponds to the loss predictions for the feed system oscillations and dribble mass loss. The remaining data scatter corresponds to thermal and priming shifts for warm dry starts and cold restarts. The relative losses were the same for chamber pressures of 172 and 345 N/cm^2 (250 and 500 psia).

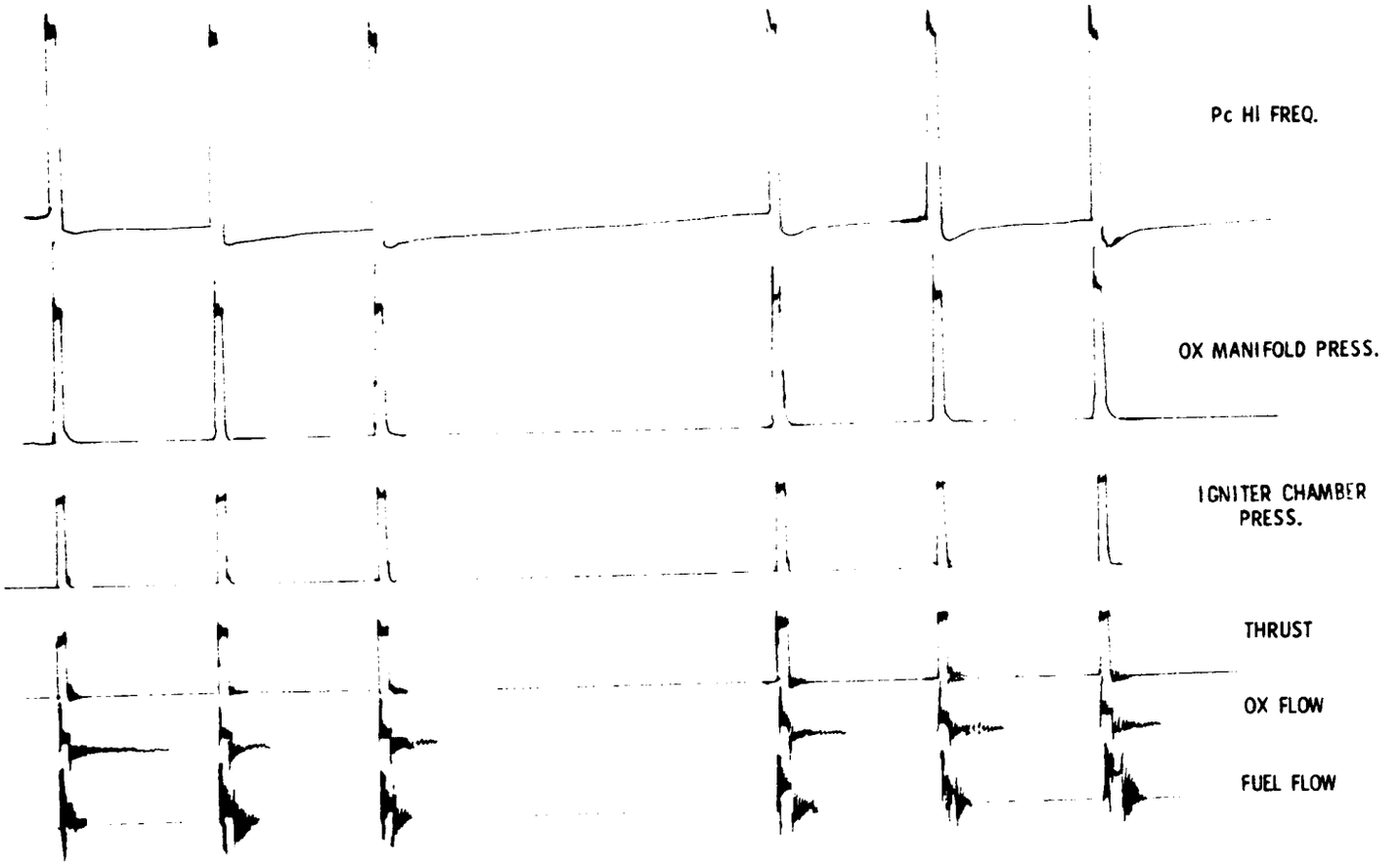

Figure 27. LH_2/LO_2 .105 sec Electric Pulse Test Series, Test 053

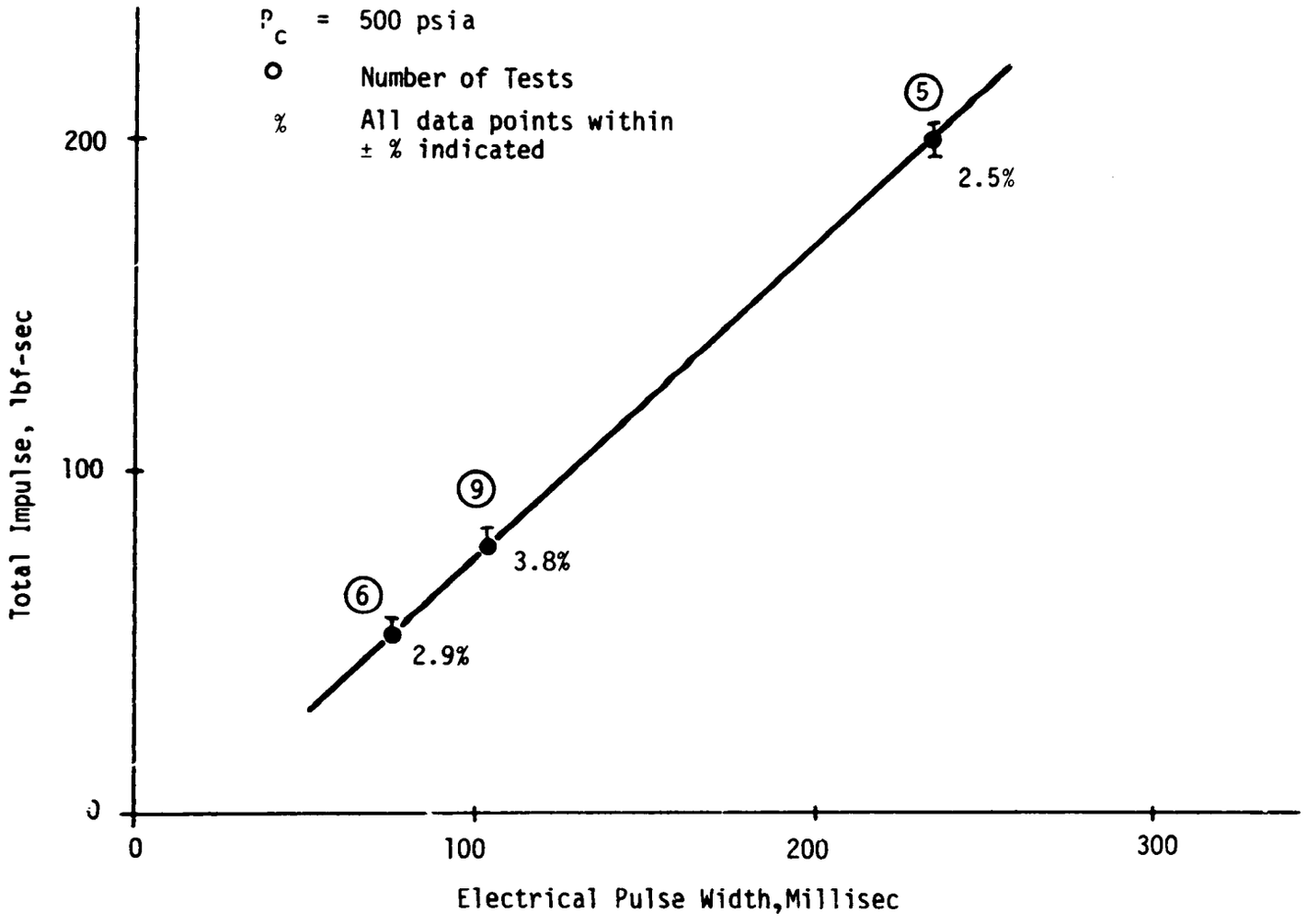

Figure 28. Total Impulse vs Electrical Pulse Width

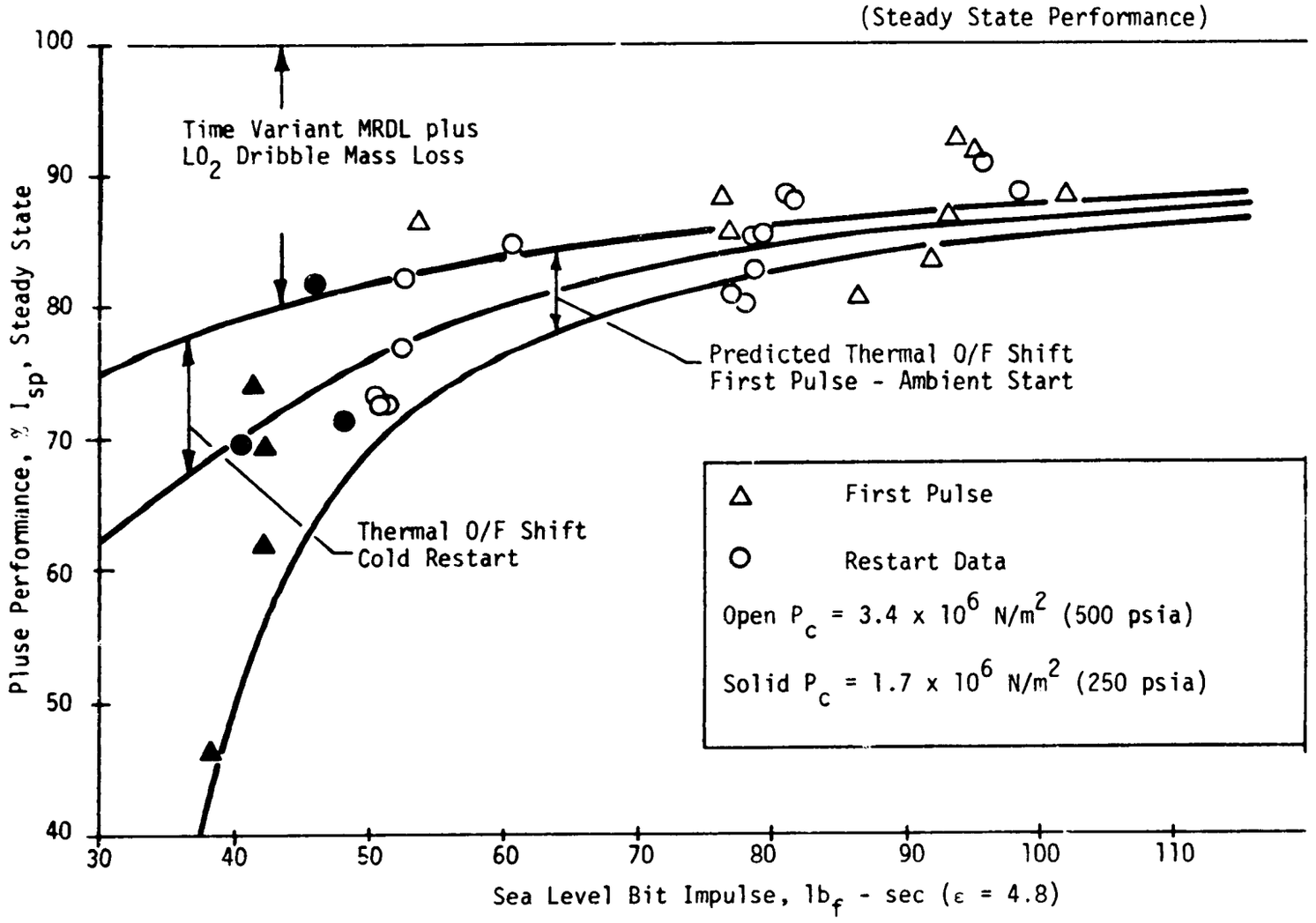

Figure 29. Effect of Bit Impulse on LH_2/LO_2 Performance

VI, B, Full Thruster Testing (cont.)

c. Steady State Performance

Tests were conducted in 35 and 43 cm (14 and 17 in.) L* chambers. The steady-state thrust based energy release efficiency at the design mixture ratio of 4.5 is as follows:

	35 L*	43 L*
LH_2/LO_2	91%	95%

The effect of MR and chamber pressure on performance is shown in Figure 30. P_c effects were found to be small. The predicted deliverable vacuum specific impulse of a 17 L* (43 cm) 40:1 area ratio cooled chamber is 4187 N-sec/Kg (427 lb-sec) for the liquid-liquid thruster.

d. Injector Hydraulics

Injector flow coefficients ($Kw = \frac{\dot{w}}{\sqrt{\Delta P \cdot SG}}$) were computed from water flow data and from complete engine firings. Comparisons are made in the following table:

TABLE VII

L/L INJECTOR FLOW COEFFICIENTS

	Kw ox.	Kw fuel
Water	.159	.127
Hot fire	.170	.126
% Change	+7%	Nil

Although no significant difference in total impulse was reported between first pulses and subsequent pulses, a difference was noted in pulse performance. This is due to a greater shift to an oxidizer rich mixture ratio in the first pulse when the manifold is warm than in subsequent pulses when the manifold is colder. The MR shift effect is shown in Figure 31.

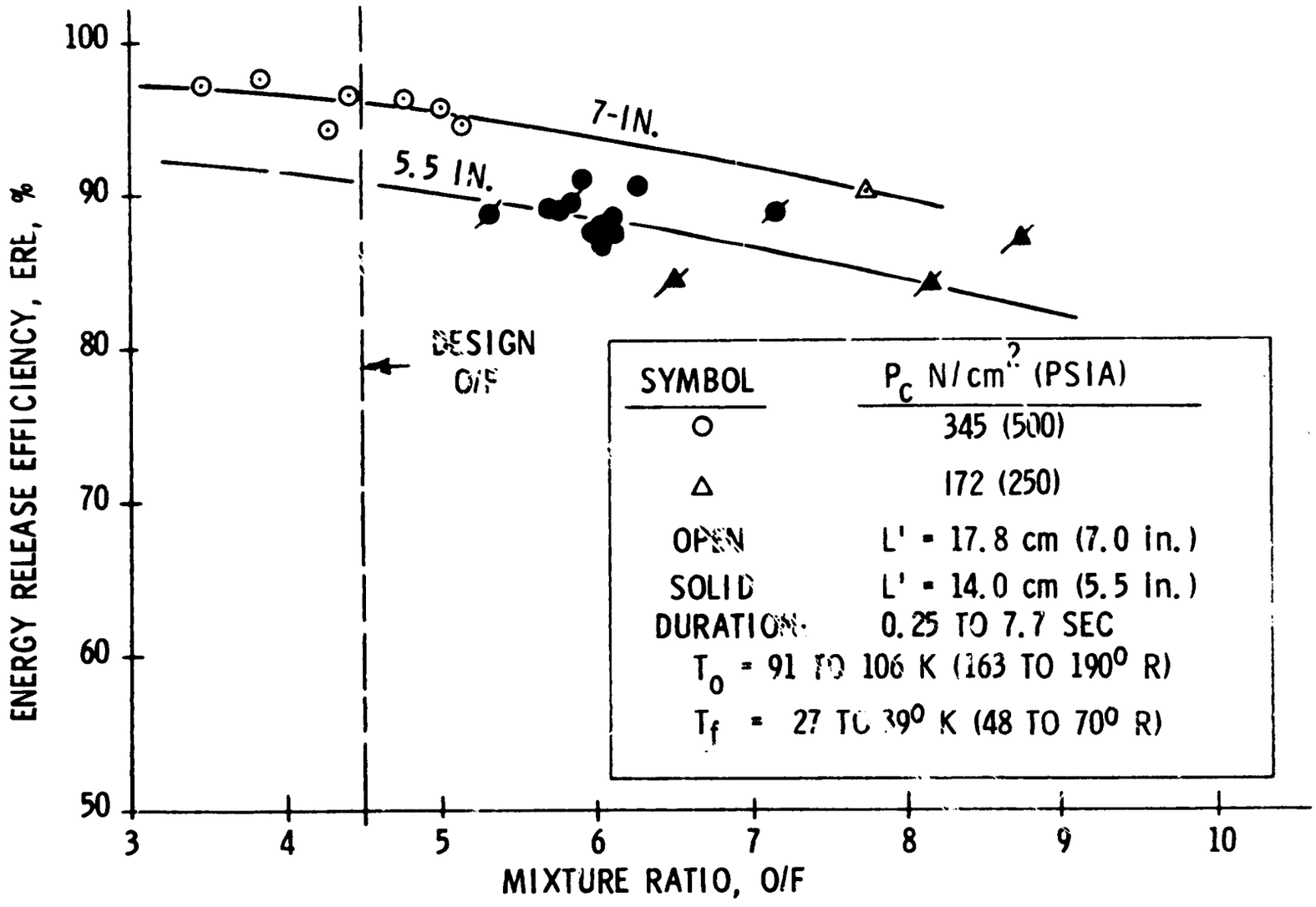

Figure 30. Steady State L/L Pulsing Performance

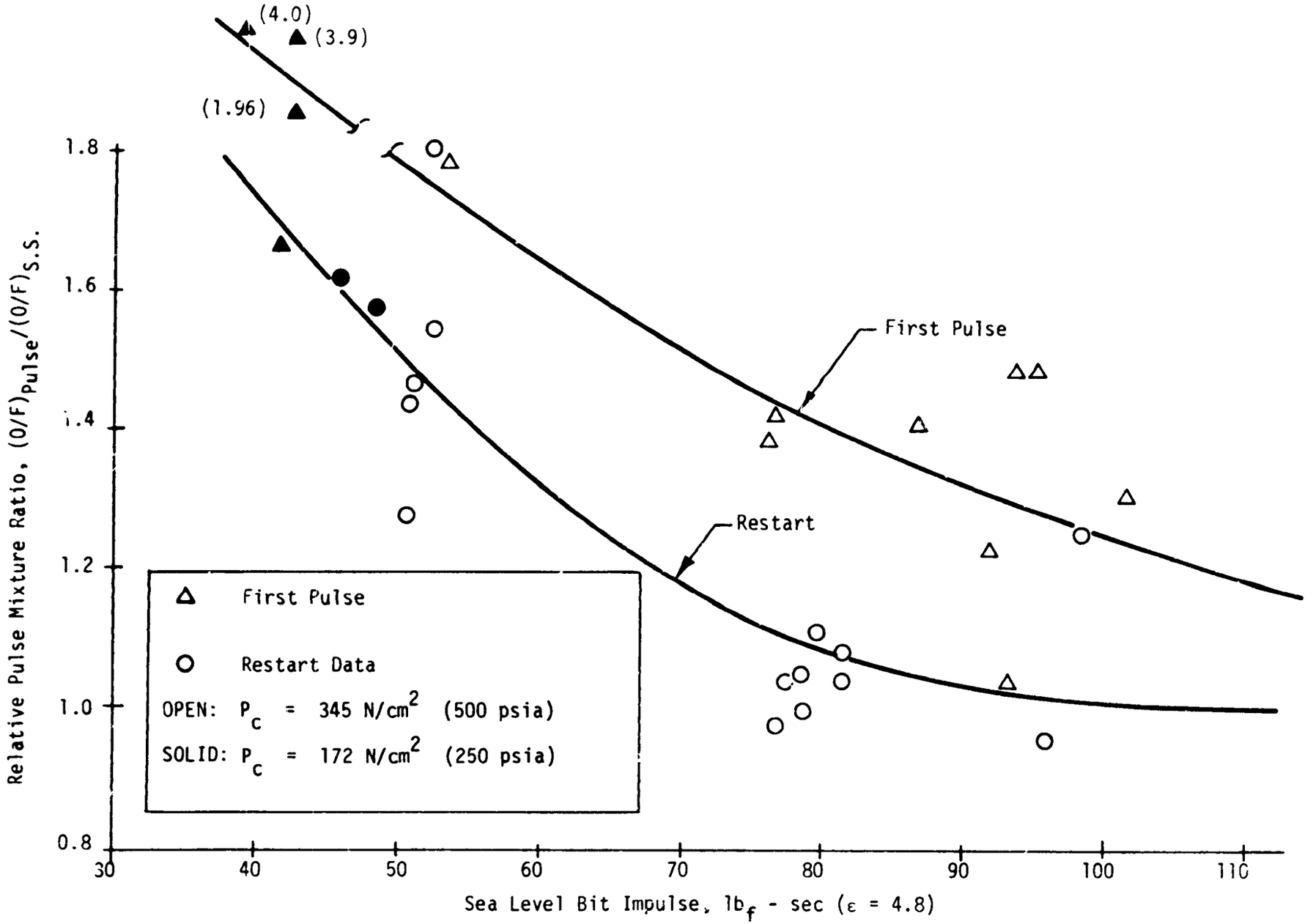

Figure 31. Bit Impulse Effect on LH_2/LO_2 Pulse Mixture Ratio

VI, B, Full Thruster Testing (cont.)

e. Stability

The LH_2/LO_2 engine was found to be stable with quarter wave tube corner resonators tuned to 17,000 Hz. The LH_2/LO_2 thruster, when bombed with 2 gr RDX charges was found to recover from 100% over pressure in 1 millisecond. The recovery from one of several such bomb tests as recorded by a Photocon 307 transducer, is shown in Figure 32. Throttling to 50% of the design flow was demonstrated without encountering chugging.

f. Thermal Results

Test durations ranged from .05 sec of fire to 7.7 sec. All essential components were instrumented to determine the maximum temperatures and time required to achieve steady-state thermal conditions. Typical measurements, shown in Figure 33, indicated the injector face was operating below 394°K (250°F). No component overheating or damage was noted in the 66 hot fire tests conducted.

Figure 34 shows the measured temperature of the valves, manifolds, flanges and injector face in a 6 firing, 200 MS pulse series. One of the face thermocouples spikes up on start and then cools as the engine continues to fire. The reason for this is not fully understood and may be due to faulty instrumentation. In the six firing pulse series shown, there is no evidence of heat soak problems or thermal pump up effects.

Figure 35 shows the local adiabatic wall temperature data points computed from the transient surface wall temperature measurements made on the heat sink copper chambers. These data for MR 4.5 were fed into the ALRC barrier film cooling model to establish certain required empirical mixing parameters. The model was then employed to provide a family of curves for other mixture ratios. These are seen to compare favorably to the test data at these other mixture ratios.

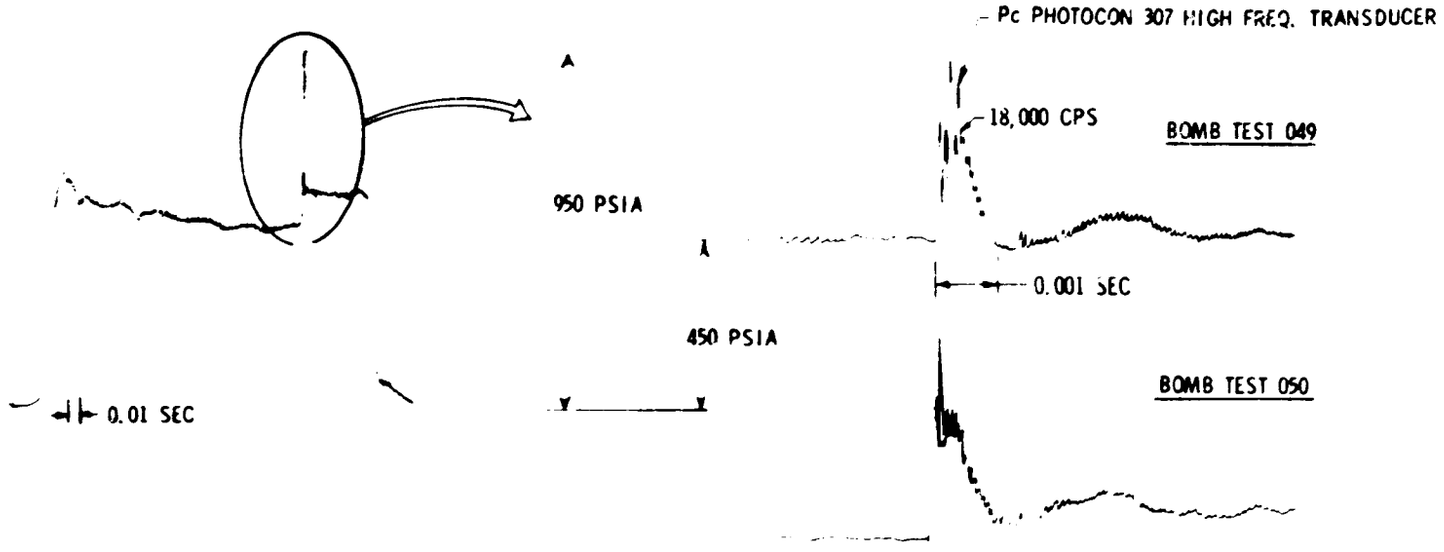

Figure 32. Pressure Recovery from 2 GR RDX Pulse

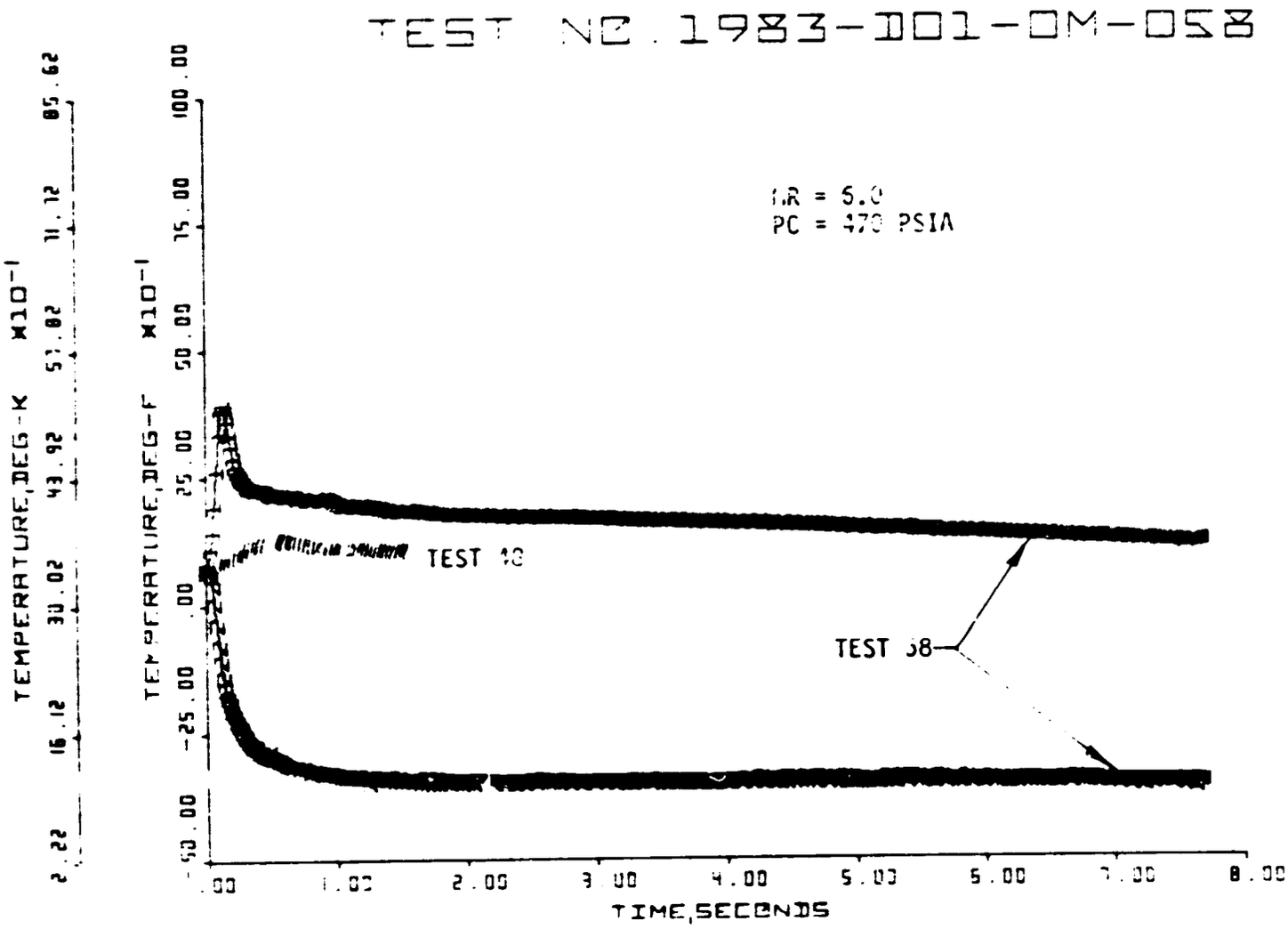

Figure 33. Injector Face Temperature

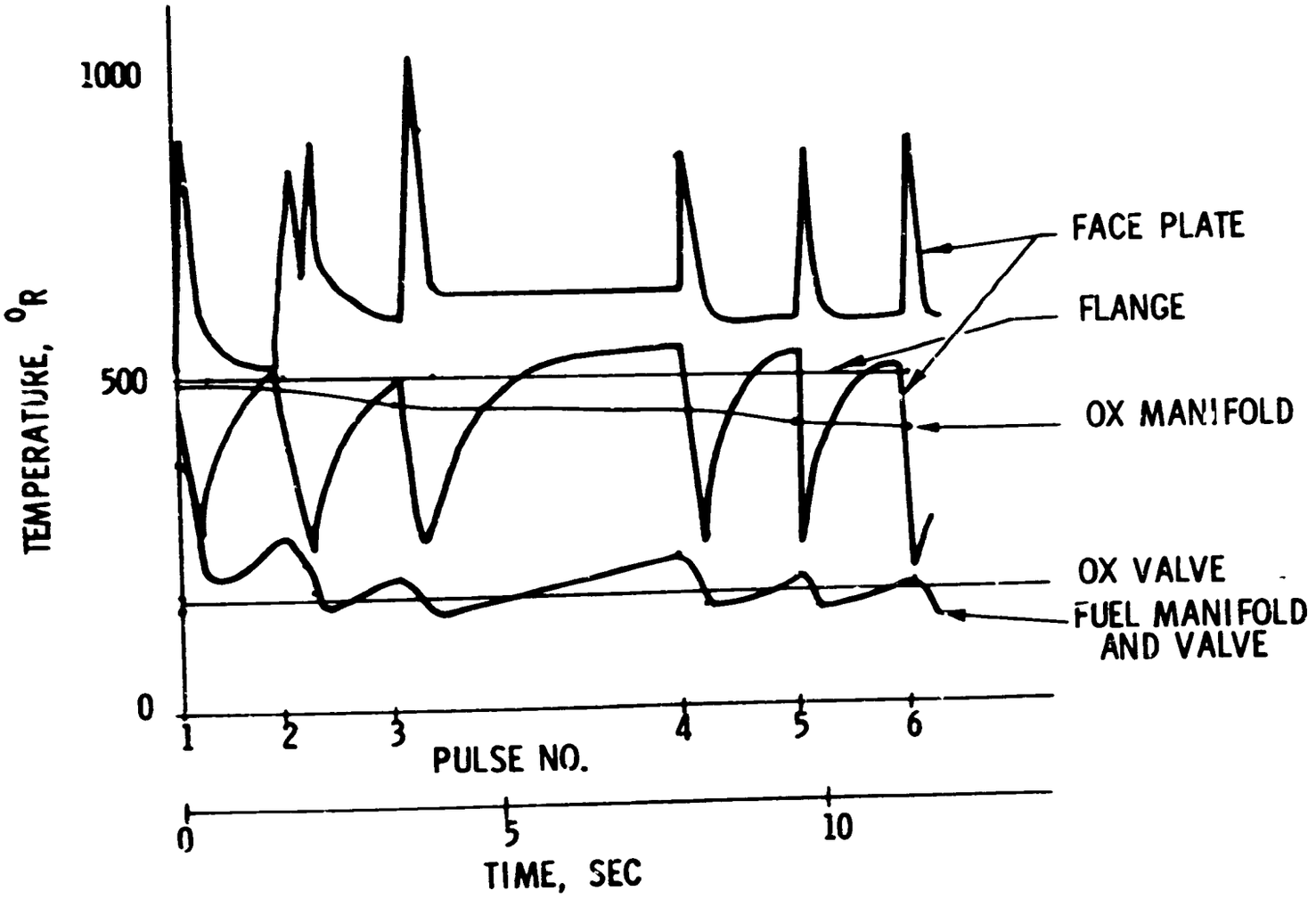

Figure 34. Injector Temperatures, Test 051

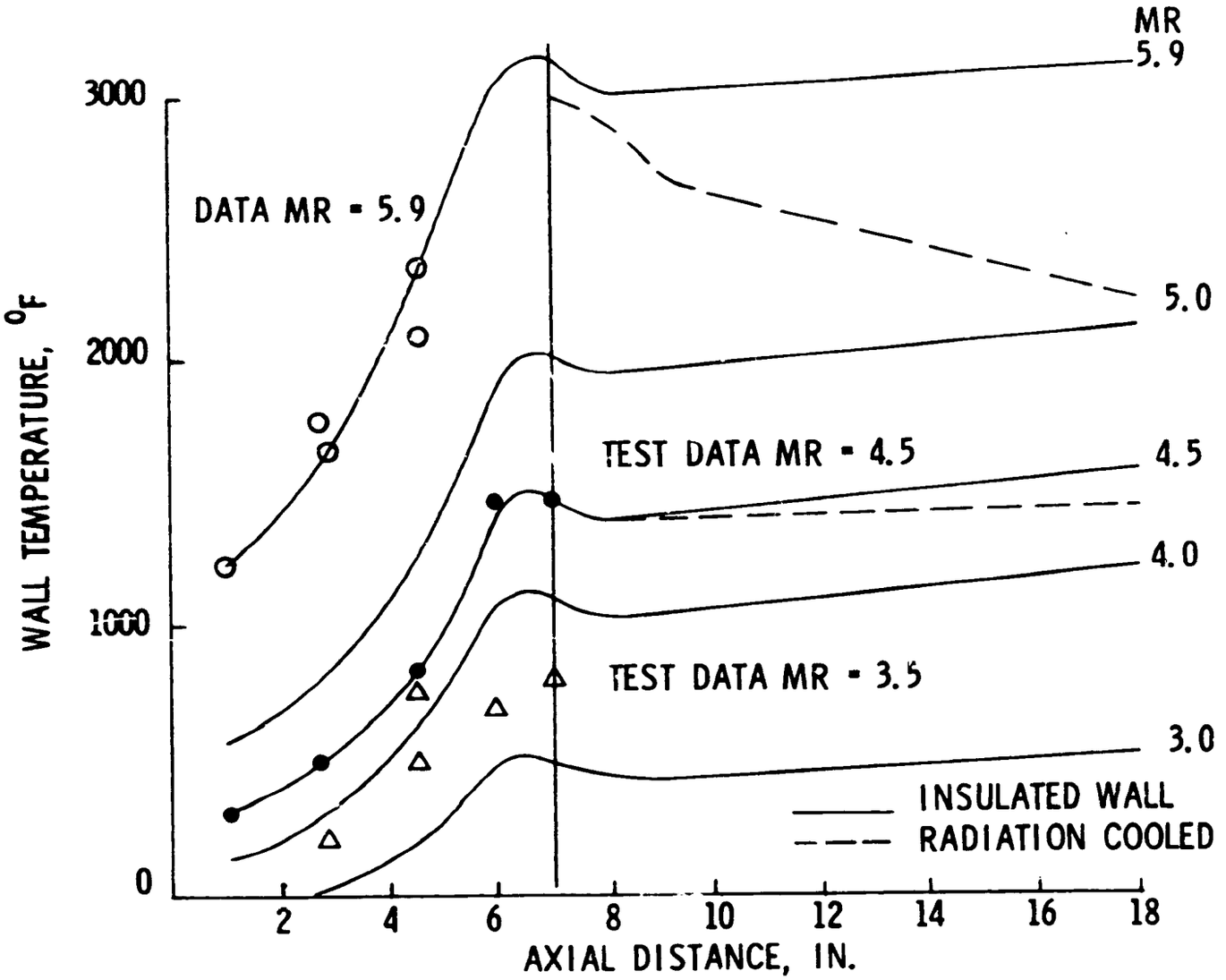

Figure 35. Axial Wall Temperature 7 in. Barrier Cooled Chamber

VI, B, Full Thruster Testing (cont.)

The significance of the data of Figure 35 is that the outer row of fuel elements of the selected injector is providing sufficient cooling to allow the use of a simple lightweight 40:1 free standing insulated wall or radiation cooled chamber provided no high temperature localized streaks exist. The design point maximum wall temperature (MR = 4.5, P_c = 500) of (1088°K) (1500°F) is sufficiently conservative when used with state-of-the-art columbium materials and fused silicide coatings to provide confidence that the scores of hours and hundreds of thousands of pulses required for future missions can be attained. The wide design margins also allow significant mixture ratio shifts to be tolerated for sustained firing and permit the chamber to operate in a heat sink mode for short periods of time when the fuel is in a full vapor locked condition.

2. GH_2/LO_2 Testing

A series of 48 injector firings (Table VII) were conducted at the Design Point 2 conditions using the thruster assembly shown in Figure 23. Table VIII provides a summary of the conditions demonstrated. Table IX provides a listing of the test conditions.

TABLE VIII

SUMMARY OF GH_2/LO_2 INJECTOR TEST CONDITIONS (48 FIRINGS)

P_c	168 - 345 N/cm^2 (243 - 501 psia)
MR	2.2 - 8.7
Fuel Temperature	41 - 100°K (74 - 181°R)
Ox Temperature	90 - 107°K (162 - 192°R)
Injector Body Temp	250 - 292°K (450 - 526°R)
Injector Face Temp	353 (635°R)
Duration min/max	0.075/0.50

a. Pulsing Characteristics

Figure 36 is a record of the first and last pulses of Test No. 013. The electrical pulse width of 0.103 sec resulted in an impulse of

TABLE IX

SUMMARY OF GH_2/LO_2 TESTING - 1983-D01-OM-XXX

Test #	Date	Time	Pulse	Sec Duration	MR	psia P_c	in. L*	°R T_{oM}	°R T_F	°R T_o	Valve Sequence & Flow Time/Millisec From FS 1 IOV	IFV	MOV	MFV	FMO/FMF	T_{ign}/E_{ign}	90% F	Comments
001	3/22	1930	I	.1							12	12	0	5				Igniter only IFN.
002	3/23	1600	I	.15														Igniter only IFN.
003	3/23	1615	I	.1														Igniter cold flow.
004	3/23	1628	A	.2	8.7	481	7.0	503	181	186					80/86	25/90	93	
005	3/23	1644	A	.2	7.5	439		490	154	192					80/86	30/90	93	
006	3/23	1655	A	.2	8.0	453		497	163	189					80/84	30/87	89	
007	3/24	1422	A	.5	6.6	497		522	137	177					65/75	25/70	77	
008	3/24	1437	A	.5	6.5	490		526	174	180				10	60/75	25/88	89	(Hard start)
009	3/25		I	.15										5				Igniter only IFN.
010			A	.15	3.3	381		510	119	170					65/76	30/77	80	
011			A	.075				511										No ignition He in igniter fuel line.
			B	.50														
			C	.075														
012		1930	I, I	.1								8						Igniter only in igniter fuel line.
013		1940	A	.075	5.5	482		512	133	181					62/76	25/76	79	No digital data on pulse B & C.
		+10 sec	B	.50											60/70	25/70	73	
		+20 sec	C	.075											60/70	25/70	73	
014		2000	A	.5	8.7	272		515	86	175					60/72	25/70	77	
015		2010	A	.50	6.9	248		507	80	173					60/71	20/70	72	
016		2012	A	.075				508							55/72	20/70	75	
		+10 sec	B	.5	6.8	243		439	86	173					55/70	23/70	75	
		+20 sec	C	.075				467							55/70	20/70	75	
017	3/27	1351	A	.075	4.0	192	5.5	516	107	163					60/70	22/70	75	
018		1414	A	.075	4.0	501		524	103	162					62/72	25/70	75	
		+10 sec	B	.50											60/65	22/66	85	No digital data pulse B & C.
		+20 sec	C	.075											60/65	22/65	85	Step start due to fuel advance.
019		1439	A	.075				535							60/-	22/70	74	Fuel flow meter not functioning.
		+10 sec	B	.50				522							60/-	25/68	73	
		+20 sec	C	.075				480							58/-	22/66	85	
020		1937	A	.075											60/65	22/70	75	
		+10 sec	B	.50	6.6	450		491	112	180					55/65	22/65	68	
		+20 sec	C	.075				456							55/65	22/62	64	
021		1928	A	.075				511							60/65	23/68	70	
		+10 sec	B	.50	4.0	450		489	104	180					55/66	23/67	68	
		+20 sec	C	.075				461							60/64	23/62	65	
022		1945	A	.075				508							60/67	24/67	70	
		+10 sec	B	.50	3.1	494		497	90	186					55/65	24/63	66	
		+20S	C	.075				460							59/64	23/62	67	
023		2034	A	.075				520							60/68	23/70	71	
		+10 sec	B	.50	2.9	432		511	89	186					60/65	23/65	74	
		+20 sec	C	.075				476							58/62	23/62	62	
024		2017	A	.075				512							60/68	23/69	73	
		+10 sec	B	.50	2.4	439		501	81	182					55/62	23/68	70	
		+20 sec	C	.075				468							55/62	23/63	68	
025		2100	A	.075				510							60/70	20/71	73	Ignition slows as fuel valve advances on openings.
		+10 sec	B	.50	4.2	241		502	93	181					60/66	20/66	84	
		+20 sec	C	.075				470							60/62	20/65	90	
026		2111	A	.075				501							63/64	21/65	75	
		+10 sec	B	.50	2.2	229		498	85	182					65/62	21/65	80	
		+20 sec	C	.075				474							61/63	21/63	80	
027		2122	A	.075				493							60/65	21/65	70	
		+10 sec	B	.50	3.0	247		478	74	184					62/64	21/63	80	
		+20 sec	C	.075				450							60/62	21/62	80	

NOTE: Same abbreviations as Table VI.

IFN - Igniter Function Normal

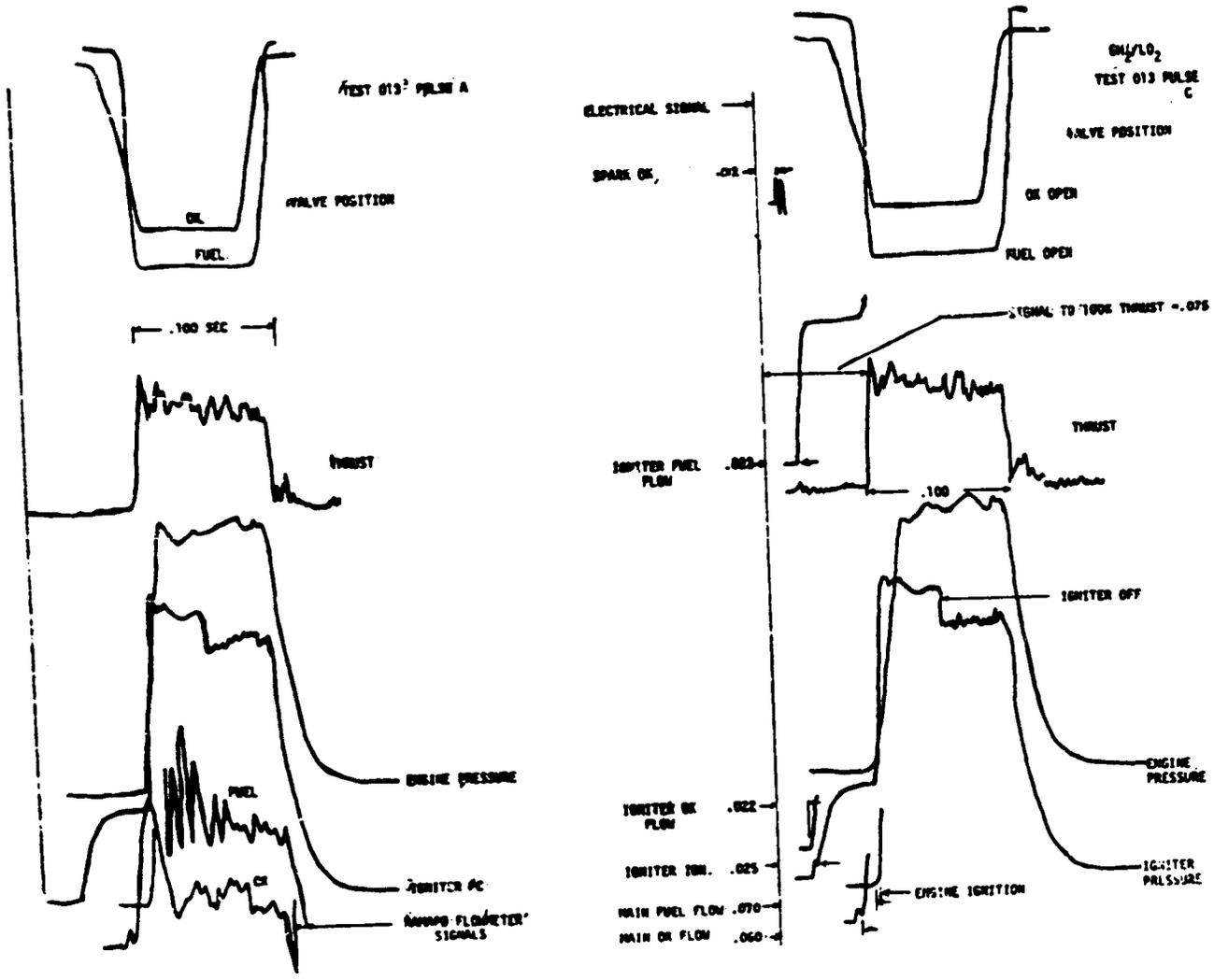

Figure 36. GH_2/LO_2 Sequence and Response Data Pulse Test Series 013

387 N-sec (86.3 lb_f sec). The relationship between valve position, propellant flow, thrust, and engine pressures can be noted on the first pulse. For clarity only, the initial rise of flows and igniter manifold pressures were reproduced on the second pulse.

In this test series the time from main stage ignition to the achievement of 90% thrust averaged about 0.003 sec at 345 N/cm^2 (500 psia) in the 55 to 111°K (100 to 200°R) fuel temperature range. This time tended to increase with reduction in chamber pressure and decreased oxidizer lead times, as illustrated in Figure 37, and is simply due to the feed system inertial effects of the high density LO_2. The effect becomes more significant at lower operating pressures with fill times increasing to up to 0.02 sec. The effect of fuel temperature is estimated to be slight based on the larger band of data for longer oxidizer leads at the higher operating pressure.

The number of different pulse widths run in this phase of the test program were insufficient to generate an impulse vs pulse width curve for the Gas/Liquid system.

b. Pulsing Performance

The pulsing performance efficiency expressed as a % of steady state is shown in Figure 38. The variables which influence the bit impulse are chamber pressure and fire duration. The data suggest the first pulse performance is slightly better than that of restart pulses. The reason for this and the apparent loss in relative efficiency for the longer chamber length is not clear. The data in mass, however, clearly demonstrate that it is possible to maintain in excess of 90% of steady state performance down to about $\approx$ 445 N-sec (100 lb_f sec) impulse with the Gas/Liquid system. This is comparable to the Liquid/Liquid system.

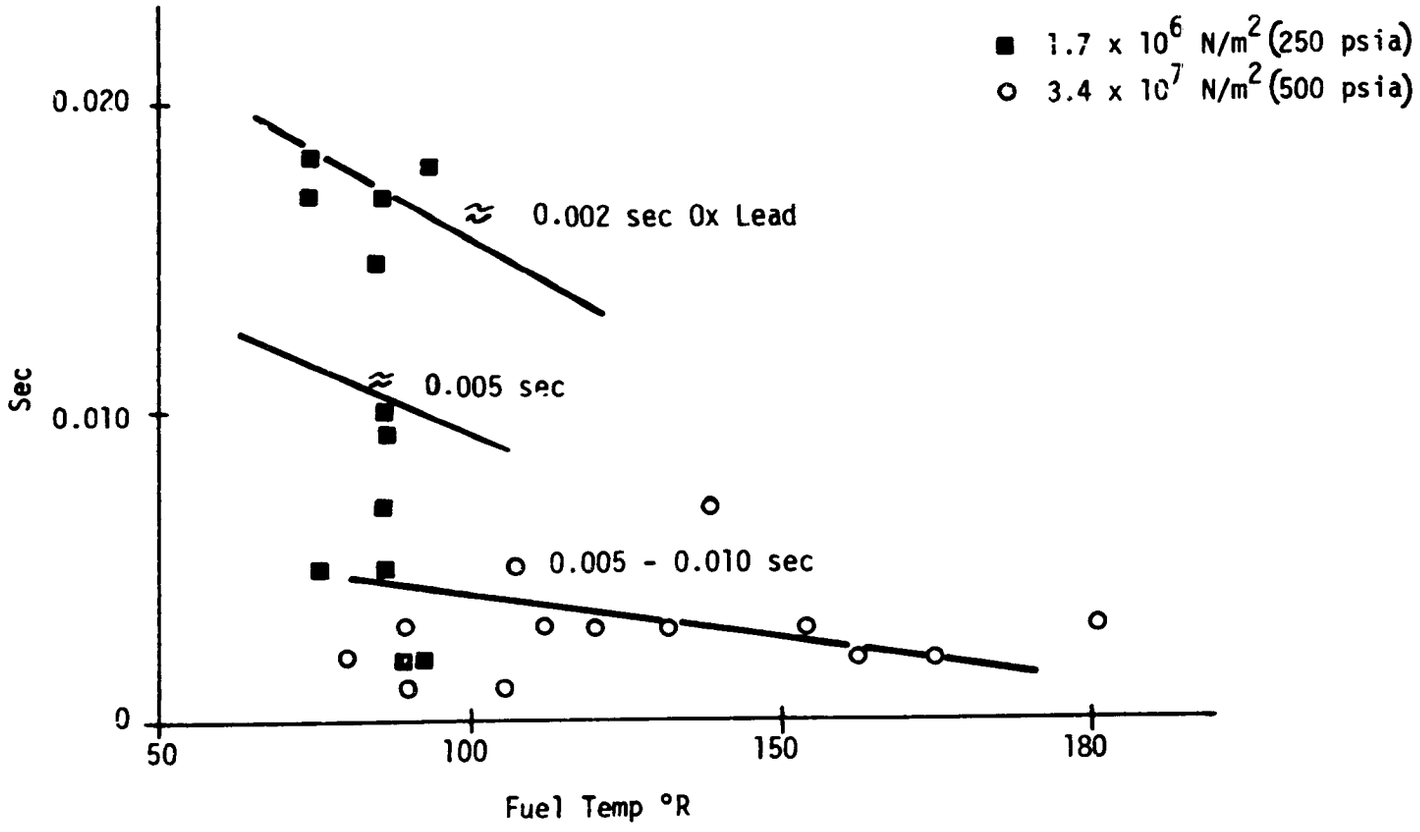

Figure 37. Time from Ignition to 90% Thrust

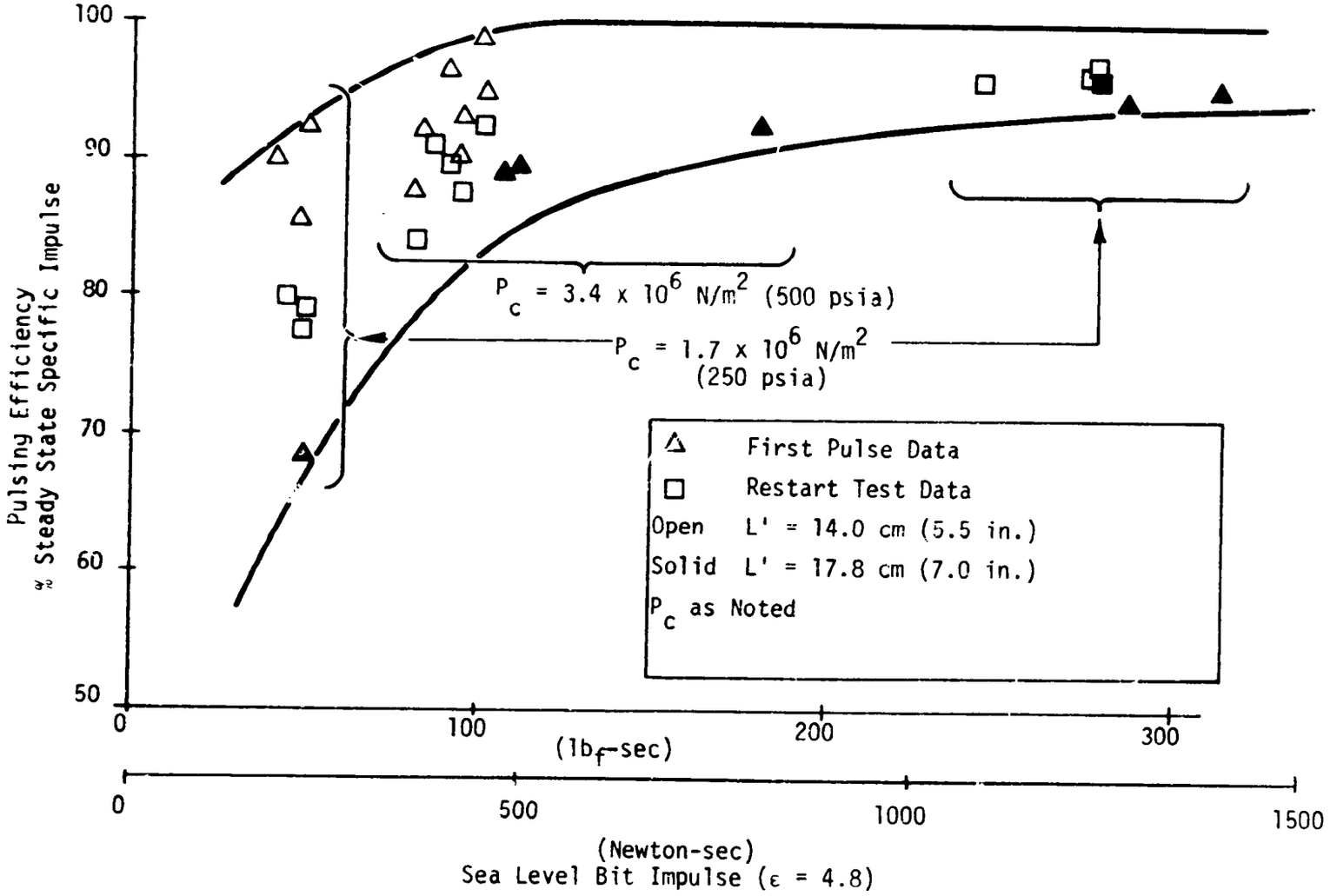

Figure 38. GH_2/LO_2 Pulsing Efficiency

VI, B, Full Thruster Testing (cont.)

Figure 39 shows the shift in pulse MR as the total impulse is reduced. Operation at reduced chamber pressure is noted to result in a lower shift in pulse MR because it slows the LO_2 entry more than the GH_2 entry. The Gas-Liquid system thus appears capable of providing better pulsing capabilities at lower operating pressures. For the conditions demonstrated, there is little difference between first pulse data and that of restart test data.

c. Steady State Performance

The steady state energy release efficiency calculated from the thrust measurements are shown in Figure 40 for 2 chamber lengths and different pressure levels. All test configurations resulted in energy release efficiencies (ERE) greater than 97.5% at the design pressure over a range of mixture ratios from 2.0 to 7.0. The ERE at the nominal MR was 99+ %. Slightly lower values were experienced at the 50% throttled condition.

d. Stability

Chamber pressure in all test firings was monitored by a Kistler 601A transducer located within the resonator cavity. Selected additional tests contained additional flush mounted Photocon 307 tranducers in the heat sink chamber segments. Analyses of these data showed no tendency for unstable operation.

Throttling to 50% chamber pressure was accomplished without encountering unstable operation.

e. Thermal Results

The 0.5 sec injector tests were not of sufficient duration to allow the measurement of the steady state injector face temperatures. The 3 locations of the injector face sampled (Figure 41) indicated that face temperature

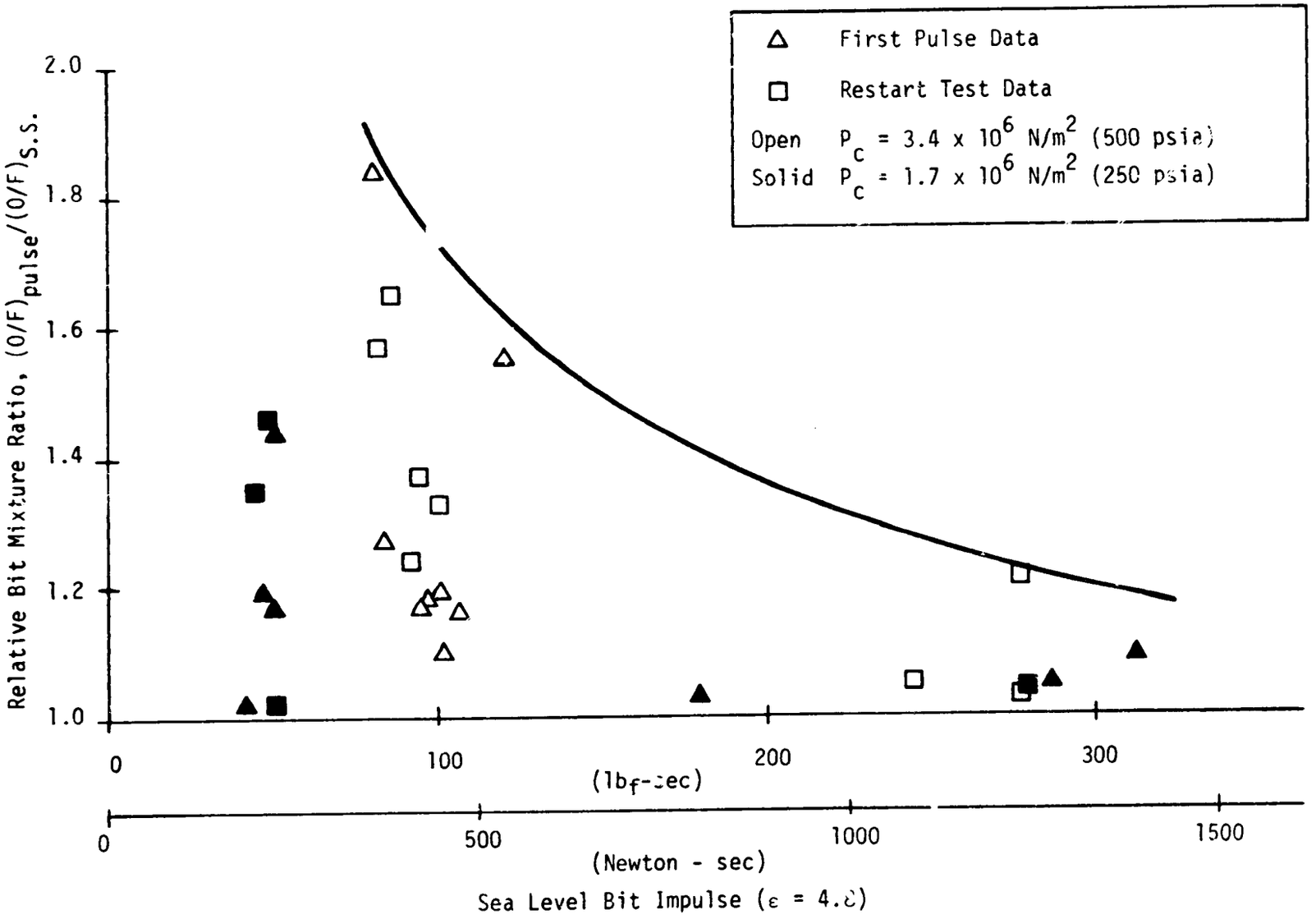

Figure 39. Bit Impulse Effect on Pulse Mixture Ratio, GH_2/LO_2

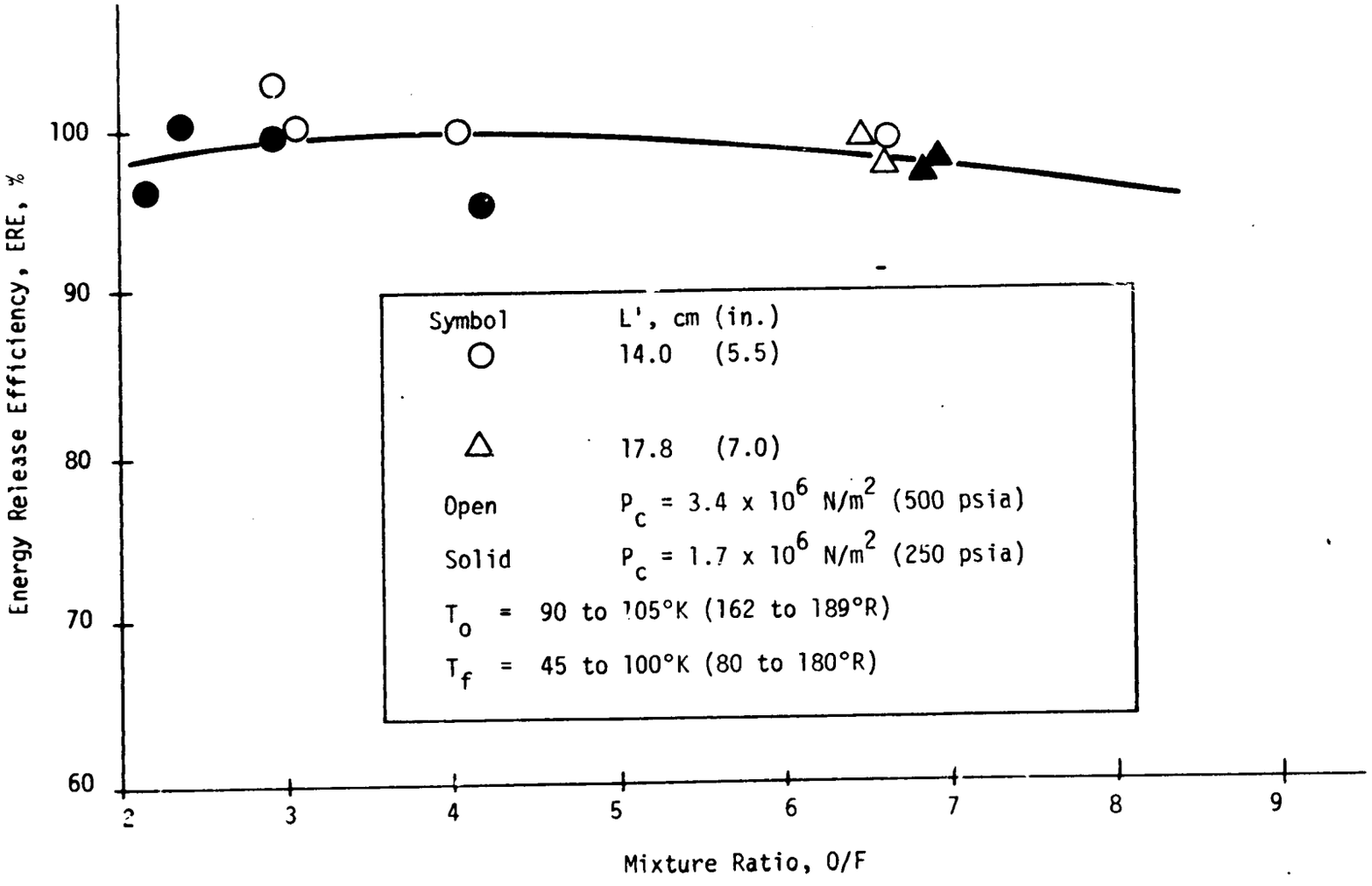

Figure 40. Steady State GH_2/LO_2 Injector Performance

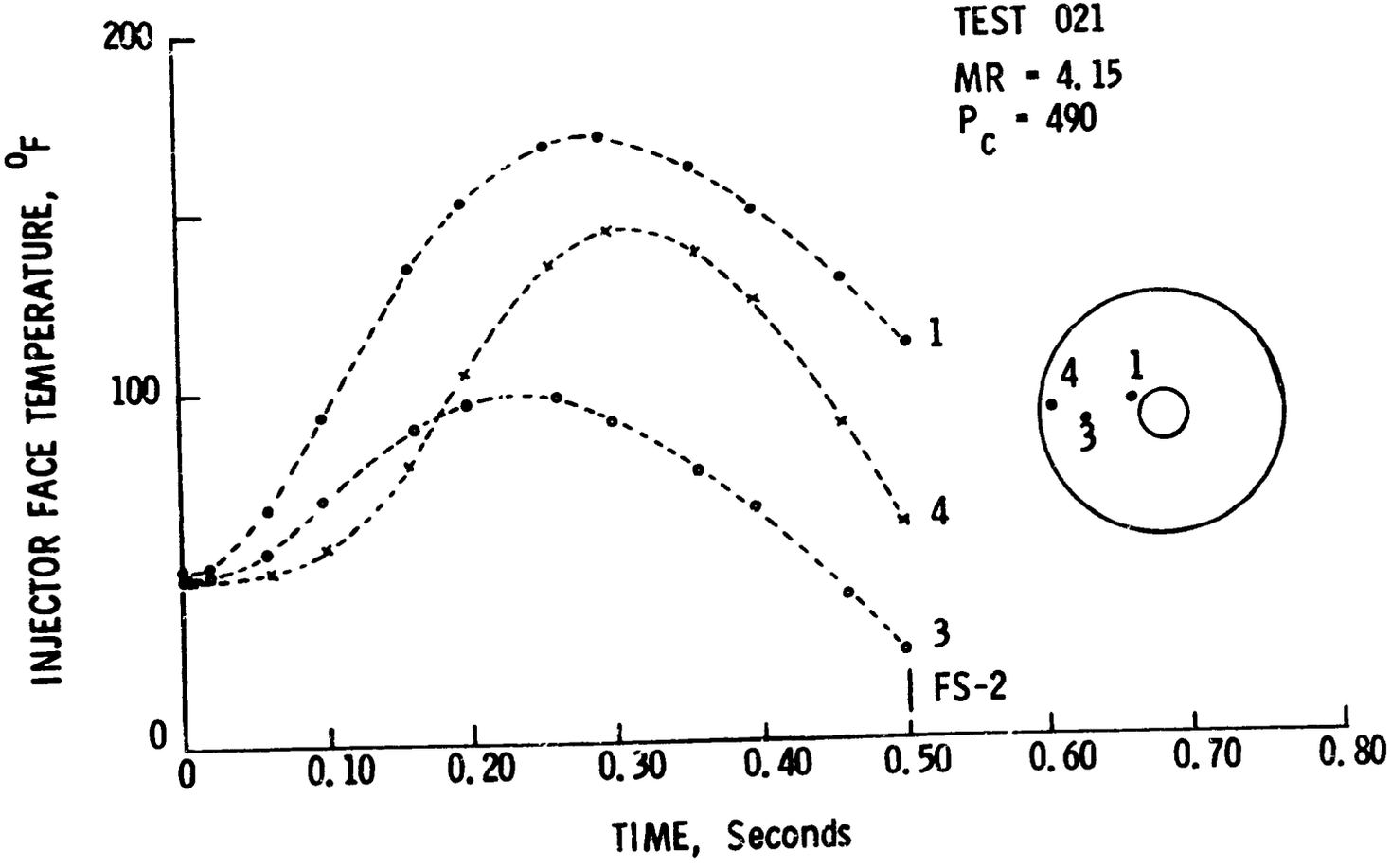

Figure 41. GH_2/LO_2 Injector Face Temperature

increased for the first 0.3 sec of the firing and then dropped. Injector face temperatures did not exceed a peak value of 367°K (200°F) and all data indicated that the steady state operating temperature would be less than 311°K (100°F). This rise and fall thermal behavior is due to the use of the thick face which is cooled from the back and orifices and is heated from the front. The thermocouples are located on the flame side half way between orifices and are influenced first by heating and later by the penetration of the remote surface cooling.

Figure 42 compares the measured and predicted gas-side wall temperatures and the coolant bulk temperature rise of the regeneratively cooled combustion chamber. Steady state wall temperatures were reached rapidly in the chamber because the relatively thin wall thicknesses employed; the design analyses is noted to be conservative.

The effect of higher mixture ratio is noted to become more pronounced at the end of the cylindrical section of the chamber. This is due to the consumption of the excess fuel near the wall and probably some streaking caused by unvaporized oxidizer separating from the lower density gases turning into the nozzle. The maximum regeneratively cooled chamber temperatures at the design MR and PC are about 561°K (550°F) which is about 56°K (100°F) below the design predictions and thus assures an adequate life for this component.

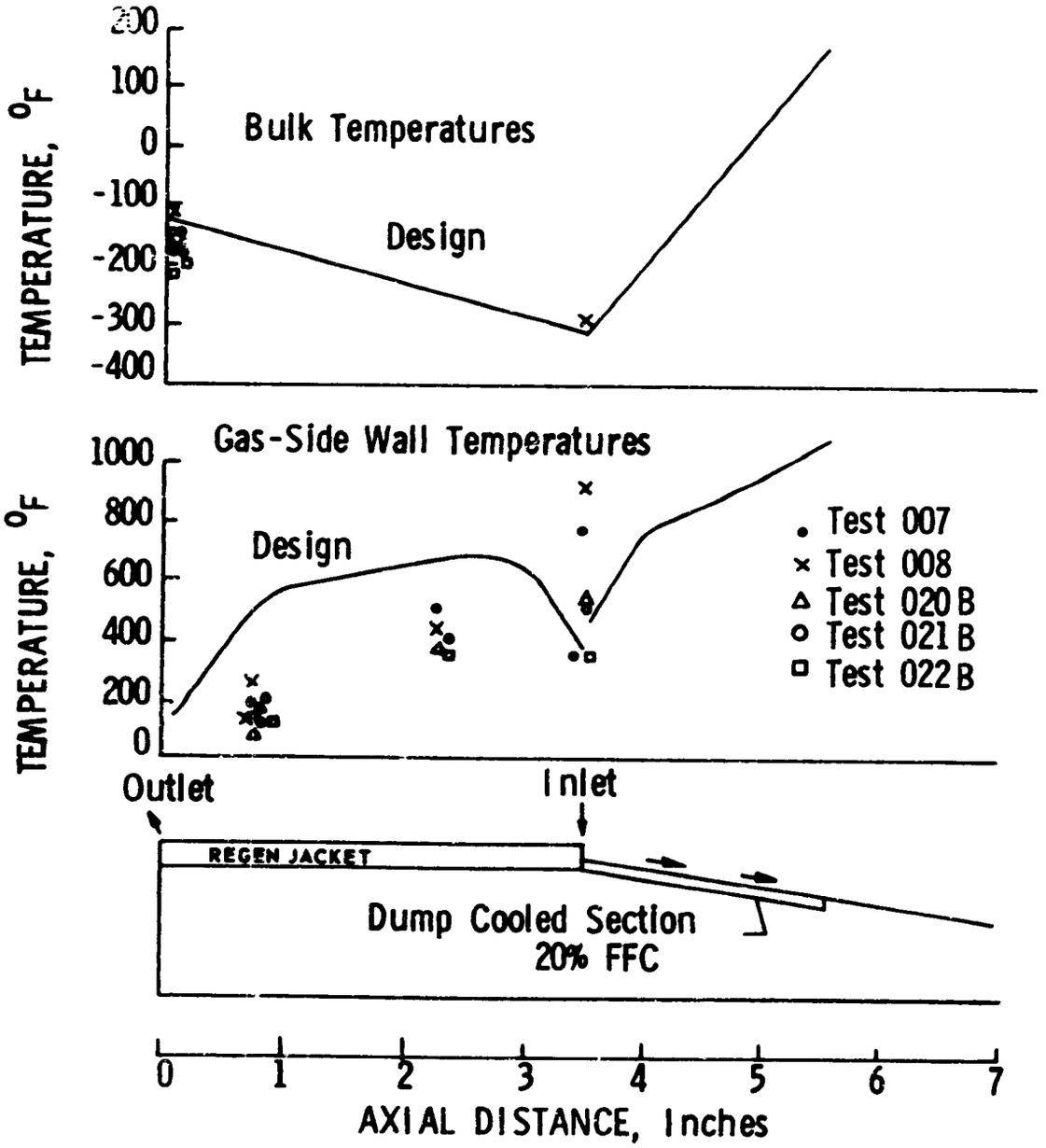

Figure 42. GH_2/LO_2 Cooled Thrust Chamber Thermal Data

VII COOLED CHAMBER DESIGN AND FABRICATION

A. DESIGN ANALYSIS

1. Liquid/Liquid (Design Point 1)

Three cooled chamber designs that exploit the barrier cooling characteristics of the liquid/liquid injector were considered and are shown in Figure 43. The thermal "stand off" concept was introduced to reduce the heat load that soaks back into the injector after firing. The cooled duct approach was the most conservative since it would permit additional hydrogen film coolant to be introduced into the chamber to supplement the barrier cooling.

A study was made of the effect of chamber length and percent of supplemental FFC on wall temperature, performance and material selection. The results are shown in Figure 44 for 17.8 cm (7.0 in.) and 21.6 cm (8.5 in.) barrier cooled designs (with or without thermal stand off) and for 17.9 cm (7.0 in.) and 21.6 cm (8.5 in.) chambers utilizing dump cooled ducts to introduce supplemental film cooling. Both ducts account for 3.81 cm (1.5 in.) of the chamber length. The 12.1 cm (4.75 in.) duct extends 8.26 cm (3.25 in.) into the 20.3 cm (8 in.) chamber and the 8.26 cm (3.25 in.) duct extends 4.45 cm (k.75 in.) into the 17.8 cm (7 in) chamber so that in both cases the film coolant would be introduced 7.62 cm (3 in.) upstream of the throat. The 17.8 cm (7 in.) barrier cooled columbium design concept was selected for fabrication since it was the simplest and provided adequate thermal margin for operation over the required 3.5 to 5.0 MR range with very little sacrifice in performance (See Figure 44).

Of the candidate columbium alloys the selection was narrowed down to Cb 103 and FS 85. The FS 85 alloy was selected for the chamber because of its higher melting point and its 24,133 N/cm^2 (35,000 psi) ultimate tensile strength at 1093 °C (2000°F) versus 17,238 N/cm^2 (25,000 psi) for Cb 103. The coating that was selected was R512E. The chamber design is shown in Figure 45 (PN 1164223-6).

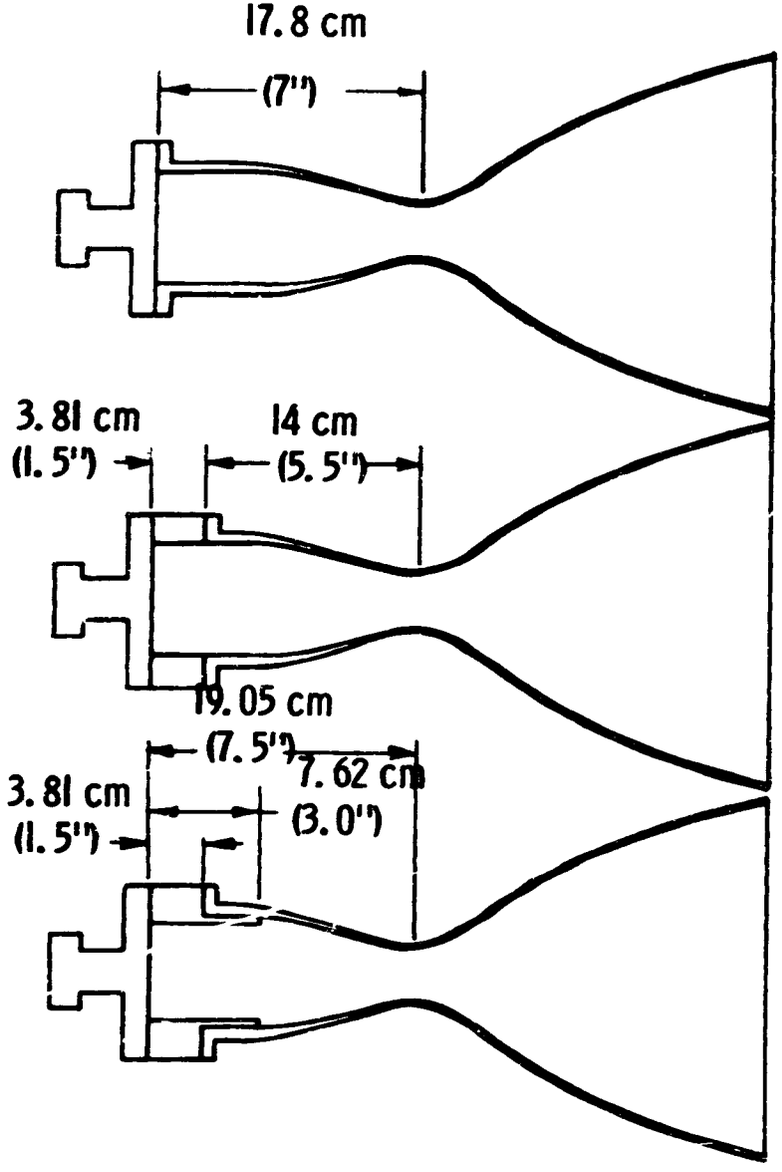

FREE STANDING 17.8 cm (7") L' COLUMBIUM

FREE STANDING 14 cm (5.5") L' COLUMBIUM CHAMBER WITH 3.81 cm (1.5") STEEL THERMAL STAND OFF

FREE STANDING 14 cm (5.5") L' COLUMBIUM OR STEEL NOZZLE WITH 7.62 cm (3") COOLED DUCT

Figure 43. Candidate Cooled Chamber Designs

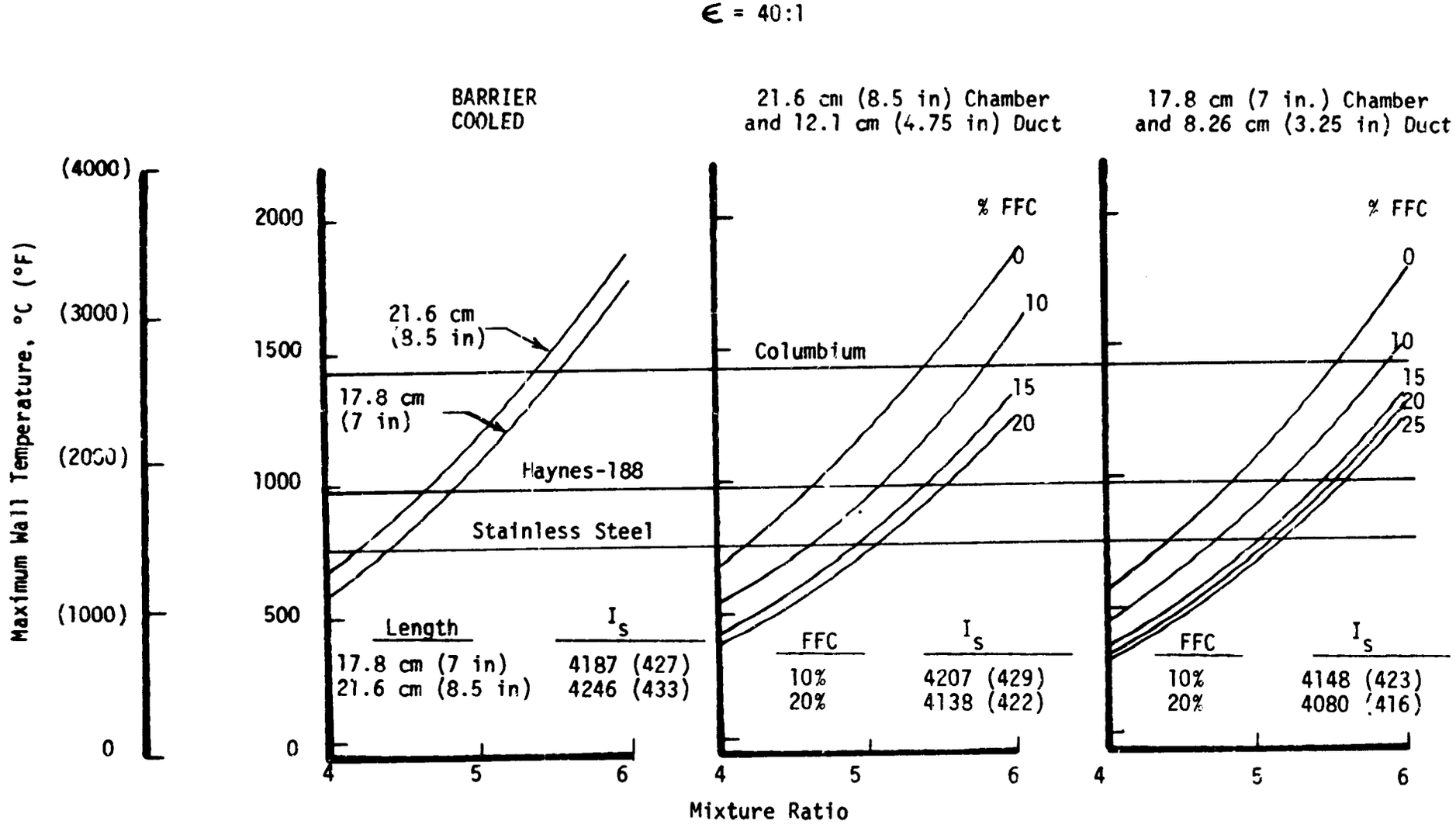

Figure 44. Thruster Length and Cooling Optimization

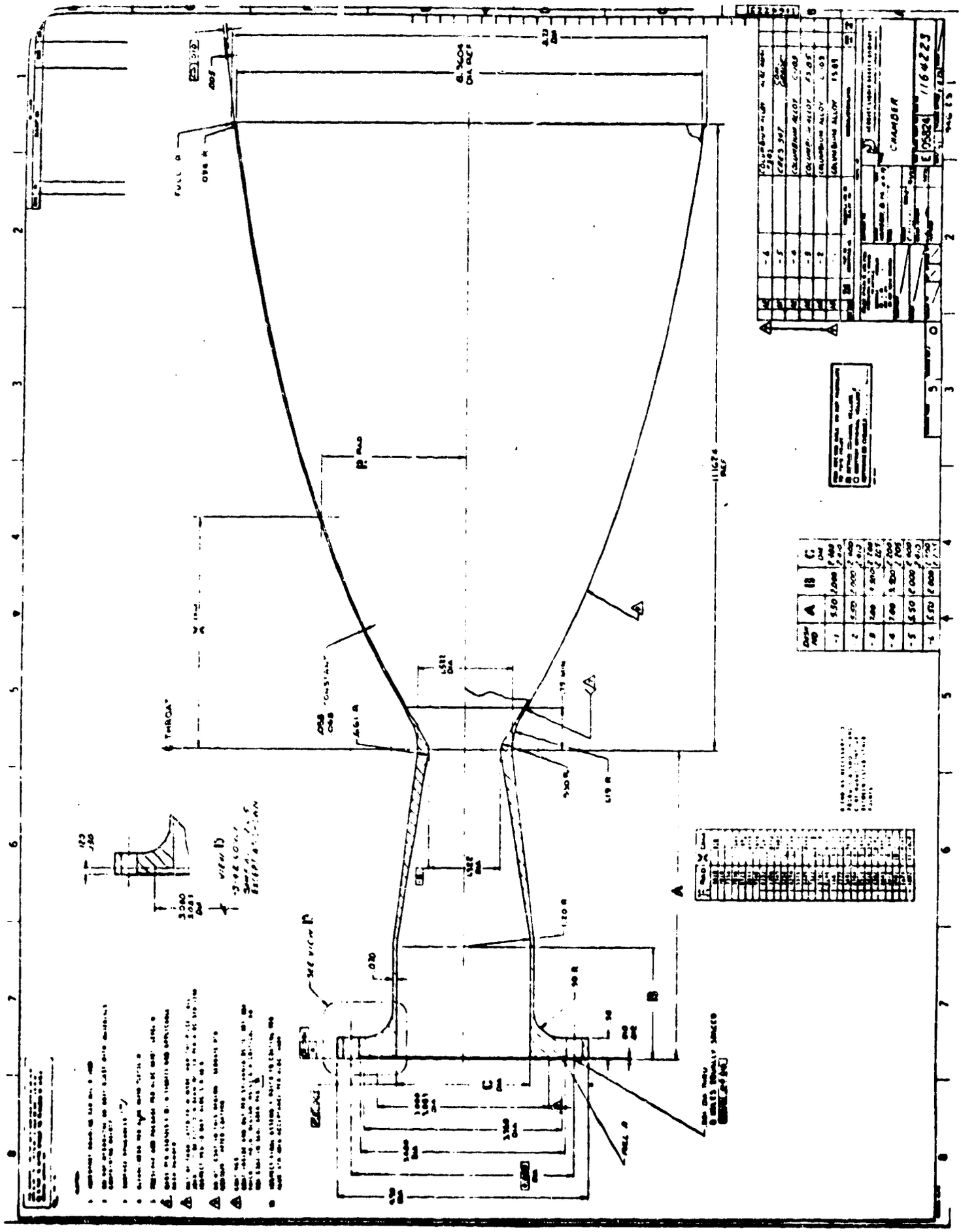

Figure 45. Chamber Drawing

VII Cooled Chamber Design and Fabrication (cont.)

The design of the uncooled spacer that serves as a thermal stand off to reduce heat soak from the columbium chamber to the injector is shown in Figure 46. A double walled (concentric cylinder) design was used to minimize mass (thermal capacitance). The inner wall serves as the pressure barrier and the outer wall transmits the load to the crush gasket sealing surfaces on the forward and aft flanges (Note ⚠ in Figure 46). The uncooled spacer contained four gas side thermocouples and a pressure tap into the resonator cavity formed between the spacer and the injector face.

The liquid/liquid thruster was predicted to operate at nominal design point 1 conditions with a 816 °C (1500°F) throat temperature and 4187 N-sec/kg (427 lbf-sec/lbm) specific impulse.

2. Gas/Liquid (Design Point 2)

The gas/liquid thruster design consisted of the injector and regen section shown in Figure 23, a film cooled nozzle and a dump cooled section that introduced the film coolant into the nozzle. The Design Point 2 cooled chamber concept is shown in Figure 47. Fuel was introduced at the aft end of the regen section. A tap off located 180° from the inlet to the regen section was used to supply hydrogen from the regen section to the dump cooled section via a u-shaped tube. The split of hydrogen between the regen passages/injector circuit and the dump/film coolant circuit was controlled by a dishpan orifice located at the inlet to the dump cooled section.

The details of the dump cooled section are shown in Figure 48. It consisted of a CRES shell (Item 1) into which was furnace brazed an OFHC copper liner (Item 2). The dump cooled passages were machined into the OD of the liner as 90 - .0813 cm wide x .0686 cm deep (.032 in. wide x .027 in. deep) rectangular passages. The film cooling slots were designed for a FFC flow that was 27% of the total fuel flow rate. There were provisions for

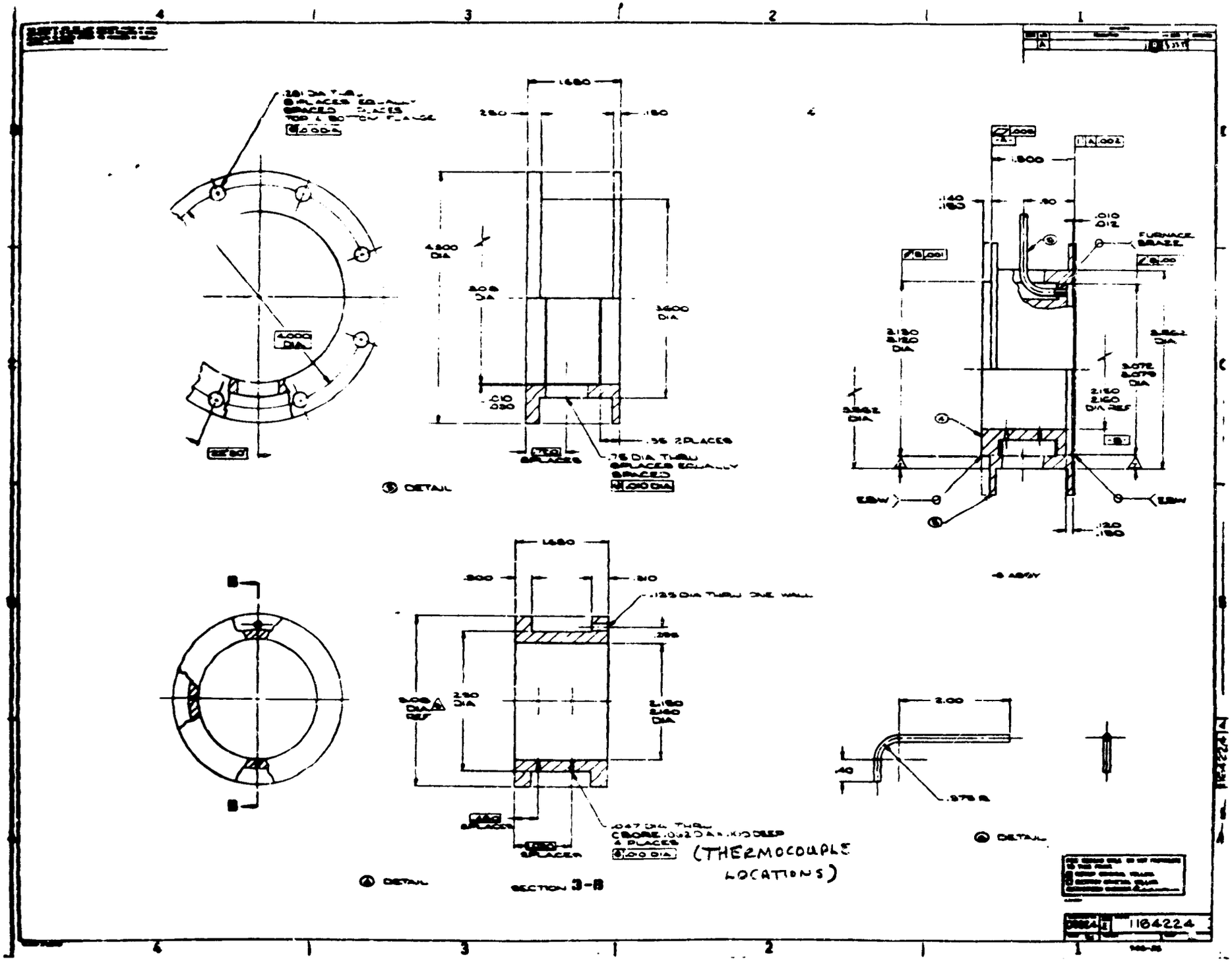

Figure 46. Uncooled Spacer

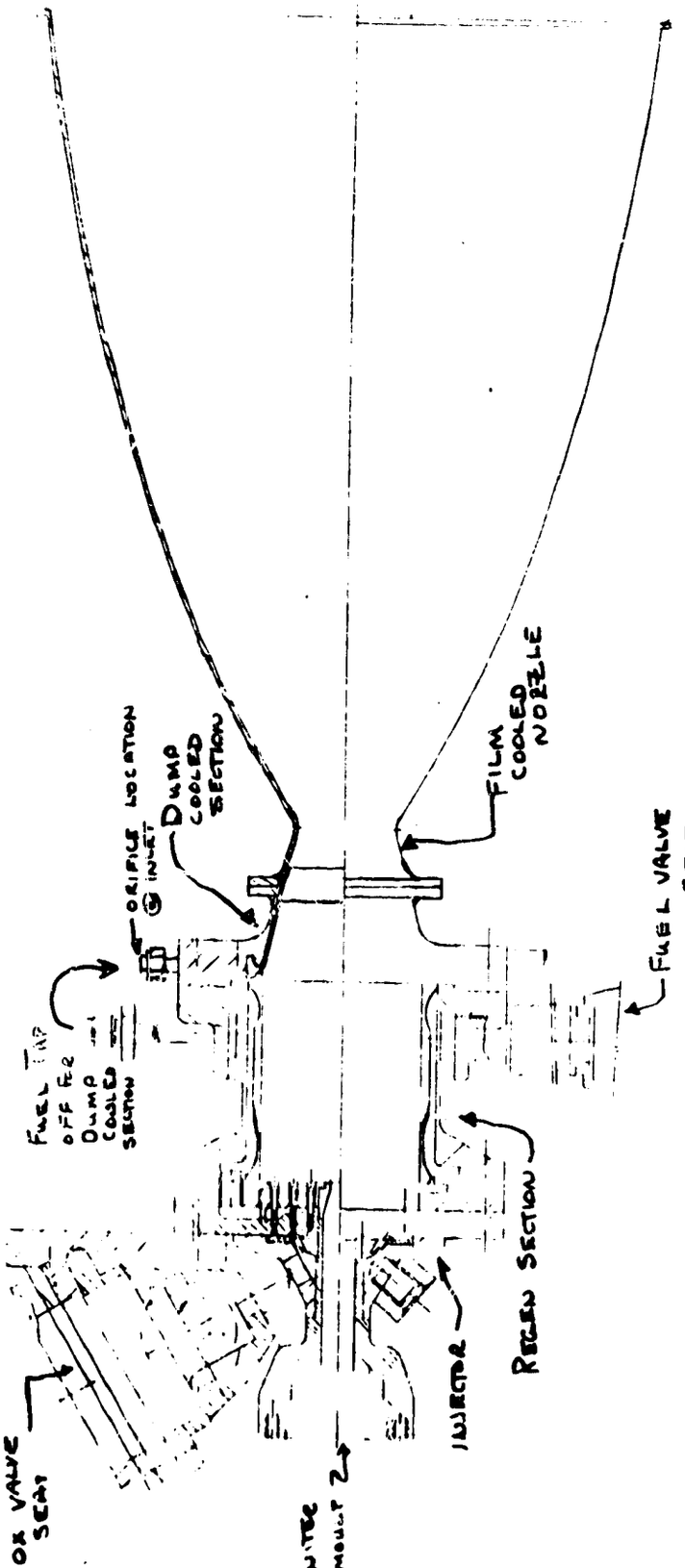

Figure 47. Design Point 2 Thruster Concept

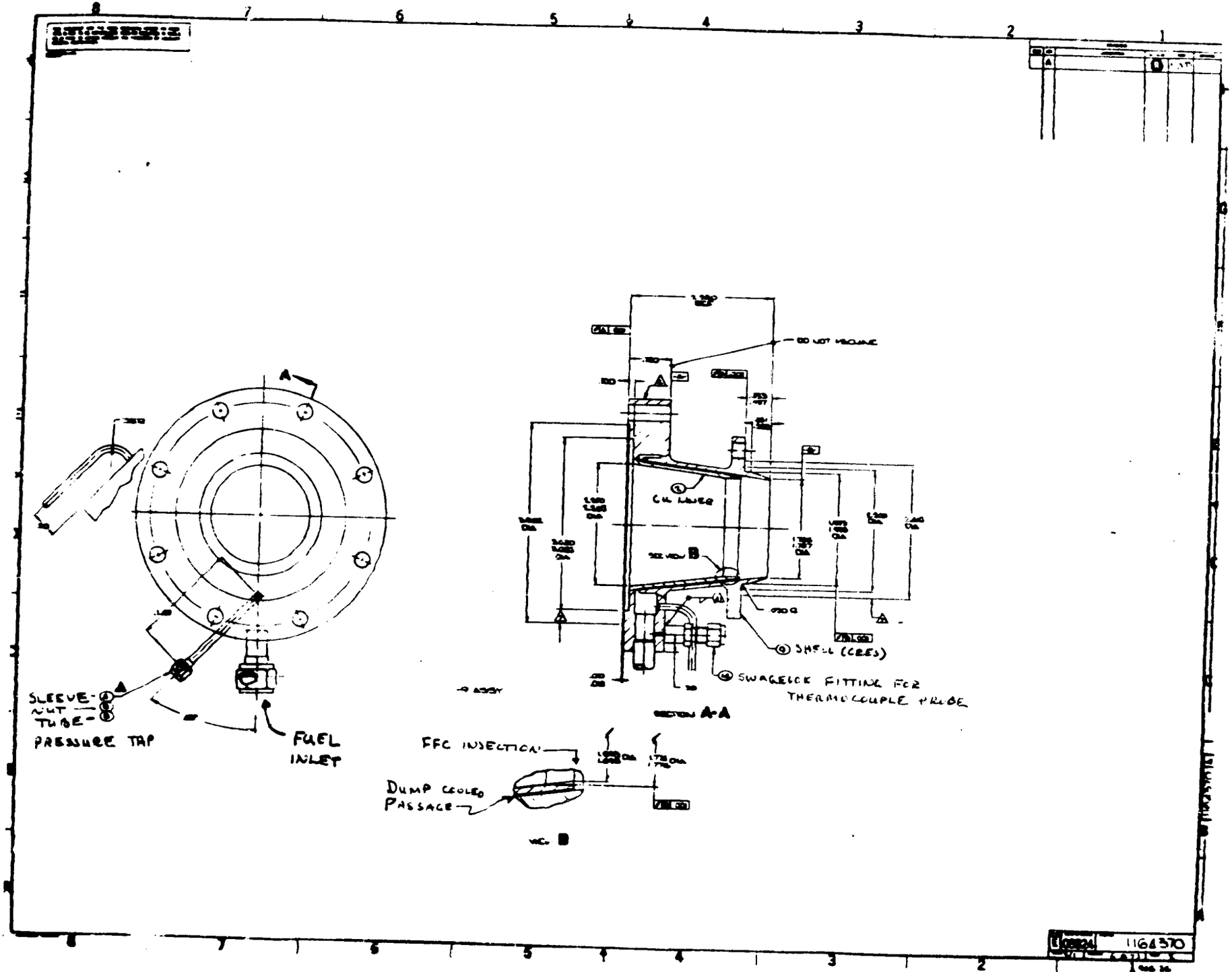

Figure 48. Dump Cooled Chamber Assembly

measuring temperature and pressure of the coolant in the manifold via a pressure tap (tube, Item 6) and a Swagelok fitting (Item 14) by which a thermocouple probe was secured in the manifold.

The design of the nozzle is illustrated in Figure 49. Candidate materials were stainless steel, Haynes 188 and columbium. The PN 1163877-4 (Haynes) nozzle was selected. The excellent creep strength (1149 °C (2100 °F) limit), oxidization resistance and high yield strength (over 27,580 N/cm^2 (40,000 psi) at elevated temperatures (871 °C (1600 °F)) of Haynes-188 resulted in it being selected over CRES. The coolant flow requirements of the dump cooled section limited the adiabatic wall temperatures in the throat, as will be shown subsequently, to low enough temperatures that the high temperature capabilities of columbium were not required.

The dump cooled section was designed to operate with a 549 °C (1020 °F) maximum wall temperature with 27% FFC. On the basis of the sea level test results the following predictions were made for the cooled chamber design operating with 27% FFC:

Performance: 3222 N-sec/kg (328.5 lbf-sec/lbm)
Thermal Characteristics

Throat Temperature: 449 °C (840 °F)
Maximum Skirt Temperature: 538 °C (1000 °F)

To achieve the program goal of 4266 N-sec/kg (435 lbf-sec/lbm) it was predicted that the FFC flow rate would have to be reduced to 20.5% of the total fuel flow rate. With 20.5% FFC at nominal operating conditions the thermal characteristics were predicted to be:

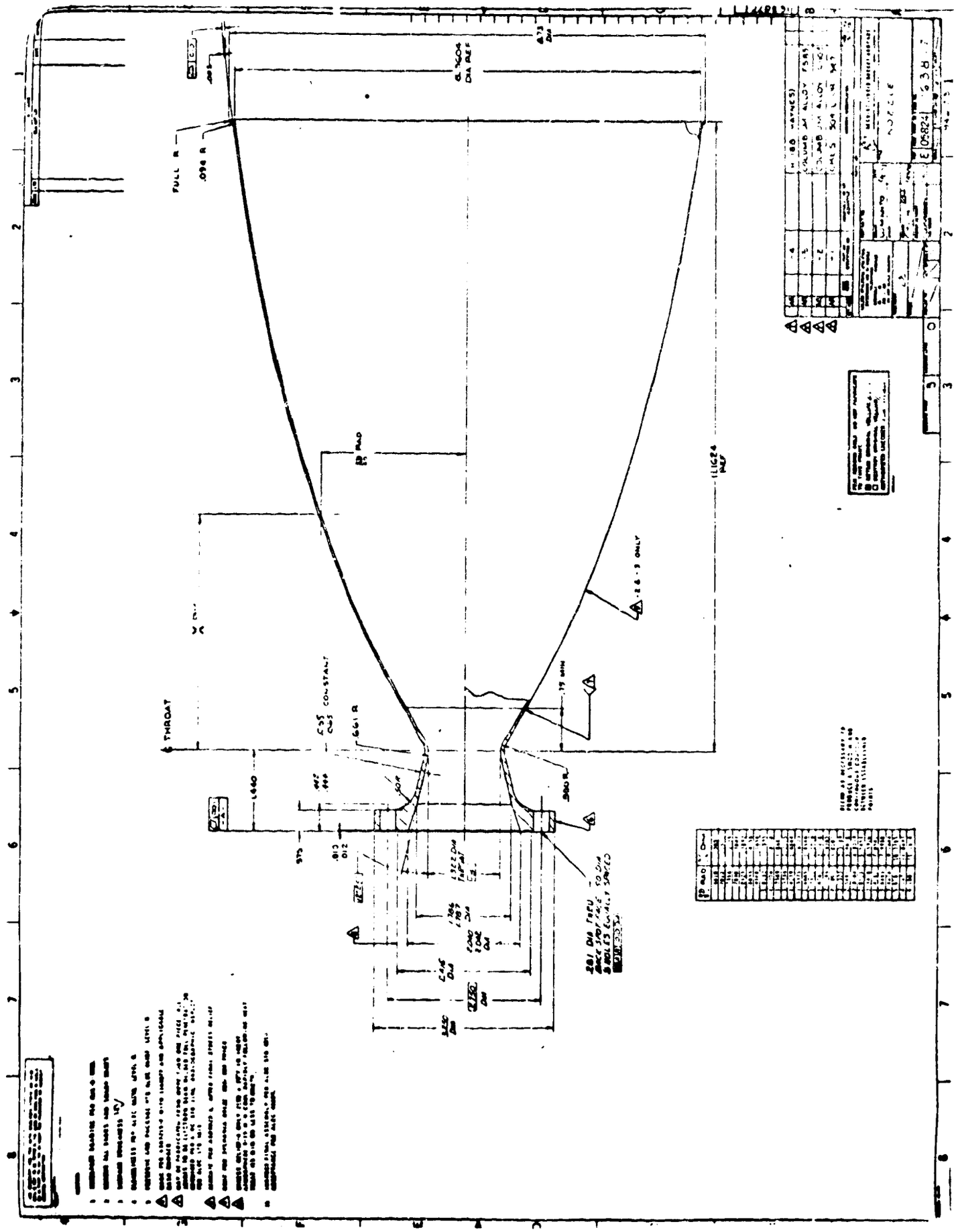

Figure 49. Nozzle Configuration

VII Cooled Chamber Design and Fabrication (cont.)

Throat Temperature:	616 °C (1140 °F)
Maximum Skirt Temperature:	804 °C (1480 °F)
Maximum Temperature, Dump Section:	635 °C (1175 °F)

The thermal limits were considered to be 871 °C (1600 °F) in the throat (high temperature strength), 1149 °C (2100 °F) for the skirt (Creep) and 649 °C (1200 °F) for copper (strength and oxidization resistance). The dump cooled section was not designed for operation with less than 19% FFC. The throat and skirt were predicted to reach their limit at approximately a 16% FFC flow rate.

B. COOLED THRUST CHAMBER FABRICATION

1. Liquid/Liquid (Design Point 1) Hardware

The uncooled spacer was fabricated per print. No difficulties were encountered.

Four gas-side chromel/alumel thermocouples were installed on the uncooled spacer. These thermocouples extended through the wall of the spacer with the thermocouple bead flush with the chamber ID. They were furnace brazed in place to effect a good thermal contact with the wall, minimizes discontinuities and provide the gas seal. The uncooled spacer was also instrumented with four exterior chromel/alumel thermocouples at the location of the gas-side ones (provides ΔT through wall). The locations of the thermocouples are shown in Figure 46.

Three problems were encountered in the fabrication of the columbium chamber. The chamber was made in three parts. The flange and chamber were made from separate forgings; the skirt was made from sheet metal. The first problem was fracture of one of the raw material billets (chamber) during the forging operation. Fracture was attributed to operator error in orientating the grain relative to the forming process. The second billet (flange) and a replacement billet for the chamber forging were formed without incident.

VII Cooled Chamber Design and Fabrication (cont.)

A second problem was encountered in the fabrication of the nozzle. Sheet stock .152 cm (.060 inch) thick was welded into a cone, the weld ground flush and the nozzle rough formed on a die. An anneal cycle following the weld was omitted from the planning and the material adjacent to the weld cracked during the forming operation. Because it was readily available, the nozzle was made from .0762 cm (.030 inch) thick Cb 103. A .0762 cm (.030 inch) thick aluminum liner was used to permit the existing dies to be used to accomodate the difference in material thickness. The aluminum liner was used on the exterior of the nozzle so that the inside contour was smooth. The chamber/nozzle joint was blended on the exterior to avoid a step change in thickness at the interface of the .152 cm (.060 inch) thick chamber wall with the .0762 cm (.030 inch) thick nozzle.

The third problem occurred in joining the nozzle to the chamber. A .0762 cm (.030 inch) thick Cb 103 nozzle extension was fabricated and welded to the FS-85 chamber. The weld was not annealed. Some distortion of the nozzle extension at the weld joint had occurred, so the nozzle extension was reshaped on the forming die. This resulted in circumferential cracks in the weld area and one longitudinal crack in the FS-85. The FS-85 is not as forgiving as the Cb 103 and apparently the heat treat after weldment cannot be omitted.

The .0762 cm (.030 inch) thick Cb 103 nozzle extension was machined off and second .0762 cm (.030) thick Cb 103 replacement nozzle extension was made. The longitudinal crack in the FS-85 chamber was repaired by EB welding. The nozzle extension was welded to the FS-85 chamber and the assembly heat treated. The weld area was ground smooth on the inside of the chamber to remove the penetration. The joint was satisfactory.

It is the opinion of the ALRC personnel who followed the fabrication of the Columbium chamber that the problems resulted from lack of experience with FS-85 by the vendor. There is nothing basically wrong with FS-85. It is not as forgiving as Cb-103 and therefore more difficult to

fabricate, but this is offset by the advantage of its higher melting temperature and higher strength at elevated temperatures. More frequent heat treat is required.

The PN 1164223-6 chamber is shown in Figure 50 after coating with the R512E fused silicide.

Seventeen chromel alumel thermocouples were installed on the Columbium chamber as shown in Figure 51. Eleven thermocouples were in line to measure the axial temperature profile. There were four additional thermocouples in the throat area located circumferentially from the line of axial thermocouples. Two thermocouples in addition to the axial one, were installed on the weld on the divergent section of the chamber.

The high voltage cable that conducts the spark from the exciter to the spark plug was frequently a cause of no ignition. Vacuum conditions combined with the moisture from the steam ejection system and thruster combustion products causes electrical shorts in the connectors. On the other hand, all testing done on the ITA program (Ref. 9) with the integral exciter/spark plug was accomplished with 100% reliability. Use of an integral exciter unit on this program was therefore investigated.

The geometry of the ETR spark plug was sufficiently different from that in the electrode area of the integral exciter/spark plug units that the integral unit could not be machined to replace the ETR spark plug. Instead, the spark plug was modified to permit the integral unit to be used with the ETR spark plug. The adapter on the aft end of the spark plug that normally mates to the high voltage cable was modified to mate to the integral ITA unit. A teflon guide and spring were made to fit inside the spark plug porcelain and complete the electrical contact between the aft end of the spark plug electrode and the discharge end (forward end) of the electrode and the integral unit. A spring contact is used on jet engine spark systems. The advantage of the modified system over the cable and remote exciter system is the

Figure 50. Columbium Chamber

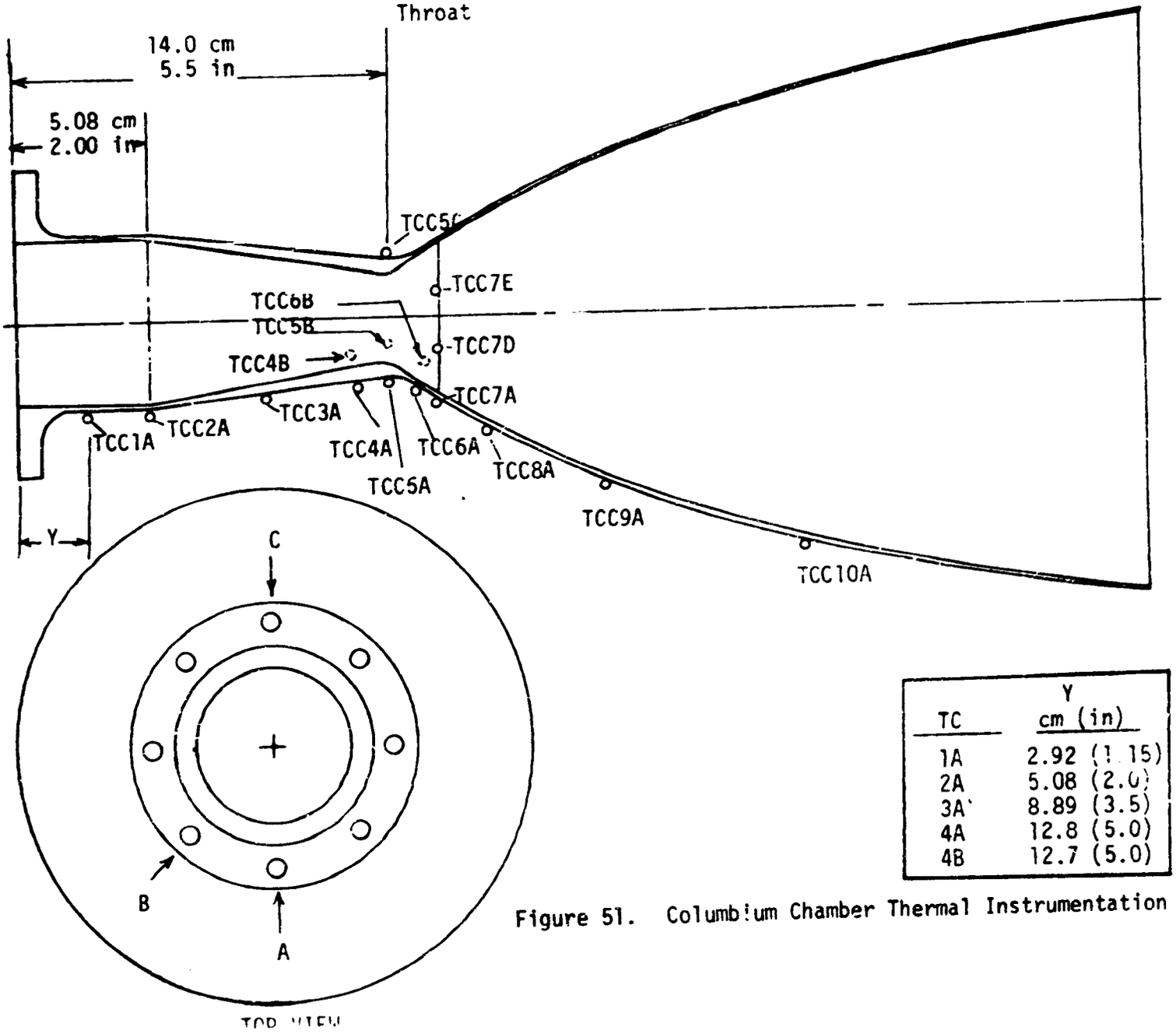

TC	Y cm (in)
1A	2.92 (1.15)
2A	5.08 (2.0)
3A	8.89 (3.5)
4A	12.8 (5.0)
4B	12.7 (5.0)

Figure 51. Columbium Chamber Thermal Instrumentation

reduction in the number of high voltage connections from four to one. A sketch of the spark plug assembly is shown in Figure 52.

2. Gas/Liquid (Design Point 2) Hardware

No major problems were encountered in the fabrication of the Haynes-188 nozzle or the dump cooled section. Haynes-188 nozzles (throat sections and skirts) were fabricated for the contract NAS 3-15850 (Ref. 9) hardware. There were brittle fracture problems associated with the anneal cycles and the attempt by the vendor to make the skirt in one piece. The Haynes-188 nozzle for this program was made in two pieces and none of the contract NAS 3-15850 problems were encountered. The experience on this program supports the Ref. 9 conclusion that the contract NAS 3-15850 problem was one of vendor methodology and not inherent on the Haynes-188 material.

Two thermocouples were installed forward and aft on the exterior shell of the dump cooled section at the circumferential location of the coolant inlet. Fourteen thermocouples were installed on the Haynes nozzle as shown in Figure 53. Eight thermocouples("A" designation on Figure 53) were installed in a line to measure the axial temperature profile; five thermocouples were located in one quadrant (#3 station in Figure 53), to measure the circumferential temperature distributions in the throat; three thermocouples were installed at the approximate location of the maximum temperature (#5 station in Figure 53) recorded with the gas-gas hydrogen/oxygen regen-dump-film cooled thruster tested on contract NAS 3-15850 (Ref. 9).

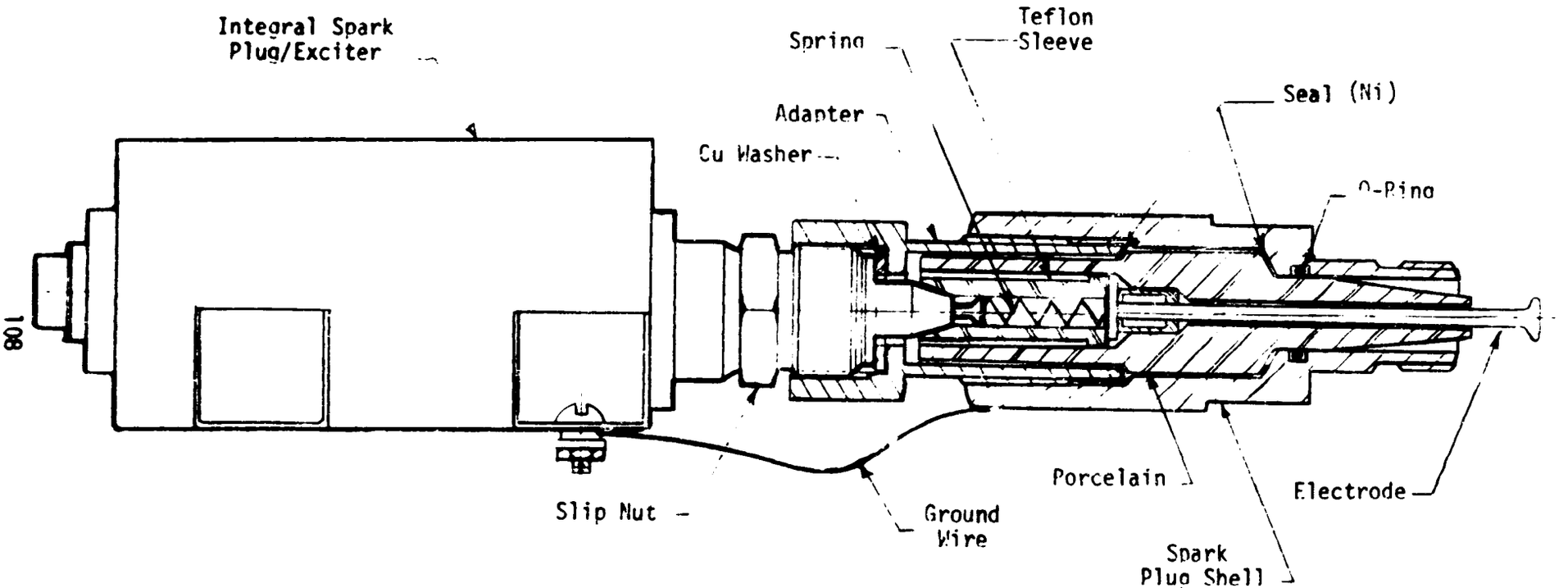

Figure 52. Spark Plug/Exciter Assembly

TC	X-DIM cm	X-DIM in	ANGLE
1A	1.91	0.75	0°
2A	2.79	1.1	0
3A	3.66	1.44	0
3B	3.66	1.44	22.5
3C	3.66	1.44	45
3D	3.66	1.44	67.5
3E	3.66	1.44	90
4A	4.32	1.7	0
5A	5.08	2.0	0
5E	5.08	2.0	90
5F	5.08	2.0	180
6A	10.2	4.0	0
7A	15.2	6.0	0
8A	24.1	9.5	0

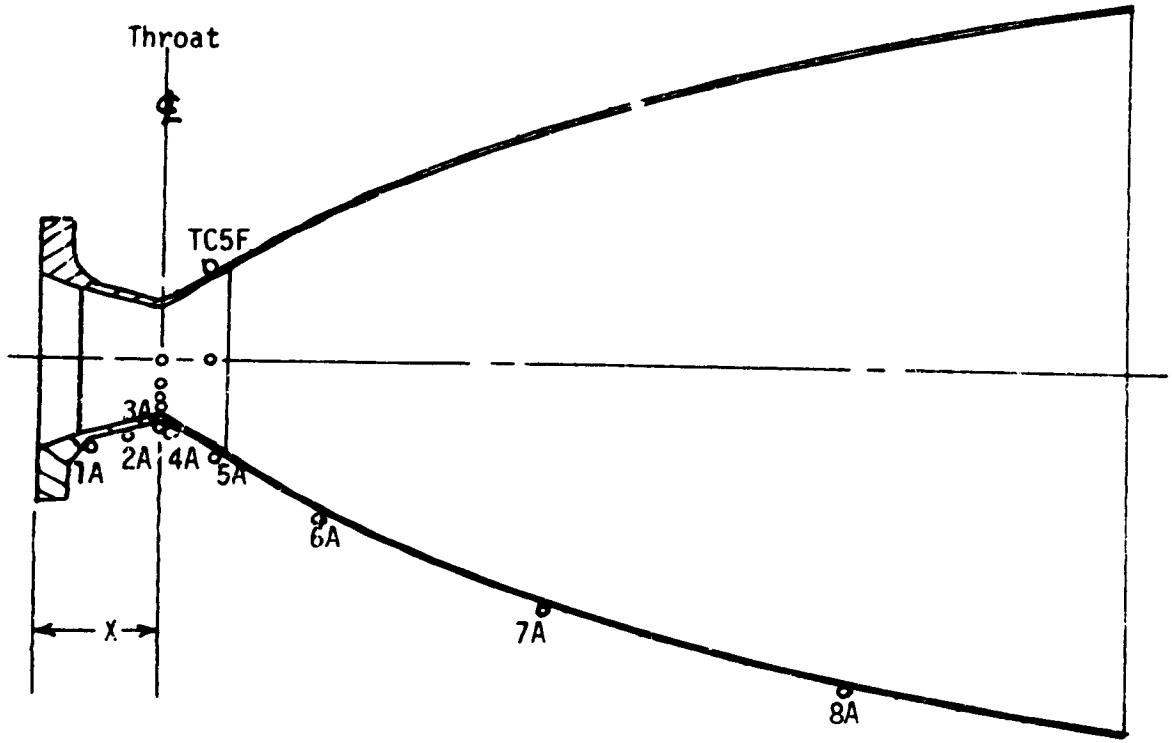

Figure 53. Haynes Nozzle Thermal Instrumentation

VIII COOLED CHAMBER TESTING

A. LIQUID/LIQUID (DESIGN POINT 1)

The injector, igniter and valves were installed on test stand J-4 and the injector flowed for pattern check and Kw (flow coefficients). The ox lines, injector and igniter were then removed and cleaned to "Level E" (oxygen service). All components were then reinstalled on the test stand and pressure checked. The test stand buildup was then completed with the installation of the uncooled spacer, the Columbium chamber, transducers, and the spark plug assembly (shown in Figure 52). The set-up was the same, except for the exciter, duplicate flowmeters and additional propellant temperature monitors as that used for the sea level testing.

The Ramapo flow meters were recalibrated using water. A sensitivity to electrical line length (input voltage reduction with line length) was noted and was factored into the calibration. Backup turbine type flow meters were installed for the liquid-liquid testing. The oxidizer flow meter was located in a straight line section downstream of the accumulator. The hydrogen flow meter was located at the entrance to the cell (break in vacuum jacket). These flow meters were intended to serve as references for the Ramapo meters during the steady state tests.

The igniter valves were operated with GN_2 inlet pressures ranging from 311 to 683 N/cm^2 (450 psia to 990 psia). An electrical booster was used to provide a high voltage initiation signal to the valves. After the initial high voltage impulse, the voltage is held at 28 vdc. The data obtained with the electrical booster are compared in Figure 54 to those obtained previously with the normal 28 vdc power supply. The response of the fuel valve varied by only 4 msec over the entire range of pressures. The oxidizer valve was erratic in opening at pressures in excess of 587 N/cm^2 (850 psia) and would not open at 683 N/cm^2 (990 psia). The fuel valve leaked at the conclusion of the these valve tests and was replaced. On the basis of these tests the valve inlet pressure was limited to 587 N/cm^2 (850 psia).

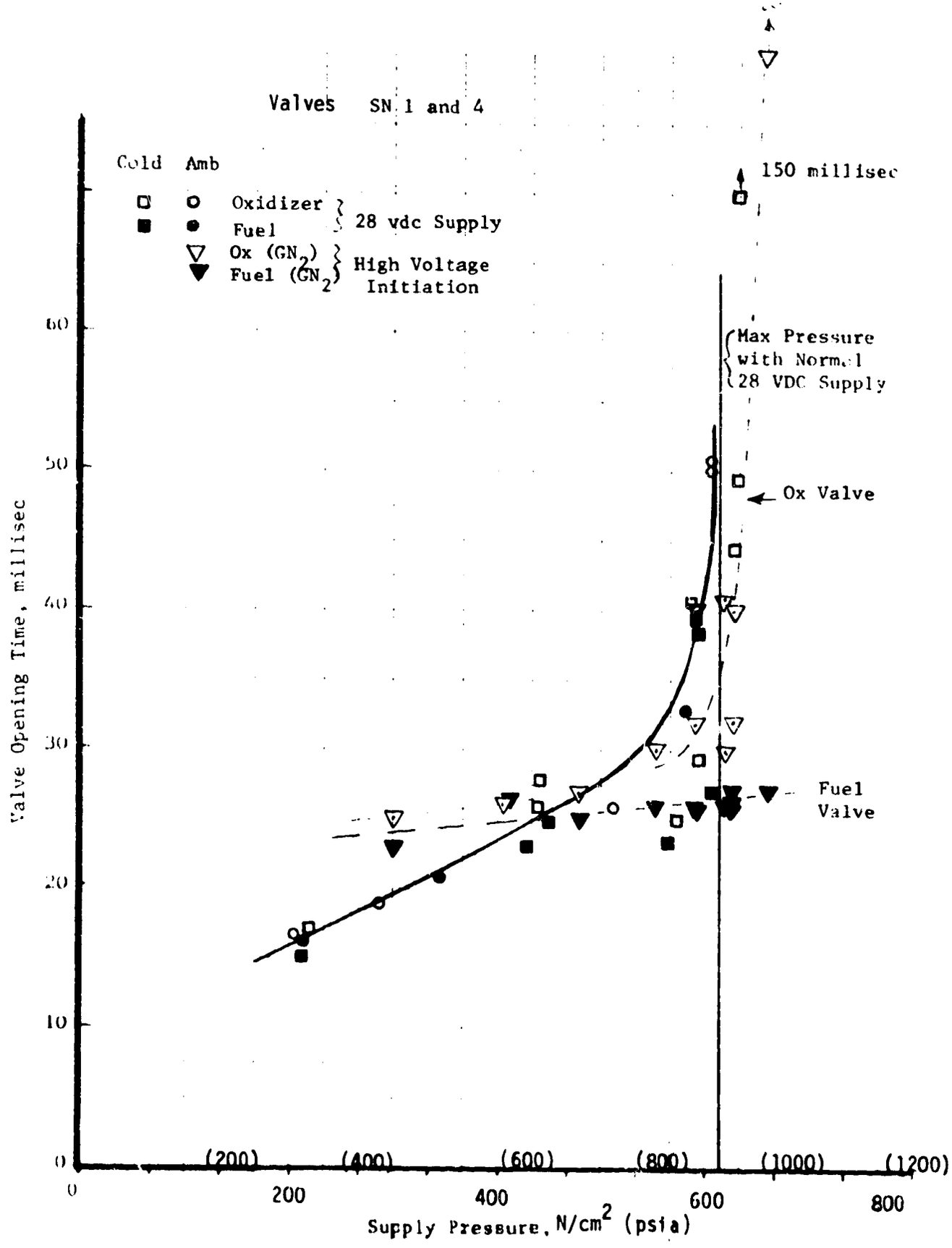

Figure 54. Valcor Igniter Valve Response

VIII Cooled Chamber Testing (cont.)

Ten tests were made with the liquid/liquid injector that was previously tested in the sea level tests and the columbium chamber. Testing was conducted in test cell J-4 of the ALRC altitude facility. The tests are summarized in Table X.

There were two streaks that could be seen in the columbium chamber after Test -003. These streaks were narrow bands of discoloration in the convergent section and throat of the chamber and occurred at the location corresponding to one of the two fuel inlets. The throat temperatures transient that was measured during Test -004 indicated that the heat transfer coefficient was lower (slower response) and the recovery temperature higher than had been inferred from the data generated in the sea level testing with a copper heat sink chamber as shown in Figure 55.

The throat temperature response data from Test -004 were analyzed using a flat plate conduction model to represent the columbium chamber wall. The recovery temperature that was correlated from the Test -004 data was 1260°C (2300 °F); the limit on the coating was considered to be 1371 °C (2500°F), the temperature at which it was cured.

The columbium chamber was rotated to bring the bulk of the thermocouples into the area where the heat streaking was observed. Test -006 was made to evaluate throat temperature response with the thermocouples in their new position. The duration was not extended beyond that previously demonstrated for fear that the temperatures in the heat streak area would be significantly higher than those measured elsewhere in the chamber. The temperature data were similar to the Test -004 data. The test duration was then extended to 1 sec (Test -008). The thermocouple data from the tests made after Test -004 compared favorably with the temperature response projected from the Test -004 data as shown in Figure 56.

TABLE X

SUMMARY OF LIQUID/LIQUID COOLED CHAMBER TESTING

Date 1974	Test 1983-D02 OM	Duration (sec)	Chamber Pressure (N/cm^2)	Chamber Pressure (psia)	MR	Oxygen Inlet Temperature (°C)	Oxygen Inlet Temperature (°F)	Hydrogen Inlet Temperature (°C)	Hydrogen Inlet Temperature (°F)	COMMENTS
1-25	001	.06	-	-	-	-	-	-	-	Igniter Only Checkout
1-29	002	.11	316	458		90.6	163	31	56	Short Duration Checkout
1-30	003	.47	320	464	3.5	87.8	158	28	51	Checkout - Streak Discoloration at 6:00 O'Clock
1-30	004	.69	326	473	3.6	88.3	159	29	53	Throat Temperature Shutdown - Trip Set at 982 °C (1800°F)
1-31	005	.11	310	449	4.2	91.7	165	28	51	Low Thrust Shutdown Due to Fuel Valve Delay on Opening
1-31	006	.66	336	488	3.7	87.8	158	28	51	Repeat Test for Comparison with -004
1-31	007	.61	346	502	3.8	91.7	165	27	49	Inadvertent Shutdown - Electrical Malfunction
1-31	008	1.01	345	500	3.7	89.4	161	27	49	Temperature Shutdown - Trip Set at 1093 °C (2000°F)
1-31	009	3.60	319	462	3.3	90.0	162	29	52	Temperature Shutdown - Minor Surface Erosion in Throat - Two Locations: 11:00 & 1:00 O'Clock
2-4	010	.98 & .99	349	506	4.8	89.4	161	31	55	Two pulses - Burned through Chamber on Second Pulse at 6:00 O'Clock Location

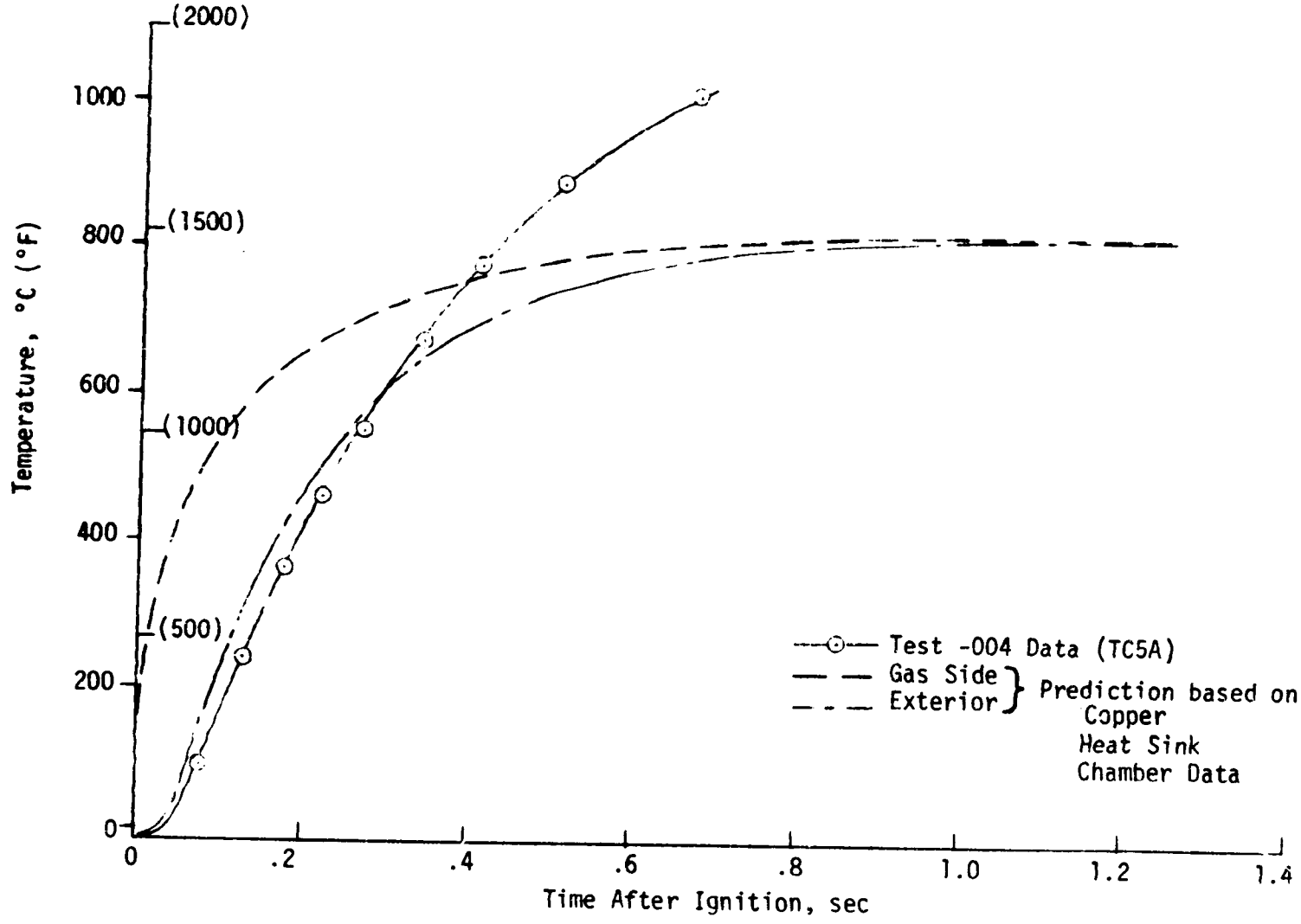

Figure 55. Throat Temperature Transient

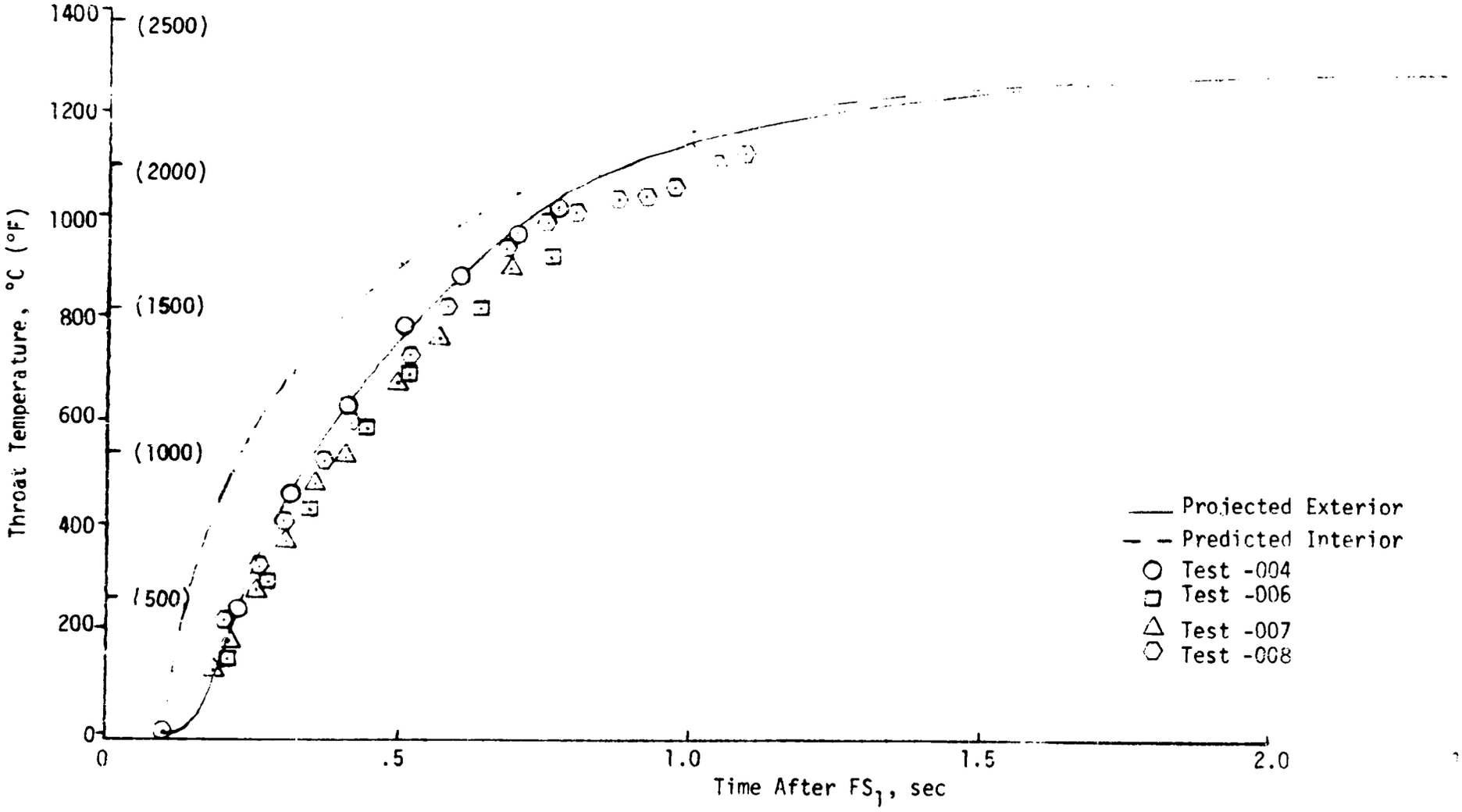

Figure 56. Projection of Throat Temperature Transient Based on Test -004 Data

VIII Cooled Chamber Testing (cont.)

On the basis of the analysis of the throat temperature data, as shown in Figure 56, it appeared that the steady state recovery temperature would be 1260 °C (2300 °F) or less. Test -009 was set for a 40 sec duration; it was terminated in 3.6 sec by a high temperature trip. There were two streaks in the chamber starting in the convergent section and extending through the throat into the divergent section. The coating in the streaks was removed and there was minor erosion of the columbium surface in one of the streaks. These streaks occurred 180° from those originally observed; thus, there were no chamber thermocouples in the vicinity of the streaks. The streaks occurred at a circumferential location corresponding to the second fuel inlet.

The temperature response of the two throat thermocouples during Test -009 are shown in Figure 57. The throat temperatures steadied out in about two seconds in good agreement with the results from earlier testing as shown in Figure 58. The decay and subsequent rise shown by thermocouple TC5A two seconds after FS_1 (Figure 57) was exhibited by all the thermocouples that were in line axially with TC5A except those on the nozzle extension which had not reached steady state. None of the thermocouples in the B location (in line axially with TC5B) showed the excursion.

Because of the loss of the oxidation resistant coating in the two streaks, it was decided to conduct no additional steady state tests and to continue the program with testing in the pulse mode of operation. The chamber was rotated to move the streaks into a location which exhibited low temperature on the basis of the chamber coloration pattern. Test -010 was scheduled to be a ten pulse test with a duty cycle consisting of one second firing times and one second coast between pulses. Testing was terminated on the second pulse by a low thrust shutdown. The chamber had burned through at the location of the less severe of the two streaks produced by Test -009.

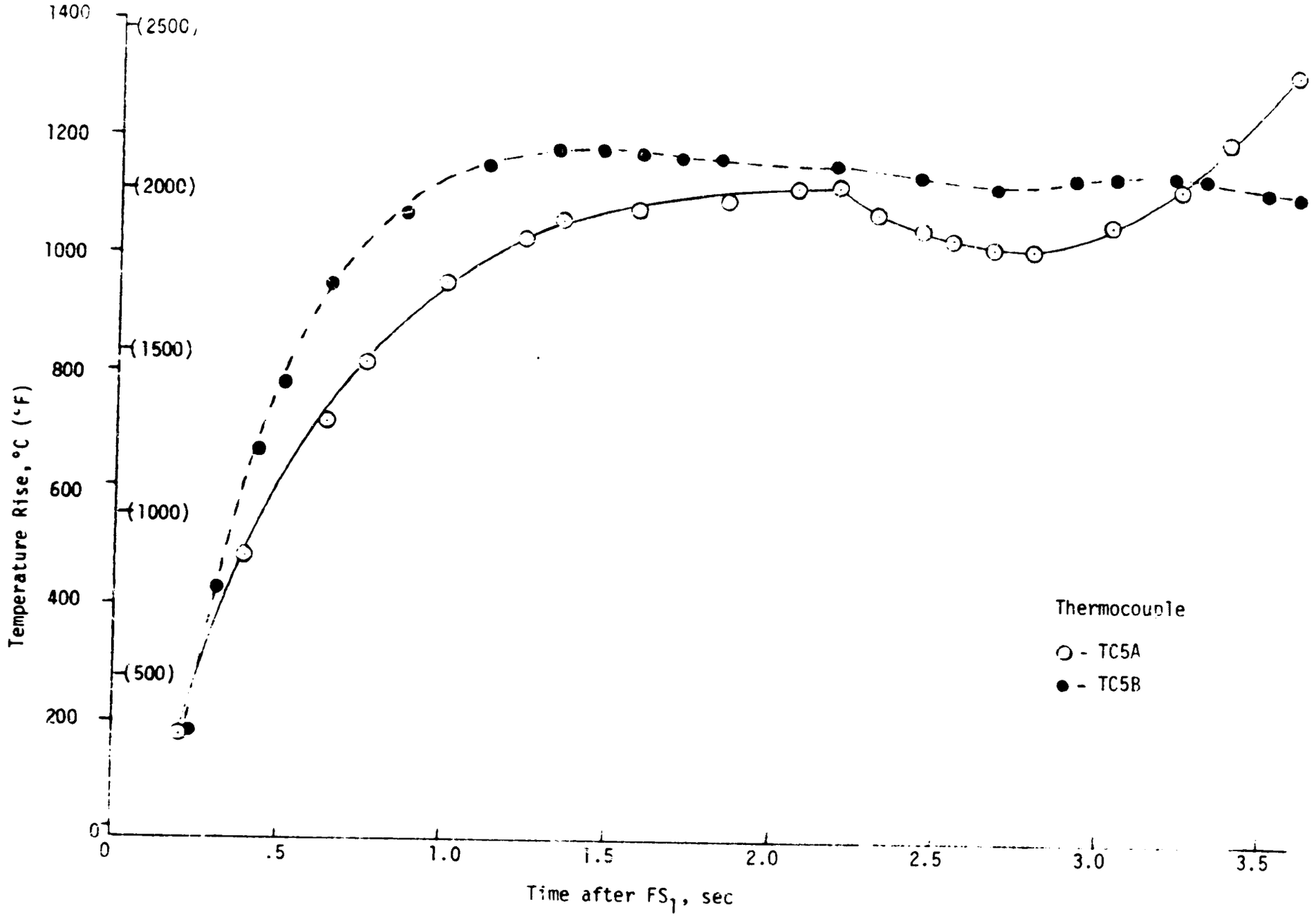

Figure 57. Throat Temperature Transient, Test -009

VIII, Cooled Chamber Testing (cont.)

The response of three of the thermocouples in the throat area is shown in Figure 58 for comparison with the data already discussed; data from thermocouple TC6B are shown as representative of the B location (TC5B was inoperative); data from thermocouple TC5A are shown to provide a basis of comparison for the TC6B data and to show by comparison to the TC5A data that there was little difference in the throat temperatures as measured at the axial location at the -5 and -6 thermocouples. (See Figure 51 for thermocouple locations.) As in the case of Test -009 thermal data, the throat temperatures exhibit the normal start up transient and then the thermocouples at one location; in this case the B location, rise rapidly.

A postfire picture of the columbium chamber is shown in Figure 59, to illustrate the discoloration streaks that were present in the chamber. A postfire picture of the uncooled section is shown in Figure 60. There were 16 heat marks next to the injector corresponding roughly to the location of the 16 peripheral oxidizer doublets. The injector is shown in Figure 61. The longer streaks on the aft end of the uncooled section extended into the columbium chamber as shown in Figure 59. The streaks in the columbium chamber originated upstream and were not the result of a discontinuity between the uncooled section and the columbium chamber.

It is fairly obvious that the injector produced the heat streaks in the chamber. In order to ascertain whether this was due to the basic design of the injector or the result of plugging, icing, etc., several bench tests were performed on the injector. Particular emphasis was placed on the oxidizer circuit since its hydraulic resistance during testing was not the same as measured previously or in the pretest water flow.

In the event that the injector could have been plugged with a water soluble compound the injector was flowed with GN_2 and a low resistance probe (3% of total ΔP) was used to collect the flow from each element. A gas flow turbine meter was used to measure the flow rate. No doublet either in the

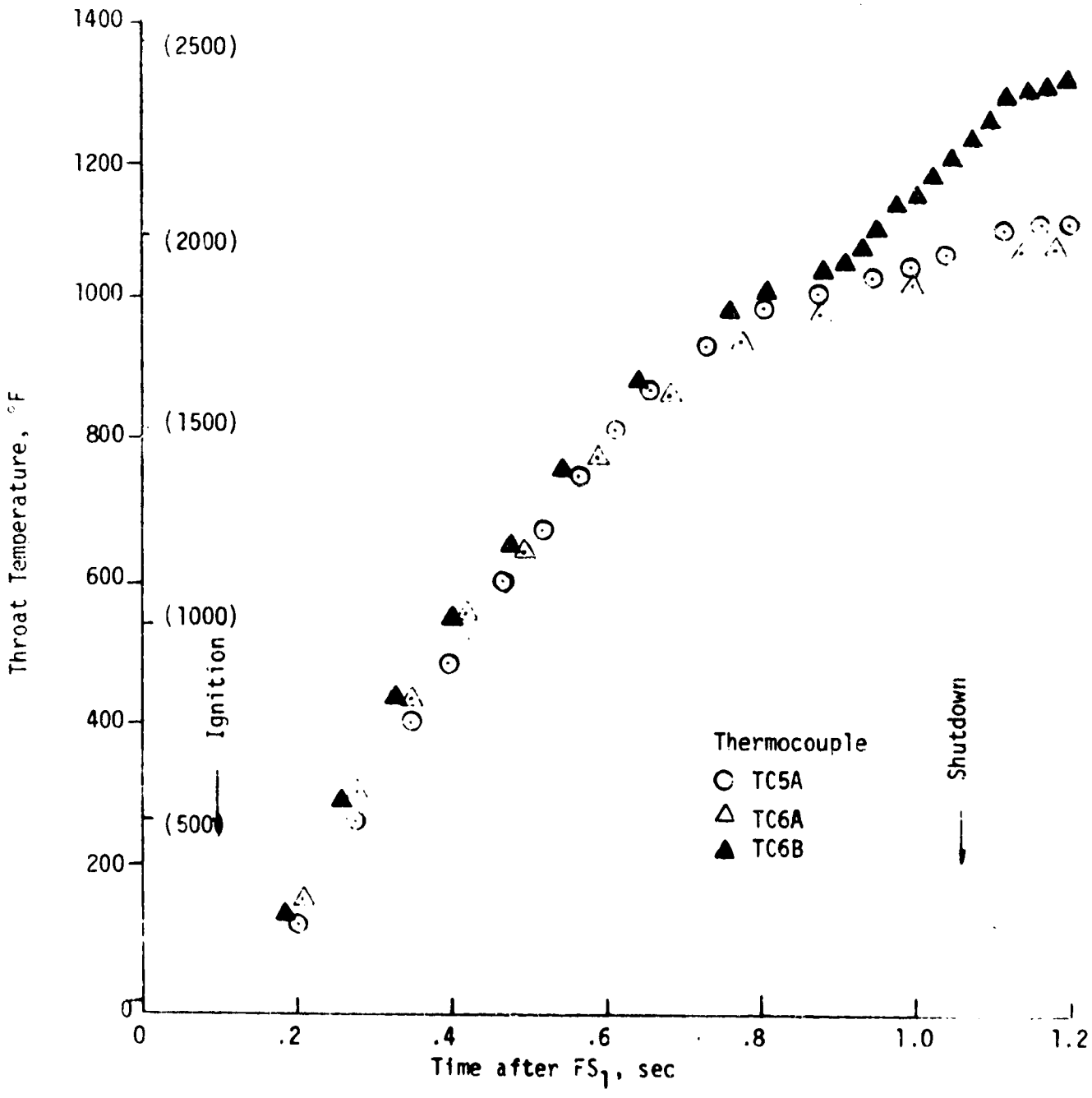

Figure 58. Throat Temperature Transients, Test -010, First Pulse

CHAMBER

VIEW OF THROAT FROM FORWARD END

Figure 59. Postfire Condition of Columbium Chamber Showing Streaks

FORWARD END

AFT END

Figure 60. Postfire Photograph of Uncooled Spacer Showing Heat Marks

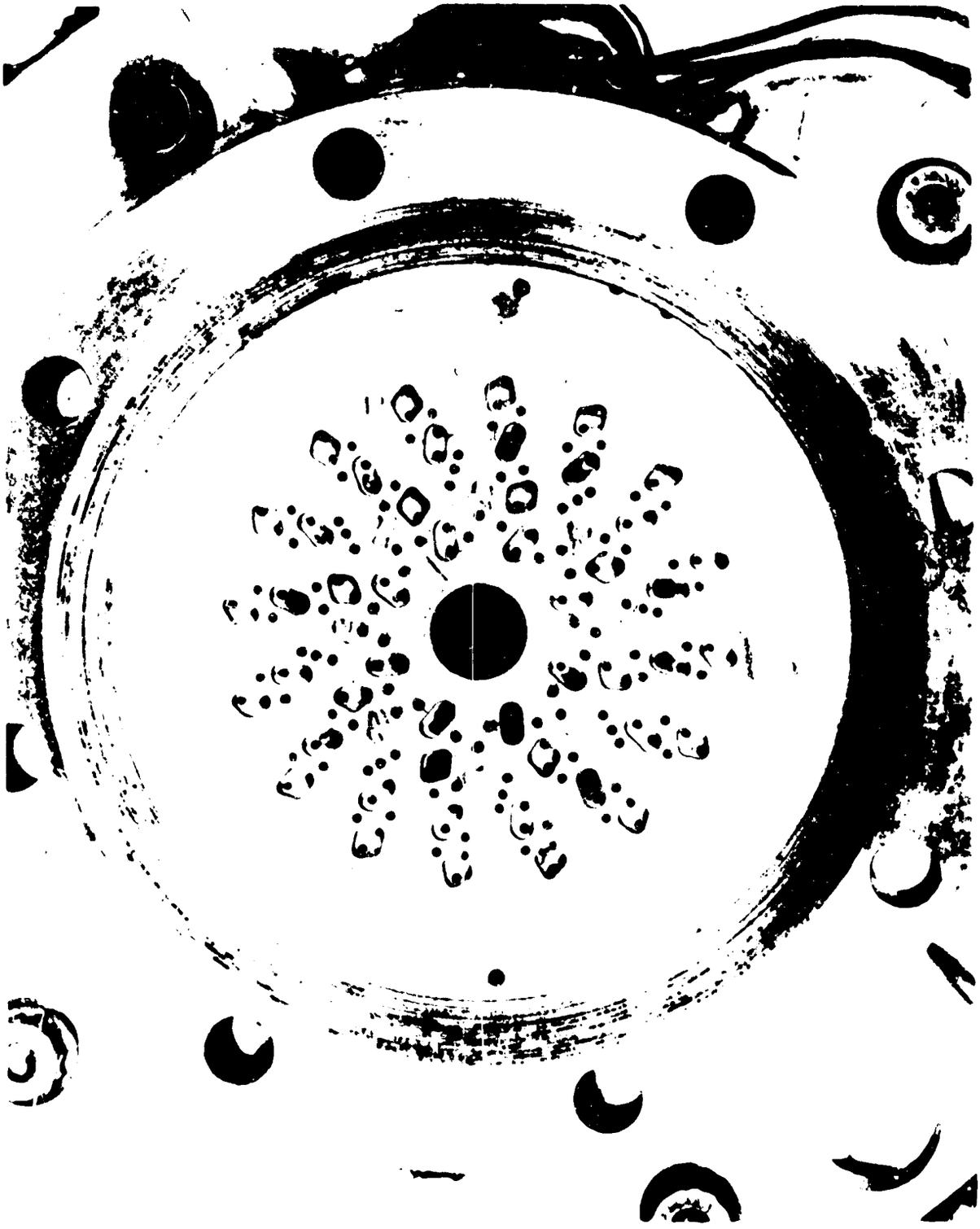

Figure 61. Liquid/Liquid Injector after Testing

VIII Cooled Chamber Testing (cont.)

fuel or oxidizer circuit showed any blockage or abnormality. The oxidizer data are shown in Figure 62 for comparison with the data that were obtained prior to the sea level testing.

After the GN_2 cold flow test a water flow test was made to re-evaluate the injector flow coefficients (K_w values). The injector was then backflushed into a filter paper; no particulate matter was found. The K_w values (K_w = flow rate/square root of the product of the pressure drop and fluid specific gravity) are shown in Table XI.

TABLE XI

COMPARISON OF LIQUID/LIQUID INJECTOR FLOW COEFFICIENTS

Condition	K_w Ox	K_w Fuel
Prior Water Flow	.147	.127
Cooled Chamber Pretest Water Flow	.145	.121
Cooled Chamber Testing (-009)	.130	.127
Cooled Chamber Post Test Water Flow	.155	-

The fuel circuit K_w was generally the same for every condition. The oxidizer circuit shows a significantly lower resistance during the cooled chamber test firings. This is the opposite of what was experienced in the sea level testing. As was shown earlier in Table VII, the K_w values shown in Table VII were based on injector manifold pressures and those in Table XI on the pressure at the inlet to the valves.

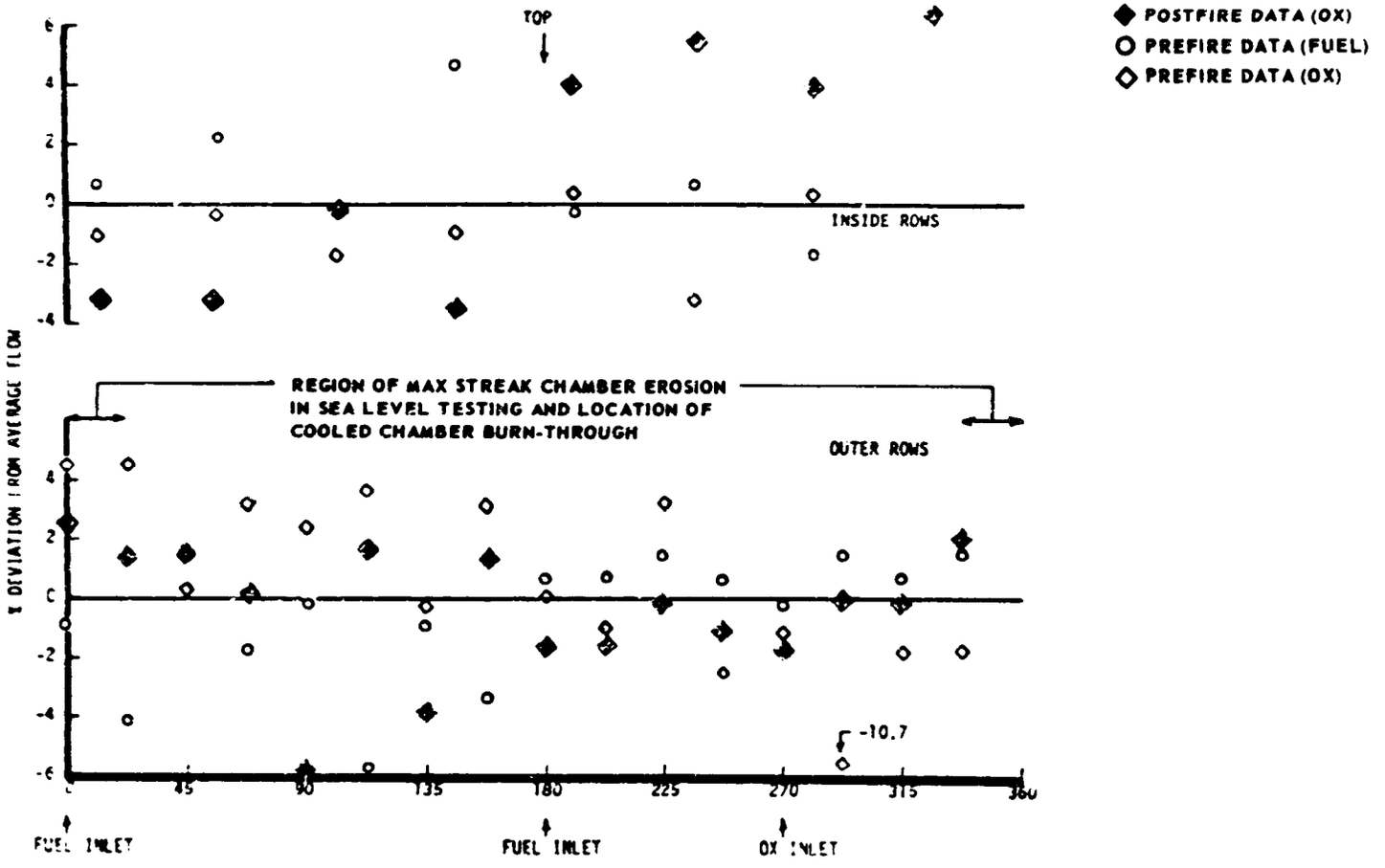

Figure 62. Liquid-Liquid Injector Cold Flow Data

VIII, Cooled Chamber Testing (cont.)

B. GAS/LIQUID (DESIGN POINT 2)

The gas/liquid injector was installed on the test stand (Figure 63) and the ox circuit flowed with water for a visual pattern check and to determine its hydraulic characteristics (K_w). The ox circuit was flowed with GN_2 and an element-by-element flow measurement made. The injector and lines were removed, cleaned to "level E" (oxygen service) and reinstalled. The regen chamber, dump cooled chamber and Haynes nozzle were installed.

A total of 44 tests were run with the gas/liquid hardware. Table XII is a summary of the range of operating conditions. Table XIII is a description of the tests. The thruster was pulsed 402 times at 12 combinations of chamber pressure, mixture ratio and fuel temperature. Thirty checkout and steady state tests were made.

Test -014 (Table XIII) was run at approximately 165 N/cm^2 (240 psia) chamber pressure. There was an oscillation observed in all chamber pressure parameters. It was not seen in any of the system parameters or at the inlet to the valves. The propellant flow rates were increased to give a chamber pressure of approximately 207 N/cm^2 (300 psia) and no oscillation occurred.

Upon demonstration of the chamber at the low pressure with ~28% ffc (Test -021) the coolant flow rate was reduced to ~25% ffc. With this coolant flow rate, tests were made at approximately 207 N/cm^2 (300 psia) (Test -023), 276 N/cm^2 (400 psia) (Test -024) and 348 N/cm^2 (500 psia) (Test -026). The coolant flow rate was then reduced to 20% of the total fuel flow and Test -028 made. The dump cooled section was designed for a 27% ffc flow rate.

The next series of tests were pulse tests and were run using a sequence in which a fixed firing and coast times were repeated. The pulse width was systematically reduced (Tests -029 through -032 and -036). The valve sequencing was varied to change ox lead on startup and fuel lag on shutdown (-032 & -033, and -036 through -039). Various combinations of on and off times were investigated (-040 through -042).

TABLE XII

SUMMARY OF GAS/LIQUID COOLED CHAMBER TEST CONDITIONS

Number of Tests	44
Chamber Pressure Range, N/cm^2 (psia)	152 to 345 (220 to 500)
Mixture Ratio Range	2.3 to 6.2
Fuel Inlet Temperature Range, °K (°R)	36 to 116 (64 to 208)
Maximum Duration, sec	20
Minimum Impulse Bit, N-sec (lbf-sec)	187 (42)
Range of % ffc	-37 to -20
Thrust Range, N (lbf)	2224 to 5560 (500 to 1250)
Cumulative Firing Duration, sec	273
Number of Firings	417

TABLE XIII

GAS/LIQUID COOLED THRUSTER TEST CONDITIONS

Date 1974	Test No. 1983-D02-012	Dur. Sec	Nominal % ffc	P_c, N/cm^2 (psia)	MR	T_O, °K (°R)	T_F, °K (°R)	Mode of Operation	Comments
2-19	-011	.07	28	152 (220)	-	83 (150)	83 (150)	Steady State	Checkout
	-012	.1	28	181 (262)	-	90 (162)	86 (155)	"	Low thrust shutdown-trip set too high
	-013	.1	28	183 (266)	2.3	92 (166)	85 (153)	"	Repeat - low thrust shutdown - trip set too high
	-014	.5	28	165 (239)	2.5	87 (157)	78 (140)	"	Thrust chamber pressure oscillate
	-015	2	28	221 (320)	3.6	86 (154)	75 (132)	"	Increased pressures-no oscillation
2-20	-016	.5	28	219 (318)	3.6	88 (159)	81 (145)	"	Checkout at higher MR
	-017	2	28	226 (328)	4.5	87 (157)	86 (154)	"	Increased MR - igniter fuel valve did not close
	-018	-	-	-	-	-	-	-	No ignition - igniter fuel valve open from prior test
2-21	-019	5	28	212 (307)	4.7/ 5.6	87 (157)	86 (154)	"	Checkout
	-020	.1	28	226 (328)	-	87 (157)	82 (148)	"	Low thrust shutdown-fuel valve delayed opening
	-021	20	28	223 (323)	4.4	87 (157)	84 (151)	"	1st long duration test
2-22	-022	.5	25	232 (336)	5.0	89 (160)	95 (171)	"	Reduced % ffc - checkout
	-023	20	25	225 (326)	4.4	89 (160)	94 (170)	"	Long duration test with lower % ffc
	-024	20	25	285 (413)	5.0	91 (164)	91 (163)	"	Increased pressure - MR high because of no checkout test
	-025	.5	25	345 (500)	4.9	87 (156)	88 (158)	"	Increased pressure - checkout
	-026	20	25	317 (460)	4.8	90 (162)	94 (170)	"	Fuel temperature higher than planned

TABLE XIII (cont.)

Date 1974	Test No. 1983-D02-012	Dur. Sec	Nominal % ffc	P_c, N/cm^2 (psia)	MR	T_o, °K (°R)	T_F, °K (°R)	Mode of Operation	Comments
2-25	-027	.1	20	327 (474)	-	96 (172)	94 (170)	Steady State	Reduced % ffc - checkout
	-028	20	20	319 (463)	4.6	90 (162)	88 (158)	"	Near nominal long duration test
2-25	-029	10 @ 1 sec ea.	20	347 (504)	4.9	88 (158)	88 (158)	Pulse	First pulse test
2-26	-030	10 @ .2 sec ea.	20	331* (480)	4.6 5.1	97/ 102 (175/ 183)	92/ 116 (165/ 208)	"	Reduced pulse width
	-031	10 @ .15 sec ea.	20	338 (490)	4.7/ 5.4	93 (168)	114 (205)	"	Reduced pulse width
	-032	10 @ .07 sec ea.	20	338 (490)	3.8/ 4.25	89 (160)	97 (175)	"	Reduced pulse width
	-033	10 @ .07 sec ea	20	338 (490)	3.3/ 3.7	89 (160)	94 (170)	"	Delayed fuel valve closing by .01 sec
	-034	10 @ .07 sec ea.	20	-	-	-	-	No Ignition	Igniter of valve did not close - igniter froze up
	-035	10 @ .07 sec ea.	20	-	-	-	-	"	Same - run back to back with short delay after -034
	-036	10 @ .07 sec ea.	20	327 (475)	3.9/ 4.4	89 (160)	100 (180)	Pulse	Repeat of Test -032
	-037	10 @ .07 sec ea.	20	327 (475)	3.3/ 3.7	87 (157)	96 (173)	Pulse	Repeat of Test -033
	-038	10 @ .07 sec ea.	20	327 (475)	2.8/ 2.9	87	94	Pulse	Repeat of Test -034, delayed fuel valve closing by .01 sec.
	-039	10 @ .07 sec ea.	20	327 (475)	3.3/ 3.5	86 (155)	93 (167)	"	Repeat of Test -035, increased ox lead on opening by .005 sec.
	-040	20 @ 1 sec ea.	20	324 (470)	4.4/ 4.6	88 (158)	86 (155)	"	.5 sec coast between pulses, 1 sec firing time
	-041	20 @ .07 sec ea.	20	327 (475)	2.8/ 3.0	97 (175)	86 (154)	"	.5 sec coast between pulses, .07 sec firing time

TABLE XIII (cont.)

Date 1974	Test No. 1983-D02-012	Dur. Sec	Nominal % ffc	P_c, N/cm^2 (psia)	MR	T_c, °K (°R)	T_F, °K (°R)	Mode of Operation	Comments
2-26	-042	152 @ .07 sec ea.	20	~327 (~475)	2.6/ 3.4	96 (172)	84 (151)	Pulse	.3 sec coast between pulses, .07 sec firing time
	-043	5 @ 1 sec 5 @ .07 sec 1 @ 9 sec	20	310/ 331 (450/ 480)	5.3/ 6.3	89 (161)	50/ 83 (90/ 150)	Pulse + Steady State	Coast times varied: .?, .5, 2, 3 & 4 sec. Fuel temp. increase resulted in high temp. shutdown during steady state operation.
4-11	-044	10 @ .07 sec 1 @ 10 sec	20	347 (504)	2.3	89 (160)	36/ 46 (64/ 83)	Pulse + Steady State	Shortened pulse widths to avoid fuel temp increase
	-045	"	20	324** (470)	4.5/ 4.9	89	67/ 74 (120/ 134)	"	Planned nominal conditions, fuel temperature low
	-046	"	20	202 (293)	3.5/ 4.4	88 (159)	44/ 61 (80/ 100)	"	Low P_c, cold propellant
	-047	"	20	198 (287)	3.4	89 (161)	75 (135)	"	Low P_c, planned nominal MR and fuel temp (near nominal)
	-048	"	20	310 (450)	4.7/ 4.8	89 (160)	42/ 60 (75/ 108)	"	High MR, cold fuel temp.
	-049	"	20	272 (395)	6.0/ 6.2	89 (160)	66/ (118/ 135)	"	High MR, nominal fuel temp.
4-12	-050	"	20	192 (278)	3.1	93 (167)	103 (185)	"	Warm fuel temp., low P_c
	-051	"	20	281 (408)	3.8	93 (168)	109 (196)	"	Warm fuel temp., planned nominal P_c & MR
	-052	"	20	303 (440)	4.5	92 (165)	111 (200)	"	Warm fuel temp., planned high MR

TABLE XIII (cont.)

Date 1974	Test No. 1983-DO2-012	Dur. Sec	Nominal % ffc	P_c, N/cm^2 (psia)	MR	T_o, °K (°R)	T_F, °K (°R)	Mode of Operation	Comments
4-12	-053	10 @ .07 sec 1 @ 2 sec	18	321 (465)	4.8	88 (158)	92 (165)	Pulse + Steady State	Reduced % ffc - checkout test
	-054	10 @ .07 sec 1 @ 10	18	327 (475)	4.6	87 (157)	87 (156)	"	Increased ox lead on startup. Planned nominal conditions

* Pc-1 plugged to prevent burnout of tube during pulse mode of operation Pc-i (igniter Pc) used for measure of chamber pressure during pulse mode of operation. Pc-j traditionally read low; for example on Test -028, Pc-1 read 336 N/cm^2 (487 psia) vs. 345 N/cm^2 (500 psia) for Pc-1

** Pc-i froze up @ 324 N/cm^2 (470 psia)

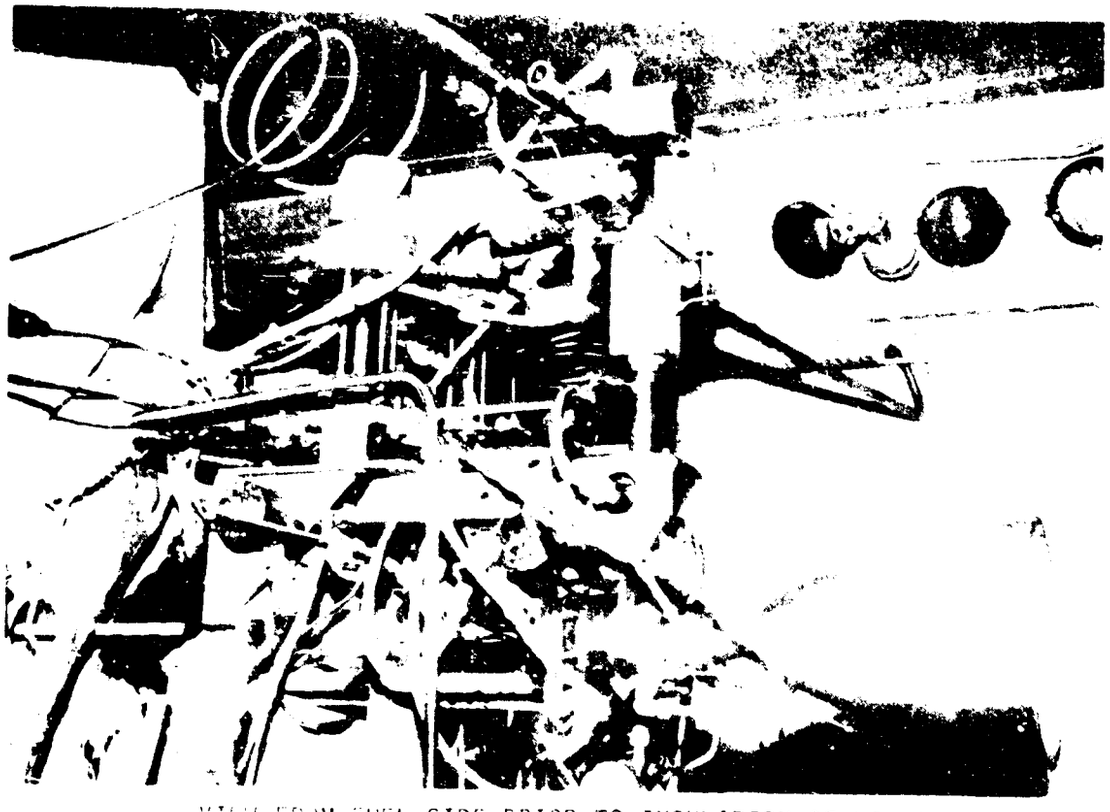

VIEW FROM FUEL SIDE PRIOR TO INSULATION OF LINES

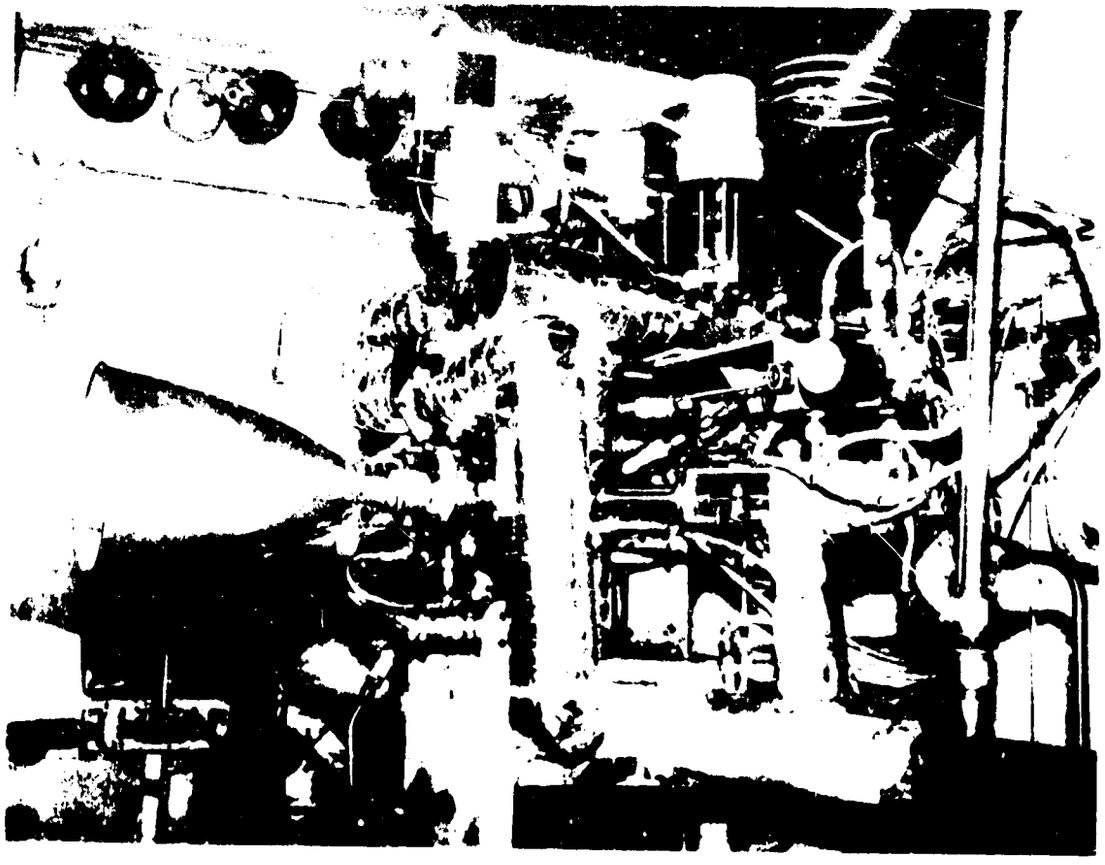

VIEW FROM OX SIDE AFTER INSULATION OF LINES

Figure 63. G/L Test Installation

VIII, B, Gas/Liquid (Design Point 2) (cont.)

There were three tests in which no-ignition occurred. On Test -018 the fuel valve to the igniter did not close. Tests -034 and -035 did not result in ignition because the electrical cable to the igniter had been damaged.

The final series of tests consisted of ten pulses followed by a steady state test. Ten of these combination pulse-steady state tests were made with fuel temperature, mixture ratio and chamber pressure being varied.

Test -043 was run with a duty cycle that consisted of the following firing and coast times.

Pulse	1	2	3	4	5	6	7	8	9	10	11
On (sec)	1	1	1	1	1	0.07	0.07	0.07	0.07	0.07	10*
Off (sec)	0.5	0.5	2	2	0.3	0.3	2	2	3	4	-

*Steady state test following ten pulses.

However, fuel inlet temperatures less than the temperature of the LH_2 in the heat exchanger could not be maintained for the 1.5 + sec cumulative firing duration. For subsequent tests, all pulse widths were reduced to 0.07 sec so that the steady state test could be made with cold fuel. The final two tests were made with the fuel film cooling reduced to ~18% of the total fuel flow. The steady state portion of Test -053 was reduced to 2 sec and a check of throat temperatures made before conducting Test -054 with a 10 sec steady state firing duration. The testing with ~18% ffc was done last since this was well below the 27% design value for the dump cooled section.

VIII, B, Gas/Liquid (Design Point 2) (cont.)

No duty cycle limits were encountered (Test -040 through -043) and operation over the required range of fuel temperatures, 56 to 111°K (100 to 200°R) and mixture ratios (3.5 to 5) was demonstrated both in steady state and the pulsing mode.

The hardware after the testing was visually inspected and was in excellent condition. Post-fire pictures of the thruster components are shown in Figures 64, 65 and 66. The streaks that can be seen on the interior of the components were simply discoloration without metal removal.

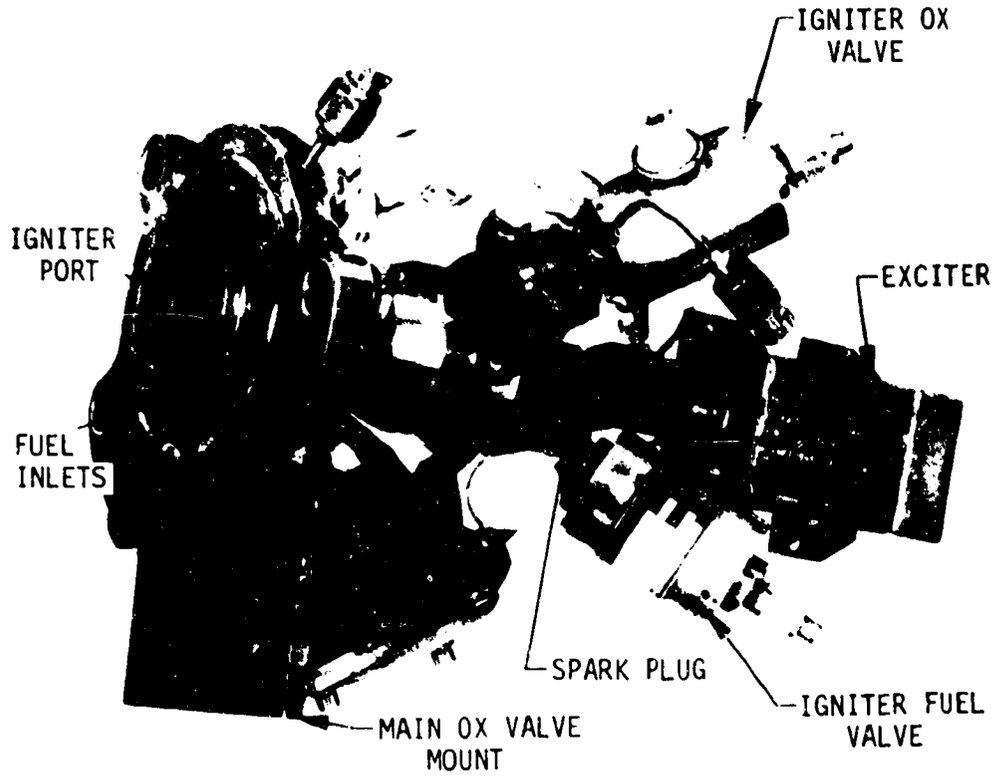

INJECTOR/IGNITER ASSEMBLY

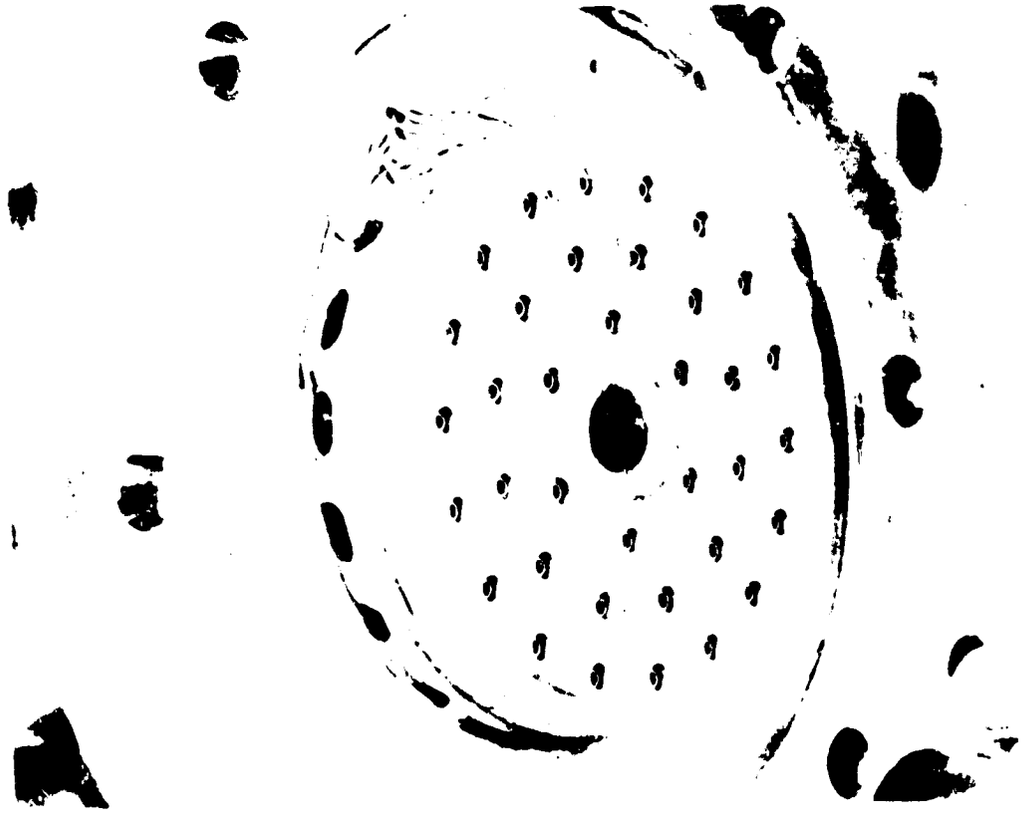

INJECTOR FACE

Figure 64. 4L Injector After Testing

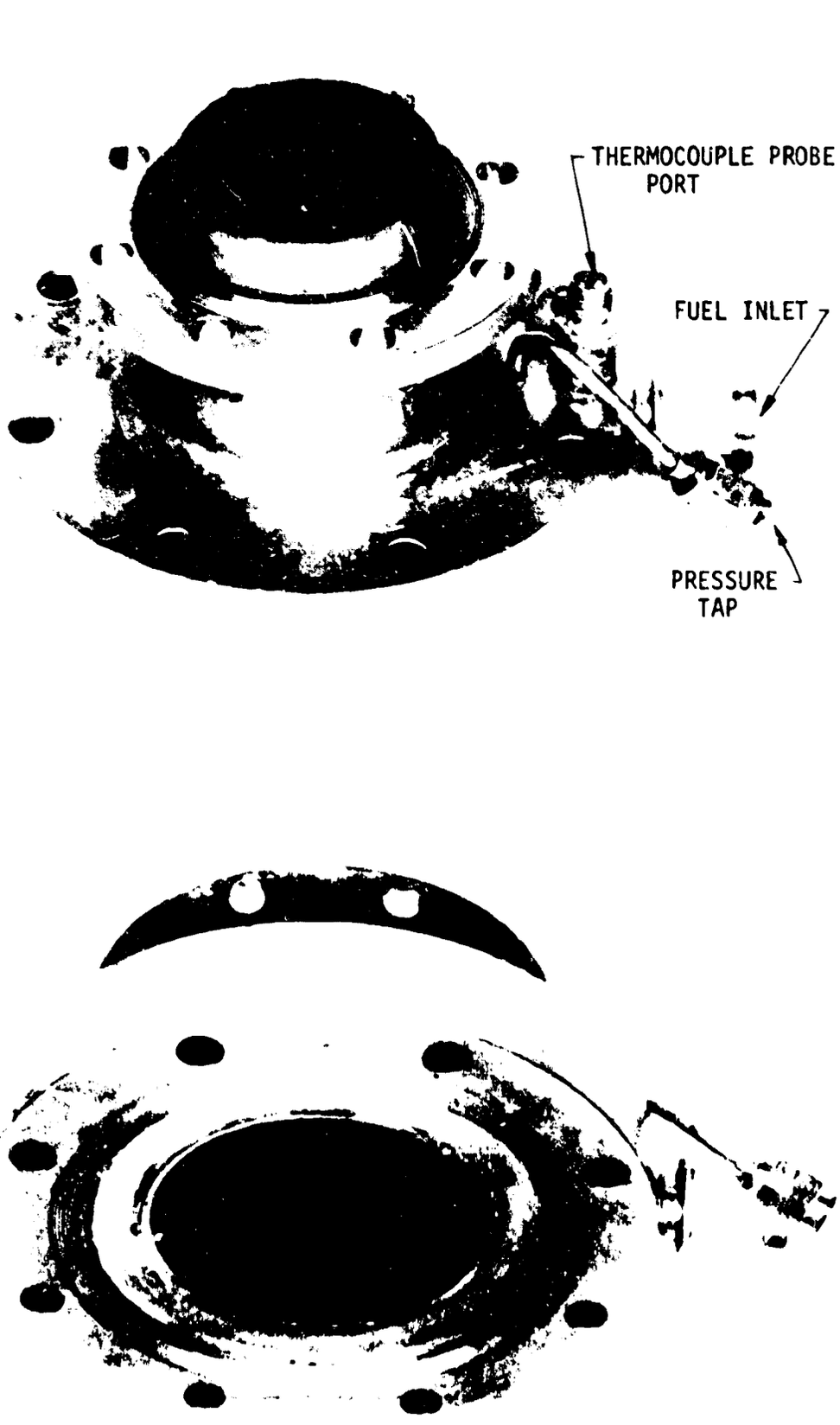

Figure 65. Dump-Cooled Section After Testing

EXTERIOR

FORWARD END

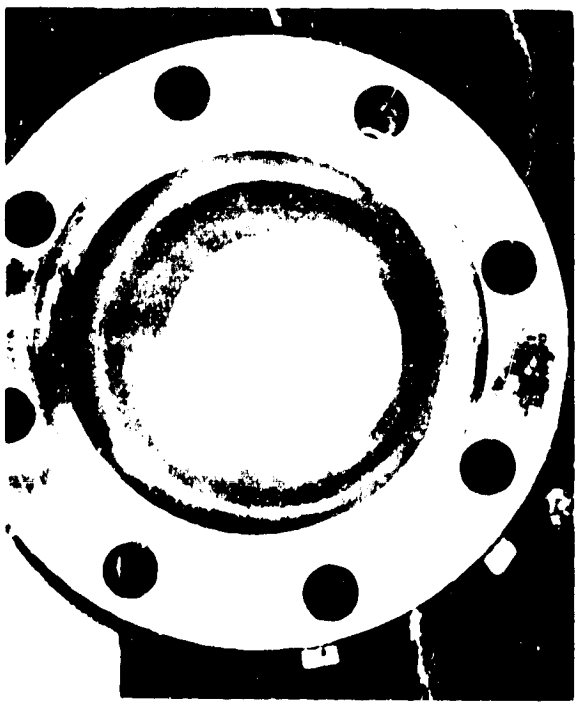

THROAT

SKIRT

Figure 66. Haynes After Test

IX. COOLED CHAMBER TEST RESULTS

A. LIQUID/LIQUID (DESIGN POINT 1)

1. Heat Transfer

The recovery temperatures that were measured in the cooled chamber testing, 1090 to 1150°C (2000 to 2100°F) were substantially higher than the 815°C (1500°F) temperature inferred from the sea level test data (Section VI, B, 1) as shown in Figure 67. The recovery temperatures were determined in the cooled chamber testing by measuring the steady state adiabatic wall temperatures of the columbium chamber (see Figure 56). The recovery temperatures that were obtained from the sea level data were extrapolated from the heat flux-wall temperature plots as shown in Figure 68.

As can be seen from Figure 68, based on the average of the change in heat flux with wall temperature an 815°C (1500°F) recovery temperature would be predicted. However, it can also be seen that the last few data points suggest a recovery temperature in agreement with the 1150°C (2100°F) recovery temperature measured with the columbium chamber or even a higher recovery temperature. Thus, in hindsight, the copper chamber data appear to indicate a change in recovery temperature as the test progressed that could perhaps have been the result of conduction from an hotter zone, that is a hot streak. The spread in the peak heat flux valves (Figure 68) are also indicative of streaking.

Figure 69 shows the response of the cooled chamber thermocouples during Test -009. The rate at which the thermocouples rise is proportional to the heat flux. Thus, the throat thermocouples rose more rapidly than those in the cylindrical section or in the supersonic portion of the nozzle. The thermocouples at the B location (see Figure 51) rose more rapidly and steadied out at a higher temperature than the thermocouples at the A location (45° from B location). The response of the thermocouples at the two locations indicated a difference in both recovery temperature and heat transfer coefficient - that is, they showed evidence of streaking.

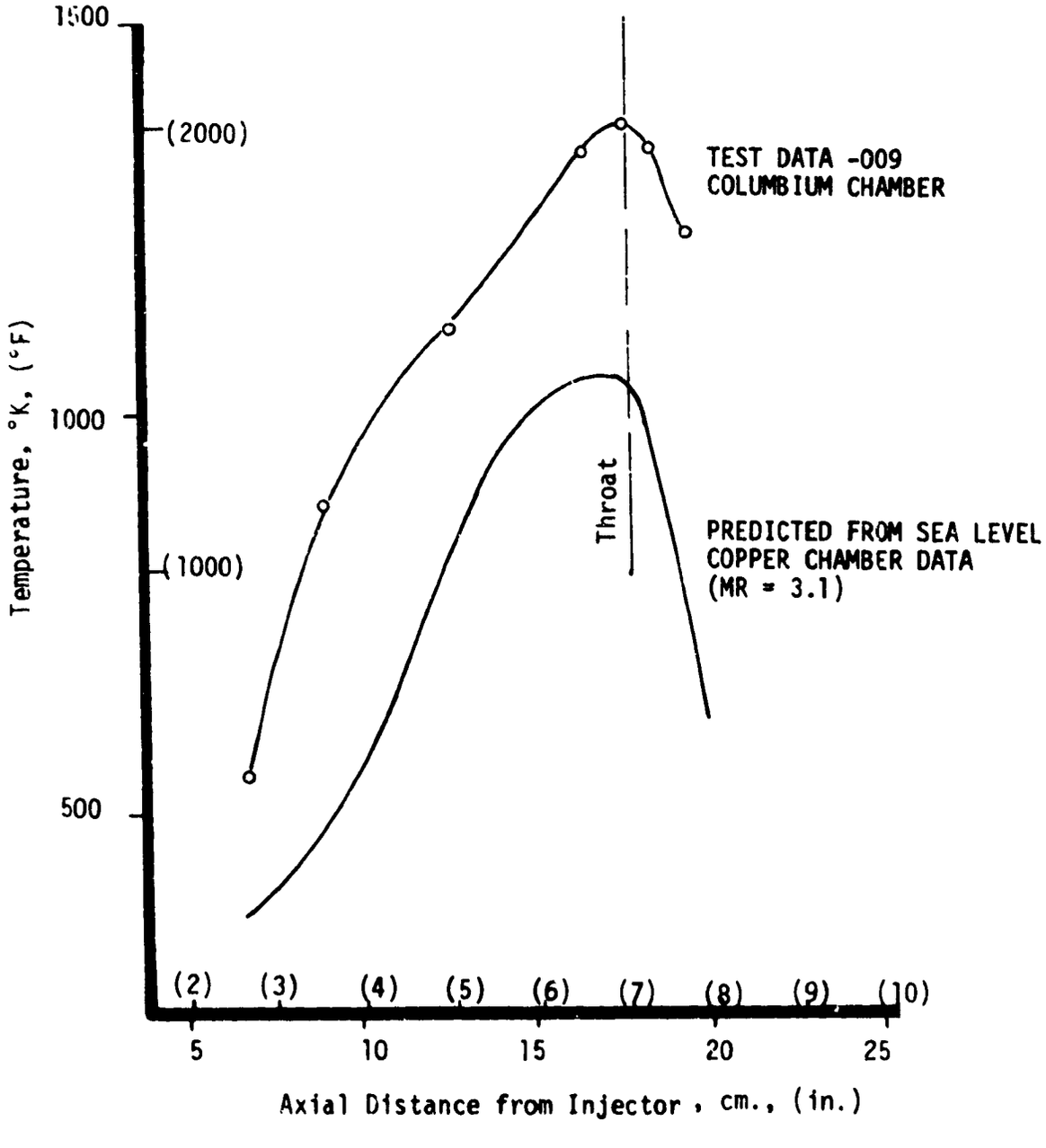

Figure 67. Gas Recovery Temperature

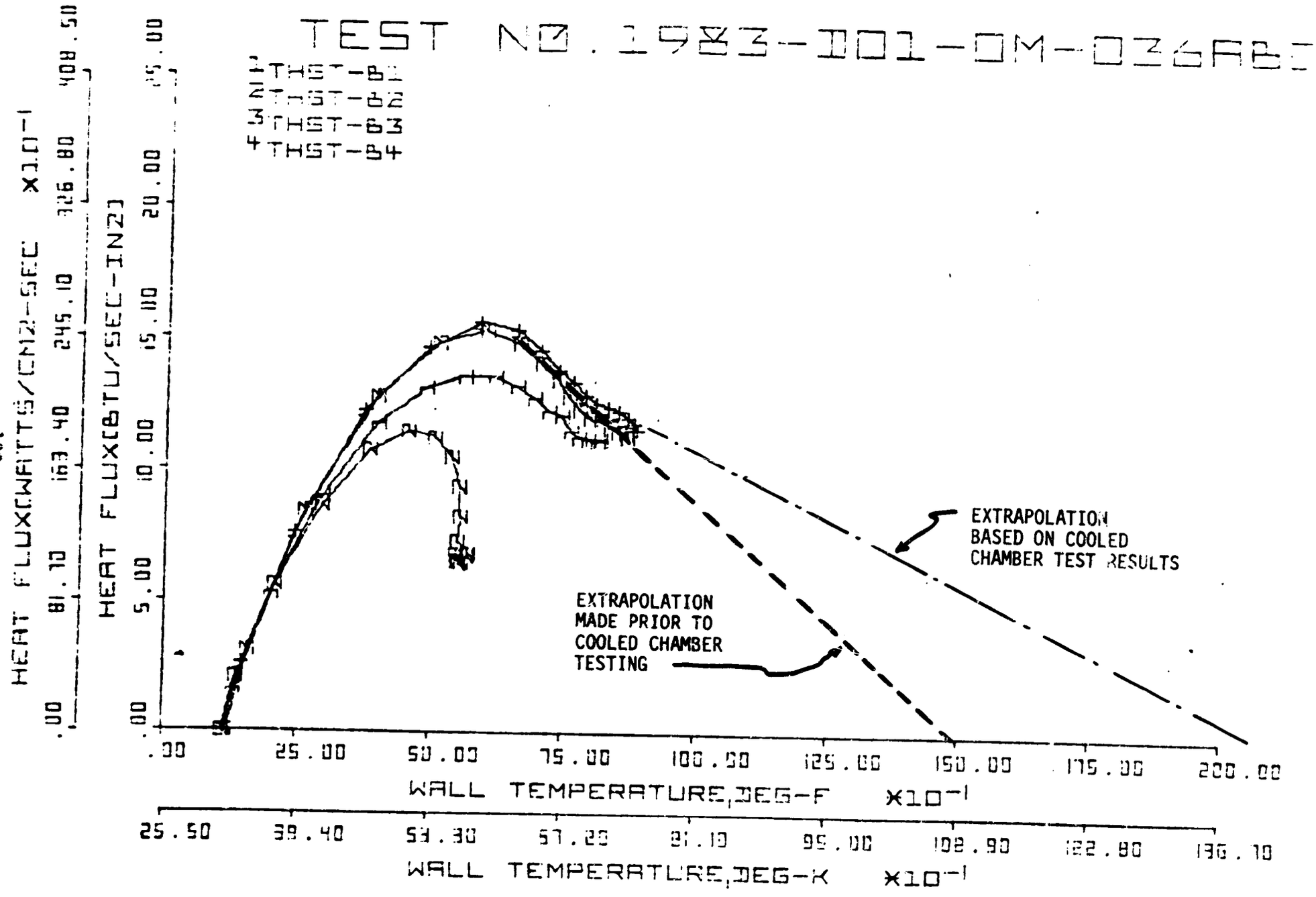

Figure 68. Heat Flux Wall Temperature Plots

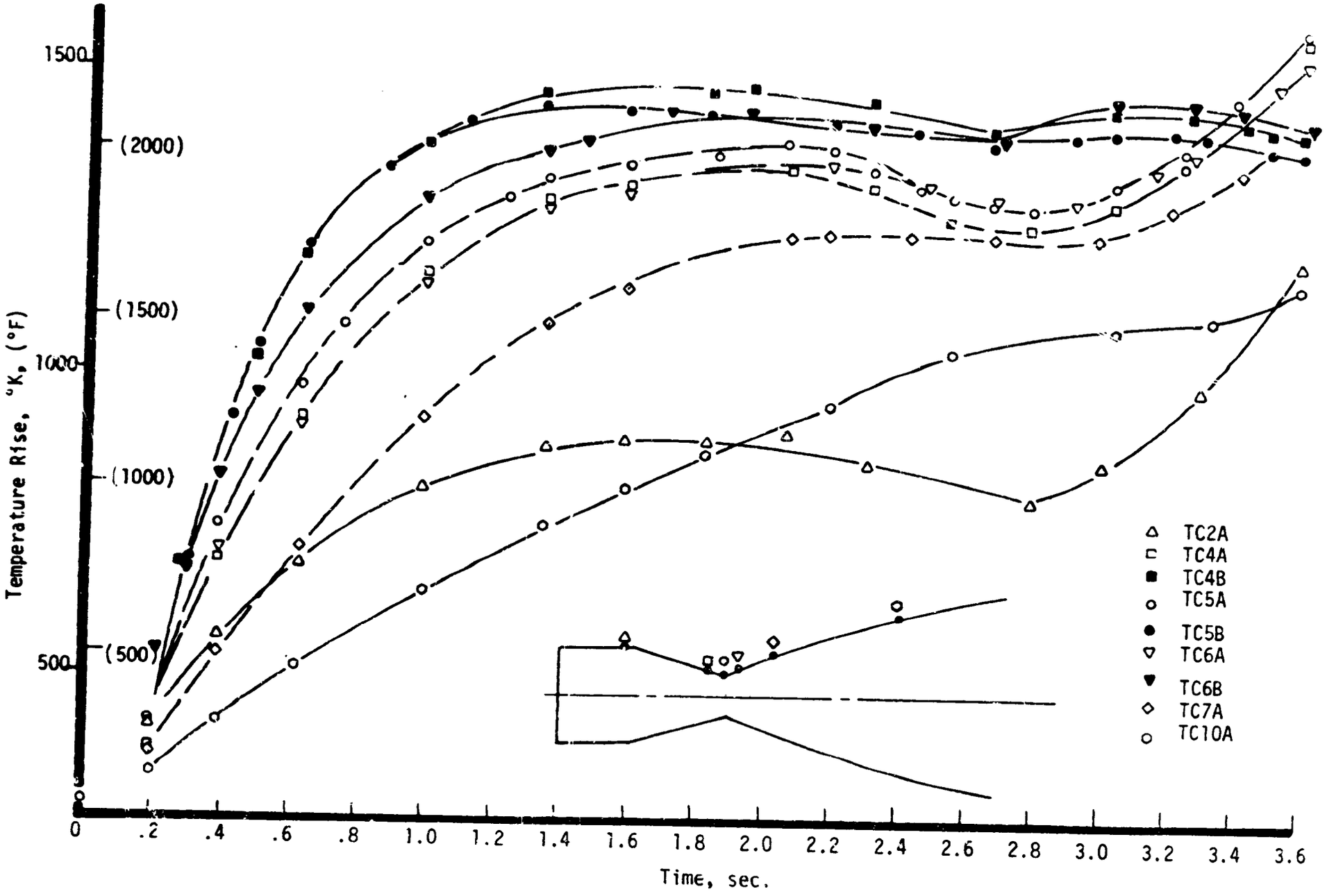

Figure 69. Test -009 Wall Temperature Transients

IX, A, Liquid/Liquid (Design Point #1)

The rise in the temperatures at the A location, 2.8 seconds into Test -009 (see Figure 69), probably corresponds to the surface erosion. However, the A thermocouples were not in an area that showed any evidence of high temperatures based on discoloration of the chamber. The rise in adiabatic wall temperature after steadying out at a lower level also occurred on Test -010 as shown in Figure 68. In this instance, the thermocouples were in the general area where erosion occurred.

The heat streaks that are evidenced in both the sea level and altitude thermal data could also be seen visually. The discoloration of the uncooled spacer (Figure 60) and on the forward end of the columbium chamber (Figure 59) evidence nonuniform heating.

The surface plane of the R512E coating on columbium typically contains 30 atom percent columbium and 67 atom percent silicon (Ref. 10). This atomic percent corresponds to the compound $CbSi_2$ which has a melting temperature of 1930°C (3506°F) (Ref. 11). The erosion of the coating on the columbium chamber in four places therefore suggests the presence of heat streaks of very high temperature.

There were 16 heat marks on the forward end of the uncooled spacer: they occurred in the space between the 16 outboard fuel elements. Thus, it would appear that the injector produced high temperature heat streaks that caused the columbium chamber erosion. The excellent thermal conductivity of the copper heat sink chamber mitigated the effect of these streaks during sea level testing.

The injector thermocouple data were reviewed to determine if there was any indication of temperatures that could have resulted in cryopumping and ice formation in the manifolding. The injector thermocouples were operating and were all above 4.4°C (40°F) prior to the Test -009 and -010. The injector temperatures did not suggest cryopumping. There was no apparent valve leakage that would have chilled down the injector.

IX, A, Liquid/Liquid (Design Point #1)

Both the fuel and ox circuits flowed uniformly when flowed with GN_2 at the conclusion of the testing. There was no evidence in the element-by-element flow data of any blockage. The results for the ox circuit are shown in Figure 62. The prior gas flow test data are shown for comparison.

The oxidizer and fuel K_w values are shown in Table XIV. The ox hydraulic resistance is low during the firing compared to the water flow data. This is the opposite of what was observed in the sea level testing (Table VII). There was a shift in ox K_w as determined by the pre and post-fire hydraulics tests but no visible reason for this shift could be found. The difference between cold flow and hot fire K_w's suggests that there was a pressure drop at the injector face that was combustion dependent and not duplicated in the water flow tests - even though the water flow tests were made to back pressure via a back pressure fixture.

Table XV is a tabulation of some of the performance data from the liquid/liquid testing. These data, coupled with the data on operating conditions given in Table XIV, show that there was no change in any measured parameter at the time the temperature excursion was occurring.

Specific impulse is in agreement with the extrapolation of the sea level results to a prediction of 4187 N-sec/kg (427 lbf-sec/lbm) at altitude for nominal conditions and, thus, there is no indication of change or abnormal operation in the performance data.

On the basis of the consistency in the liquid/liquid performance, the absence of any anomaly in the operating pressures and flows at the time of the temperature excursion, and the fact that no plugging or icing was observed, it was concluded that the heat streaks in the columbium chamber are the result of the injector pattern. There are areas in the pattern that appear as "bowling alleys", that is, lanes generally running radially outward that have no elements as indicated in Figure 70. Flow into these low mass areas could result in a

TABLE XIV

INJECTOR HYDRAULIC CHARACTERIZATION

Test	Time Sec aft FS_1	$\dot{W}_o$, Kg/sec (lb/sec)	$\dot{W}_f$, Kg/sec (lb/sec)	SG_o	SG_F	P_{OTCV} N/cm^2 (psia)	P_{FTCV} N/cm^2 (psia)	P_c N/cm^2 (psia)	K_W ox	K_W Fuel
-004	0.3745	.912 (2.011)	.240 (0.529)	1.155	0.0673	470 (682)	594 (797)	307 (445)	64.5 (0.118)	59.5 (0.109)
	0.5995	.933 (2.056)	.253 (0.558)	1.195	0.0673	475 (689)	549 (796)	320 (464)	69.4 (0.127)	64.5 (0.118)
	0.7585	.917 (2.022)	.257 (0.556)	1.160	0.0680	466 (676)	549 (797)	309 (448)	67.7 (0.124)	63.4 (0.116)
-005	0.1990	.912 (2.010)	.209 (0.460)	1.144	0.0692	467 (677)	556 (807)	300 (435)	66.1 (0.121)	49.7 (0.091)
-006	0.4495	.991 (2.184)	.253 (0.557)	1.161	0.692	498 (723)	554 (804)	320 (464)	68.8 (0.126)	62.8 (0.115)
	0.739	.996 (2.195)	.261 (0.575)	1.163	0.690	496 (720)	552 (801)	322 (467)	69.9 (0.128)	65.6 (0.120)
-007	0.4495	.980 (2.161)	.256 (0.565)	1.142	0.070	499 (724)	556 (807)	319 (462)	68.3 (0.125)	62.8 (0.115)
	0.6895	1.030 (2.270)	.257 (0.567)	1.146	0.070	516 (748)	555 (805)	332 (481)	71.0 (0.130)	65.0 (0.119)
-008	0.4495	.994 (2.191)	.255 (0.562)	1.150	0.070	498 (723)	552 (801)	323 (468)	69.9 (0.128)	63.4 (0.116)
	0.7495	1.035 (2.281)	.258 (0.569)	1.152	0.0696	512 (743)	551 (799)	332 (481)	11.6 (0.131)	66.1 (0.121)
	1.0780	1.021 (2.250)	.259 (0.571)	1.153	0.0699	513 (744)	552 (800)	334 (485)	71.0 (0.130)	66.6 (0.122)

Nomenclature

$\dot{W}_o$ - oxidizer flowrate

$\dot{W}_f$ - fuel flowrate

SG_o - oxidizer specific gravity

SG_f - fuel specific gravity

P_{OTCV} - oxidizer inlet pressure

P_{FTCV} - fuel inlet pressure

P_c - chamber pressure

K - flow coefficient

TABLE XIV (cont.)

Test	Time Sec aft FS_1	$\dot{W}_o$, Kg/sec (lb/sec)	$\dot{W}_f$, Kg/sec (lb/sec)	SG_o	SG_F	P_{OTCV} N/cm^2 (psia)	P_{FTCV} N/cm^2 (psia)	P_c N/cm^2 (psia)	K_W ox	K_W Fuel
-009	0.4495	.903 (1.903)	.243 (0.536)	1.144	0.0622	463 (671)	544 (789)	311 (451)	68.8 (0.126)	63.9 (0.117)
	0.7495	.911 (2.009)	.259 (0.570)	1.148	0.0650	466 (676)	543 (787)	316 (458)	69.4 (0.127)	67.2 (0.123)
	1.0495	.909 (2.004)	.264 (0.582)	1.149	0.0664	465 (674)	544 (789)	317 (460)	69.9 (0.128)	68.3 (0.125)
	1.6495	.918 (2.023)	.267 (0.589)	1.150	0.0673	465 (675)	544 (789)	319 (462)	70.5 (0.129)	68.8 (0.126)
	2.2495	.919 (2.025)	.269 (0.594)	1.151	0.0678	465 (675)	544 (789)	819 (463)	71.0 (0.130)	68.8 (0.126)
	3.6395	.917 (2.021)	.272 (0.600)	1.152	0.0684	465 (675)	544 (789)	321 (465)	71.0 (0.130)	69.4 (0.127)
-010	0.4495	1.072 (2.363)	.218 (0.480)	1.147	0.0641	517 (750)	518 (752)	327 (475)	72.7 (0.133)	62.3 (0.114)
	0.7495	1.112 (2.451)	.225 (0.496)	1.152	0.0655	524 (760)	516 (749)	336 (487)	75.4 (0.138)	65.6 (0.120)
	1.048	1.104 (2.434)	.230 (0.508)	1.153	0.0665	518 (752)	516 (749)	335 (486)	75.9 (0.139)	66.1 (0.121)
Water Flow - Prior Testing (Sea Level)									80.3 (0.147)	69.4 (0.121)
- Prior to Cooled Thruster Tests									79.2 (0.145)	66.1 (0.121)
- After Cooled Thruster Tests									84.7 (0.155)	-

$$K_W = \frac{\dot{W}}{\sqrt{(\Delta P)\ (SG)}}$$

TABLE XV

LIQUID/LIQUID PERFORMANCE SUMMARY

Test No.	Time Sec aft FS_1	$(\dot{W}_O)_T$ Kg/sec (lb/sec)	$(\dot{W}_F)_T$ Kg/sec (lb/sec)	MR Total	TOTCV °K (°R)	TFTCV °K (°R)	$(I_s)_{VAC}$ N-sec/kg (lb_f-sec/lb_m)
-003	0.3745	.910 (2.007)	.255 (0.563)	3.57	88 (159)	28.1 (50.5)	4175 (425.7)
	0.5485	.926 (2.042)	.263 (0.579)	3.53	88 (158)	28.9 (52.0)	4200 (428.3)
-004	0.3745	.912 (2.011)	.247 (0.544)	3.70	89 (160)	29.8 (53.7)	4233 (431.6)
	0.5995	.933 (2.056)	.259 (0.571)	3.60	88 (159)	29.8 (53.7)	4235 (431.9)
	0.7585	.917 (2.022)	.263 (0.580)	3.49	88 (159)	29.2 (52.5)	4233 (431.6)
-005	0.1990	.912 (2.010)	.215 (0.475)	4.23	92 (165)	28.1 (50.6)	4107 (418.8)
-006	0.4495	.991 (2.184)	.259 (0.572)	3.82	88 (159)	28.1 (50.5)	4101 (418.2)
	0.739	.996 (2.195)	.267 (0.589)	3.73	88 (158)	28.3 (50.9)	4148 (422.9)
-007	0.4495	.980 (2.161)	.263 (0.581)	3.73	91 (164)	27.6 (49.6)	4170 (425.2)
	0.6895	1.030 (2.270)	.263 (0.581)	3.90	91 (164)	27.6 (49.6)	4170 (425.2)
-008	0.4495	.994 (2.191)	.261 (0.576)	3.80	91 (163)	27.3 (49.1)	4069 (414.9)
	0.7495	1.034 (2.280)	.265 (0.584)	3.91	90 (162)	27.6 (49.7)	4146 (422.7)
	1.0495	1.012 (2.231)	.271 (0.597)	3.74	89 (161)	27.5 (49.5)	4166 (424.8)
-009	0.4495	.903 (1.991)	.251 (0.554)	3.60	91 (164)	33.8 (60.9)	4179 (426.[illegible]
	0.7495	.912 (2.010)	.265 (0.584)	3.44	91 (163)	31.6 (56.9)	[illegible] (426.2)
	1.0495	.909 (2.004)	.270 (0.596)	3.36	91 (163)	30.5 (54.9)	4183 (426.5)
	1.6495	.917 (2.022)	.274 (0.605)	3.34	91 (163)	29.8 (53.6)	4179 (426.1)
	2.2495	.918 (2.025)	278 (0.612)	3.31	89 (162)	29.3 (52.8)	4179 (426.1)

TABLE XV (cont.)

Test No.	Time Sec aft FS_1	$(\dot{W}_o)_T$ Kg/sec (lb/sec)	$(\dot{W}_F)_T$ Kg/sec (lb/sec)	MR Total	TOTCV °K (°R)	TFTCV °K (°R)	$(I_s)_{VAC}$ N-sec/kg (lb_f-sec/lb_m)
-009 (cont.)	2.8495	..920 (2.028)	.279 (0.616)	3.29	89 (162)	28.9 (52.0)	4182 (426.5)
	3.4495	.920 (2.029)	.282 (0.621)	3.27	89 (162)	28.7 (51.7)	4180 (426.2)
-010	0.4495	1.072 (2.363)	.224 (0.493)	4.80	91 (164)	31.7 (57.5)	4161 (424.3)
	0.7495	1.112 (2.451)	.231 (0.509	4.82	89 (162)	30.8 (55.5)	4157 (423.8)
	1.048	1.104 (2.434)	.237 (0.522)	4.66	89 (162)	30.1 (54.2)	4175 (425.7)

radial flow at these locations toward the wall and result in stoichiometric combustion products being carried to the wall. There are 16 bowling alleys in the pattern (Figure 70 shows the two that the pattern repeats symmetrically eight times) that correspond to 16 heat marks on the uncooled spacer at the injector face. Compatibility could probably be improved by moving elements to break up the bowling alleys or by enlarging the outer element of the fuel doublet to force the fuel fans inward.

2. Vacuum Test Performance Analysis

Steady state performance data from eight of the altitude tests with LH_2/LO_2 are summarized in Table XVI. The like doublet injector was tested with a 17.8 cm (7.0 in.) chamber length from injector face to throat together with a 40 exit area ratio nozzle.

Engine mixture ratios from 3.3 to 4.8 were evaluated. The ε = 40:1 vacuum experimental energy release efficiencies (ERE) are shown vs. O/F on Figure 71 and for reference, the sea level ERE vs. O/F line is also shown. The sea level (ε = 4.8) and vacuum (ε = 40) ERE data are in agreement. The c* efficiency data are shown in Figure 71; the ERE and c* data are comparable although the latter exhibit somewhat greater scatter.

The steady state performance was achieved very quickly with the LH_2/LO_2 engine as shown on Figure 72 for Test 1983-002-0M-009. Delivered vacuum specific impulse, ERE, and c* efficiency, are all stabilized and constant within 0.25 to .50 second. This was made possible due to the rapid injector chilldown characteristic of this engine design. The steady state specific impulse of the design point 1 engine was 4178 to 4187 N-sec/kg (426 to 427 lbf-sec/lbm) which is in agreement with extrapolated sea level performance data (see Section VI, B, 1, c).

TABLE XVI

LIQUID/LIQUID ENGINE PERFORMANCE

********** ETR ENGINE TEST DATA AND PERFORMANCE SUMMARY **********

TEST SERIES: 1983-002-0X-XXX

DESIGN POINT 1: LIKE DOUBLET INJECTOR

**** ENGINE SYSTEM DATA ****

			START	STOP	COMBT PC	F VAC	MR	AF	WFC	WT	%EFC	ISPV	CSTAR	MW	MRC	TMW	TO	TF
			.49	.49	[illegible]	1694.2	2.0072	.5629	.0000	2.6701	.0	425.7	8107.	3.57	3.57	1186.	159.	56.
			.50	.50	[illegible]	1122.7	2.0421	.5702	.0000	2.6213	.0	426.3	7974.	3.63	3.63	1466.	156.	53.
			.50	.50	[illegible]	1102.4	2.0158	.5637	.0000	2.6545	.0	431.6	8352.	3.70	3.70	1151.	160.	54.
			.50	.50	[illegible]	1135.0	2.0365	.5714	.0000	2.6279	.0	431.9	7768.	3.60	3.60	1435.	159.	53.
			.50	.50	[illegible]	1123.0	2.0218	.5680	.0000	2.6018	.0	431.6	8080.	3.49	3.49	1714.	159.	53.
			.49	.49	[illegible]	[illegible]	2.0084	.4753	.0000	2.4851	.0	419.8	7972.	4.23	4.23	671.	145.	51.
			.49	.49	[illegible]	1153.1	2.1844	.5725	.0000	2.7569	.0	418.2	7774.	3.82	3.82	1241.	155.	56.
			.50	.50	[illegible]	1127.4	2.1953	.5891	.0000	2.7844	.0	422.9	7743.	3.73	3.73	1751.	154.	51.
			.49	.49	[illegible]	1144.4	2.1668	.5793	.0000	2.7461	.0	417.8	7759.	3.73	3.73	1240.	154.	49.
			.50	.50	[illegible]	1216.6	2.2703	.5815	.0000	2.8518	.0	426.2	7769.	3.90	3.90	1689.	166.	56.
			.49	.49	[illegible]	1154.1	2.1910	.5762	.0000	2.7672	.0	414.9	7800.	3.80	3.80	1345.	163.	53.
			.50	.50	[illegible]	1210.6	2.2608	.5835	.0000	2.8443	.0	422.7	7741.	3.91	3.91	1862.	169.	54.
			1.00	1.00	[illegible]	1231.4	2.2315	.5674	.0000	2.8289	.0	424.7	7717.	3.74	3.74	2027.	161.	48.
			1.00	1.00	[illegible]	1211.9	2.2406	.5660	.0000	2.8356	.0	434.1	7851.	3.84	3.84	2041.	161.	49.
			.49	.49	[illegible]	1064.4	1.4911	.5546	.0000	2.5447	.0	426.1	7820.	3.60	3.60	1214.	164.	61.
			.50	.50	[illegible]	1104.8	2.0046	.5638	.0000	2.5324	.0	426.2	7807.	3.44	3.44	1582.	163.	57.
			1.00	1.00	[illegible]	1109.3	2.0043	.5964	.0000	2.6007	.0	426.5	7813.	3.36	3.36	1839.	163.	55.
			1.00	1.00	[illegible]	1116.9	2.0207	.6012	.0000	2.6219	.0	426.8	7789.	3.36	3.36	1954.	162.	55.
			1.00	1.00	[illegible]	1119.8	2.0225	.6058	.0000	2.6283	.0	426.1	7795.	3.34	3.34	2033.	163.	54.
			1.00	1.00	[illegible]	1124.0	2.0341	.6071	.0000	2.6412	.0	425.6	7737.	3.35	3.35	2076.	162.	54.
			1.00	1.00	[illegible]	1124.7	2.0254	.6118	.0000	2.6372	.0	426.1	7752.	3.31	3.31	2076.	162.	53.
			1.00	1.00	[illegible]	1125.4	2.0328	.6152	.0000	2.6480	.0	425.6	7720.	3.30	3.30	2081.	162.	53.
			1.00	1.00	[illegible]	1127.8	2.0281	.6161	.0000	2.6442	.0	426.5	7771.	3.29	3.29	2043.	162.	53.
			1.00	1.00	[illegible]	1126.6	2.0331	.6180	.0000	2.6511	.0	425.8	7734.	3.29	3.29	2112.	162.	52.
			1.00	1.00	[illegible]	1127.3	2.0247	.6209	.0000	2.6496	.0	426.2	7732.	3.27	3.27	2056.	161.	52.
			.49	.49	[illegible]	1211.8	2.3631	.4926	.0000	2.8557	.0	424.3	7650.	4.80	4.80	1252.	164.	57.
			.79	.79	[illegible]	1254.0	2.4506	.5085	.0000	2.9591	.0	423.8	7561.	4.82	4.82	1706.	162.	55.
			1.00	1.00	[illegible]	1258.2	2.4337	.5218	.0000	2.9555	.0	425.7	7570.	4.66	4.66	1935.	162.	54.
			2.00	2.00	[illegible]	1245.2	2.4760	.5074	.0000	2.9834	.0	417.4	7323.	4.88	4.88	2182.	163.	53.
			3.47	3.47	[illegible]	946.3	3.2387	.6688	.0000	3.9075	.0	255.0	3510.	4.84	4.84	1991.	161.	50.

TABLE XVI (cont.)

TEST.42076.1.100 25 FEB 74 16:31:03 PAGE 20

********** ETR ENGINE TEST DATA AND PERFORMANCE SUMMARY **********

TEST SERIES: 1983-002-0M-XXX

DESIGN POINT 1: LIKE DOUBLET INJECTOR

**** PERFORMANCE DATA ****

			PC		%PEC	TO	TF	CSTAR	CSTART	%C*	ISPV	ISPT	%ISP	KL	OL	HL	MRL	FCL	EBL	EBF
		1	471.8	3.57	.0	158.9	50.5	8107.	7989.	101.5	425.7	452.5	94.1	1.1	2.1	10.2	.0	.0	13.3	97.1
		2	473.3	3.53	.0	157.7	52.0	7974.	7952.	99.8	428.3	452.2	94.7	1.0	2.2	8.6	.0	.0	12.2	97.3
		1	483.1	3.70	.0	160.4	53.7	8352.	7982.	104.6	431.6	453.4	95.2	1.2	2.2	10.7	.0	.0	7.8	98.3
		2	483.4	3.60	.0	159.1	53.7	7788.	7988.	97.5	431.9	452.8	95.4	1.2	2.2	8.4	.0	.0	9.2	98.0
		3	476.0	3.49	.0	158.7	52.5	8080.	7994.	101.1	431.6	452.0	95.5	1.0	2.2	7.9	.0	.0	9.3	97.9
		1	448.6	4.23	.0	164.7	50.6	7972.	7917.	100.7	418.8	455.4	92.0	2.1	2.1	13.1	.0	.0	19.3	95.8
		1	485.3	3.82	.0	158.6	50.5	7774.	7970.	97.5	418.2	453.9	92.1	1.3	2.1	9.6	.0	.0	22.6	95.0
		2	488.2	3.73	.0	157.6	50.9	7743.	7978.	97.1	422.9	453.5	93.3	1.2	2.1	8.1	.0	.0	18.2	96.8
		1	481.4	3.73	.0	165.6	49.3	7759.	7978.	97.2	417.8	453.5	92.1	1.2	2.1	9.5	.0	.0	22.9	94.9
		2	501.7	3.90	.0	164.5	49.6	7769.	7962.	97.6	425.2	454.4	93.6	1.4	2.1	8.3	.0	.0	17.4	96.2
		1	486.7	3.80	.0	162.7	49.1	7800.	7971.	97.8	414.9	453.9	91.4	1.3	2.1	8.5	.0	.0	27.1	94.0
		2	502.1	3.91	.0	161.6	49.7	7741.	7961.	97.2	422.7	454.4	93.0	1.4	2.1	7.9	.0	.0	20.3	95.5
		3	498.2	3.74	.0	151.5	49.5	7717.	7977.	96.7	424.7	453.5	93.6	1.2	2.1	7.6	.0	.0	18.5	95.9
		4	508.1	3.96	.0	161.5	49.5	7851.	7968.	98.5	434.1	454.0	95.6	1.3	2.2	7.1	.0	.0	8.4	97.9
		1	450.6	3.60	.0	164.5	60.9	7820.	7992.	97.8	426.1	453.1	94.1	1.2	2.1	9.5	.0	.0	14.1	96.9
		2	458.3	3.44	.0	163.1	56.9	7807.	7999.	97.6	426.2	451.8	94.3	1.0	2.1	7.6	.0	.0	14.9	96.7
		3	460.1	3.36	.0	162.7	54.9	7813.	8000.	97.7	426.5	451.1	94.6	.9	2.1	6.6	.0	.0	15.0	96.7
		4	462.4	3.36	.0	162.3	54.6	7789.	8000.	97.4	426.8	451.1	94.6	.9	2.1	6.1	.0	.0	15.1	96.6
		5	461.5	3.34	.0	162.6	53.6	7755.	8000.	96.9	426.1	450.9	94.5	.9	2.1	5.9	.0	.0	15.9	96.5
		6	462.7	3.35	.0	161.9	53.6	7737.	8000.	96.7	425.6	451.0	94.4	.9	2.1	5.9	.0	.0	16.5	96.3
		7	462.9	3.31	.0	162.6	52.8	7752.	8000.	96.9	426.1	450.6	94.6	.8	2.1	5.8	.0	.0	15.7	96.5
		8	462.4	3.30	.0	161.8	52.3	7720.	8000.	96.5	425.0	450.5	94.3	.8	2.1	5.8	.0	.0	16.7	96.3
		9	463.3	3.29	.0	161.6	52.0	7771.	8000.	97.1	426.5	450.4	94.7	.8	2.1	5.8	.0	.0	15.1	96.7
		10	462.3	3.29	.0	161.8	51.9	7734.	8000.	96.7	425.8	450.4	94.5	.8	2.1	5.8	.0	.0	15.9	96.5
		11	463.9	3.27	.0	161.5	51.7	7732.	8000.	96.7	426.2	450.2	94.7	.8	2.1	5.6	.0	.0	15.4	96.6
		1	494.7	4.80	.0	164.0	57.5	7650.	7823.	97.8	424.3	456.0	93.1	2.5	2.1	10.5	.0	.0	16.5	96.4
		2	506.0	4.82	.0	162.2	55.5	7561.	7819.	96.7	423.8	455.9	92.9	2.5	2.1	8.7	.0	.0	18.9	95.9
		3	506.6	4.66	.0	161.8	54.2	7570.	7848.	96.5	425.7	456.0	93.4	2.3	2.1	7.8	.0	.0	18.1	96.0
		4	494.7	4.88	.0	162.9	59.0	7529.	7807.	93.8	417.4	455.9	91.5	2.7	2.1	7.0	.0	.0	26.8	94.1
		5	510.6	4.84	.0	161.4	53.4	3510.	7792.	45.0	255.0	455.5	56.0	4.6	1.3	3.4	.0	.0	191.2	58.0

TABLE XVI (cont.)

25 FEB 74 16:31:03 PAGE 21

[illegible]

************ ETR ENGINE TEST DATA AND PERFORMANCE SUMMARY **********

TEST SERIES: 1993-002-OM-XXX

DESIGN POINT 1: LIKE DOUBLET INJECTOR

******HYDRAULIC DATA ****

TEST	DATE	RUN	PC	MR	AO	KF	AC	AF	CDU	CUF	ΔPOX	ΔPFL	VOX	VFUEL	TOJ	TEJ	DN	VF/VO	MORAT	FRC
[illegible]	[illegible]	[illegible]	[illegible]	[illegible]	[illegible]	[illegible]	[illegible]	[illegible]	.600	.800	193.2	345.8	[illegible]	935.6	178.9	[illegible]	.317	5.77	1.62	97.1
[illegible]	[illegible]	[illegible]	[illegible]	.53	[illegible]	.5782	[illegible]	.02956	.600	.800	149.3	374.9	[illegible]	985.8	177.7	[illegible]	[illegible]	6.09	1.76	[illegible]
[illegible]	[illegible]	[illegible]	[illegible]	[illegible]	[illegible]	[illegible]	[illegible]	[illegible]	.600	.800	194.6	339.2	163.0	950.2	180.4	[illegible]	[illegible]	5.83	[illegible]	[illegible]
[illegible]	[illegible]	[illegible]	[illegible]	[illegible]	[illegible]	.5714	[illegible]	[illegible]	.600	.800	202.9	340.5	166.1	1014.2	179.1	63.7	.307	6.11	[illegible]	[illegible]
[illegible]	[illegible]	[illegible]	[illegible]	3.49	[illegible]	[illegible]	[illegible]	[illegible]	.600	.800	195.9	378.7	163.1	[illegible]	178.7	62.5	[illegible]	6.09	[illegible]	[illegible]
[illegible]	[illegible]	[illegible]	[illegible]	[illegible]	[illegible]	[illegible]	[illegible]	[illegible]	.600	.800	196.7	250.5	164.8	802.7	184.7	[illegible]	[illegible]	4.87	[illegible]	[illegible]
[illegible]	[illegible]	[illegible]	[illegible]	[illegible]	[illegible]	[illegible]	[illegible]	[illegible]	.600	.800	228.6	355.3	176.2	945.2	178.6	60.5	.348	[illegible]	[illegible]	[illegible]
[illegible]	[illegible]	[illegible]	[illegible]	[illegible]	[illegible]	[illegible]	[illegible]	[illegible]	.600	.800	230.3	378.9	176.6	977.1	177.6	61.9	[illegible]	[illegible]	[illegible]	[illegible]
[illegible]	[illegible]	[illegible]	[illegible]	[illegible]	[illegible]	[illegible]	[illegible]	[illegible]	.600	.800	227.9	357.9	177.6	[illegible]	185.6	[illegible]	[illegible]	[illegible]	[illegible]	[illegible]
[illegible]	[illegible]	[illegible]	[illegible]	[illegible]	[illegible]	[illegible]	[illegible]	[illegible]	.600	.800	250.8	359.4	186.0	941.2	184.5	59.6	.367	[illegible]	[illegible]	[illegible]
[illegible]	[illegible]	[illegible]	[illegible]	[illegible]	[illegible]	[illegible]	[illegible]	.02956	.600	.800	232.5	352.1	178.7	930.5	182.7	59.1	.354	5.21	[illegible]	[illegible]
[illegible]	[illegible]	[illegible]	[illegible]	[illegible]	[illegible]	[illegible]	[illegible]	[illegible]	.600	.800	251.2	362.3	185.5	945.6	181.6	59.7	.365	[illegible]	[illegible]	[illegible]
[illegible]	[illegible]	[illegible]	[illegible]	4.91	[illegible]	[illegible]	[illegible]	.02956	.600	.800	240.4	379.8	181.4	958.2	181.5	59.5	.344	5.34	[illegible]	[illegible]
[illegible]	[illegible]	[illegible]	[illegible]	[illegible]	[illegible]	[illegible]	[illegible]	.02956	.600	.800	244.3	363.1	182.9	943.7	181.5	59.3	.358	[illegible]	1.34	[illegible]
[illegible]	[illegible]	[illegible]	[illegible]	[illegible]	[illegible]	[illegible]	[illegible]	[illegible]	.600	.800	192.9	491.9	163.2	[illegible]	184.5	70.9	[illegible]	[illegible]	[illegible]	[illegible]
[illegible]	[illegible]	[illegible]	[illegible]	[illegible]	[illegible]	[illegible]	[illegible]	[illegible]	.600	.800	195.6	446.2	164.0	1163.9	183.1	[illegible]	.267	7.10	[illegible]	[illegible]
[illegible]	[illegible]	[illegible]	[illegible]	.44	[illegible]	[illegible]	.04358	.02956	.600	.800	194.6	429.6	163.5	1097.1	182.7	64.9	.273	6.71	[illegible]	96.7
[illegible]	[illegible]	[illegible]	[illegible]	3.36	[illegible]	[illegible]	.04358	.02956	.600	.800	197.5	431.7	164.6	1093.5	182.3	64.6	.275	6.64	[illegible]	96.6
[illegible]	[illegible]	[illegible]	[illegible]	[illegible]	2.0267	[illegible]	.04358	.02956	.600	.800	198.0	427.4	164.9	1074.6	182.6	63.6	.278	6.52	1.95	[illegible]
[illegible]	[illegible]	[illegible]	[illegible]	3.34	[illegible]	[illegible]	.04358	.02956	.600	.800	200.0	[illegible]	165.5	1075.7	181.9	63.6	.279	6.50	1.94	96.3
[illegible]	[illegible]	[illegible]	[illegible]	[illegible]	2.0341	[illegible]	[illegible]	[illegible]	.600	.800	198.3	427.9	164.9	1065.0	182.0	62.8	.278	6.46	[illegible]	[illegible]
[illegible]	[illegible]	[illegible]	[illegible]	3.31	[illegible]	[illegible]	.04358	.02956	.600	.800	199.6	428.4	165.4	1060.4	181.8	62.3	.279	6.41	1.94	96.3
[illegible]	[illegible]	[illegible]	[illegible]	3.30	[illegible]	[illegible]	.04358	.02956	.600	.800	199.6	426.5	164.9	1054.3	181.6	62.0	.279	6.39	1.94	96.7
[illegible]	[illegible]	[illegible]	[illegible]	[illegible]	2.0241	[illegible]	[illegible]	.02956	.600	.800	199.6	428.7	165.3	1056.3	181.6	61.9	.279	6.39	1.94	96.5
[illegible]	[illegible]	[illegible]	[illegible]	[illegible]	[illegible]	[illegible]	[illegible]	[illegible]	.600	.800	198.7	[illegible]	164.9	1057.8	181.5	61.7	.276	6.41	1.96	96.6
[illegible]	[illegible]	1	[illegible]	[illegible]	[illegible]	.4926	.04358	.02956	.600	.800	271.4	313.5	193.4	969.1	184.0	67.5	.418	5.01	1.04	96.4
[illegible]		2	[illegible]	[illegible]	[illegible]	[illegible]	.04358	.02956	.600	.800	299.5	306.3	199.6	917.3	182.2	65.5	.440	4.60	.95	95.9
[illegible]		3	[illegible]	[illegible]	2.4337	.5218	.04358	.02956	.600	.800	286.2	311.5	198.0	909.2	181.8	64.2	.432	4.59	.98	96.0
[illegible]		[illegible]	[illegible]	[illegible]	[illegible]	.5074	.04358	[illegible]	.600	.800	247.1	355.9	202.0	1068.2	182.9	63.0	.409	5.29	1.08	94.1
[illegible]		5	310.6	[illegible]	[illegible]	[illegible]	.04358	.02956	.600	[illegible]	596.2	732.4	263.2	1067.8	141.4	63.9	.364	6.34	1.31	58.0

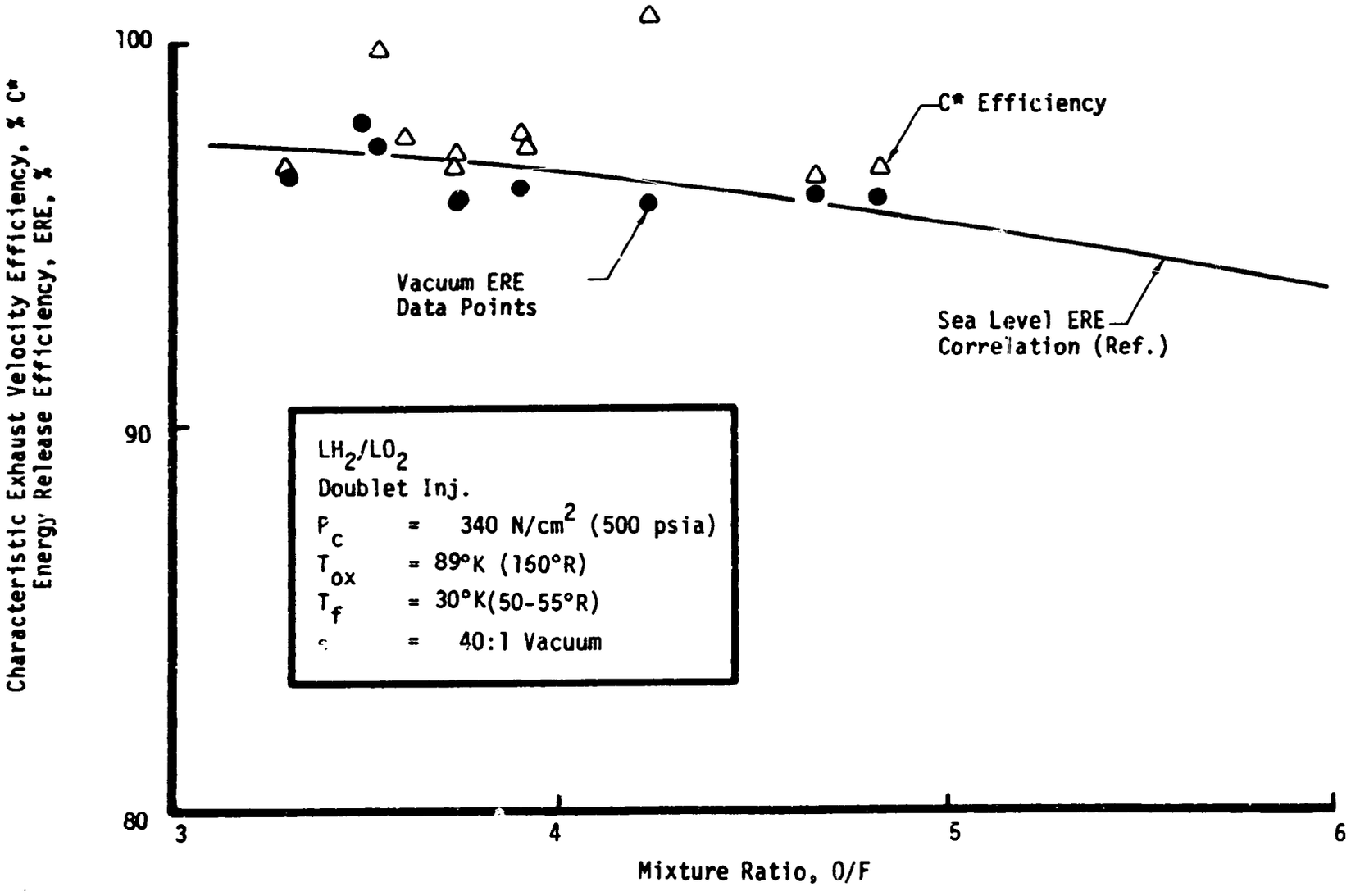

Figure 71. Mixture Ratio Effect on LH_2/LO_2 Performance Efficiency

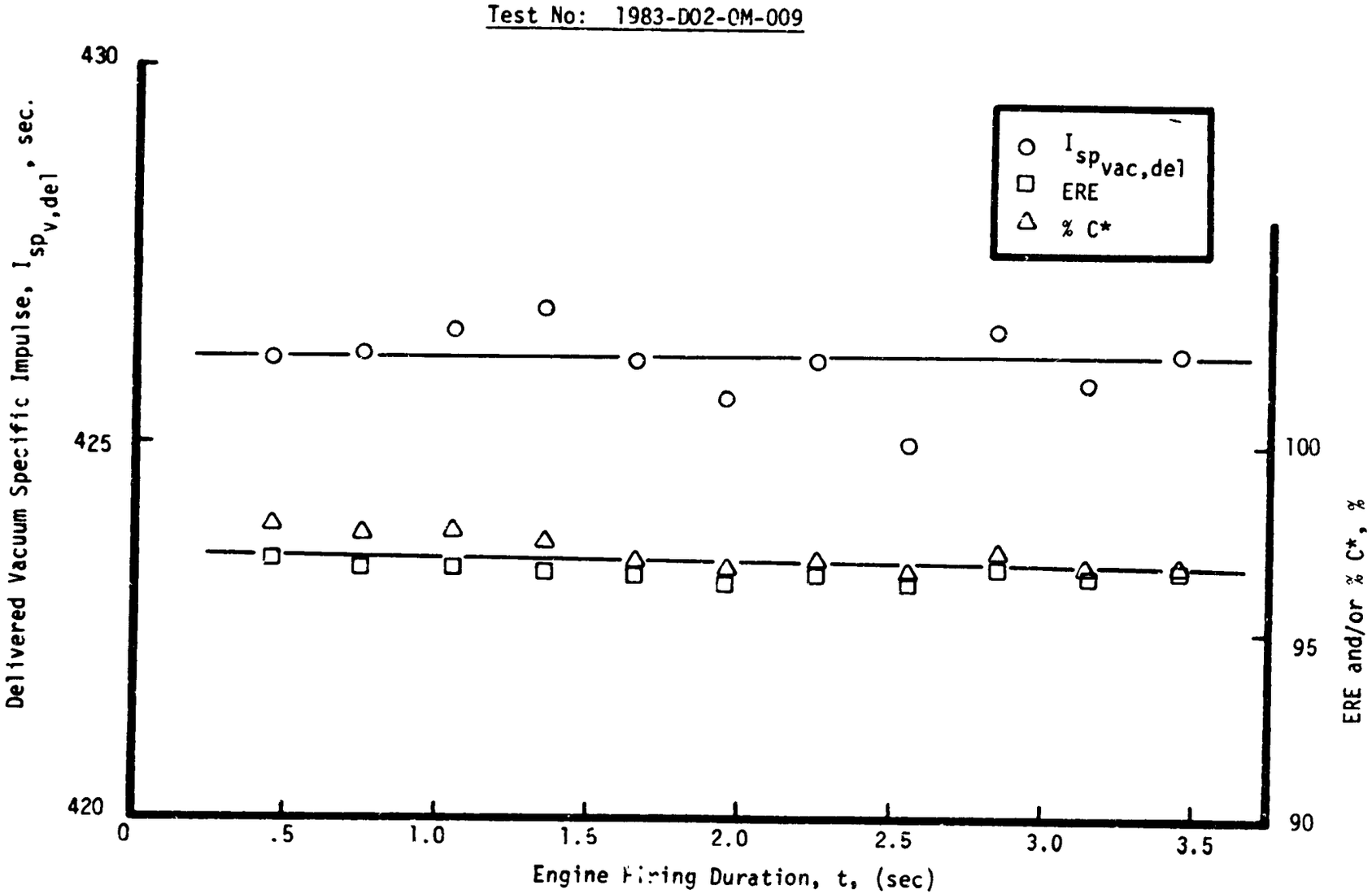

Figure 72. LH_2/LO_2 Engine Performance vs Firing Duration

IX. Cooled Chamber Test Results (cont.)

B. GAS/LIQUID (DESIGN POINT #2)

1. Heat Transfer

Test conditions for the gas/liquid thruster are given in Table X. The tests of most interest from a heat transfer standpoint are: (1) long duration tests 021, 023, 024, 026 and 028; (2) pulse tests 029 through 043; (3) pulsed tests followed by a steady burn with varied fuel temperatures 044 through 052, and (4) reduced fuel film cooling test 054.

The following major results have been found and will be discussed in detail in following sections.

1. Injector face temperatures do not exceed 380°K (225°F) for nominal conditions (P_c = 345 N/cm^2 (500 psia), MR = 4.5, T_{fuel} = 83°K (150°R). Chilling of the fuel to temperatures of less than 56°C (100°R) has the effect of producing a substantial decrease in injector face temperatures.

2. Regeneratively cooled thrust chamber data are in excellent agreement with previously attained sea level data and with the design predictions.

3. Steady state throat wall temperatures exhibited a strong effect due to film cooling flow rate and a surprisingly strong effect with chamber pressure. The most severe thermal conditions occur at minimum film cooling flow rate and at a chamber pressure of 296 N/cm^2 (430 psia). Maximum wall temperature recorded was at thermocouple TCC-A7 which was located 11.54 cm (4.56 inches) downstream of the throat.

a. Injector Face Temperatures

Injector face temperatures are plotted in Figure 73 and 74 for tests having a duration of ten seconds or longer. Thermocouples TF-1

ETR GAS/LIQUID INJECTOR FACE TEMPERATURES
STEADY FIRINGS - NOMINAL FUEL TEMPERATURE

PART A

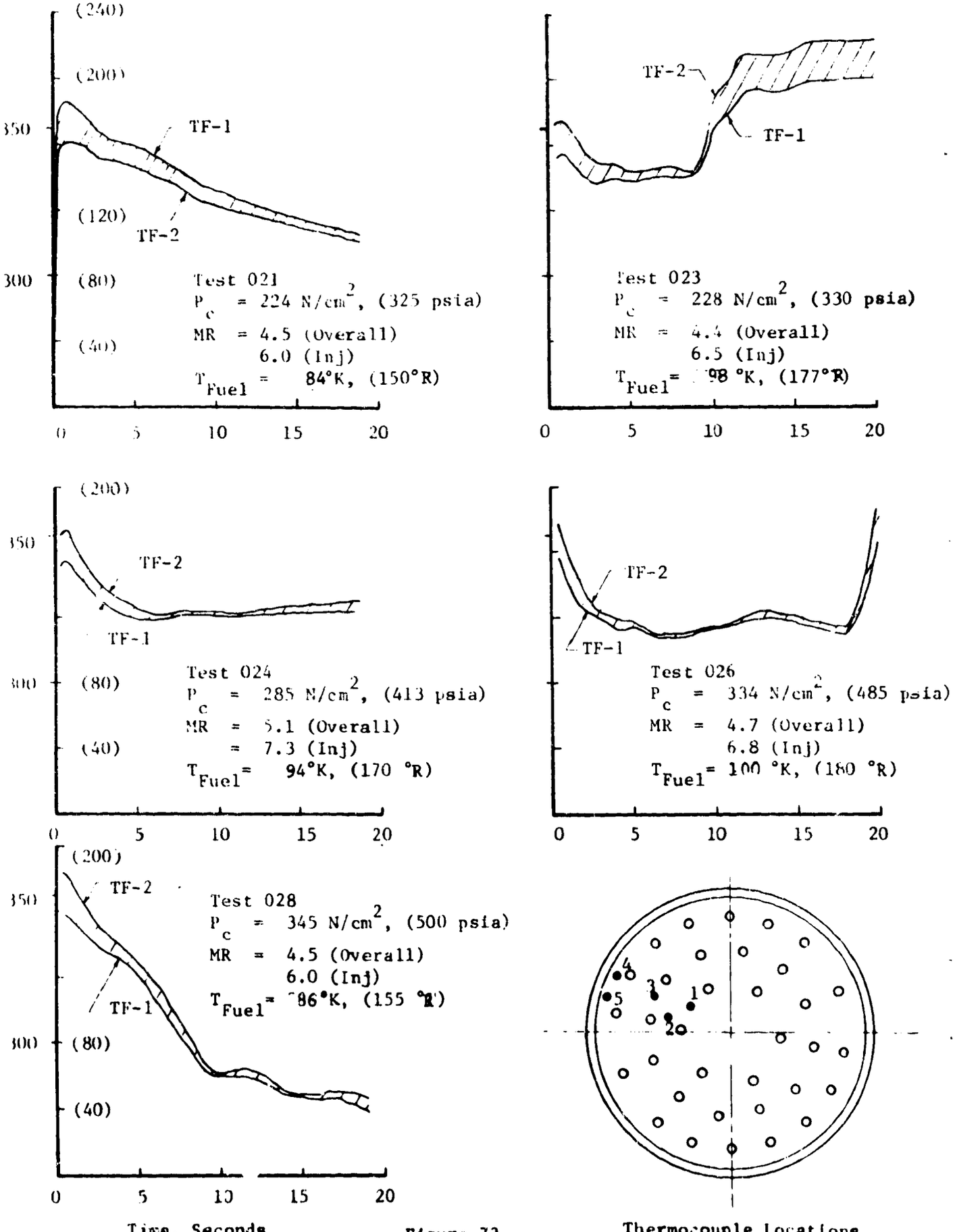

Figure 73

ETR GAS/LIQUID INJECTOR FACE TEMPERATURES
STEADY FIRINGS - NOMINAL FUEL TEMPERATURE

PART B

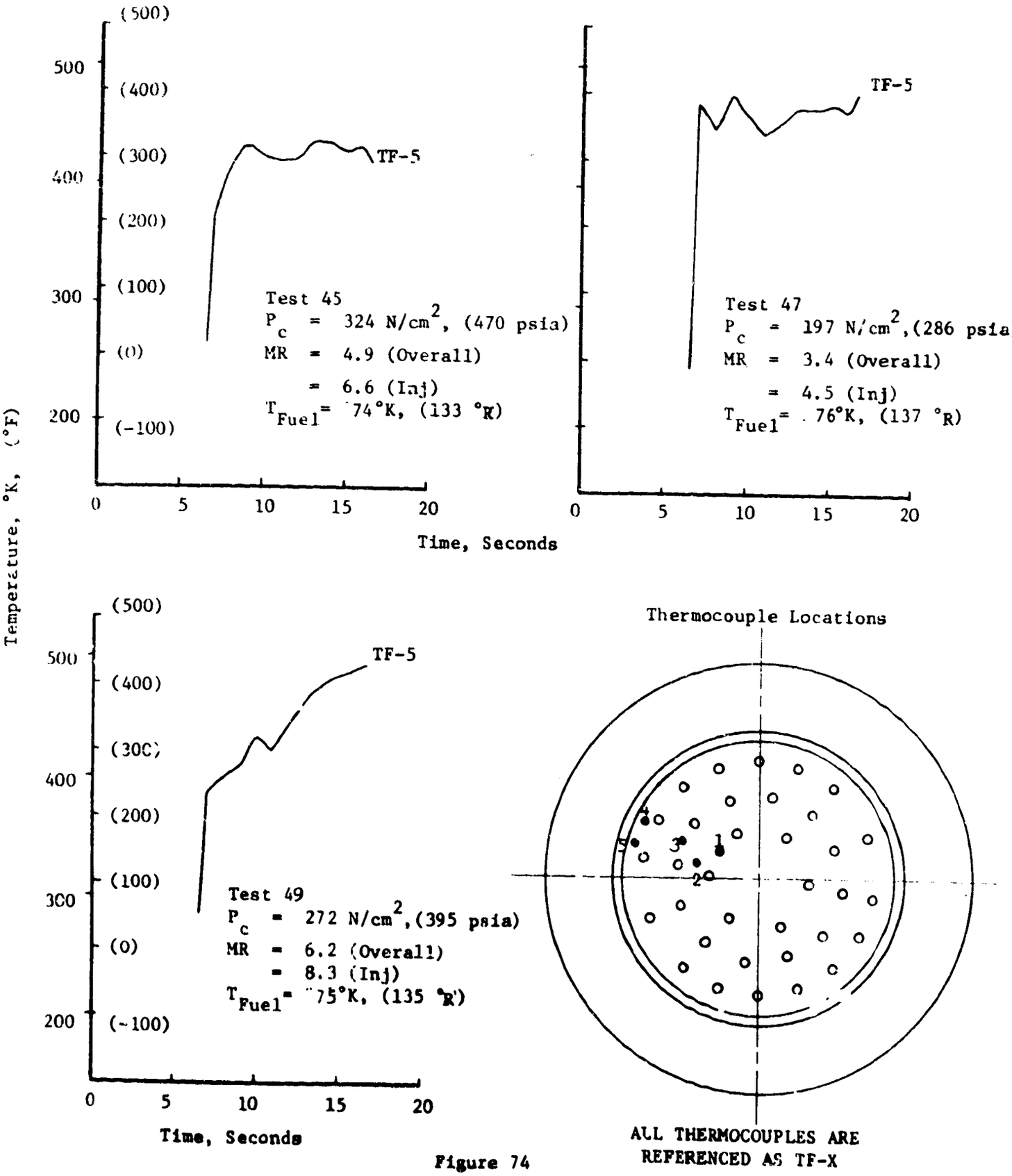

Figure 74

and TF-2 were monitored on all twenty second tests. Thermocouple TF-5 was monitored on all ten second tests; these data are presented in Figures 73 and 74, respectively. Also shown on these figures are the relative thermocouple locations.

The most obvious feature of these curves is the change in temperature with time including the sudden upturn of temperatures at 10 seconds for Test 023 and 19 seconds for Test -026. Test -023 ultimately settles out at a maximum temperature of 379°K (223°F), an increase of approximately 44°K (80°F) over its previous steady value. Test -026 may have steadied out also, however, the test was terminated by a normal shutdown. The change in injector face temperatures was the result of fuel temperature changes at the inlet to the thruster. These propellant changes caused changes in the flow, mixture ratio and heat input through the regen section. During Test -023, the fuel inlet temperature increased by 23°K (42°R). During Test -026, the fuel inlet temperature was initially at 88.3°K (159°F) and increased by the end of the run to 100.5°K (181°F). The fuel inlet temperature decreased for the first 10 sec of Test -028. The injector face temperatures during these tests seemed to reflect the fuel inlet temperatures. Injector face temperatures are plotted as a function of fuel inlet temperature in Figure 75.

The injector face temperature was more sensitive to hydrogen flow rate than the fuel temperature (as long as it is above 50°K (90°R) (Figure 75)). As may be seen on Figure 73, Test -028 has a 21% fuel film cooling flow rate which means more fuel within the injector and a colder face temperature than any of the other tests. Colder fuel temperatures on Test -028 most certainly contributes to cooler face temperatures. Pressure effects upon the injector face temperature appear to be negligible.

Figure 74 is a plot of all 10 second tests with nominal fuel temperature and test conditions. These data, however, are for temperatures taken at TF-5 which is outboard of the last ring of elements. Temperatures at

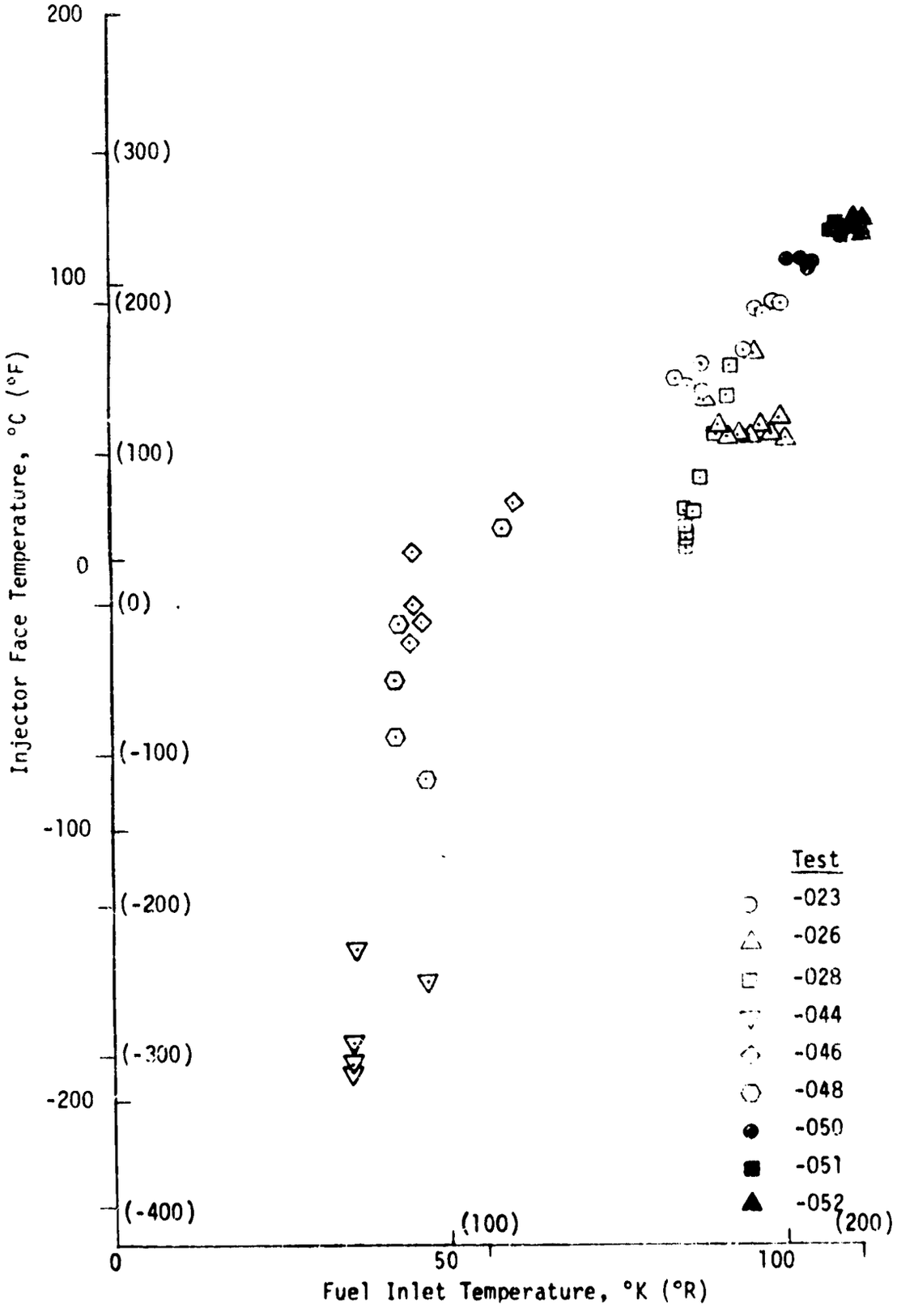

Figure 75. Effect of Propellant Temperature on Injector Face Temperature TC - TF-1 or TF-2

this location are well-behaved, however, the maximum temperature recorded here is 494°K (430°F) compared with 379°K (223°F) at the TF-2 location indicating a higher heat transfer rate at this point due possibly to either a lack of cooling or to increased hot gas circulation locally.

Figure 76 illustrates the injector face temperatures at the TF-5 location for the off-nominal fuel temperature tests. Tests -046, -048 and -044 had cold propellant temperatures while Tests -050, -051 and -052 had above nominal propellant temperatures. The cold propellant tests all exhibit a substantial decrease in face temperatures during the 10 second tests and then a marked increase near the end of the test. This is a direct result of an increased fuel flow in the middle of the test which is reflected in the flow meter readings. Generally, the fuel temperature decreased to a minimum in the middle of the test as the hardware and lines chilled down and then rose toward the end of the run by 10 to 16°K (18 to 29°R) as the supply of cold hydrogen was exhausted. This resulted in a changing fuel flow rate and mixture ratio. The fuel enters the system as a near-liquid which goes through a psuedo-phase change primarily in the regeneratively cooled jacket. Large density changes result from small temperature changes. This same phenomenon occurs in the dump cooled and film cooled regions where wall temperatures are changing long after they normally have steadied out.

The warmer fuel test results are given in Figure 76. Maximum injector face temperatures experienced was 561°K (550°F) and this occurred on Test -052 where the fuel temperature was 111°K (200°R). The propellant temperatures for these tests was constant (unlike the cold propellant tests). There was no change in fuel flow rate or MR and thus the injector face temperatures did not change.

b. Regeneratively Cooled Thrust Chamber

Approximately 75-80% of the fuel was introduced at the aft end of the cylindrical thrust chamber, flowed through the regeneratively

ETR GAS/LIQUID INJECTOR FACE TEMPERATURES
STEADY FIRINGS - OFF-NOMINAL FUEL TEMPERATURES

Test	P_c N/cm^2	P_c (Psia)	O/A	Core	T_{Fuel} °K	T_{Fuel} (°R)
44	345	(500)	2.4	2.5	37	(67)
46	201	(291)	3.8	3.9	47	(85)
48	324	(470)	4.7	4.8	42	(76)

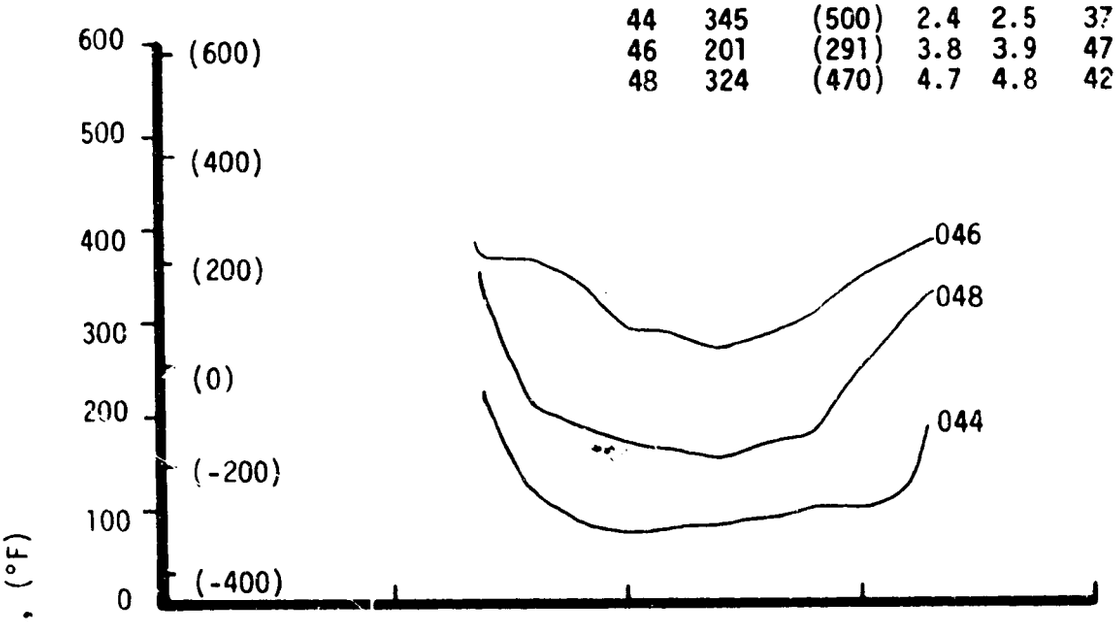

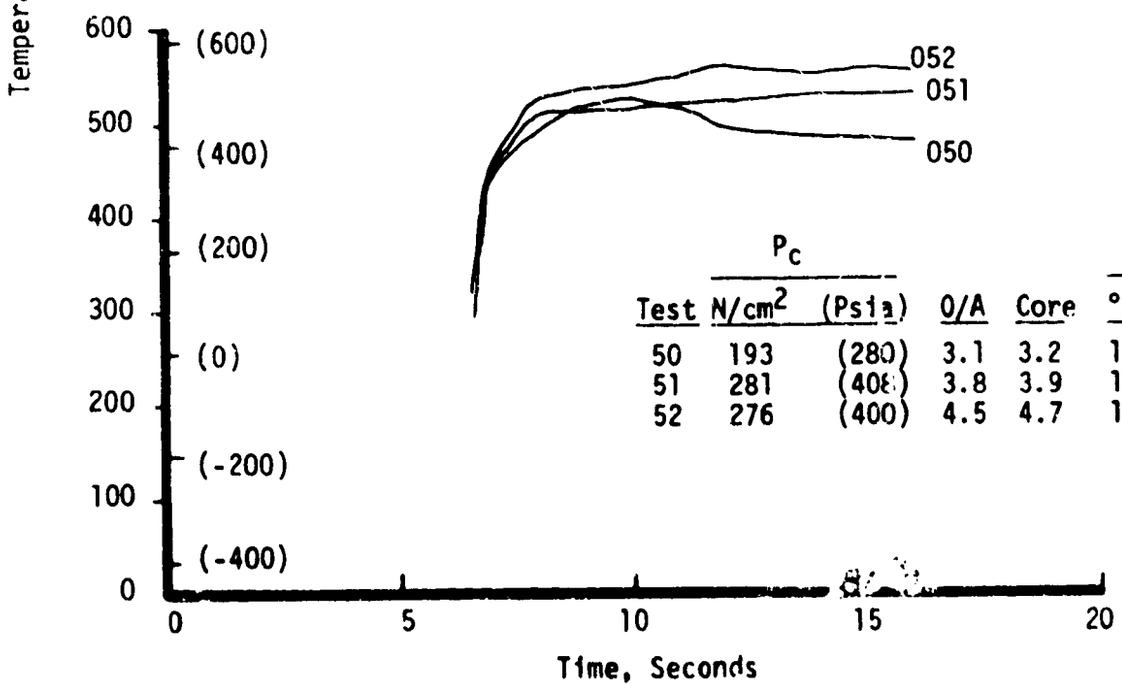

Temperature, °K, (°F)

Time, Seconds

Test	P_c N/cm^2	P_c (Psia)	O/A	Core	T_{Fuel} °K	T_{Fuel} (°R)
50	193	(280)	3.1	3.2	103	(186)
51	281	(408)	3.8	3.9	108	(195)
52	276	(400)	4.5	4.7	111	(200)

Figure 76

cooled thrust chamber, and then was injected into the thrust chamber via the injector. Fuel flow thus was a one-pass counter flow arrangement. Original predictions indicated a bulk temperature rise of approximately 111°K (200°F) under nominal test conditions. This prediction was based on the sea level data and as can be seen in Figure 77, was verified by the altitude test data. In this figure are plotted the bulk temperature rise and the liquid-side wall temperatures. Included on each of these curves are the original predictions and for comparison purposes the sea level data from two representative tests. Excellent agreement between the three sources is obtained on the bulk temperature curve and between the two sets of test data on the wall temperature curve. At the forward end of the chamber, the wall temperature prediction is substantially higher than data. A good deal of this apparent discrepancy is due to the difficulty of accurately placing the thermocouple on the thrust chamber surface and accurately locating it between coolant channels where thermal gradients are severe. Nevertheless, the altitude data are in excellent agreement with the sea level data and well within the bounds of acceptable operation.

c. Film Cooled Wall Temperatures

Typical throat temperature transients are given in Figure 78 for two representative tests, -021 and -028. The wall temperatures peak at about three seconds into the test and then decay slightly. This slight drop-off in temperature is probably the result of a small increase in film coolant flow rate as the regen chamber heats up and the chamber and injector resistance rises relative to that of the film cooling circuit. Temperatures around the throat generally fall into a tolerance band of about 56°K (100°F). One thermocouple, TCC-3B, consistently read much lower than other throat thermocouples and eventually failed. This low reading as shown on Test -028, has therefore been discounted as a faulty thermocouple and is shown here for comparison purposes only.

Steady state axial variation of adiabatic wall temperature for all long duration tests is given in Figure 79. In this figure the temperature

ETR REGENERATIVELY COOLED THRUST CHAMBER

COMPARISON OF BULK TEMPERATURES AND WALL TEMPERATURES

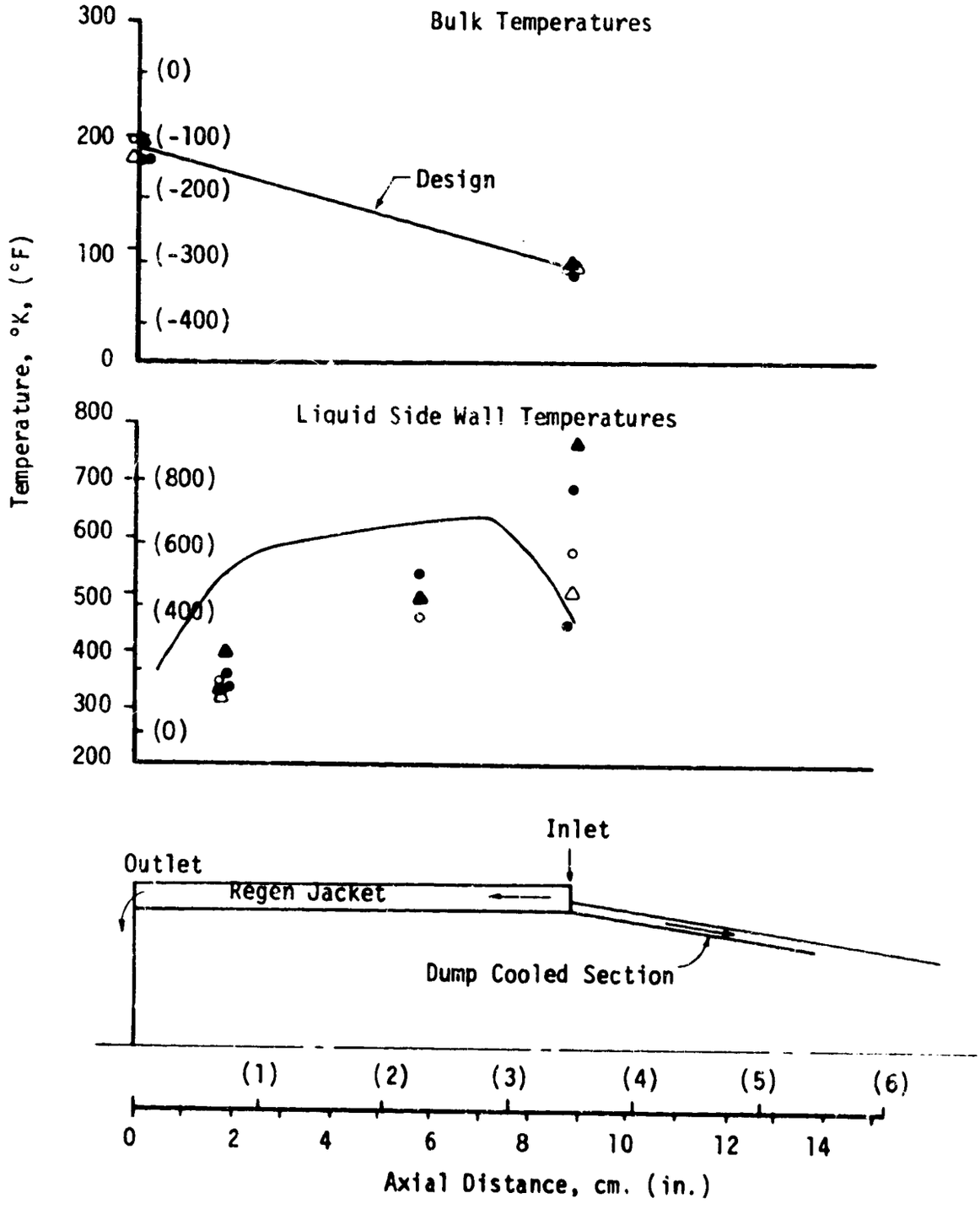

Symbol	Test No.	Inj. MR	P_c N/cm^2	(Psia)	S/L-Alt.
●	007	6.6	343	(497)	S/L
▲	008	6.5	338	(490)	S/L
○	026	6.8	331	(480)	Alt.
△	028	6.0	345	(500)	Alt.

Figure 77

TYPICAL THROAT WALL TEMPERATURE

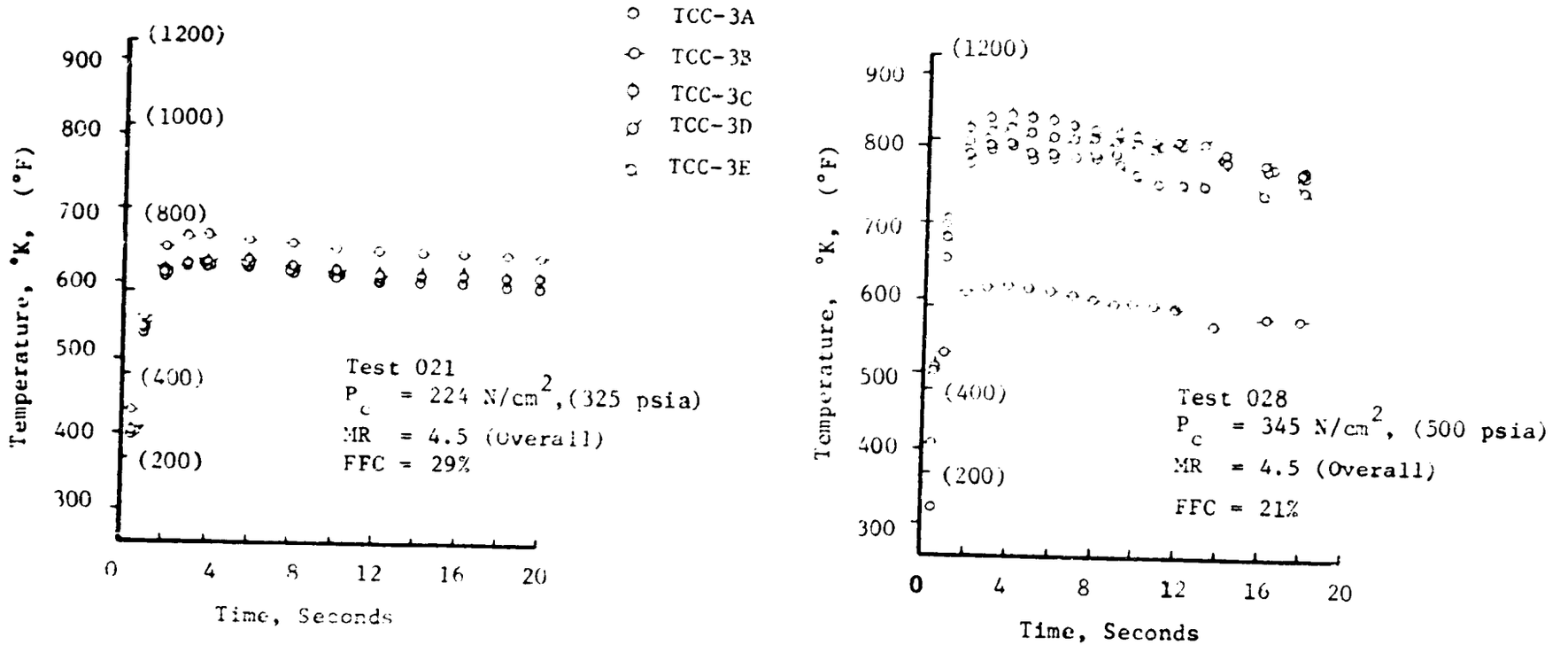

Figure 78

GAS/LIQUID THRUSTER TEMPERATURES ALONG ROW A,
STEADY FIRINGS

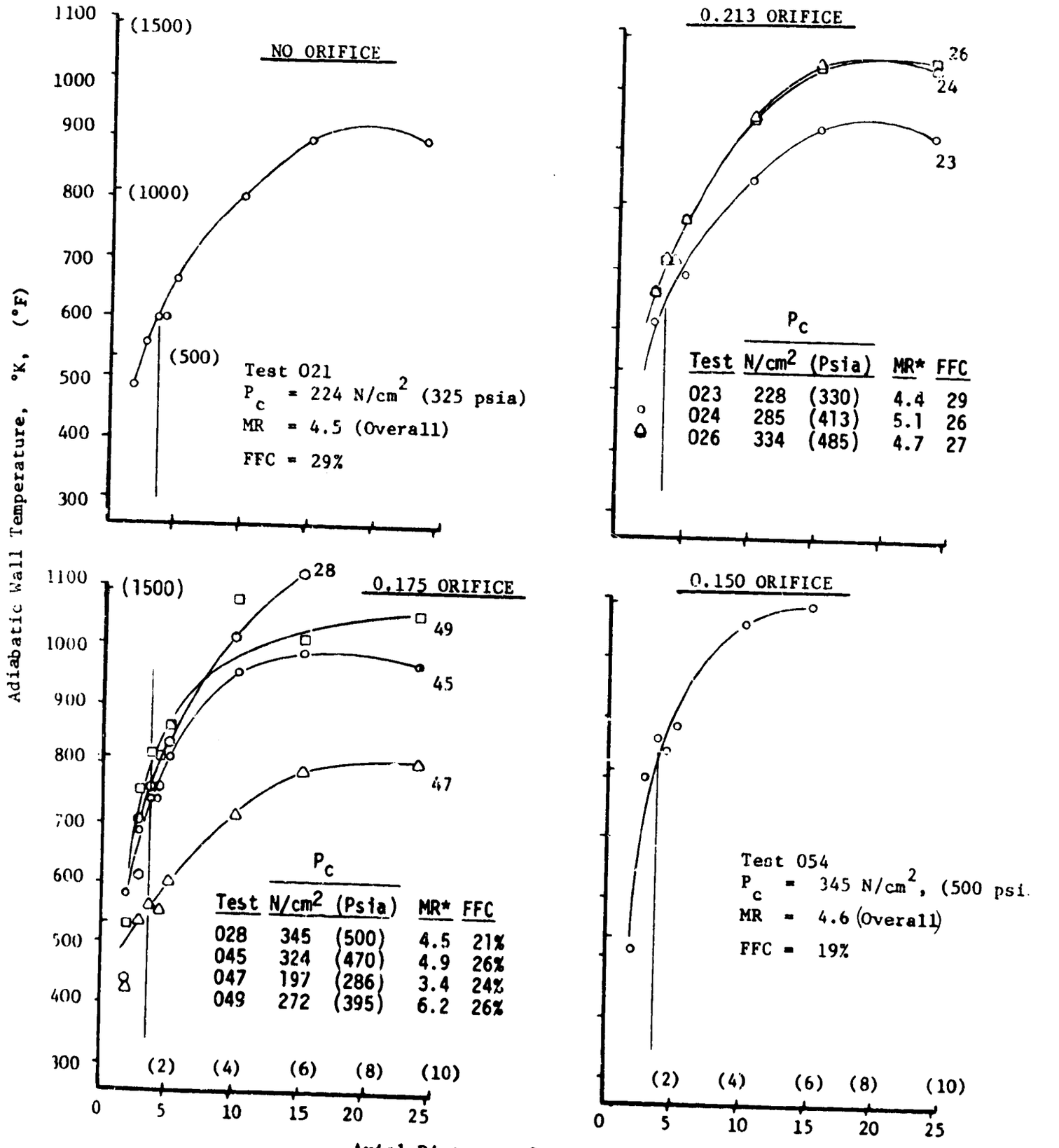

Figure 79

*Overall Mixture Ratio

profiles are grouped according to which film cooling orifice was used for that particular test. Of course, the smaller the orifice the less fuel film cooling and, for all other conditions being equal, the higher the wall temperature. The peak adiabatic wall temperature occurs downstream of the throat at approximately 19 cm (7.5 in.) from the flange. This, or course, is due to mixing of free stream gases into the boundary layer. The following dicussion will center on two nozzle locations: the throat because the temperatures steady out quite rapidly and because the instrumentation density is highest, and the point of maximum temperature (TCC-A7) because it is that point which limits operation.

The single most effective parameter in correlating the film cooling thermal data was found to be the film coolant flow rate expressed as a precentage of total propellant flow. This is shown in Figure 80 in which the throat temperature and maximum wall temperature are shown as a function of the percentage coolant flow rate. These data cover a chamber pressure range from 207 to 345 N/cm^2 (300 to 500 psia) and a mixture ratio range from 3.5 to 6.5. It can be seen in this figure that the throat data correlate quite well. The data at the maximum wall temperature correlate well when the long duration runs are considered alone as evidenced by the line drawn through those points. Apparently the 10 second runs had not reached steady state. Allowing for a practical limit of 1144°K (1600°F) for the Haynes alloy at the throat and a 1420°K (2100°F) creep limit it may be seen that considerable reduction in the film cooling could have been made before the throat reached 1144°K or the skirt reached 1420°K.

d. Pulsing Thermal Data

Temperature traces of throat thermocouples during selected pulsing tests are shown on Figure 81. Peak temperatures, on most runs, are reached somewhere between 2 seconds and 8 seconds. Following the peak temperatures, a slow decay of temperature was experienced. Test -042

ETR GAS/LIQUID THRUSTER WALL TEMPERATURE VS.
FILM COOLING FRACTION

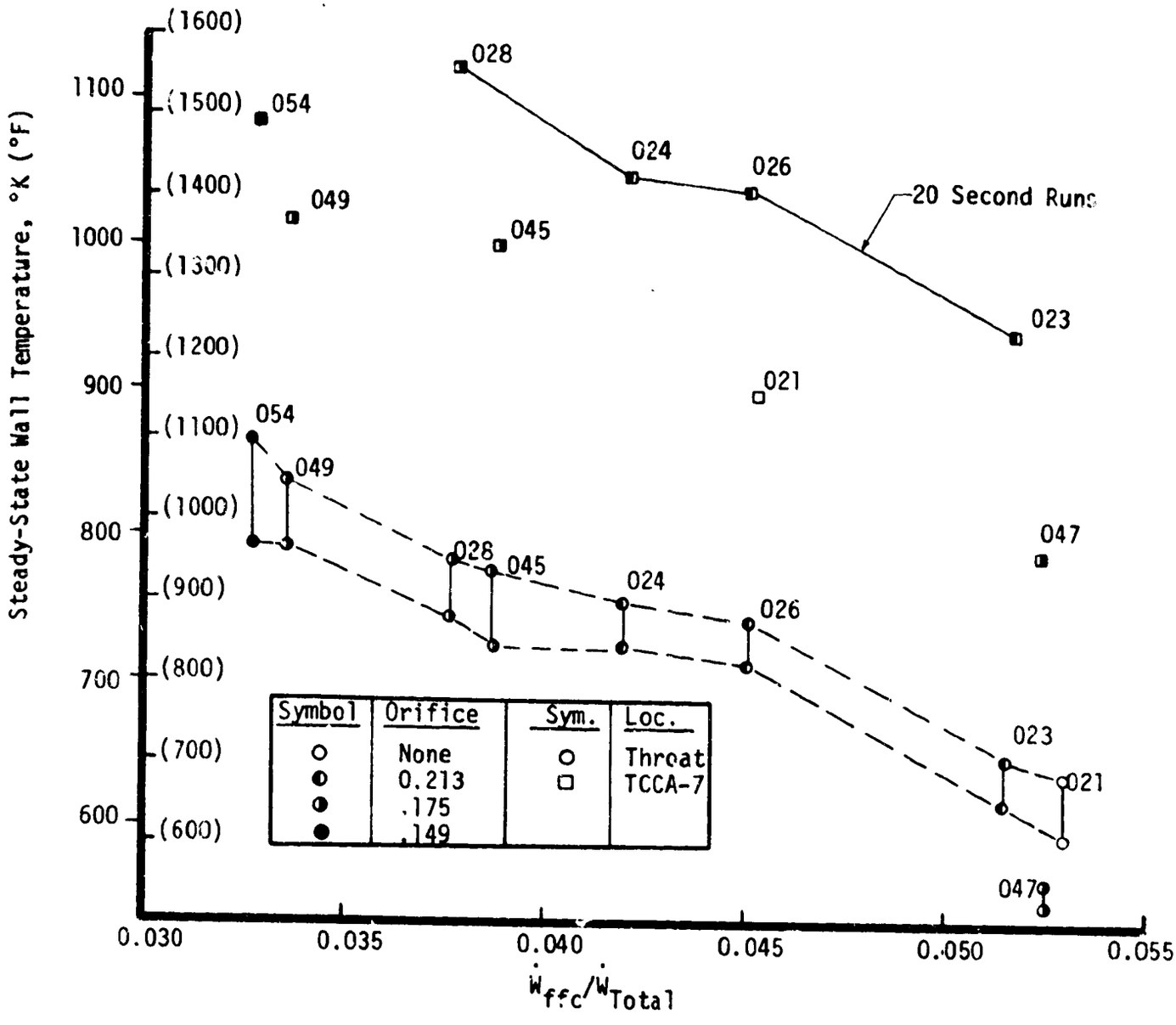

Test	P_c N/cm^2	P_c (Psia)	$\dot{W}_{Total}$	MR	$\dot{W}_{ffc}$ lb/sec
021	224	(325)	1.89	4.5	0.102
023	228	(330)	1.86	4.6	0.0960
024	276	(400)	2.45	5.0	0.103
026	331	(480)	2.84	5.0	0.128
028	345	(500)	2.86	4.7	0.108
045	328	(475)	2.83	5.0	0.109
047	207	(300)	1.68	3.5	0.0880
049	283	(410)	2.50	6.5	0.0840
054	345	(500)	2.78	4.6	0.091

Figure 80

MAXIMUM THROAT TEMPERATURE - G/L PULSE TEST

(TCC-3F)

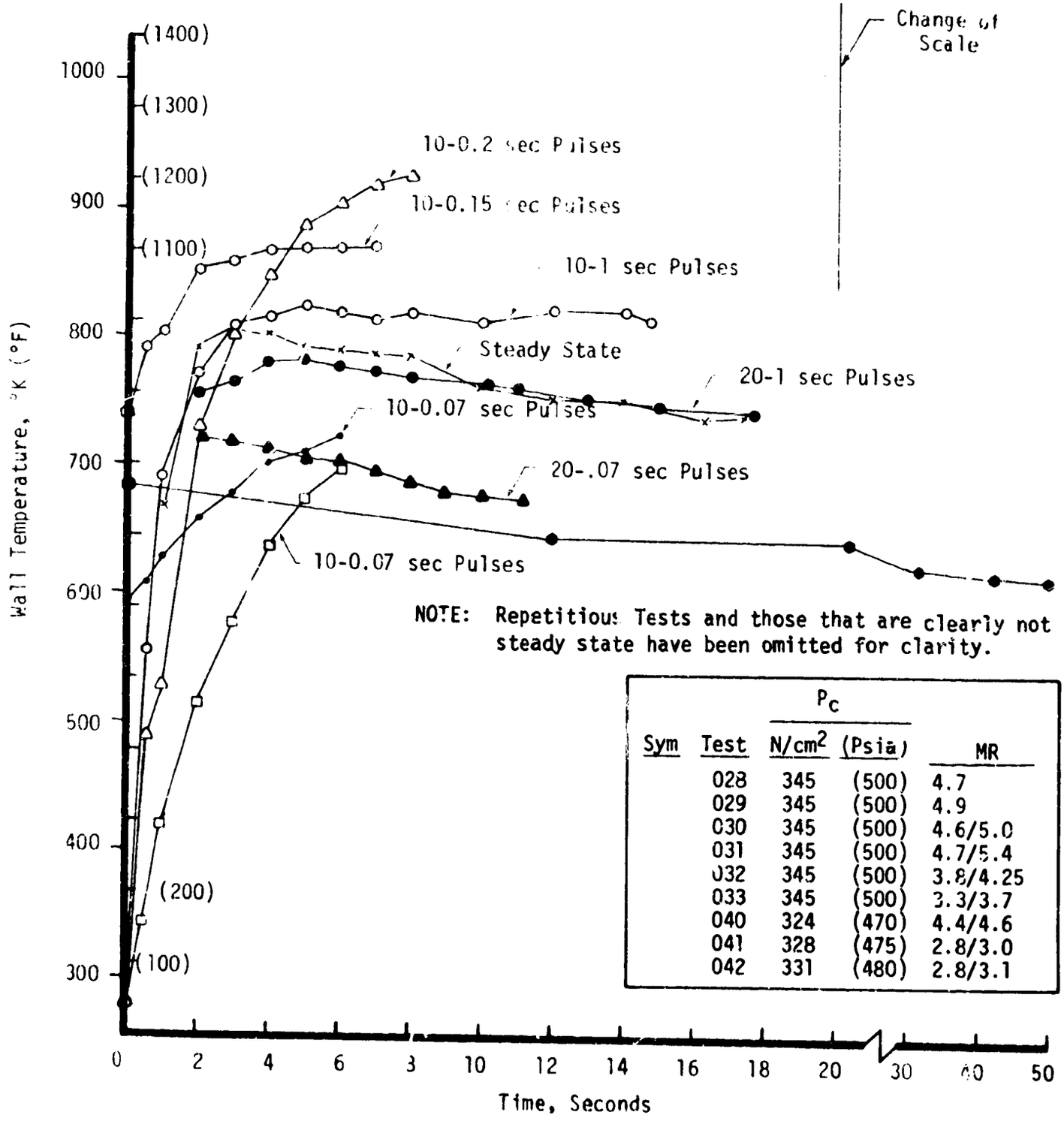

NOTE: Repetitious Tests and those that are clearly not steady state have been omitted for clarity.

Sym	Test	P_c N/cm²	P_c (Psia)	MR
	028	345	(500)	4.7
	029	345	(500)	4.9
	030	345	(500)	4.6/5.0
	031	345	(500)	4.7/5.4
	032	345	(500)	3.8/4.25
	033	345	(500)	3.3/3.7
	040	324	(470)	4.4/4.6
	041	328	(475)	2.8/3.0
	042	331	(480)	2.8/3.1

Figure 81

which had a total duration in excess of 50 seconds, was still experiencing a slight decay of temperatures at shutdown. This decay is probably the result of a gradual shift in the relative hydraulic resistances of the injector, chamber, and film cooling ring as they heat up, producing a slight increase in the film coolant flow rate.

The data of Figure 81 have been analyzed to determine what parameters control the steady state temperatures achieved during pulsing. When plotted as a function of percentage on time it was found that the maximum throat temperature was nearly independent of the duty cycle over the range tested. This result reflects the fact that at steady state the throat operates in a nearly adiabatic mode. The heat loss between firings or heat pick-up during firing is minimal, giving a throat temperature which doesn't vary much with duty cycle. A very significant conclusion from this is that the throat sees a pulse series as nearly equivalent to a single deep thermal cycle from the cycle life point of view, thereby greatly enhancing the cycle life characteristics of the design.

The steady state throat temperature is a strong function of the overall mixture ratio as shown in Figure 82. This result is in agreement with the results of Figure 81 where it was shown that the wall temperature is primarily a function of the percentage of the total propellant flow which is used as film coolants. Since the pulsing data are for a constant fuel split the mixture ratio dependance is really reflecting the coolant flow rate dependance.

2. Vacuum Test Performance Analysis

The steady state altitude performance for the GH_2/LO_2 design point 2 engine is summarized in Table XVII. All tests were conducted with the regeneratively cooled cylindrical chamber and GH_2 film cooled nozzle throat.

EQUILIBRIUM THROAT WALL TEMPERATURE AS A FUNCTION OF
MIXTURE RATIO FOR PULSE TESTS

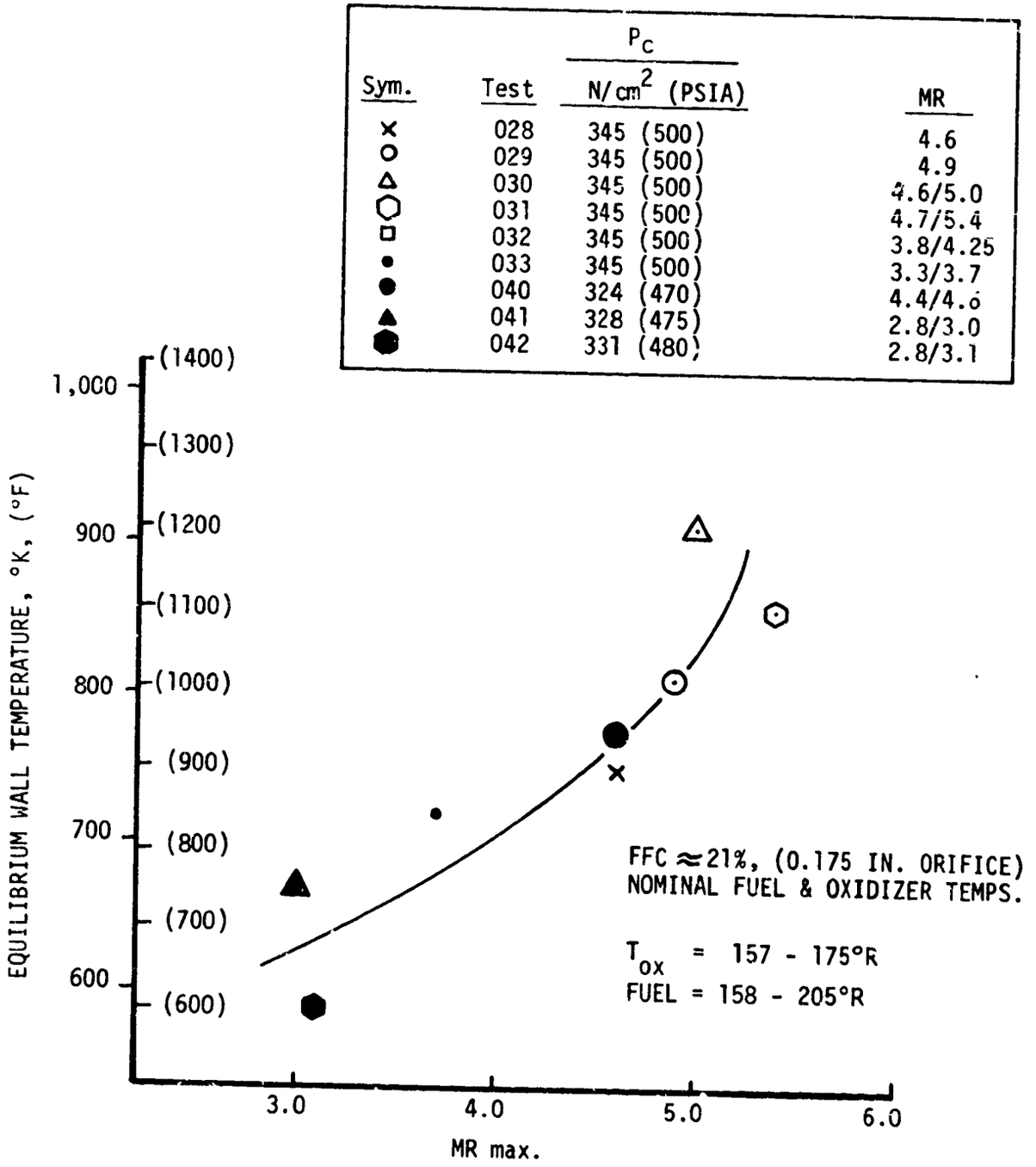

Figure 82.

TABLE XVII

GAS/LIQUID ENGINE PERFORMANCE

********** ETR ENGINE TEST DATA AND PERFORMANCE SUMMARY **********

TEST SERIES: 1983-D02-0M-XXX

DESIGN POINT 2: SHEAR COAXIAL INJECTOR

**** ENGINE SYSTEM DATA ****

TEST	DATE	PER	START	STOP	DURAT	PC	F VAC	WO	WF	WFC	WT	%FFC	ISPV	CSTAR	MR	MRC	TWM	TO	TF
12	02/19/74	1	.19	.19	.00	262.6	619.5	1.1564	.2544	.0944	1.5052	27.1	411.6	7704.	3.32	4.55	540.	162.	155.
13	02/19/74	1	.20	.20	.00	265.9	613.2	1.1625	.2754	.0926	1.5305	25.2	400.7	7649.	3.16	4.22	540.	166.	153.
14	02/19/74	1	.44	.44	.00	234.7	535.7	.9107	.2795	.1004	1.2906	26.4	415.1	8030.	2.40	3.26	545.	158.	140.
14		2	.61	.61	.00	238.6	553.0	.9452	.2748	.1004	1.3204	26.8	418.8	7979.	2.52	3.44	550.	157.	141.
15	02/19/74	1	.64	.64	.00	317.8	761.3	1.3807	.2978	.0963	1.7748	24.4	428.9	7907.	3.50	4.64	615.	156.	132.
15		2	2.10	2.10	.00	320.1	775.7	1.4091	.2960	.0963	1.8014	24.5	430.6	7847.	3.59	4.76	819.	154.	132.
16	02/20/74	1	.24	.24	.00	320.4	761.3	1.3619	.2986	.1042	1.7647	25.9	431.4	8017.	3.38	4.56	540.	161.	146.
16		2	.54	.54	.00	318.4	766.0	1.3932	.2626	.1042	1.7800	26.9	430.3	7699.	3.60	4.93	680.	159.	146.
17	02/20/74	1	.64	.64	.00	317.8	778.0	1.4694	.2411	.0993	1.8098	29.2	429.9	7754.	4.32	6.09	680.	164.	159.
17		2	2.10	2.10	.00	312.7	770.9	1.4747	.2315	.0993	1.8055	30.0	427.0	7648.	4.46	6.37	968.	163.	163.
19	02/21/74	1	.24	.24	.00	321.9	789.0	1.5200	.2489	.0771	1.8460	23.7	427.4	7700.	4.66	6.11	550.	159.	156.
19		2	.54	.54	.00	326.2	819.0	1.7014	.2289	.0771	2.0074	25.2	408.0	7220.	5.56	7.43	680.	157.	154.
21	02/21/74	1	1.14	1.14	.00	322.1	795.7	1.5620	.2361	.1020	1.9007	30.2	418.6	7483.	4.62	6.62	819.	160.	155.
21		2	3.14	3.14	.00	322.0	800.5	1.5678	.2389	.1020	1.9087	29.9	419.4	7449.	4.60	6.56	1060.	160.	156.
21		3	5.14	5.14	.00	322.1	802.2	1.5614	.2438	.1020	1.9072	29.5	420.6	7458.	4.62	6.40	1110.	160.	155.
21		4	10.14	10.14	.00	323.3	803.6	1.5517	.2500	.1020	1.9037	29.0	422.1	7499.	4.41	6.21	1160.	158.	151.
21		5	15.14	15.14	.00	323.4	803.0	1.5459	.2535	.1020	1.9014	28.7	422.3	7511.	4.35	6.10	1210.	157.	149.
21		6	19.14	19.14	.00	323.2	802.6	1.5479	.2543	.1020	1.9042	28.6	421.5	7495.	4.34	6.09	1234.	156.	148.
22	02/22/74	1	.30	.30	.00	339.1	819.2	1.7077	.2496	.0896	2.0469	26.4	400.2	7316.	5.03	6.84	550.	161.	172.
22		2	.50	.50	.00	333.0	804.1	1.7323	.2561	.0896	2.0780	25.9	387.0	7077.	5.01	6.76	675.	160.	171.
23	02/22/74	1	2.14	2.14	.00	332.6	817.8	1.5632	.2664	.0960	1.9256	26.5	424.7	7632.	4.31	5.87	988.	162.	154.
23		2	6.14	6.14	.00	332.3	824.4	1.5734	.2660	.0960	1.9354	26.5	426.0	7582.	4.35	5.92	1181.	161.	154.
23		3	10.14	10.14	.00	330.4	817.6	1.5632	.2615	.0960	1.9207	26.9	425.7	7597.	4.37	5.98	1246.	161.	170.
23		4	16.14	16.14	.00	321.6	795.5	1.5312	.2499	.0960	1.8771	27.8	423.8	7571.	4.43	6.13	1275.	159.	177.
23		5	20.10	20.10	.00	321.8	795.9	1.5356	.2478	.0960	1.8794	27.9	423.5	7561.	4.47	6.20	1305.	158.	181.
24	02/22/74	1	2.14	2.14	.00	413.3	1029.7	2.0068	.3148	.1030	2.4246	24.7	424.7	7528.	4.80	6.37	1033.	170.	150.
24		2	6.14	6.14	.00	413.0	1037.8	2.0261	.3147	.1030	2.4438	24.7	424.7	7463.	4.85	6.44	1258.	168.	156.
24		3	10.14	10.14	.00	413.9	1039.8	2.0421	.3089	.1030	2.4540	25.0	423.7	7439.	4.96	6.61	1338.	166.	162.
24		4	16.14	16.14	.00	412.9	1040.4	2.0640	.3012	.1030	2.4682	25.5	421.5	7388.	5.11	6.85	1404.	162.	171.
24		5	20.10	20.10	.00	413.4	1041.0	2.0724	.2966	.1030	2.4720	25.8	421.1	7385.	5.19	6.99	1438.	161.	175.
25	02/22/74	1	.34	.34	.00	501.5	1245.8	2.4434	.3689	.1210	2.9333	24.7	424.7	7550.	4.99	6.62	580.	158.	158.
25		2	.54	.54	.00	491.4	1217.7	2.3620	.3739	.1210	2.8569	24.4	426.2	7597.	4.77	6.32	721.	156.	158.
26	02/22/74	1	2.14	2.14	.00	491.6	1226.1	2.3475	.3823	.1280	2.8578	25.1	429.0	7597.	4.60	6.14	1077.	156.	158.
26		2	5.14	5.14	.00	489.9	1225.8	2.3623	.3759	.1280	2.8662	25.4	427.7	7548.	4.69	6.28	1258.	157.	158.
26		3	10.14	10.14	.00	488.2	1229.0	2.3761	.3679	.1280	2.8720	25.8	427.9	7507.	4.79	6.46	1364.	158.	164.
26		4	15.14	15.14	.00	489.1	1228.4	2.3697	.3670	.1280	2.8647	25.9	428.8	7540.	4.79	6.46	1395.	161.	170.
26		5	19.14	19.14	.00	485.3	1221.3	2.3544	.3673	.1280	2.849	25.8	428.6	7521.	4.75	6.41	1422.	169.	178.
27	02/25/74	1	2.14	2.14	.00	496.9	1241.0	2.3852	.3856	.1078	2.8796	21.8	431.1	7623.	4.83	6.19	1206.	156.	182.
28		2	6.14	6.14	.00	493.9	1247.2	2.3845	.3906	.1078	2.8829	21.6	432.6	7566.	4.78	6.10	1432.	157.	161.
28		3	10.14	10.14	.00	494.5	1248.1	2.3755	.4035	.1078	2.8868	21.1	432.3	7565.	4.65	5.89	1485.	158.	163.
28		4	16.14	16.14	.00	493.6	1245.5	2.3548	.4138	.1078	2.8764	20.7	433.0	7655.	4.51	5.69	1498.	165.	157.
28		5	20.14	20.14	.00	499.2	1243.4	2.3442	.4159	.1078	2.8679	20.6	433.6	7687.	4.48	5.64	1512.	169.	154.
29	02/25/74	1	1.00	1.00	.00	487.7	1241.0	2.3695	.3948	.0995	2.8638	20.1	433.3	7521.	4.79	6.00	1030.	158.	154.
29		2	2.52	2.52	.00	487.7	1245.0	2.4014	.3901	.0995	2.8916	20.3	430.6	7450.	4.90	6.16	1246.	157.	154.
29		3	4.04	4.04	.00	491.3	1251.4	2.4250	.3861	.0995	2.9106	20.5	429.9	7453.	4.99	6.28	1330.	157.	161.

TABLE XVII (cont.)

28 MAR 74 15:11:37 PAGE 20

		4	8.59	8.59	.00	469.4	1249.0	2.4028	.3929	.0995	2.8952	20.2	431.4	7465.	4.88	6.12	1403.	157.	163.
		5	14.65	14.65	.00	491.4	1242.7	2.4133	.3955	.0995	2.9083	20.1	427.3	7464.	4.98	6.10	1436.	157.	159.
		1	1.00	1.00	.00	467.9	1190.6	2.2600	.3907	.1002	2.7509	20.4	432.8	7512.	4.60	5.78	922.	156.	156.
		2	2.52	2.52	.00	467.8	1195.7	2.2535	.3935	.1002	2.7472	20.3	435.2	7520.	4.56	5.73	1110.	156.	158.
		3	4.04	4.04	.00	467.6	1195.0	2.2519	.3950	.1002	2.7471	20.2	435.0	7507.	4.55	5.70	1217.	156.	160.
		4	8.59	8.5	.00	466.1	1183.5	2.2729	.3997	.1002	2.7726	20.0	426.8	7423.	4.55	5.69	1323.	157.	160.
		5	14.65	14.65	.00	467.4	1175.1	2.2965	.4091	.1032	2.7788	20.1	422.9	7428.	4.42	5.54	1346.	157.	156.
		6	22.23	22.23	.00	465.5	1181.0	2.2542	.4096	.1043	2.7681	20.3	426.6	7427.	4.39	5.50	1363.	161.	152.
		7	29.81	29.81	.00	463.7	1184.9	2.2549	.4091	.1060	2.7689	20.6	427.9	7396.	4.39	5.53	1357.	166.	152.
		1	1.00	1.00	.00	475.8	1217.1	2.4835	.3822	.0871	2.9531	18.6	412.1	7115.	5.29	6.50	1121.	161.	152.
		2	2.52	2.52	.00	478.6	1218.2	2.4864	.3782	.0871	2.9517	18.7	412.7	7164.	5.34	6.57	1182.	161.	151.
		3	4.04	4.04	.00	477.0	1219.1	2.4806	.3793	.0871	2.9470	18.7	412.3	7148.	5.32	6.54	1264.	162.	151.
		4	8.59	8.59	.00	465.8	1192.4	2.5981	.3629	.0871	3.0081	21.2	396.4	6938.	6.34	8.05	1335.	162.	151.
		1	15.64	15.64	.00	501.6	1208.1	2.0660	.7504	.1018	2.9182	11.9	414.0	7594.	2.42	2.75	867.	160.	108.
		1	15.69	15.69	.00	469.6	1196.3	2.3710	.3775	.1032	2.8517	21.5	419.5	7272.	4.93	6.28	1439.	161.	67.
		1	14.69	14.69	.00	291.2	722.2	1.3641	.2923	.0662	1.7226	18.5	419.2	7465.	3.81	4.67	1060.	161.	133.
		1	15.69	15.69	.00	286.1	710.5	1.3084	.2972	.0869	1.6935	22.6	419.8	7526.	3.41	4.40	1078.	137.	85.
		1	15.69	15.69	.00	471.3	1167.7	2.3406	.4170	.0839	2.8415	16.7	418.0	7359.	4.67	5.61	1153.	161.	137.
		1	14.69	14.69	.00	394.6	1011.7	2.1765	.2614	.0863	2.5182	24.6	401.8	6920.	6.24	8.30	1545.	160.	74.
		1	15.69	15.69	.00	278.2	692.4	1.2313	.3087	.0882	1.6282	22.2	425.3	7545.	3.10	3.99	1135.	155.	135.
		1	15.64	15.69	.00	408.5	1031.9	1.8922	.3687	.1101	2.3910	22.1	431.6	7545.	3.79	4.87	1345.	164.	188.
		1	15.64	15.69	.00	480.0	1112.3	2.1164	.3657	.1051	2.5872	22.3	429.9	6828.	4.50	5.79	1406.	163.	146.
		1	7.44	7.69	.00	482.6	1184.3	2.2795	.3950	.0867	2.7610	18.0	429.9	7400.	4.73	5.77	1321.	154.	2[illegible].
		1	15.65	15.65	.00	475.6	1214.9	2.2839	.4187	.0916	2.7942	18.0	434.8	7517.	4.48	5.65	1270.	157.	146.

Nomenclature

Per	- Date Period	ISPV	- Vacuum Specific Impulse, sec
Start	- Time at Start of Data Sample, sec	MK	- Engine Mixutre Ratio
Stop	- Time at Stop of Data Sample, sec	MRC	- Injector Mixture Ratio
Durat	- Duration of Data Sample	TWM	- Average Wall Temperature, °R
PC	- Chamber Pressure, psia	TO	- Oxidizer Temp, °R
FVAC	- Thrust, lbf	TF	- Fuel Temp, °R
WO	- Oxidizer Flow Rate, lb/sec		
WF	- Fuel Flow Rate to Injector, lb/sec		
WFC	- Fuel Film Coolant Flow Rate, lb/sec		
WT	- Total Propellant Flow Rate, lb/sec		
%FFC	- % of Fuel Used as Film Coolant		

TABLE XVII (cont.)

********** ETR ENGINE TEST DATA AND PERFORMANCE SUMMARY **********

TEST SERIES: 1983-D02-0M-xxx

DESIGN POINT 2: SHEAR COAXIAL INJECTOR

**** PERFORMANCE DATA ****

TEST	DATE	PER	PC	MR	%FFC	TC	TF	CSTAR	CSTART	%C*	ISPV	ISPT	%ISP	KI	DL	PL	MRL	FCL	FFL	FDF
19	03/19/74	1	282.0	3.32	27.1	161.9	155.1	7704.	8043.	95.8	412.6	453.9	90.7	1.6	2.1	6.8	.0	6.4	25.8	94.3
20	03/19/74	1	289.4	3.16	25.2	166.4	152.6	7649.	8047.	95.1	400.7	452.5	88.5	1.3	2.0	6.1	.0	4.3	18.1	91.6
21	03/19/74	1	234.7	3.60	26.4	157.7	139.6	8038.	7995.	100.4	415.1	442.5	93.8	.0	2.1	5.5	.0	.0	19.8	95.5
22		2	230.6	3.52	26.8	157.1	141.5	7979.	8012.	99.6	418.8	444.4	94.2	.1	2.1	5.6	.0	.2	17.5	94.1
23	03/19/74	1	317.8	3.50	24.4	155.8	131.7	7967.	8024.	98.5	428.9	454.5	94.4	1.7	2.2	6.5	.0	6.2	9.0	93.0
24		2	326.1	3.59	24.5	154.3	132.4	7847.	8017.	97.9	430.6	455.0	94.6	1.8	2.2	6.4	.0	7.0	7.0	93.5
25	03/20/74	1	320.4	3.38	25.9	161.5	146.5	8017.	8038.	99.7	431.4	454.1	95.0	1.4	2.2	6.5	.0	5.7	6.3	93.5
26		2	318.4	3.60	26.1	158.6	145.6	7899.	8023.	98.5	430.3	455.6	94.5	1.8	2.2	6.6	.0	6.3	6.4	93.6
27	03/21/74	1	317.8	3.32	29.2	164.0	159.0	7754.	7933.	97.7	429.9	458.3	93.8	3.2	2.2	7.2	.0	16.6	-.8	100.2
28		2	312.7	3.46	30.0	163.0	163.0	7648.	7907.	96.7	427.0	458.4	93.1	3.5	2.1	7.1	.0	18.6	.1	100.0
29	03/21/74	1	321.8	3.46	28.7	159.0	156.0	7700.	7864.	97.9	427.4	458.1	93.3	3.9	2.1	7.6	.0	15.4	1.7	99.6
30		2	329.2	3.56	29.2	157.0	154.0	7220.	7646.	94.4	408.0	455.3	89.6	5.7	2.1	7.6	.0	23.7	8.3	96.2
31	03/21/74	1	322.1	3.62	30.2	160.0	155.0	7483.	7872.	95.1	418.6	458.1	91.4	3.8	2.1	7.1	.0	20.0	6.5	98.6
32		2	322.0	3.61	29.9	160.0	156.0	7449.	7877.	94.6	419.4	458.2	91.5	3.7	2.1	6.9	.0	19.6	6.5	98.6
33		3	322.1	3.62	29.9	160.0	155.0	7438.	7893.	94.5	420.6	458.2	91.8	3.5	2.1	6.8	.0	18.5	6.5	98.6
34		4	323.3	3.61	29.8	158.0	151.0	7439.	7912.	94.8	422.1	458.1	92.2	3.3	2.1	6.7	.0	17.2	6.6	98.6
35		5	323.4	3.65	28.7	157.0	149.0	7511.	7923.	94.8	422.3	458.0	92.2	3.2	2.1	6.6	.0	16.4	7.2	94.4
36		6	323.2	3.64	28.6	156.0	148.0	7495.	7923.	94.6	421.5	457.9	92.0	3.2	2.1	6.6	.0	16.4	8.2	98.2
37	03/22/74	1	334.1	3.03	25.4	161.0	172.0	7316.	7788.	93.9	400.2	457.8	87.4	4.4	2.0	7.4	.0	20.1	23.6	94.8
38		2	332.0	3.01	25.4	160.0	171.0	7077.	7793.	90.8	387.0	457.8	84.5	4.5	1.9	7.0	.0	19.6	37.9	91.8
39	03/22/74	1	332.5	3.31	26.5	162.0	154.0	7532.	7933.	96.2	424.7	458.1	92.7	3.1	2.1	6.8	.0	14.4	7.0	98.5
40		2	332.3	3.35	26.5	161.0	164.0	7552.	7930.	95.6	426.0	458.4	92.9	3.1	2.1	6.7	.0	14.7	5.8	99.7
41		3	330.4	3.37	26.9	161.0	170.0	7597.	7927.	95.8	425.7	458.6	92.8	3.2	2.1	6.7	.0	15.2	5.7	98.8
42		4	321.8	3.43	27.8	159.0	177.0	7571.	7914.	95.6	423.8	458.7	92.4	3.4	2.1	6.7	.0	16.5	6.2	98.6
43		5	321.8	3.47	27.9	158.0	181.0	7561.	7912.	95.6	423.5	458.8	92.3	3.5	2.1	6.7	.0	16.9	6.1	98.7
44	03/22/74	1	413.3	3.86	24.7	170.0	150	7528.	7845.	96.0	424.7	458.1	92.7	3.2	2.1	6.8	.0	15.5	-.8	98.7
45		2	413.6	3.89	24.7	168.0	156.0	7463.	7836.	95.2	424.7	458.1	92.7	3.2	2.1	6.7	.0	15.8	5.6	98.8
46		3	413.9	3.96	25.0	166.0	162.0	7449.	7814.	95.3	423.7	458.0	92.5	3.4	2.1	6.7	.0	16.8	5.2	98.9
47		4	412.9	3.11	25.5	162.0	171.0	7388.	7781.	95.0	421.5	457.7	92.1	3.7	2.1	6.7	.0	18.3	5.3	98.8
48		5	413.4	3.19	25.8	161.0	175.0	7385.	7762.	95.1	421.1	457.5	92.0	3.8	2.1	6.7	.0	19.2	4.6	99.0
49	03/22/74	1	501.5	4.93	24.7	158.0	158.0	7550.	7814.	96.6	424.7	457.9	92.7	2.7	2.1	7.1	.0	15.4	6.0	98.7
50		2	491.4	4.77	24.4	156.0	158.0	7597.	7859.	96.7	426.2	458.3	93.0	2.4	2.1	6.9	.0	13.9	6.8	98.5
51	03/22/74	1	491.6	4.80	25.1	156.0	158.0	7597.	7893.	96.3	429.0	458.5	93.6	2.2	2.2	6.5	.0	13.2	5.4	98.8
52		2	489.9	4.89	25.4	157.0	158.0	7562.	7876.	95.8	427.7	458.4	93.3	2.3	2.1	6.4	.0	14.0	5.9	98.7
53		3	488.2	4.79	25.8	156.0	164.0	7507.	7857.	95.5	427.9	458.4	93.3	2.5	2.2	6.4	.0	15.0	4.5	99.0
54		4	484.1	4.79	25.9	161.0	170.0	7540.	7860.	95.9	428.8	458.6	93.5	2.5	2.2	6.4	.0	15.0	3.8	99.2
55		5	485.3	4.75	25.7	159.0	178.0	7521.	7871.	95.6	428.6	458.6	93.4	2.4	2.2	6.3	.0	14.8	4.6	99.0
56	03/25/74	1	496.5	4.83	27.8	156.0	182.0	7623.	7854.	97.1	431.1	458.6	94.0	2.5	2.2	6.6	.0	12.4	4.0	99.1
57		2	493.9	4.78	27.6	157.0	181.0	7566.	7858.	96.3	432.6	458.4	94.4	2.4	2.2	6.4	.0	11.9	2.8	99.4
58		3	494.5	4.85	27.1	158.0	183.0	7565.	7886.	96.9	432.7	458.6	94.3	2.2	2.2	6.2	.0	10.7	4.9	99.3
59		4	498.6	4.91	27.7	165.0	157.0	7655.	7911.	96.8	433.0	458.6	94.4	2.0	2.2	6.2	.0	9.6	5.5	98.8
60		5	499.2	4.98	28.6	169.0	154.0	7687.	7917.	97.1	433.6	458.5	94.6	2.0	2.2	6.2	.0	9.3	5.3	98.8
61	03/25/74	1	487.7	4.79	27.1	158.0	154.0	7521.	7853.	95.8	433.3	458.2	94.6	2.5	2.2	6.5	.0	11.1	2.5	99.5
62		2	484.1	4.90	27.3	157.0	154.0	7450.	7829.	95.2	430.6	458.0	94.0	2.7	2.2	6.5	.0	11.9	4.2	99.1
63		3	481.1	4.99	27.5	157.0	161.0	7453.	7812.	95.4	429.9	457.9	93.9	2.8	2.2	6.5	.0	12.4	4.1	99.1

TABLE XVII (cont.)

		4	465.4	4.38	20.2	157.0	163.0	7465.	7938.	95.2	431.4	458.2	94.1	2.6	2.2	6.4	.0	11.6	4.1	90.1
		5	471.4	4.48	20.1	157.0	159.0	7464.	7938.	95.2	427.3	458.2	93.3	2.6	2.1	6.4	.0	11.5	4.3	90.2
		1	467.9	4.60	20.4	156.0	156.0	7512.	7899.	95.2	432.8	458.4	94.4	2.4	2.2	6.6	.0	10.4	4.1	90.1
		2	467.8	4.56	20.3	156.0	158.0	7520.	7898.	95.2	435.2	458.4	94.9	2.3	2.2	6.4	.0	10.1	2.3	90.5
		3	467.3	4.55	20.2	156.0	160.0	7507.	7901.	95.0	435.0	458.5	94.9	2.3	2.2	6.3	.0	9.9	2.7	90.4
		6	466.1	4.55	20.0	157.0	160.0	7423.	7912.	93.9	426.8	458.5	93.1	2.3	2.1	6.2	.0	9.3	11.2	87.6
		7	467.4	4.42	20.1	157.0	156.0	7428.	7923.	93.8	422.9	458.4	92.3	2.1	2.1	6.1	.0	9.1	16.0	86.5
		8	465.5	4.39	20.3	161.0	152.0	7427.	7929.	93.7	426.6	458.3	93.1	2.1	2.1	6.3	.0	9.0	12.4	87.3
		7	463.7	4.34	20.0	160.0	152.0	7396.	7930.	93.3	427.9	458.4	93.4	2.1	2.2	6.0	.0	9.2	10.9	87.6
		1	475.6	5.29	18.6	161.0	152.0	7115.	7737.	92.0	412.1	456.8	90.2	3.4	2.1	6.5	.0	12.7	20.0	85.6
		2	474.3	5.34	18.7	161.0	91.0	7164.	7744.	92.9	412.7	456.4	90.6	3.4	2.1	6.5	.0	13.0	17.6	86.1
		3	474.3	5.12	18.7	162.0	91.0	7145.	7715.	92.7	412.3	456.5	90.5	3.4	2.1	6.5	.0	12.9	18.4	86.0
		4	472.2	5.25	18.2	162.0	91.0	7034.	7695.	91.8	396.4	456.3	88.0	5.6	2.0	6.5	.0	21.6	18.1	86.0
	45/74	1	481.3	2.42	11.8	160.0	148.0	7484.	7979.	95.2	414.0	441.6	93.7	.3	2.1	4.3	.0	.6	20.5	95.4
	46/74	1	476.8	4.05	21.5	161.0	67.0	7272.	7746.	93.3	419.5	456.0	92.0	2.9	2.1	6.3	.0	13.1	12.2	91.3
	47/74	1	481.2	3.91	1.5	161.0	137.0	7465.	7947.	93.3	419.2	456.2	91.9	2.5	2.1	6.2	.0	6.4	10.7	91.7
	48/74	1	484.1	3.41	22.1	137.0	85.0	7324.	7832.	94.1	419.6	457.0	92.0	1.7	2.1	5.8	.0	5.1	17.6	91.1
	49/74	1	471.5	4.07	18.7	161.0	137.0	7353.	7871.	93.5	418.9	457.9	91.3	2.5	2.1	6.3	.0	8.4	21.6	85.5
	50/74	1	474.5	4.24	19.4	159.0	76.0	7320.	7859.	92.8	401.4	458.4	89.2	4.5	2.0	5.7	.0	27.0	7.4	88.6
	51/74	1	476.6	3.10	22.2	155.0	135.0	7345.	8038.	93.9	427.3	451.4	94.2	1.1	2.1	5.4	.0	2.9	14.4	92.8
	52/74	1	469.5	3.79	22.1	156.0	144.0	7345.	8028.	94.0	431.6	457.9	94.3	1.6	2.2	5.7	.0	6.6	13.2	93.8
	53/74	1	466.0	4.90	22.3	161.0	136.0	7428.	7930.	86.2	429.9	459.4	93.6	2.8	2.2	5.6	.0	11.9	7.0	86.5
	54/74	1	462.4	4.74	19.3	158.0	150.0	7401.	7874.	93.9	428.9	459.3	93.4	2.6	2.2	6.3	.0	9.7	9.5	87.9
	55/74	1	473.0	4.45	21.1	157.0	166.0	7517.	7914.	94.9	434.9	459.7	94.8	2.2	2.2	6.0	.0	8.1	4.4	90.8

Nomenclature

CSTART - Theoretical C*, ft/sec

ISPT - Theoretical Is

KL - Kinetics Loss, sec

DL - Divergence Loss, sec

BL - Boundary Layer Loss, sec

MRL - Mixture Ratio Loss, sec

FCL - Film Cooling Loss, sec

ERL - Energy Release Loss, sec

ERE - Energy Release Efficiency

TABLE XVII (cont.)

********** ETR ENGINE TEST DATA AND PERFORMANCE SUMMARY **********

TEST SERIES: 1983-D02-0M-XXX

DESIGN POINT 2: SHEAR COAXIAL INJECTOR

****HYDRAULIC DATA ****

TEST	DATE	PER	PC	MRC	WO	WF	AO	AF	CDO	CDF	ΔPOX	ΔPFL	VOX	VFUEL	TOJ	TFJ	RN	OF/VO	MORAT	EFF
12	02/19/74	1	302.0	4.55	1.1564	.2544	.02980	.115001.190	.850		35.1	109.3	59.42704.6	181.9	350.0	445.	38.98	8.57	94.3	
13	02/19/74	1	305.9	4.22	1.1625	.2754	.02980	.115001.190	.850		35.9	129.8	70.62967.0	186.4	360.0	552.	42.03	9.96	91.6	
14	02/19/74	1	234.7	3.26	.9107	.2795	.02980	.115001.190	.850		21.5	136.8	54.03080.7	177.7	324.0	963.	57.01	17.50	95.5	
14		2	235.0	3.44	.9[illegible]	.2748	.02980	.115001.190	.850		23.2	131.7	56.03017.3	177.1	329.0	851.	53.88	15.87	96.1	
15	02/19/74	1	317.8	4.64	1.3407	.2978	.02980	.115001.190	.850		49.3	117.7	81.52487.4	175.8	331.0	509.	30.51	6.58	98.0	
15		2	320.1	4.76	1.3491	.2960	.02980	.115001.190	.850		51.1	116.1	82.92469.6	176.3	333.0	482.	29.80	6.26	98.5	
16	02/20/74	1	320.4	4.56	1.3619	.2986	.02980	.115001.190	.850		48.7	118.4	81.62496.4	181.5	334.0	520.	30.58	6.70	98.5	
16		2	318.4	4.43	1.3932	.2826	.02980	.115001.190	.850		50.6	106.7	82.92377.2	178.8	334.0	424.	28.67	5.83	98.6	
17	02/20/74	1	317.8	6.09	1.4004	.2411	.02980	.115001.190	.850		57.0	85.3	88.72228.2	184.0	360.0	233.	25.13	4.12	100.2	
17		2	316.7	5.57	1.4747	.2315	.02980	.115001.190	.850		57.3	84.4	88.72294.1	183.0	391.0	206.	25.85	4.06	100.0	
18	02/21/74	1	321.4	6.11	1.5200	.2489	.02980	.115001.190	.850		60.2	88.5	90.52238.3	179.0	363.0	243.	24.73	4.05	99.6	
18		2	328.2	7.43	1.7014	.2289	.02980	.115001.190	.850		75.1	75.6	110.82079.7	177.0	376.0	152.	20.64	2.78	98.2	
21	02/21/74	1	322.1	6.02	1.5626	.2361	.02980	.115001.190	.850		63.8	79.6	93.32121.9	180.0	363.0	196.	22.74	3.44	98.6	
21		2	322.0	5.96	1.5678	.2389	.02980	.115001.190	.850		64.3	81.3	93.62142.4	180.0	362.0	202.	22.89	3.49	98.6	
21		3	322.1	6.00	1.5614	.2438	.02980	.115001.190	.850		63.7	83.0	93.22163.8	180.0	354.0	216.	23.21	3.62	98.6	
21		4	323.3	6.21	1.5617	.2500	.02980	.115001.190	.850		62.6	86.2	92.12171.4	178.0	351.0	237.	23.56	3.86	98.6	
21		5	323.4	6.10	1.5459	.2535	.02980	.115001.190	.850		62.0	87.9	91.62183.7	177.0	348.0	250.	23.85	3.91	98.4	
21		6	323.2	6.09	1.5479	.2543	.02980	.115001.190	.850		62.0	88.8	91.42197.8	176.0	349.0	252.	24.04	3.95	98.2	
22	02/22/74	1	330.1	6.84	1.7077	.2496	.02980	.115001.190	.850		76.4	84.8	102.22137.8	181.0	364.0	193.	20.91	3.06	94.8	
22		2	333.0	6.76	1.7323	.2561	.02980	.115001.190	.850		78.4	92.0	103.42260.6	180.0	369.0	203.	21.86	3.23	91.8	
23	02/22/74	1	332.8	6.87	1.5632	.2664	.02980	.115001.190	.850		64.2	96.4	93.82278.1	182.0	356.0	280.	24.28	4.14	98.5	
23		2	332.3	6.92	1.5734	.2660	.02980	.115001.190	.850		64.9	98.4	94.22329.9	181.0	365.0	276.	24.74	4.18	98.7	
23		3	330.4	6.98	1.5632	.2615	.02980	.115001.190	.850		64.1	104.1	93.62505.8	181.0	390.0	265.	26.78	4.48	98.8	
23		4	321.9	6.13	1.5312	.2494	.02980	.115001.190	.850		61.1	105.6	91.22660.4	179.0	430.0	243.	29.18	4.76	98.6	
23		5	321.8	6.20	1.5356	.2478	.02980	.115001.190	.850		61.3	105.4	91.22676.7	178.0	436.0	236.	29.35	4.74	98.7	
24	02/22/74	1	413.3	6.37	2.0068	.3148	.02980	.115001.190	.850		108.1	104.8	123.12096.5	190.0	342.0	274.	17.04	2.67	98.7	
24		2	413.0	6.45	2.0261	.3147	.02980	.115001.190	.850		109.6	106.9	123.62137.5	188.0	349.0	270.	17.30	2.69	98.8	
24		3	413.9	6.61	2.0421	.3089	.02980	.115001.190	.850		110.8	105.4	123.92148.4	186.0	359.0	253.	17.34	2.62	98.9	
24		4	412.9	6.85	2.0640	.3012	.02980	.115001.190	.850		112.0	103.2	123.92157.7	182.0	370.0	232.	17.42	2.54	98.8	
24		5	413.4	6.99	2.0724	.2986	.02980	.115001.190	.850		112.6	101.7	124.12158.7	181.0	377.0	220.	17.40	2.49	98.8	
25	02/22/74	1	501.5	6.62	2.4434	.3689	.02980	.115001.190	.850		155.2	135.3	145.11967.1	178.0	331.0	307.	13.56	2.05	98.7	
25		2	491.4	6.32	2.3520	.3739	.02980	.115001.190	.850		144.3	122.6	139.52064.4	176.0	336.0	344.	14.80	2.34	98.5	
26	02/22/74	1	491.6	6.14	2.3475	.3823	.02980	.115001.190	.850		142.5	126.3	138.72079.0	176.0	331.0	372.	14.99	2.44	98.8	
26		2	489.4	6.28	2.3523	.3759	.02980	.115001.190	.850		144.7	126.1	139.92111.6	177.0	341.0	349.	15.09	2.40	98.7	
26		3	488.2	6.46	2.3761	.3679	.02980	.115001.190	.850		146.8	124.8	141.12136.1	178.0	352.0	322.	15.14	2.34	99.0	
26		4	489.1	6.46	2.3697	.3670	.02980	.115001.190	.850		147.2	126.6	141.92171.0	181.0	360.0	319.	15.30	2.37	99.2	
26		5	485.3	6.41	2.3544	.3673	.02980	.115001.190	.850		148.4	131.6	144.02255.4	189.0	372.0	317.	15.66	2.44	99.0	
28	02/25/74	1	496.2	6.19	2.3852	.3856	.02980	.115001.190	.850		147.2	130.1	140.92124.0	176.0	339.0	370.	15.07	2.44	99.1	
28		2	493.9	6.15	2.3845	.3908	.02980	.115001.190	.850		147.5	133.5	141.22152.1	177.0	337.0	384.	15.24	2.50	99.4	
28		3	494.5	6.29	2.3755	.4035	.02980	.115001.190	.850		146.7	141.1	141.12201.2	178.0	334.0	425.	15.60	2.65	98.9	
28		4	498.6	6.69	2.3548	.4138	.02980	.115001.190	.850		146.9	145.9	142.52219.2	185.0	331.0	458.	15.58	2.74	98.8	
28		5	499.2	6.84	2.3442	.4159	.02980	.115001.190	.850		147.1	142.6	143.42159.1	189.0	321.0	465.	15.06	2.67	98.8	
29	02/25/74	1	487.7	6.35	2.3695	.3948	.02980	.115001.190	.850		146.0	141.1	140.72090.3	179.0	321.0	461.	14.85	2.68	99.5	
29		2	487.7	6.15	2.3814	.3961	.02980	.115001.190	.850		149.6	141.3	142.22118.7	177.0	324.0	457.	14.[illegible]	2.62	99.1	
29		3	491.5	6.29	2.3859	.3861	.02980	.115001.190	.850		152.5	138.3	143.02[illegible].7	177.0	334.0	454.	14.[illegible]	2.51	99.1	

TABLE XVII (cont.)

			5.12	2.4928	.3923	.02980	.115001	.190	.850	149.7	133.5	142.82	139.7	177.0	334.0	385.	15.03	2.46	99.1
			5.1	2.4133	.3955	.02980	.115001	.190	.850	151.0	128.9	142.92	050.9	177.0	314.0	389.	14.35	2.35	98.2
		1	5.79	2.4600	.3907	.02980	.115001	.190	.850	132.1	130.6	133.62	104.2	176.0	313.0	429.	15.76	2.72	99.1
		6	5.73	2.4535	.3935	.02980	.115001	.190	.850	131.4	133.4	133.12	134.5	176.0	315.0	441.	16.03	2.80	99.5
		1	5.70	2.4614	.3950	.02980	.115001	.190	.850	131.2	141.4	133.02	52.7	176.0	330.0	446.	16.93	2.97	99.4
		4	5.59	2.4769	.3947	.02980	.115001	.190	.850	134.0	148.5	134.62	338.3	177.0	338.0	453.	17.37	3.05	97.6
			5.54	2.4855	.4041	.02980	.115001	.190	.850	133.2	156.4	134.22	407.0	177.0	341.0	484.	17.93	3.24	96.5
		8	5.50	2.4542	.4096	.02980	.115001	.190	.850	133.2	155.2	134.92	385.5	181.0	336.0	490.	17.68	3.21	97.3
		7	5.53	2.4548	.4081	.02980	.115001	.190	.850	135.0	153.3	136.82	365.0	186.0	333.0	478.	17.29	3.13	97.6
		1	5.56	2.4483	.3822	.02980	.115001	.190	.850	161.7	103.9	148.71	711.5	181.0	269.0	328.	11.91	1.77	95.5
			5.57	2.4466	.3742	.02980	.115001	.190	.850	162.0	101.1	148.81	683.3	181.0	268.0	317.	11.31	1.72	96.1
			5.54	2.4505	.3793	.02980	.115001	.190	.850	161.7	106.4	148.91	765.6	182.0	272.0	321.	11.76	1.81	96.0
		1	5.5	2.4341	.3229	.02980	.115001	.190	.850	177.4	94.4	155.91	840.6	182.0	323.0	180.	11.80	1.47	96.0
		1	5.75	2.4995	.7504	.02980	.115001	.190	.850	111.6	132.8	123.31	617.0	180.0	148.0	*500.	13.11	4.76	94.4
		1	5.44	2.4716	.3775	.02980	.115001	.190	.850	147.4	132.9	141.92	217.0	181.0	340.0	347.	15.62	2.89	97.3
		1	5.47	2.4743	.3940	.02980	.115001	.190	.850	48.8	108.6	81.72	339.0	181.0	294.0	487.	28.63	7.14	95.7
		1	5.41	2.4742	.3980	.02980	.115001	.190	.850	42.2	140.3	73.72	471.6	187.0	353.0	501.	40.32	9.16	94.1
		1	5.3	2.4170	.3170	.02980	.115001	.190	.850	143.6	106.5	140.11	517.2	181.0	217.0	480.	10.83	1.93	95.5
		1	5.30	2.4154	.2614	.02980	.115001	.190	.850	123.2	89.7	123.62	159.8	180.0	203.0	138.	10.67	2.01	98.6
		1	5.44	2.4311	.3487	.02980	.115001	.190	.850	40.2	177.3	74.53	615.6	185.0	411.0	496.	48.54	12.17	94.8
		1	5.47	2.4346	.3687	.02980	.115001	.190	.850	94.6	199.1	114.23	224.9	184.0	424.0	520.	25.75	5.38	97.8
		1	5.49	2.4114	.3457	.02980	.115001	.190	.850	118.0	190.1	127.43	272.5	183.0	447.0	504.	20.69	4.68	98.5
		1	5.37	2.4345	.3950	.02980	.115001	.190	.850	135.1	162.7	135.42	42.6	179.0	391.0	434.	19.15	3.32	97.9
		1	5.45	2.4341	.4167	.02980	.115001	.190	.850	135.3	164.5	135.52	33.7	177.0	396.0	510.	14.73	1.87	98.8

Nomenclature

- AO - Injector Oxidizer Orifice Area
- AF - Injector Fuel Oxidizer Orifice Area
- CDO - Oxidizer Orifice Discharge Coef
- CDF - Fuel Orifice Discharge Coef
- ΔPOX - Oxidizer Pressure Dorp, psi
- ΔPF - Fuel Pressure Drop, psi
- VOX - Oxidizer Injection Velocity, ft/sec
- VFUEL - Fuel Injection Velocity, ft/sec
- TOJ - Oxidizer Temp in Injector, °R
- TFJ - Fuel Temp in Injector, °R
- MORAT - Oxidizer to Fuel Momentum Ratio

IX, B, Gas/Liquid (Design Point #2) (cont.)

All design point 2 engine tests were conducted with approximately 20 to 30% fuel film coolant (ffc) flowrates as listed in Table XV. The film cooling was the main difference from the previous uncooled sea level tests. Thus, to compare film cooled vacuum performance data with previous uncooled sea level performance requires that the performance loss due to ffc be determined. The performance loss attributable to ffc was calculated as shown in Figure 83 as a function of coolant flow fraction and overall engine O/F. This performance loss was calculated with a thermal exchange model which accounts for the heating of the H_2 film coolant with a corresponding enthalpy reduction of the core combustion gases. The performance loss accounts for both the Isp change due to the core mixture ratio shift and its effect on the kinetic interaction. The losses calculated for Figure 83 were based upon a thermal exchange rate corresponding to heating the H_2 coolant to 1670°K (3000°R) at the nozzle exit plane.

After accounting for the film coolant losses in the above manner, the resultant energy release efficiencies for all steady state tests were plotted vs. engine O/F as shown on Figure 84. Examination of Figure 84 leads to the following conclusions:

1. The ERE's for 20%, 25%, and 30% ffc are consistent.
2. The ERE's for both nominal P_c = 340 N/cm^2 (500 psia) and low P_c = 170 N/cm^2 (250 psia) are consistent.
3. Cold fuel T_f = 55°K (100°R) results in approximately 2.5% ERE reduction from nominal T_f = 83°K (150°R) at the nominal engine O/F = 4.5; but the difference diminishes at both high and low O/F's.
4. Hot fuel T_f = 110°K (200°R) results in nearly equal to slightly lower ERE's than at the design fuel inlet temperature.

From the fact that a consistent 99% ERE is indicated at the design engine O/F for all P_c's and ffc's implies that the film coolant performance losses and kinetic losses listed in Table XV for each test condition must be correct. This value of 99% ERE is also in agreement with the sea level test results.

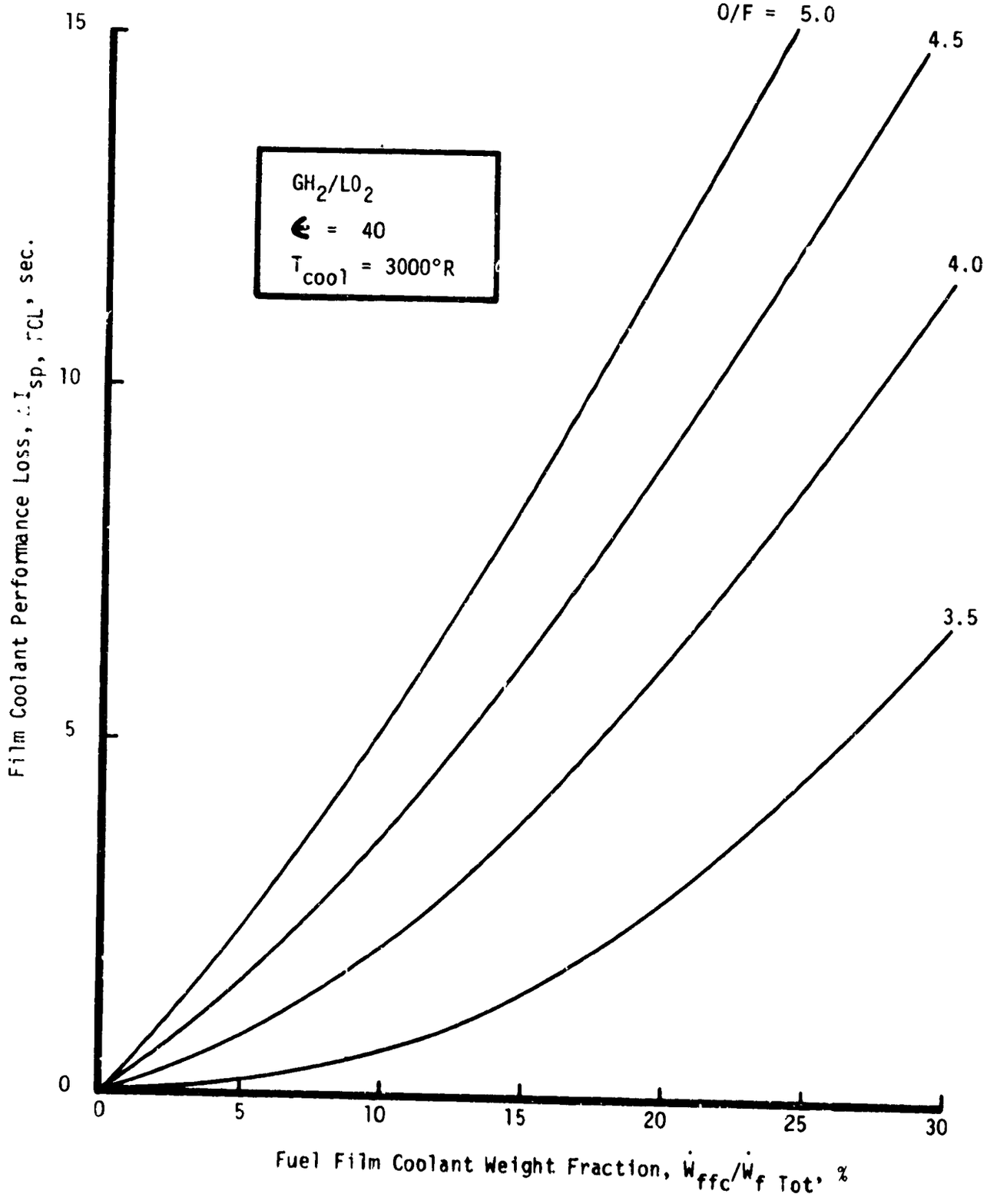

FIGURE 83 . THERMAL EXCHANGE FILM COOLANT PERFORMANCE LOSS

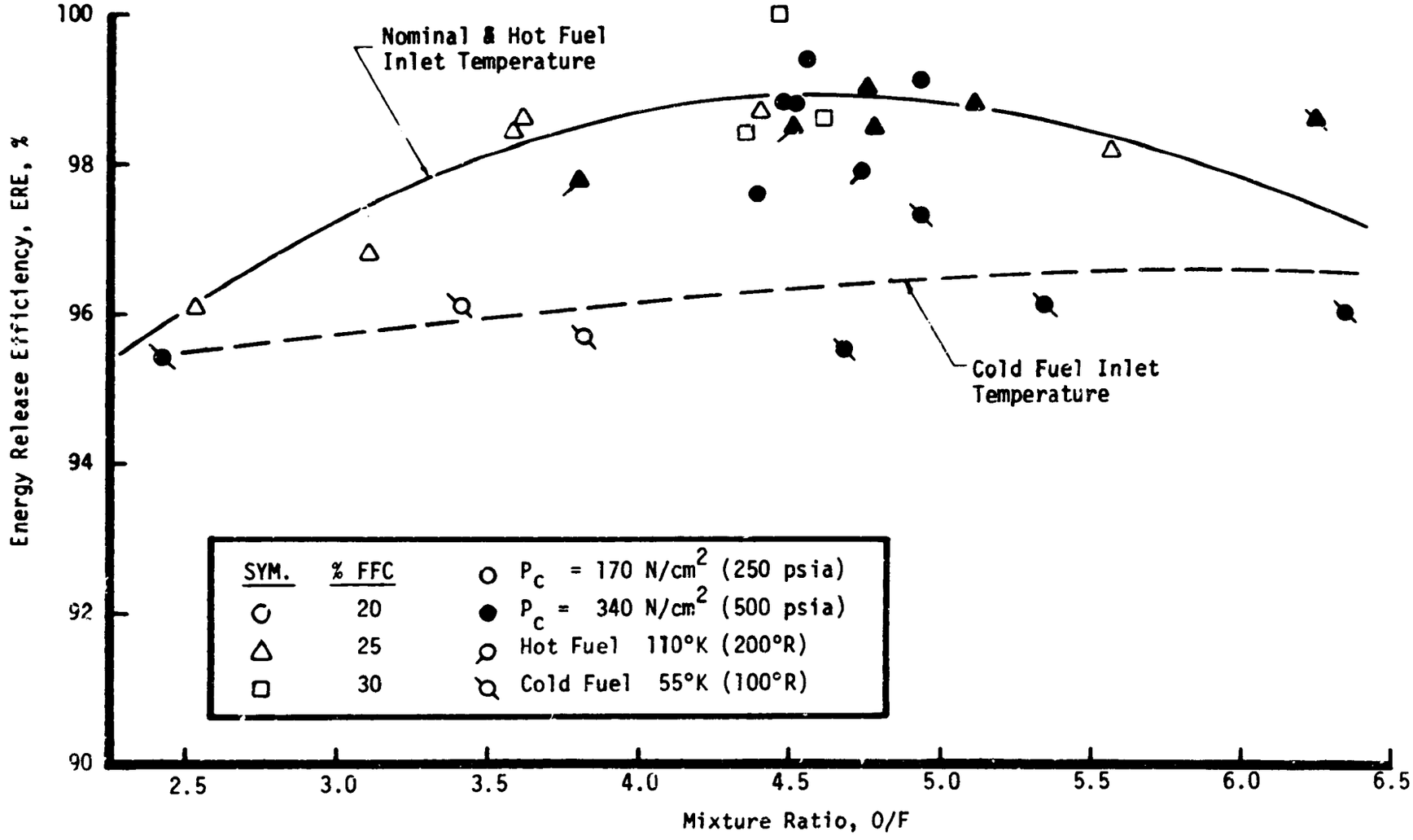

FIGURE 84. SHEAR COAXIAL ENERGY RELEASE EFFICIENCY

IX, B, Gas/Liquid (Design Point #2) (cont.)

Table XVII shows that the largest variability in delivered performance is attributable to the amount of ffc utilized. These data are plotted on Figure 85. The 435 sec delivered engine I_{sp} goal was met with the ffc at approximately 18% of the total fuel flowrate. At the 30% maximum ffc flowrate tested, engine I_{sp} was approximately 420 sec.

Pulsing tests were conducted with the GH_2/LO_2 engine as tabulated in Table XVIII. The effect of electrical pulse width (EPW) to the propellant valves upon total impulse is plotted in Figure 86; the inset shows that near the minimum impulse bit (MIB), valve sequencing becomes an important operating factor. Because of the low GH_2 density and low fuel mass capacitance of the engine, a fuel valve closing lag provides additional fuel to combust the residual LO_2 contained in the oxidizer manifold at shutdown. During engine start, an oxidizer valve lead of approximately 5 millisec results in closer to simultaneous start at the injector face and higher start transient performance as implied by the data of Figure 87. Figure 87 shows that long (.030 sec) fuel shutdown lags reduce pulse performance because the additional impulse increment occurs at the expense of higher GH_2 consumption. The highest MIB pulse performance tested was obtained with the 5 millisec oxidizer lead on start and 10 to 20 millisec fuel valve lag on shutdown. Under these conditions the pulse performance can exceed 400 sec I_{sp} even for the MIB of 222 N-sec (50-lbf-sec).

Test -053 and -54 were run with the same electrical pulse width. The oxidizer lead was increased by .005 sec for Test -054. The sequence was selected on the basis of the results of earlier tests and should have been nearly optimum. For Test -053, the specific impulse was 3649 N-sec/kg (372 lb_f-sec/lb_m) for a 197.5 N-sec (44.4 lb_f-sec) bit impulse. Increasing the oxidizer lead by .005 sec resulted in a 246.4 N-sec (55.4 lb_f-sec) bit impulse with a 3987.8 N-sec/kg (406.5 lb_f-sec/lb_m) specific impulse. The pulse repeatibility was good. The standard deviation of the pulses from the average value was 1.94% on Test -053 and 2.34% on Test -054. The program goal of a 334 N-sec (75 lb_f-sec) bit impulse with 3924 N-sec/kg (400 lb_f-sec/lb_m) performance was met and bettered.

TABLE XVIII

G/L PULSING PERFORMANCE

Test No.	029										030									
Pulse No.	1	2	3	4	5	6	7	8	9	10	1	2	3	4	5	6	7	8	9	10
	EPW = .989 sec										EPW = .249									
I_T Lbf-sec	285.09	288.60	289.57	290.54	292.01	287.78	284.96	282.76	282.72	282.27										
WOT Lbm/sec	.5518	.5539	.5626	.5779	.5794	.5724	.5685	.5680	.5670	.5669										
WFT	.1147	.1207	.1175	.1174	.1142	.1132	.1120	.1105	.1109	.1108										
WTT	.6664	.6746	.6801	.6953	.6936	.6857	.6805	.6785	.6779	.6777										
O/F_{Tot} -	4.813	4.588	4.787	4.921	5.074	5.056	5.076	5.141	5.110	5.116										
ISP_i sec	427.78	427.82	425.77	417.84	421.02	419.71	418.75	416.74	417.03	416.50										
O/F_{core} -	4.959	4.722	4.929	5.109	5.250	5.218	5.242	5.312	5.280	5.286										
ISP_{cum} sec	427.8	427.8	427.1	424.7	424.0	423.3	422.6	421.9	421.4	420.9										

Nomenclature

EPW - Electrical Pulse Width
I_T - Total Impulse lbf-sec
WOT - Total Oxidizer Flow, lbm
WFT - Total Fuel Flow, lbm
WTT - Total Propellant Flow, lbm
O/F - Mixture Ratio
ISP_i - Specific Impulse for Individual Pulse, sec
ISP_{cum} - Cumulative Specific Impulse for Pulse Train, sec

TABLE XVIII (cont.)

Test No.	031										032									
Pulse No.	1	2	3	4	5	6	7	8	9	10	1	2	3	4	5	6	7	8	9	10
	EPW = .149 sec										EPW = .069 sec									
I_T	171.21	169.86	160.70	164.08	162.96	161.87	161.59	161.10	161.94	160.81	60.37	67.51	68.80	66.89	66.46	66.29	66.33	67.18	66.03	67.01
WOT	.3436	.3429	.3373	.3341	.3346	.3305	.3321	.3289	.3306	.3265	.1235	.1330	.1330	.1318	.1342	.1314	.1321	.1421	.1362	.1363
WFT	.0696	.0702	.0628	.0704	.0704	.0690	.0695	.0689	.0693	.0698	.0300	.0327	.0330	.0342	.0330	.0343	.0332	.0334	.0337	.0344
WTT	.4133	.4131	.4001	.4045	.4050	.3995	.4015	.3978	.3999	.3962	.1535	.1657	.1660	.1660	.1672	.1657	.1653	.1756	.1698	.1707
O/F_{TOT}	4.934	4.886	5.370	4.744	4.753	4.787	4.779	4.770	4.771	4.681	4.114	4.063	4.031	3.848	4.064	3.826	3.983	4.250	4.045	3.962
ISP_i	414.28	411.21	401.6	405.6	402.4	405.2	402.4	405.0	404.9	405.9	393.3	407.4	414.4	403.0	397.6	400.0	401.2	382.7	388.8	392.6
O/F_{core}	5.114	5.088	5.606	4.918	4.923	4.947	4.935	4.926	4.927	4.835	4.219	4.160	4.132	3.937	4.163	3.911	4.078	4.356	4.140	4 052
ISP_{cum}	414.3	412.7	409.1	408.3	407.1	406.8	406.2	406.0	405.9	405.9	393.3	400.6	405.3	404.7	403.3	402.7	402.5	399.9	398.6	398.0

TABLE XVIII (cont.)

Test No.	033										036									
Pulse No.	1	2	3	4	5	6	7	8	9	10	1	2	3	4	5	6	7	8	9	10
	FPW = .069 sec										EPW = .064									
I_T	66.72	70.95	71.00	68.52	68.72	70.57	68.98	69.62	70.64	69.04	54.96	55.88	56.71	56.87	57.10	57.34	57.42	57.51	57.38	
WOT	.1292	.1435	.1493	.1469	.1338	.1481	.1431	.1443	.1459	.1454	.1057	.1118	.1105	.1133	.1142	.1203	.1211	.1176	.1164	
WFT	.0389	.0398	.0402	.0397	.0406	.0399	.0400	.0409	.0412	.0403	.0269	.0274	.0280	.0276	.0273	.0277	.0273	.0286	.0278	
WTT	.1681	.1833	.1895	.1823	.1744	.1880	.1832	.1852	.1871	.1857	.1326	.1393	.1384	.1409	.1415	.1480	.1484	.1462	.1442	
O/F_{TOT}	3.326	3.605	3.711	3.698	3.293	3.715	3.575	3.530	3.540	3.607	3.923	4.074	3.949	4.110	4.177	4.346	4.444	4.116	4.185	
ISP_i	396.99	387.2	374.6	367.0	393.9	375.4	376.6	375.8	377.7	371.8	414.4	401.3	409.6	403.6	403.5	387.6	386.9	393.3	397.8	
O/F_{core}	3.387	3.672	3.777	3.767	3.356	3.806	3.663	3.612	3.615	3.669	4.047	4.203	4.071	4.242	4.313	4.491	4.590	4.255	4.347	
ISP_{cum}	396.99	391.9	385.8	381.0	383.5	382.1	381.3	380.6	380.3	379.4	414.4	407.7	408.3	407.1	406.4	403.1	400.6	399.7	399.5	

TABLE XVIII (cont.)

Test No.	037										038									
Pulse No.	1	2	3	4	5	6	7	8	9	10	1	2	3	4	5	6	7	8	9	10
	EPW = .064										EPW = .064									
	.081										.081									
I_T	60.25	59.77	59.91	60.81	59.81	60.75	60.40	60.87	59.91		59.79	62.05	61.21	61.39	61.76	62.43	61.68	62.50	61.50	62.30
WOT	.1193	.1186	.1188	.1201	.1230	.1143	.1151	.1180	.1159		.1138	.1138	.1170	.1188	.1210	.1203	.1205	.1166	.1170	.1175
WFT	.0341	.0341	.0347	.0336	.0336	.0347	.0348	.0350	.0344		.0399	.0411	.0414	.0413	.0416	.0417	.0416	.0416	.0417	.0421
WTT	.1533	.1527	.1535	.1537	.1567	.1490	.1499	.1530	.1503		.1536	.1549	.1584	.1601	.1626	.1620	.1621	.1582	.1588	.1596
O/F_{TOT}	3.498	3.476	3.429	3.572	3.658	3.296	3.310	3.369	3.365		2.855	2.767	2.825	2.874	2.907	2.888	2.899	2.803	2.804	2.791
ISP_i	392.9	391.3	390.3	395.7	381.7	407.7	403.0	397.8	398.6		389.1	400.5	386.5	383.4	379.9	385.5	380.5	395.0	387.4	390.4
O/F_{core}	3.584	3.572	3.532	3.695	3.782	3.400	3.408	3.460	3.456		2.925	2.826	2.884	2.933	2.966	2.947	2.953	2.858	2.856	2.843
ISP_{cum}	392.9	392.1	391.5	392.6	390.4	393.?	394.6	395.0	395.4		389.1	394.8	392.0	389.8	387.8	387.4	386.4	387.4	387.4	387.7

TABLE XVIII (cont.)

Test No.	039									
Pulse No.	1	2	3	4	5	6	7	8	9	10
	EPW = .064									
I_T	66.60	70.39	68.35	68.48	68.11	68.77	67.94	68.12	68.30	68.68
WOT	.1352	.1316	.1305	.1332	.1423	.1373	.1404	.1365	.1422	.1374
WFT	.0409	.0411	.0409	.0404	.0406	.0409	.0405	.0410	.0409	.0408
WTT	.1760	.1726	.1714	.1736	.1829	.1782	.1809	.1775	.1831	.1782
O/F_{TOT}	3.308	3.202	3.190	3.297	3.506	3.356	3.466	3.326	3.469	3.364
ISP_i	378.4	407.7	398.7	394.5	372.4	386.0	375.6	383.7	373.0	385.4
O/F_{core}	3.383	3.271	3.260	3.370	3.582	3.428	3.542	3.401	3.548	3.439
ISP_{cum}	378.4	392.9	394.8	394.7	390.1	389.4	387.4	386.9	385.3	385.3

TABLE XVIII (cont.)

Test No.	041																			
Pulse No.	1	2	3	4	5	6	7	8	9	10	11	12	13	14	15	16	17	18	19	20
	EPW = .064																			
I_T	59.19	59.54	58.98	59.15	57.97	58.42	57.71	57.48	58.00	57.50	57.78	57.79	57.03	57.99	57.68	57.84	57.52	58.93	57.51	57.20
WOT	.1123	.1133	.1166	.1119	.1121	.1153	.1128	.1133	.1168	.1196	.1177	.1158	.1135	.1162	.1171	.1203	.1170	.12046	.1130	.1169
WFT	.0385	.0387	.0395	.0401	.0397	.0397	.0396	.0401	.04025	.0405	.0406	.0412	.0401	.0404	.0406	.0412	.0417	.04138	.0410	.0419
WTT	.1508	.1520	.1561	.1520	.1518	.1550	.1524	.1535	.1570	.1600	.1583	.1569	.1536	.1566	.1577	.1614	.1587	.1618	.1540	.1588
O/F_{TOT}	2.916	2.924	2.954	2.793	2.819	2.907	2.846	2.824	2.901	2.954	2.899	2.813	2.833	2.872	2.881	2.922	2.807	2.911	2.756	2.788
ISP_i	392.5	391.7	377.9	392.2	381.8	376.9	378.6	374.6	369.4	359.3	364.9	368.3	371.3	370.3	365.7	358.3	362.5	364.2	373.4	360.3
O/F_{core}	2.976	2.987	3.018	2.853	2.877	2.969	2.908	2.879	2.959	3.014	2.959	2.869	2.892	2.932	2.941	2.985	2.866	2.972	2.813	2.844
ISP_{cum}	392.5	392.1	387.3	387.8	386.6	384.9	384.0	382.9	381.3	379.0	377.7	376.9	376.5	376.0	375.3	374.2	373.5	373.0	373.0	372.4

TABLE XVIII (cont.)

Test No.	042															
Pulse No.	1	2	3	4	5	6	7	8	9	10	50	51	52	53	54	55
	EPW = .064															
I_T	59.11	60.15	58.75	58.32	59.59	58.90	58.09	57.08	58.65	56.95	58.99	58.98	59.26	59.71	58.95	58.58
WOT	.1090	.1193	.1174	.1153	.1209	.1185	.1164	.1172	.1192	.1159	.1253	.1204	.1245	.1284	.1267	.1253
WFT	.0409	.0419	.0407	.0412	.0413	.0423	.0415	.0425	.0413	.0417	.0429	.0384	.0430	.0444	.0432	.0430
WTT	.1499	.1612	.1581	.1565	.1622	.1608	.1579	.1597	.1604	.1576	.1689	.1589	.1676	.1728	.1699	.1683
O/F_{TOT}	2.665	2.846	2.881	2.802	2.929	2.805	2.806	2.759	2.888	2.784	2.928	3.132	2.894	2.890	2.936	2.912
ISP_i	394.3	373.1	371.6	372.8	367.5	366.3	367.9	357.3	365.6	361.3	351.0	371.3	353.6	345.5	346.99	348.1
O/F_{core}	2.713	2.898	2.935	2.855	2.987	2.855	2.857	2.811	2.946	2.840	2.989	3.181	2.953	2.950	2.999	2.972
ISP_{cum}	394.3	383.3	379.4	377.7	375.6	374.0	373.2	371.2	370.5	369.6						

TABLE XVIII (cont.)

Test No.	← 042 →									
Pulse No.	100	101	102	103	104	105	149	150	151	152
I_T	61.44	61.27	62.63	62.80	63.21	62.80	40.26	17.58	17.53	19.80
WOT	.1208	.1135	.1195	.1219	.1213	.1173	.1344	.1468	.1528	.1501
WFT	.0455	.0442	.0446	.0454	.0455	.0446	.0453	.0496	.0499	.0511
WTT	.1663	.1577	.1642	.1673	.1668	.1620	.1797	.1964	.2026	.2012
O/F_{TOT}	2.656	2.569	2.678	2.687	2.664	2.628	2.970	2.958	3.065	2.940
ISP_i	369.6	388.4	381.5	375.4	378.9	387.8	224.0	89.52	86.51	98.41
O/F_{core}	2.709	2.621	2.732	2.742	2.717	2.681	3.007	3.005	3.113	2.983
ISP_{cum}										

TABLE XVIII (cont.)

Test No.	053									054									
Pulse No.	1	2	3	4	5	6	7	8	9	1	2	3	4	5	6	7	8	9	10
	EPW = .059									EPW = .059									
I_T	47.58	44.44	43.61	44.28	45.04	44.95	45.99	40.83	42.49	53.26	57.58	52.16	53.12	53.40	57.70	57.34	58.70	54.97	55.97
WOT	.0842	.0876	.0894	.0922	.0944	.0996	.0921	.0911	.0893	.0938	.1018	.1062	.1084	.1086	.1087	.1153	.1074	.1091	.1058
WFT	.0267	.0278	.0276	.0281	.0286	.0292	.0282	.0287	.0287	.0260	.0299	.0298	.0298	.0299	.0308	.0307	.0304	.0306	.0303
WTT	.1109	.1154	.1171	.1203	.1230	.1288	.1203	.11974	.1179	.1198	.1317	.1360	.1363	.1385	.1395	.1460	.1378	.1396	.1361
O/F_{TOT}	3.159	3.155	3.236	3.286	3.297	3.413	3.262	3.178	3.114	3.602	3.410	3.565	3.633	3.632	3.527	3.751	3.534	3.571	3.497
ISP_i	429.2	385.2	372.5	368.0	366.1	349.0	382.2	341.0	360.3	444.4	437.3	383.6	384.1	385.5	413.7	392.8	425.9	393.5	411.4
O/F_{core}	3.234	3.226	3.316	3.366	3.377	3.496	3.342	3.258	3.188	3.71	3.493	3.66	3.733	3.734	3.629	3.867	3.64	3.686	3.605
ISP_{cum}	429.2	406.7	395.1	388.0	383.4	377.2	378.0	373.3	371.9	444.4	440.7	429.6	411.0	405.7	407.1	404.9	407.6	405.9	406.5

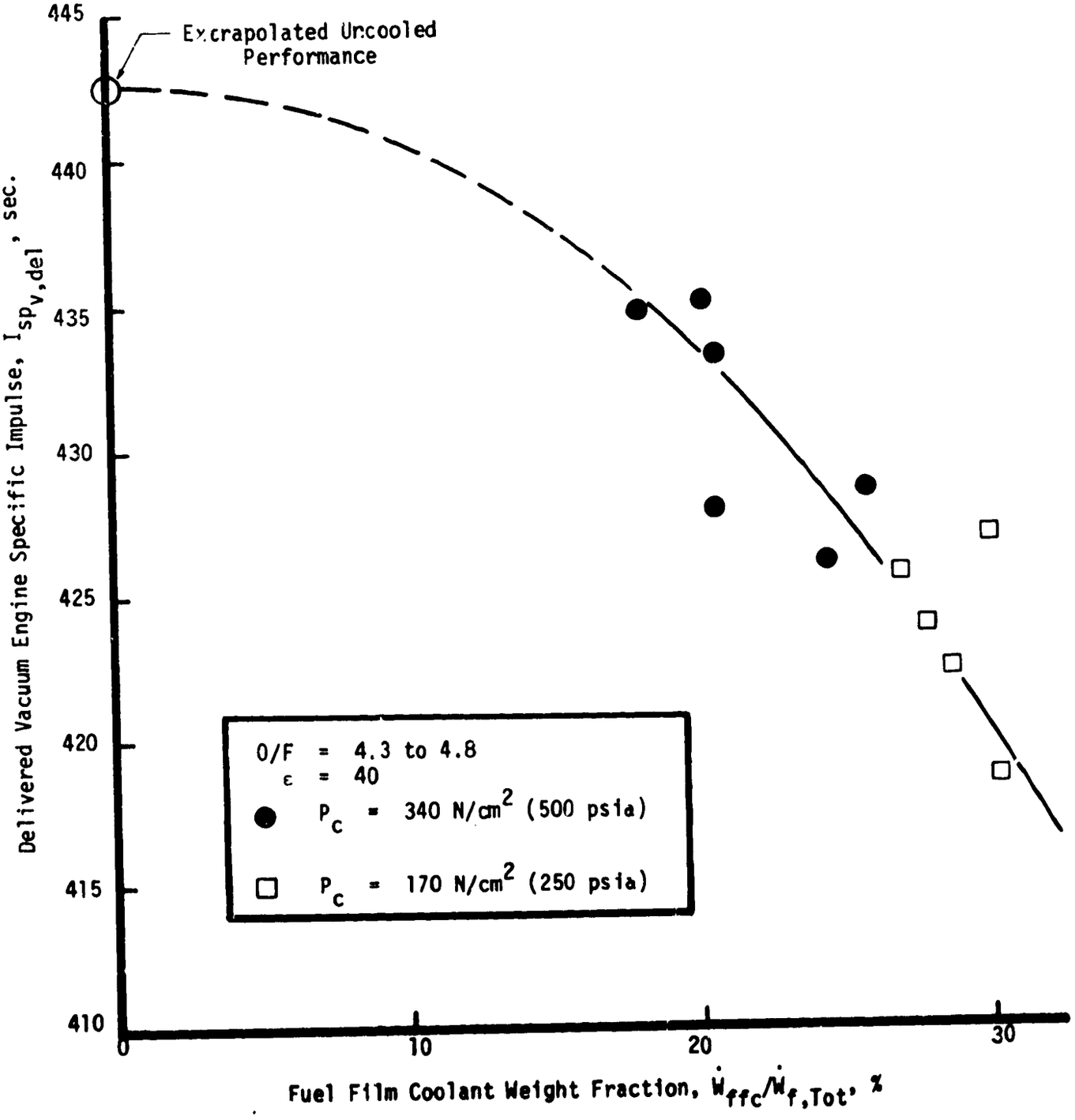

FIGURE 85. ENGINE VACUUM PERFORMANCE REDUCTION WITH FUEL FILM COOLING

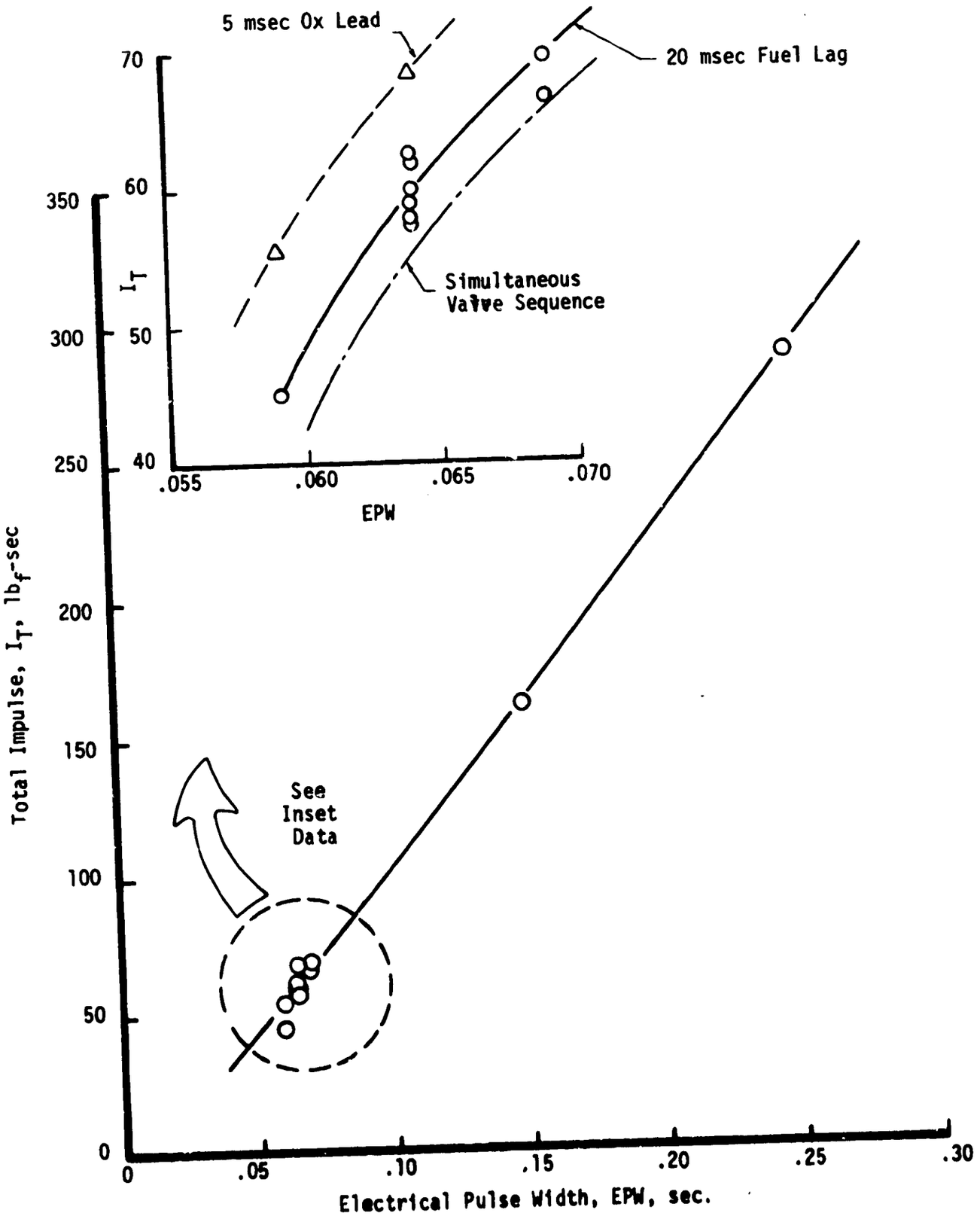

FIGURE 86. GH_2/LO_2 BIT IMPULSE VARIATION WITH ENGINE PULSE DURATION

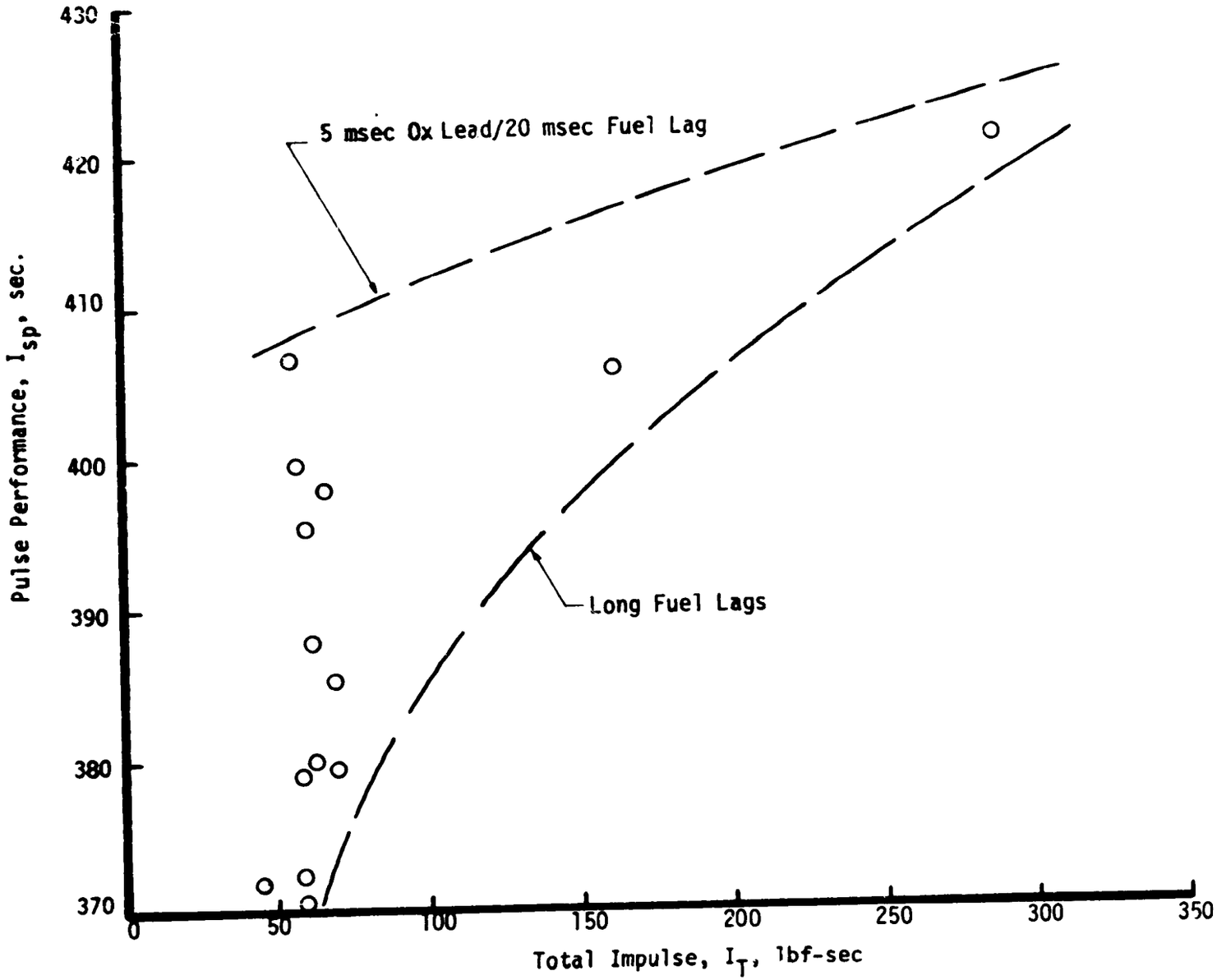

FIGURE 87. GH_2/LO_2 PULSE PERFORMANCE VARIATION WITH BIT IMPULSE

REFERENCES

1. Kelley, P. J., et al: Space Shuttle Auxiliary Propulsion System Design Study, Douglas Corporation, Interim Systems Definition Review, Contract NAS 9-12013, October, 1971.

2. Bauman, T. L. et al: Space Shuttle Auxiliary Propulsion System Design Study, McDonnell Douglas Corporation, Contract NAS 9-12013, Systems Definition Review, February, 1972. MDCE0603.

3. Akkerman, James W.: Shuttle Reaction Control System Cryogenic Liquid Distribution System Study. Auxiliary Propulsion and Pyrotechnics Branch Internal Note, Propulsion and Power Division, Manned Spacecraft Center, September, 1971.

4. Wanhainen, J. P., et al: Effect of Propellant Injection Velocity on Screech in a 20,000-Pound Hydrogen-Oxygen Rocket Engine, NASA TN D-3373, April, 1966.

5. Schoenman, L., Hydrogen-Oxygen Auxiliary Propulsion for Space Shuttle, NASA CR-120895, Aerojet Liquid Rocket Co., Sacramento, California, January, 1973.

6. Falk, A. Y., "Space Storeable Propellant Performance Gas/Liquid Like Doublet Injector Characterization", Final Report, Rocketdyne, NASA CR-120935, October, 1972.

7. Burick, R. J., Space Storable Propellant Performance Program Coaxial Injector Characterization, Final Report, Contract NAS 3-1205, NASA CR 120936, 1972.

8. Rosenberg, S. D., Aitken, A. J., Jassowski, D. M. and Royer, K. F.: Ignition Systems for Space Shuttle Auxiliary Propulsion System, NASA CR-72890, 1972. NASA Contract NAS 3-14348.

9. "Integrated Thruster Assembly Program", Final Report, Aerojet Liquid Rocket Company, NASA CR-134509, 1974. NASA Contract NAS 3-15850.

10. Reznik, B. D., "Practical Field Repair of Fused Slurry Silicide Coating for Space Shuttle T.P.S.," Space Shuttle Materials, Society of Aerospace Material and Process Engineers, Vol. 3, 1971, p. 382.

11. Sisco, F. T. and Epremian, E., Columbium and Tantalum, John Wiley and Sons, Inc., New York.

END

DATE

FILMED

OCT 14 1974